High Enthalpy Gas Dynamics

Ethirajan Rathakrishnan

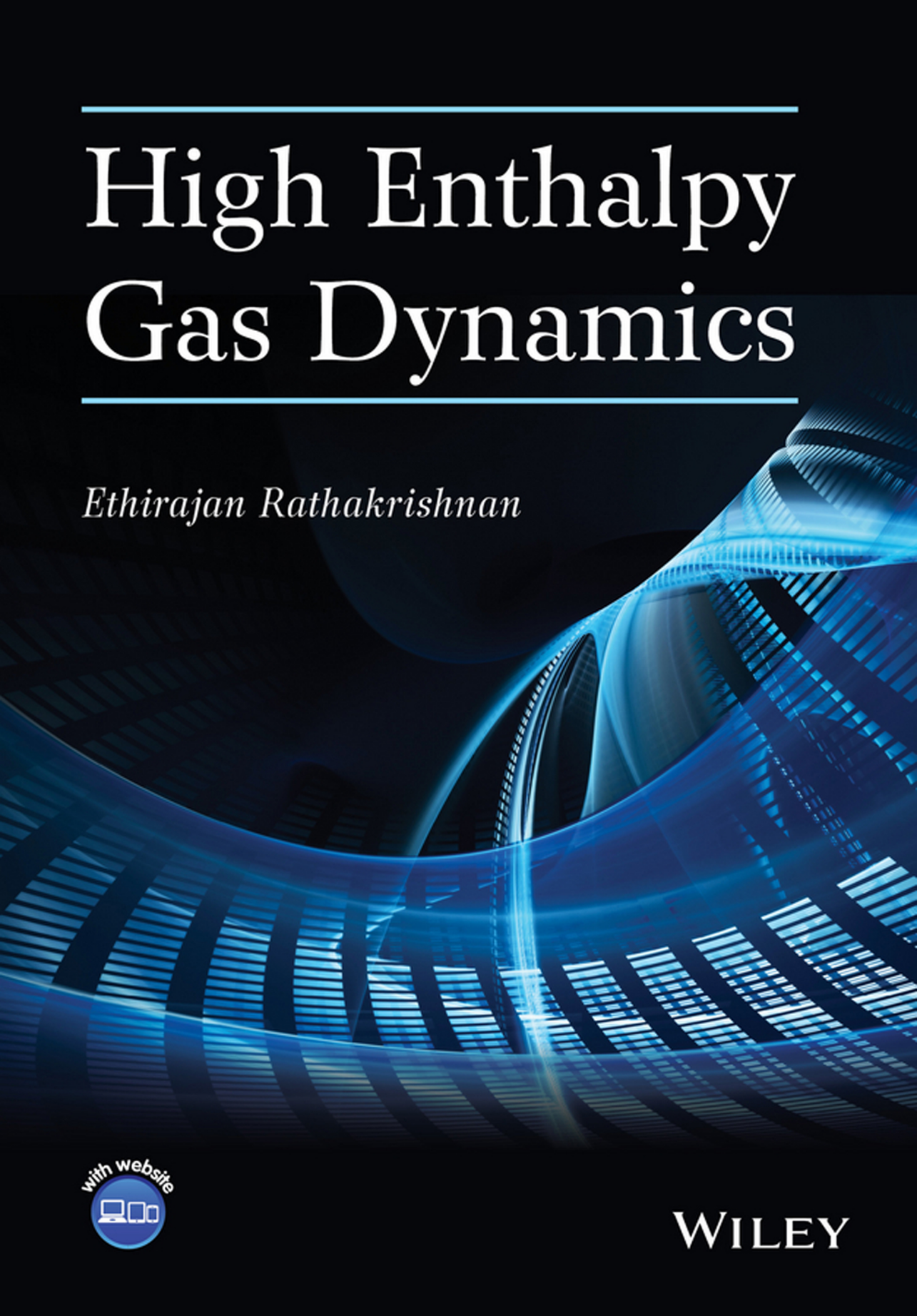

WILEY

HIGH ENTHALPY GAS DYNAMICS

HIGH ENTHALPY GAS DYNAMICS

Ethirajan Rathakrishnan

Indian Institute of Technology Kanpur, India

WILEY

This edition first published 2015

Registered office
John Wiley & Sons Singapore Pte. Ltd., 1 Fusionopolis Walk, #07-01 Solaris South Tower, Singapore 138628.

Library of Congress Cataloging-in-Publication Data

Rathakrishnan, Ethirajan, author.
High enthalpy gas dynamics / Ethirajan Rathakrishnan.
pages cm
Includes bibliographical references and index.
ISBN 978-1-118-82189-3 (cloth)
1. Gas dynamics. 2. Gases – Thermal properties. 3. Enthalpy. I. Title.
QC168.R384 2015
533′.2 – dc23

2014034305

Typeset in 11/13pt Times by Laserwords Private Limited, Chennai, India

1 2015

This book is dedicated to my parents,

Mr. Thammanur Shunmugam Ethirajan

and

Mrs. Aandaal Ethirajan

Ethirajan Rathakrishnan

Contents

About the Author

Ethirajan Rathakrishnan is Professor of Aerospace Engineering at the Indian Institute of Technology Kanpur, India. He is well known internationally for his research in the area of high-speed jets. The limit for the passive control of jets, called the *Rathakrishnan limit*, is his contribution to the field of jet research, and the concept of *breathing blunt nose (BBN)*, which reduces the positive pressure at the nose and increases the low pressure at the base simultaneously, is his contribution to drag reduction at hypersonic speeds. Positioning twin-vortex at Reynolds number around 5000, by changing the geometry from circular cylinder, for which the maximum limit for the Reynolds number for positioning twin-vortex was found to be around 160, by von Karman, to flat plate, is his addition to vortex flow theory. He has published a large number of research articles in many reputed international journals. He is Fellow of many professional societies, including the Royal Aeronautical Society. Professor Rathakrishnan serves as the Editor-In-Chief of the *International Review of Aerospace Engineering* (IREASE) and *International Review of Mechanical Engineering* (IREME) journals. He has authored 10 other books: *Gas Dynamics*, 5th ed. (PHI Learning, New Delhi, 2013); *Fundamentals of Engineering Thermodynamics*, 2nd ed. (PHI Learning, New Delhi 2005); *Fluid Mechanics: An Introduction*, 3rd ed. (PHI Learning, New Delhi 2012); *Gas Tables*, 3rd ed. (Universities Press, Hyderabad, India, 2012); *Instrumentation, Measurements, and Experiments in Fluids* (CRC Press, Taylor & Francis Group, Boca Raton, USA, 2007); *Theory of Compressible Flows* (Maruzen Co., Ltd. Tokyo, Japan, 2008); *Gas Dynamics Work Book*, 2nd ed. (Praise Worthy Prize, Napoli, Italy, 2013); *Applied Gas Dynamics* (John Wiley, New Jersey, USA, 2010); *Elements of Heat Transfer* (CRC Press, Taylor & Francis Group, Boca Raton, USA, 2012); and *Theoretical Aerodynamics* (John Wiley, New Jersey, USA, 2013).

In addition to the above technical books, Professor Ethirajan Rathakrishnan has authored the following literary books in Tamil: *Krishna Kaviam* (book on the life of LORD KRISHNA, in Classical Tamil Poetry, Shantha Publishers, Royapettah, Chennai, India, 2014) and *Naan Kanda Japan* (The Japan I Saw, in Tamil, Shantha Publishers, Royapettah, Chennai, India, 2014).

Preface

This book is designed to serve as an introductory text to graduate students who aspire to specialize in the area of *high-enthalpy gas dynamics*. A comprehensive knowledge of *gas dynamics* of perfect gases is taken as the datum for building the subject coverage of this book. The quantum mechanics and thermodynamics background necessary for the treatment of high-enthalpy flows is briefly reviewed wherever necessary. Some of the practical aspects that are essential in the application area of high-enthalpy flows, namely, shocks, nozzle flow, and transport properties, where the flow becomes chemically reactive are dealt with in detail in this book. The chapter on high-enthalpy facilities introduces the experimental devices meant for generating high-speed and high-temperature flows.

This book material has been class tested many times. The response of the students over the past two decades has refined the manuscript, to take the present form. The basic aim of this book is to make a complete text covering both the basic and applied aspects of theory of high-enthalpy flows for students, engineers, and applied physicists.

The fundamentals of thermodynamics and gas dynamics are covered, as it is treated at the undergraduate level. Considerable number of solved examples are given in these chapters to fix the concepts introduced, and a set of exercise problems along with answers are listed at the end of these chapters to test the understanding of the material studied.

To make the readers comfortable with the basic features of enthalpy and gas dynamics, vital features highlighting the concepts associated with such high-speed flows are given in Chapter 1. The material covered in this book is so designed that any user can follow it comfortably. The topics covered are broad based, starting from the basic principles and progressing toward the physics of the flow that governs the flow process.

The book is organized in a logical manner, and the topics are discussed in a systematic way. First, the basic aspects of the enthalpy, internal energy, heat, and gas dynamics are reviewed, to establish a firm basis for the subject of gas dynamic theory. Following this, thermodynamics of fluid flow is introduced with the elementary aspects, gradually proceeding to the vital aspects of thermal and calorical perfectness and entropy. The chapter on wave propagation discusses the speed of sound, flow regimes, similarity parameters, and continuum hypothesis.

The chapter on high-temperature flows presents the importance and nature of high-enthalpy flows, most probable macrostate, and counting the number of microstates in a given state, using Bose–Einstein and Fermi–Dirac statistics. Evaluation of internal energy, partition function, thermodynamic, and equilibrium properties of high-temperature air are presented systematically. Kinetic theory of gases is presented systematically. Following these, inviscid high-temperature flows are analyzed. The flow traversed by normal and oblique shocks are analyzed with appropriate equations. Frozen and equilibrium aspects of flow through nozzle are presented in detail. Inviscid high-temperature flows are analyzed, beginning with the equations governing such flows followed by nonequilibrium flow through shocks, nozzles, and over blunt-nosed bodies. The final section of this chapter presents the transport properties of high-temperature gases.

The chapter on hypersonic flows covers the physics of hypersonic flows systematically. Newtonian flow model and Mach number independence principles are discussed to the point. Characteristics of hypersonic flow are presented, highlighting the non-continuum considerations, equilibrium, and nonequilibrium aspects. The transport properties and experimental measurements in hypersonic regime are also presented.

The chapter on aerothermodynamics discusses the empirical correlations, viscous interaction with external flows, computational fluid dynamics (CFD) for hypersonic flows, and their validation. In the final chapter, the working principle of some high-enthalpy facilities, along with some of the popular working facilities, is presented. In the last section of this chapter, all the vital aspects of high-enthalpy flows are recollected.

This book is the outgrowth of lectures presented over a number of years, at both undergraduate and graduate levels. The material for these lectures were prepared referring to the following books. *Hypersonic and High Temperature Gas Dynamics*, by J. D. Anderson, McGraw-Hill, Inc. 1989; *High Temperature Gas Dynamics*, by Tarit Bose, Springer, 2004; *Kinetic Theory of Gases*, by Kennard E. H, McGraw-Hill, 1938; *Introduction to Physical Gas Dynamics*, by Vincenti W. G and Charles H. Kruger, Krieger Pub Co, 1975; *Hypersonic Flow Theory*, by Hayes W.D and Probstein R.F, Academic Press, 1959 and *Hypersonic Aerothermodynamics*, by John J Bertin, AIAA Education Series, 1984. My sincere thanks to these authors for their contribution to this high-tech science.

The student, or reader, is assumed to have a background in the basic courses of fluid mechanics, thermodynamics, and gas dynamics of perfect gases. Advanced undergraduate students should be able to handle the subject material comfortably. Sufficient details have been included so that the text can be used for self-study. Thus, the book can be useful for scientists and engineers working in the field of aerodynamics in industries and research laboratories.

My sincere thanks to my undergraduate and graduate students in India and abroad, who are directly and indirectly responsible for the development of this book.

I would like to express my sincere thanks to Dr. Yasumasa Watanabe, Assistant Professor, Department of Aeronautics and Astronautics, Graduate School of

Engineering, The University of Tokyo, Japan, for his help in making some solved examples along with computer codes and checking the manuscript at different stages of its development.

I thank Dr. Shashank Khurana, Senior Research Scholar, State Key Laboratory of Turbulence and Complex Systems, Department of Aeronautics and Astronautics, Peking University, Beijing, China, for critically checking the manuscript of this book. I thank my doctoral student Aravindh Kumar and masters student Vinay Chauhan for checking the manuscript and the solutions manual.

For instructors only, a companion solutions manual is available from John Wiley that contains typed solutions to all the end-of-chapter problems. The financial support extended by the Continuing Education Centre of the Indian Institute of Technology, Kanpur, for the preparation of the manuscript is gratefully acknowledged.

Ethirajan Rathakrishnan

1

Basic Facts

1.1 Introduction

High-enthalpy flows are those with their specific heats ratio as a function of temperature. The word *enthalpy* is based on the Greek word enthalpies, which means to put heat into. It comes from the classical Greek prefix en-, meaning to put into, and the verb thalpein, meaning "to heat." The earliest writings to contain the concept of enthalpy did not appear until 1875 when Josiah Willard Gibbs introduced "a heat function for constant pressure" [1]. However, Gibbs did not use the word "enthalpy" in his writings. Instead, the word "enthalpy" first appeared in the scientific literature in a 1909 publication by J. P. Dalton. According to that publication, Heike Kamerlingh Onnes (1853–1926) actually coined the word. Over the years, many different symbols were used to denote enthalpy [2]. It was not until 1922 that Alfred W. Porter proposed the symbol "H" as the accepted standard [3], thus finalizing the terminology still in use today.

1.1.1 Enthalpy

Enthalpy is a measure of the total energy of a thermodynamic system. It includes the internal energy, which is the energy required to create a system, and the amount of energy required to make room for it by displacing its environment and establishing its volume and pressure.

Enthalpy is a thermodynamic potential. It is a state function and an extensive quantity. The unit of measurement for enthalpy in the International System of Units (SI) is the joule, but other historical, conventional units are still in use, such as the British thermal unit and the calorie.

The enthalpy is the preferred expression of system energy changes in many chemical, biological, and physical measurements, because it simplifies certain descriptions of energy transfer. This is because a change in enthalpy takes account of energy transferred to the environment through the expansion of the system under study.

High Enthalpy Gas Dynamics, First Edition. Ethirajan Rathakrishnan.

www.wiley.com/go/rathakrishnan

The total enthalpy, H, of a system cannot be measured directly. Thus, change in enthalpy, ΔH, is a more useful quantity than its absolute value. The change ΔH is positive in endothermic reactions and negative in heat-releasing exothermic processes. ΔH of a system is equal to the sum of nonmechanical work done on it and the heat supplied to it.

The enthalpy, H, of a homogeneous system is defined as

$$\boxed{H = U + p\mathbb{V}} \tag{1.1}$$

where U, p, and $\mathbb{V}$, respectively, are the internal energy, pressure, and volume of the system.

The enthalpy is an *extensive property*. This means that for a homogeneous system, the enthalpy is proportional to the size of the system. It is convenient to work with the specific enthalpy $h = H/m$, where m is the mass of the system, or the molar enthalpy $H_m = H/n$, where n is the number of moles (h and H_m are *intensive properties*) while working with practical problems. For an inhomogeneous system, the enthalpy is the sum of the enthalpies of the subsystems composing the system.

$$H = \sum_k H_k$$

where the label k refers to the various subsystems. In a system with continuously varying p, T, and/or composition, the summation becomes an integral:

$$H = \int \rho\, h\, d\mathbb{V}$$

where ρ is the density.

The enthalpy $H(S, p)$ of a homogeneous system can be derived as a characteristic function of the entropy S and the pressure p as follows.

Let us start from the first law of thermodynamics for a closed system

$$dU = \delta Q - \delta W$$

Here, δQ is a small amount of heat added to the system and δW is a small amount of work performed by the system. In a homogeneous system, only reversible processes can take place, so the second law of thermodynamics gives

$$\delta Q = T\, dS$$

where T is the absolute temperature of the system and S is the entropy. Furthermore, if only $p\mathbb{V}$ work is done, $\delta W = pd\mathbb{V}$. For this case, from first law of thermodynamics

$$dU = TdS - pd\mathbb{V}$$

Adding $d(p\mathbb{V})$ to both sides, we have

$$dU + d(p\mathbb{V}) = TdS - pd\mathbb{V} + d(p\mathbb{V})$$

or

$$d(U + p\mathbb{V}) = TdS + \mathbb{V}dp$$

This can be expressed as

$$dH(S, p) = TdS + \mathbb{V}dp$$

The expression of dH in terms of entropy and pressure may be unfamiliar to many readers. However, there are expressions in terms of more familiar variables such as temperature and pressure [4]

$$dH = c_p\ dT + \mathbb{V}(1 - \alpha T)\ dp$$

where c_p is the heat capacity at constant pressure (that is, specific heat at constant pressure) and α is the *coefficient of (cubic) thermal expansion*

$$\alpha = \frac{1}{\mathbb{V}}\left(\frac{\partial \mathbb{V}}{\partial T}\right)_p$$

With this expression, one can, in principle, determine the enthalpy if c_p and $\mathbb{V}$ are known as the functions of p and T.

In a more general form, the first law of thermodynamics describes the internal energy with additional terms involving the chemical potential and the number of particles of various types. The differential statement for dH then becomes

$$dH = TdS + \mathbb{V}dp + \sum_i \mu_i\ dN_i$$

where μ_i is the chemical potential per particle for an i-type particle and N_i is the number of such particles. The last term can also be written as $\mu_i dn_i$ (with dn_i, the number of moles of component i added to the system, and μ_i, in this case, the molar chemical potential) or $\mu_i dm_i$ (with dm_i, the mass of component i added to the System, and μ_i, in this case, the specific chemical potential).

1.2 Enthalpy versus Internal Energy

The internal energy U can be interpreted as the energy required to create a system, and the $p\mathbb{V}$ term as the energy that would be required to "make room" for the system if the pressure of the environment remained constant. When a system, for example, n moles of a gas of volume $\mathbb{V}$ at pressure p and temperature T, is created or brought to its present state from absolute zero, energy equal to its internal energy U plus $p\mathbb{V}$, where $p\mathbb{V}$ is the work done in pushing against the ambient (atmospheric) pressure, must be supplied. In basic physics and statistical mechanics, it may be more interesting to study the internal properties of the system, and therefore, the internal energy is used. In basic chemistry, scientists are typically interested in experiments conducted at atmospheric pressure, and for reaction energy calculations, they care about the total energy in such conditions and, therefore, typically need to use enthalpy H. Furthermore, the enthalpy is the *working horse* of engineering thermodynamics as we will see later.

1.2.1 Enthalpy and Heat

In order to discuss the relation between the enthalpy increase and heat supply, let us return to the first law of thermodynamics for a closed system

$$dU = \delta Q - \delta W$$

Let us apply this to the special case that the pressure at the surface is uniform. In this case, the work term can be split in two contributions, the so-called $p\mathbb{V}$ work, given by $-p\ d\mathbb{V}$ (here p is the pressure at the surface and $d\mathbb{V}$ is the increase in the volume of the system) and other types of work $\delta W'$ such as by a shaft or by electromagnetic interaction. So we write

$$\delta W = p\ d\mathbb{V} + \delta W'$$

In this case, the first law reads

$$dU = \delta Q - pd\mathbb{V} - \delta W'$$

Using this, Equation (1.1) can be expressed as

$$dH = \delta Q + \mathbb{V}dp - \delta W'$$

From this relation, we see that the increase in enthalpy of a system is equal to the added heat

$$dH = \delta Q$$

provided that the system is under constant pressure ($dp = 0$) and that the only work done by the system is expansion work ($\delta W' = 0$).

For systems at constant pressure, the change in enthalpy is the heat received by the system. Therefore, the change in enthalpy can be devised or represented without the need for compressive or expansive mechanics; for a simple system, with a constant number of particles, the difference in enthalpy is the maximum amount of thermal energy derivable from a thermodynamic process in which the pressure is held constant. The term $p\mathbb{V}$ is the work required to displace the surrounding atmosphere in order to vacate the space to be occupied by the system.

The total enthalpy of a system *cannot* be measured directly; the enthalpy change of a system is measured instead. Enthalpy change is defined by the following equation:

$$\Delta H = H_f - H_i$$

where ΔH is the "enthalpy change" and H_f is the final enthalpy of the system, expressed in joules. In a chemical reaction, H_f is the enthalpy of the products. H_i is the initial enthalpy of the system, expressed in joules. In a chemical reaction, H_i is the enthalpy of the reactants.

For an exothermic reaction (a reaction which liberates heat) at constant pressure, the system's change in enthalpy equals the energy released in the reaction, including

the energy retained in the system and lost through expansion against its surroundings. In a similar manner, for an endothermic reaction (a reaction which absorbs heat), the system's change in enthalpy is equal to the energy absorbed in the reaction, including the energy lost by the system and gained from compression from its surroundings. A relatively easy way to determine whether or not a reaction is exothermic or endothermic is to determine the sign of ΔH. If ΔH is *positive*, the reaction is *endothermic*, that is, heat is absorbed by the system because the products of the reaction have a greater enthalpy than that of the reactants. On the other hand, if ΔH is *negative*, the reaction is *exothermic*, that is, the overall decrease in enthalpy is achieved by the generation of heat.

Although enthalpy is commonly used in engineering and science, it is impossible to measure directly, as enthalpy has no datum (reference point). Therefore, enthalpy can only accurately be used in a closed system. However, few real-world applications exist in closed isolation, and it is for this reason that two or more closed systems cannot be compared using enthalpy as a basis, although sometimes this is done erroneously.

A thorough understanding of the gas dynamic theory of perfect gases will be of great value in understanding the physics and the application aspects of high- enthalpy flows. To enjoy this advantage, let us briefly revise the gas dynamics of perfect gases in this chapter.

1.3 Gas Dynamics of Perfect Gases

Gas dynamics is the science of fluid flow in which both density and temperature changes become significant [5]. Taking 5% change in temperature as significant, it can be stated that, at standard sea level, Mach number 0.5 is the lower limit of gas dynamics. Thus, gas dynamics is the flow field with speeds Mach 0.5 and above. Therefore, gas dynamic regime consists of both subsonic and supersonic Mach numbers. Further, when the flow is supersonic, any change of flow property or direction is taking place only through waves prevailing in the flow field. That is, supersonic flows are essentially wave-dominated flows. The waves prevailing in supersonic flow fields can be grouped as *compression waves*, *expansion waves*, and *Mach waves*. The compression and expansion waves cause *finite changes* in the flow properties, but the changes caused by a Mach wave is *insignificant*. A Mach wave is the weakest isentropic wave. The compression wave, also called as the *shock* may be regarded as isentropic and non-isentropic, depending on its strength. Similarly, even though individual expansion rays are isentropic, their combination may become non-isentropic. For example, in a centered expansion fan, at the vertex of the fan, the expansion caused becomes non-isentropic.

The essence of gas dynamics is that when the flow speed is supersonic, the entire flow field is dominated by Mach waves, expansion waves, and compression or shock waves. It is only through these waves that the change of flow properties from one state to another takes place.

Example 1.1 What will be the speed of sound in air at standard sea level state?

Solution

The temperature of air at sea level state is 15°C.
The speed of sound in a perfect gas, in terms of temperature, is

$$a = \sqrt{\gamma RT}$$

where γ is the ratio of specific heats, R is the gas constant, and T is the temperature.
For air, $\gamma = 1.4$ and $R = 287\ \text{m}^2/(\text{s}^2\ \text{K})$.
Therefore, at $T = 15 + 273.15 = 288.15$ K, the speed of sound becomes

$$\begin{aligned} a &= \sqrt{1.4 \times 287 \times 288.15} \\ &= \boxed{340.26\ \text{m/s}} \end{aligned}$$

■

1.4 Compressible Flow

Compressible flow is the science of fluid flow in which the density change associated with pressure change is appreciable. Fluid mechanics is the science of fluid flow in which the temperature change associated with the flow is insignificant. *Fluid mechanics* is essentially the science of *isenthalpic* flows, and thus the main equations governing a fluid dynamic stream are only the continuity and momentum equations and the second law of thermodynamics. The energy equation is *passive* as far as fluid dynamic streams are concerned. At standard sea level conditions, considering less than 5% change in temperature as insignificant, flow with Mach number less than 0.5 can be termed as a fluid mechanics stream. A fluid mechanics stream may be compressible or incompressible. For an incompressible flow, both temperature and density changes are insignificant. For a compressible fluid dynamic stream, the temperature change may be insignificant but density change is finite.

But in many engineering applications, such as design of airplane, missiles, and launch vehicles, the flow Mach numbers associated are more than 0.5. Hence, both temperature and density changes associated with the flow become significant. Study of such flows where both density and temperature changes associated with pressure change become appreciable is called *gas dynamics*. In other words, gas dynamics is the science of fluid flow in which both density and temperature changes become significant. A gas dynamic flow is that in which the entire flow field is dominated by Mach waves, expansion waves, and shock waves when the flow speed is supersonic. Only through these waves, the change of flow properties from one state to another takes place. In the theory of gas dynamics, change of state or flow properties is achieved by the following three means.

1. With area change, treating the fluid to be inviscid and passage to be frictionless.
2. With friction, treating the heat transfer between the surrounding and system to be negligible.
3. With heat transfer, assuming the fluid to be inviscid.

These three types of flows are called the *isentropic flow*, in which the area change is the primary parameter causing the change of state; the *frictional* or *Fanno flow*, in which the friction is the primary parameter causing the change of state; and the *Rayleigh flow*, in which the change in the stagnation (total) temperature (that is, heat addition or heat removal) is the primary parameter causing the change of state.

All problems in gas dynamics can be classified under the three flow processes described above, of course with the assumptions mentioned. Although it is impossible to have a flow process that is purely isentropic or Fanno type or Rayleigh type, in practice, it is justified in assuming so, because the results obtained with these treatments prove to be accurate enough for most practical problems in gas dynamics.

1.5 Compressibility

Fluids such as water are incompressible at normal conditions. But at very high pressures (for example, 1000 atm), they are compressible. The change in volume is the characteristic feature of a compressible medium under static condition. Under dynamic conditions, that is, when the medium is moving, the characteristic feature for incompressible and compressible flow situations are the volume flow rate, $\dot{Q} = AV =$ constant at any cross section of a streamtube for incompressible flow, and the mass flow rate, $\dot{m} = \rho AV =$ constant at any cross section of a streamtube for compressible flow. In these relations, A is the cross-sectional area of the streamtube, V and ρ are, respectively, the velocity and the density of the flow at that Cross section, as illustrated in Figure 1.1.

In general, the flow of an incompressible medium is called *incompressible flow* and that of a compressible medium is called *compressible flow*. Although this statement is true for incompressible media at normal conditions of pressure and temperature, for compressible medium such as gases, it has to be modified. As long as a gas flows at a sufficiently low speed from one cross section to another of a passage, the change in volume (or density) can be neglected and, therefore, the flow can be treated as incompressible. Although the fluid (gas) is compressible, the compressibility effects may be neglected when the flow is taking place at low speeds. In other words, although there is some density change associated with every physical flow, it is often possible (for low-speed flows) to neglect it and idealize the flow as incompressible. This approximation is applicable to many practical flow situations, such as low-speed flow around an airplane during take-off and landing and flow through a vacuum cleaner.

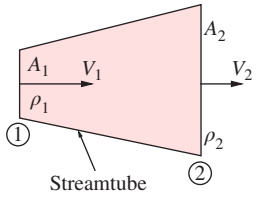

Figure 1.1 Elemental streamtube.

From the above discussion, it is clear that *compressibility is the phenomenon by virtue of which the flow changes its density with change in speed*. Now, we may question what are the precise conditions under which density changes must be considered? We will try to answer this question now.

A quantitative measure of compressibility is the *volume modulus of elasticity*, E, defined as

$$\Delta p = -E \frac{\Delta \mathbb{V}}{\mathbb{V}_i} \tag{1.2}$$

where Δp is the change in static pressure, $\Delta \mathbb{V}$ is the change in volume, and $\mathbb{V}_i$ is the initial volume. For ideal gases, the equation of state is

$$p\mathbb{V} = RT$$

For isothermal flows, this reduces to

$$p\mathbb{V} = p_i \mathbb{V}_i = \text{constant}$$

where p_i is the initial pressure.

The above equation may be written as

$$(p_i + \Delta p)(\mathbb{V}_i + \Delta \mathbb{V}) = p_i \mathbb{V}_i$$

Expanding this equation and neglecting the second-order terms, we get

$$\Delta p \ \mathbb{V}_i + \Delta \mathbb{V} \ p_i = 0$$

Therefore,

$$\Delta p = -p_i \frac{\Delta \mathbb{V}}{\mathbb{V}_i} \tag{1.3}$$

For gases, from Equations (1.2) and (1.3), we get

$$E = p_i \tag{1.4}$$

Hence, by Equation (1.3), the compressibility may be defined as the volume modulus of the pressure.

1.5.1 Limiting Conditions for Compressibility

By mass conservation, we have the mass flow rate per unit area as $\dot{m} = \rho V = \text{constant}$, where $\dot{m}$ is the mass flow rate per unit area, V is the flow velocity, and ρ is the corresponding density. This can also be written as

$$(V_i + \Delta V)(\rho_i + \Delta \rho) = \rho_i \ V_i$$

Considering only the first-order terms, this simplifies to

$$\frac{\Delta \rho}{\rho_i} = -\frac{\Delta V}{V_i}$$

Substituting this into Equation (1.2) and noting that $V = \mathbb{V}$ (that is, the flow velocity is equal to the volume) for unit area per unit time in the present case, we get

$$\Delta p = E \frac{\Delta \rho}{\rho_i} \tag{1.5}$$

From Equation (1.5), it is seen that the compressibility may also be defined as the density modulus of the pressure.

For incompressible flows, by Bernoulli's equation, we have

$$p + \frac{1}{2} \rho V^2 = \text{constant} = p_{\text{stag}}$$

where the subscript "stag" refers to stagnation condition. The above equation may also be written as

$$p_{\text{stag}} - p = \Delta p = \frac{1}{2} \rho V^2$$

that is, the change in pressure is equal to $\frac{1}{2} \rho V^2$. Using Equation (1.5) in the above relation, we obtain

$$\frac{\Delta p}{E} = \frac{\Delta \rho}{\rho_i} = \frac{\rho_i V_i^2}{2E} = \frac{q_i}{E} \tag{1.6}$$

where $q_i = \frac{1}{2} \rho_i V_i^2$ is the dynamic pressure. Equation (1.6) relates the density change with flow speed.

The compressibility effects can be neglected if the density changes are very small, that is, if

$$\frac{\Delta \rho}{\rho_i} \ll 1$$

From Equation (1.6), it is seen that for neglecting compressibility,

$$\frac{q}{E} \ll 1$$

For gases, the speed of sound "a" may be expressed in terms of pressure and density changes as [see Equation (1.11)]

$$a^2 = \frac{\Delta p}{\Delta \rho}$$

Using Equation (1.5) in the above relation, we get

$$a^2 = \frac{E}{\rho_i}$$

With this, Equation (1.6) reduces to

$$\begin{aligned} \frac{\Delta \rho}{\rho_i} &= \frac{q_i}{E} \\ &= \frac{1}{2} \frac{V^2}{E/\rho_i} \\ &= \frac{\rho_i}{2} \frac{V_i^2}{E} \end{aligned}$$

But $E/\rho_i = a^2$; therefore,

$$\frac{\Delta\rho}{\rho_i} = \frac{1}{2}\left(\frac{V}{a}\right)^2 \tag{1.7}$$

In the above equation, the subscript i for the velocity and the speed of sound are dropped to generalize the relation. The ratio V/a is called the *Mach number* M. Therefore, the condition of incompressibility for gases becomes

$$\frac{M^2}{2} \ll 1$$

Thus, the criterion determining the effect of compressibility for gases is the magnitude of M.

It is widely accepted that compressibility can be neglected when

$$\frac{\Delta\rho}{\rho_i} \leq 0.05$$

That is, when $M \leq 0.3$. In other words, the flow may be treated as incompressible when $V \leq 100$ m/s, that is, when $V \leq 360$ kmph under standard sea level conditions. The above values of M and V are widely accepted values, and they may be refixed at different levels, depending on the flow situation and the degree of accuracy desired.

Example 1.2 Air at 1.2 atm and 270 K is accelerated isothermally to a state at which the pressure is 0.8 atm. What is the speed of sound associated with this process?

Solution

Let subscripts 1 and 2 refer to the initial and final states, respectively. Given, $p_1 = 1.2$ atm, $p_2 = 0.8$ atm, and $T_1 = T_2 = 270$ K. Therefore, the corresponding densities are

$$\begin{aligned}
\rho_1 &= \frac{p_1}{RT_1} \\
&= \frac{1.2 \times 101{,}325}{287 \times 270} \\
&= 1.569 \text{ kg/m}^3 \\
\rho_2 &= \frac{p_2}{RT_2} \\
&= \frac{0.8 \times 101{,}325}{287 \times 270} \\
&= 1.046 \text{ kg/m}^3
\end{aligned}$$

Thus we have

$$\begin{aligned}\Delta\rho &= \rho_2 - \rho_1\\ &= 1.046 - 1.569\\ &= -0.523 \text{ kg/m}^3\\ \Delta p &= p_2 - p_1\\ &= 0.8 - 1.2\\ &= -0.4 \text{ atm}\\ &= -0.4 \times 101{,}325\\ &= -40{,}530 \text{ Pa}\end{aligned}$$

The speed of sound is

$$\begin{aligned}a &= \sqrt{\frac{\Delta p}{\Delta\rho}}\\ &= \sqrt{\frac{-40{,}530}{-0.523}}\\ &= \boxed{278.38 \text{ m/s}}\end{aligned}$$

■

1.6 Supersonic Flow

The Mach number M is defined as the ratio of the local flow speed V to the local speed of sound a

$$\boxed{M = \frac{V}{a}} \tag{1.8}$$

Thus M is a dimensionless quantity. In general, both V and a are functions of position and time. Therefore, Mach number is not just the flow speed made nondimensional by dividing by a constant. That is, we cannot write $M \propto V$. However, it is almost always true that M increases monotonically with V.

A flow with Mach number greater than unity is termed *supersonic flow*. In a supersonic flow, $V > a$ and the flow upstream of a given point remains unaffected by changes in conditions at that point.

1.7 Speed of Sound

Sound waves are infinitely small pressure disturbances. The speed with which sound propagates in a medium is called *speed of sound* and is denoted by a. If an infinitesimal

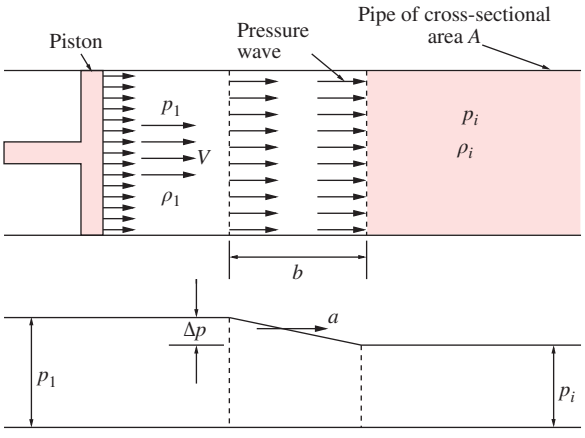

Figure 1.2 Propagation of pressure disturbance.

disturbance is created by the piston, as shown in Figure 1.2, the wave propagates through the gas at the velocity of sound relative to the gas into which the disturbance is moving. Let the stationary gas at pressure p_i and density ρ_i in the pipe be set in motion by moving the piston. The infinitesimal pressure wave created by piston movement travels with speed a, leaving the medium behind it at pressure p_1 and density ρ_1 to move with velocity V.

As a result of compression created by the piston, the pressure and the density next to the piston are infinitesimally greater than those of the gas at rest ahead of the wave. Therefore,

$$\Delta p = p_1 - p_i$$
$$\Delta \rho = \rho_1 - \rho_i$$

where the pressure change Δp and the density change $\Delta \rho$ are small.

Choose a control volume of length b, as shown in Figure 1.2. Compression of volume Ab causes the density to rise from ρ_i to ρ_1 in time $t = b/a$. The mass flow into volume Ab is

$$\dot{m} = \rho_1 AV \tag{1.9}$$

For mass conservation, $\dot{m}$ must also be equal to the mass flow rate $A\, b(\rho_1 - \rho_i)/t$ through the control volume. Thus,

$$\frac{Ab(\rho_1 - \rho_i)}{t} = \rho_1 AV$$

or

$$a(\rho_1 - \rho_i) = \rho_1 V \tag{1.10}$$

because $b/t = a$.

The compression wave caused by the piston motion travels and accelerates the gas from zero velocity to V. The acceleration is given by

$$\frac{V}{t} = V\,\frac{a}{b}$$

The mass in the control volume Ab is

$$m = Ab\overline{\rho}$$

where

$$\overline{\rho} = \frac{\rho_i + \rho_1}{2}$$

The force acting on the control volume is

$$F = A(p_1 - p_i)$$

Therefore, by Newton's law,

$$A(p_1 - p_i) = m\left(V\frac{a}{b}\right)$$

$$A(p_1 - p_i) = (Ab\overline{\rho})\left(V\frac{a}{b}\right)$$

or

$$\overline{\rho}Va = p_1 - p_i \tag{1.11}$$

Because the disturbance is very weak, ρ_1 on the right-hand side of Equation (1.10) may be replaced by $\overline{\rho}$ to result in

$$a(\rho_1 - \rho_i) = \overline{\rho}V$$

Using this relation, Equation (1.11) can be written as

$$a^2 = \frac{p_1 - p_i}{\rho_1 - \rho_i}$$

$$= \frac{\Delta p}{\Delta \rho}$$

In the limiting case of Δp and $\Delta \rho$ approaching zero, the above equation leads to

$$\boxed{a^2 = \frac{dp}{d\rho}} \tag{1.12}$$

This is Laplace equation and is valid for any fluid.

The sound wave is a weak compression wave, across which only infinitesimal change in fluid properties occur. Further, the wave itself is extremely thin, and changes

in properties occur very rapidly. The rapidity of the process rules out the possibility of any heat transfer between the system of fluid particles and its surrounding.

For very strong pressure waves, the traveling speed of disturbance may be greater than that of sound. The pressure can be expressed as

$$p = p(\rho) \tag{1.13}$$

For isentropic process of a gas,

$$\frac{p}{\rho^{\gamma}} = \text{constant}$$

where the isentropic index γ is the ratio of specific heats and is a constant for a perfect gas. Using the above relation in Equation (1.12), we get

$$a^2 = \frac{\gamma p}{\rho} \tag{1.14}$$

For a perfect gas, by the state equation,

$$p = \rho RT \tag{1.15}$$

where R is the gas constant and T the static temperature of the gas in absolute units.

Equations (1.14) and (1.15) together lead to the following expression for the speed of sound.

$$\boxed{a = \sqrt{\gamma RT}} \tag{1.16}$$

Perfect gas assumption is valid as long as the speed of gas stream is not too high. However, at hypersonic speeds, the assumption of perfect gas is not valid and we must consider Equation (1.12) to calculate the speed of sound.

Example 1.3 Calculate the speed of sound in oxygen gas at sea level state.

Solution

The temperature at sea level is 15°C, thus

$$\begin{aligned} T &= 15 + 273.15 \\ &= 288.15 \text{ K} \end{aligned}$$

For oxygen gas, molecular weight is $M = 32$. Therefore, the gas constant is

$$R = \frac{R_u}{M}$$

where $R_u = 8314$ J/(kg K) is the universal gas constant. Thus

$$\begin{aligned} R &= \frac{8314}{32} \\ &= 259.81 \text{ m}^2/(\text{s}^2 \text{ K}) \end{aligned}$$

At 288.15 K, oxygen is a perfect gas with $\gamma = 1.4$, Therefore, by Equation (1.16), the speed of sound is

$$\begin{aligned} a &= \sqrt{\gamma RT} \\ &= \sqrt{1.4 \times 259.81 \times 288.15} \\ &= \boxed{323.74 \text{ m/s}} \end{aligned}$$

■

1.8 Temperature Rise

For a perfect gas, the thermal state equation is

$$p = \rho RT$$

The gas constant R can be expressed as

$$R = c_p - c_v$$

where c_p and c_v are specific heats at constant pressure and constant volume, respectively. Also, $\gamma = c_p/c_v$; therefore,

$$R = \frac{\gamma - 1}{\gamma} c_p \tag{1.17}$$

For an isentropic change of state, an equation not involving T can be written as

$$\frac{p}{\rho^\gamma} = \text{constant}$$

Now, between state 1 and any other state, the relation between the pressure and densities can be written as

$$\left(\frac{p}{p_1}\right) = \left(\frac{\rho}{\rho_1}\right)^\gamma \tag{1.18}$$

Combining Equations (1.18) and (1.15), we get

$$\frac{T}{T_1} = \left(\frac{\rho}{\rho_1}\right)^{\gamma-1} = \left(\frac{p}{p_1}\right)^{(\gamma-1)/\gamma} \tag{1.19}$$

The above relations are very useful for gas dynamic studies. The temperature, density, and pressure ratios in Equation (1.19) can be expressed in terms of the flow Mach number.

Let us examine the flow around a symmetrical body, as shown in Figure 1.3.

In a compressible medium, there will be change in density and temperature at the stagnation point 0. The temperature rise at the stagnation point can be obtained from the energy equation.

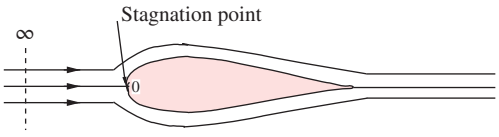

Figure 1.3 Flow around a symmetrical body.

The energy equation for an isentropic flow is

$$h + \frac{V^2}{2} = \text{constant} \tag{1.20}$$

where h is the enthalpy and V is the flow velocity.

Equating the energy at far upstream, ∞, and the stagnation point 0, we get

$$h_\infty + \frac{V_\infty^2}{2} = h_0 + \frac{V_0^2}{2}$$

But $V_0 = 0$, thus

$$h_0 - h = \frac{V_\infty^2}{2}$$

For a perfect gas, $h = c_p T$; therefore, from the above relation, we obtain

$$c_p(T_0 - T_\infty) = \frac{V_\infty^2}{2}$$

that is,

$$\Delta T = T_0 - T_\infty = \frac{V_\infty^2}{2c_p} \tag{1.21}$$

Combining Equations (1.16) and (1.17), we get

$$c_p = \frac{1}{\gamma - 1}\,\frac{a_\infty^2}{T_\infty}$$

Hence,

$$\Delta T = \frac{\gamma - 1}{2}\,T_\infty M_\infty^2 \tag{1.22}$$

that is,

$$T_0 - T_\infty = \frac{\gamma - 1}{2}\,T_\infty M_\infty^2$$

This simplifies to

$$\boxed{T_0 = T_\infty \left(1 + \frac{\gamma - 1}{2}\,M_\infty^2\right)} \tag{1.23}$$

For air, $\gamma = 1.4$, and hence,

$$T_0 = T_\infty(1 + 0.2M_\infty^2) \tag{1.24}$$

where T_0 is the temperature at the stagnation point on the body. It is also referred to as *total temperature*, for example, at the stagnation point 0 on the body shown in Figure 1.3, the flow will attain the stagnation temperature.

1.9 Mach Angle

The presence of a small disturbance is felt throughout the field by means of disturbance waves traveling at the local velocity of sound relative to the medium. Let us examine the propagation of pressure disturbance created by a moving object shown in Figure 1.4. The propagation of disturbance waves created by an object moving with velocity $V = 0$, $V = a/2$, $V = a$, and $V > a$ is shown in Figure 1.4(a), (b), (c), and (d), respectively. In a subsonic flow, the disturbance waves reach a stationary observer before the source of disturbance could reach him, as shown in Figure 1.4(a) and (b). But in supersonic flows, it takes considerable amount of time for an observer to perceive the pressure disturbance, after the source has passed him. This is one of the fundamental differences between subsonic and supersonic flows. Therefore, in a subsonic flow, the streamlines sense the presence of any obstacle in the flow field and adjust themselves well ahead of the obstacles and flow around it smoothly.

But in a supersonic flow, the streamlines feel the obstacle only when they hit it. The obstacle acts as a source, and the streamlines deviate at the Mach cone as shown in Figure 1.4(d). That is in a supersonic flow the disturbance due to an obstacle is sudden and the flow behind the obstacle has to change abruptly.

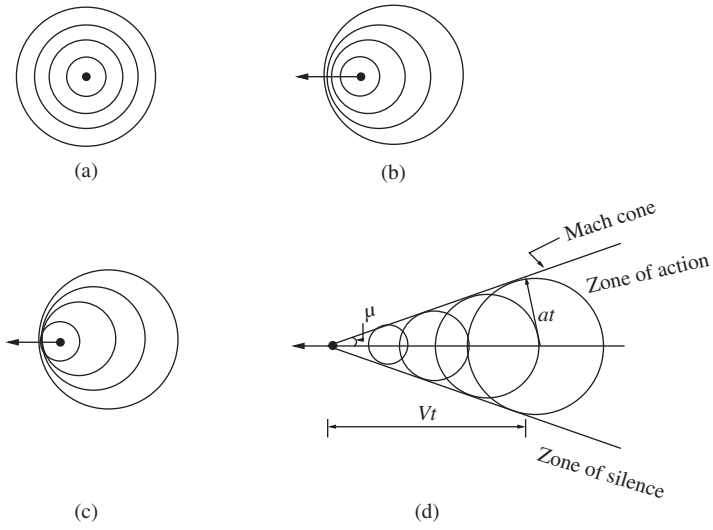

Figure 1.4 Propagation of disturbance waves. (a) $V = 0$, (b) $V = a/2$, (c) $V = a$, and (d) $V > a$.

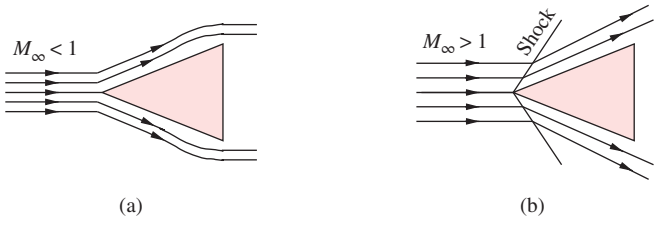

Figure 1.5 Flow around a wedge. (a) Subsonic flow and (b) supersonic flow.

Flow around a wedge, shown in Figure 1.5(a) and (b), illustrates the smooth and abrupt change in flow direction for subsonic and supersonic flow, respectively.

For $M_\infty < 1$, the flow direction changes smoothly and the pressure decreases with acceleration. For $M_\infty > 1$, there is a sudden change in flow direction at the body and the pressure increases downstream of the shock.

In Figure 1.4(d), it is shown that for supersonic motion of an object, there is a well-defined conical zone in the flow field with the object located at the nose of the cone, and the disturbance created by the moving object is confined only to the field included inside the cone. The flow field zone outside the cone does not even feel the disturbance. For this reason, von Karman termed the region inside the cone as the *zone of action* and the region outside the cone as the *zone of silence*. The lines at which the pressure disturbance is concentrated and that generate the cone are called *Mach waves* or *Mach lines*. The angle between the Mach line and the direction of motion of the body is called the *Mach angle* μ. From Figure 1.4(d), we have

$$\sin \mu = \frac{at}{Vt} = \frac{a}{V}$$

that is,

$$\boxed{\sin \mu = \frac{1}{M}} \tag{1.25}$$

From propagation of disturbance waves shown in Figure 1.4, we can infer the following features of the flow regimes.

- When the medium is *incompressible* ($M = 0$, Figure 1.4(a)) or when the speed of the moving disturbance is negligibly small compared to the local sound speed, the pressure pulse created by the disturbance spreads uniformly in all directions.
- When the disturbance source moves with a *subsonic speed* ($M < 1$, Figure 1.4(b)), the pressure disturbance is felt in all directions and at all points in space (neglecting viscous dissipation), but the pressure pattern is no longer symmetrical.
- For *sonic velocity* ($M = 1$, Figure 1.4(c)) the pressure pulse is at the boundary between subsonic and supersonic flow and the wavefront is a plane.
- For *supersonic speeds* ($M > 1$, Figure 1.4(d)), the disturbance wave propagation phenomenon is totally different from that at subsonic speeds. All the pressure disturbances are included in a cone that has the disturbance source at its apex, and the effect of the disturbance is not felt upstream of the disturbance source.

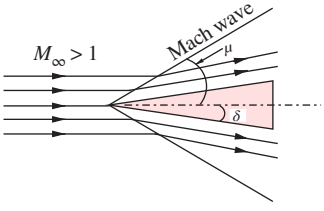

Figure 1.6 Mach cone.

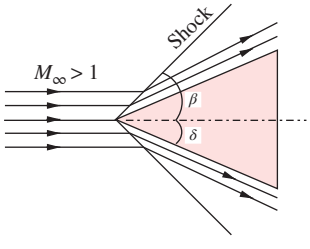

Figure 1.7 Shock wave.

1.9.1 Small Disturbance

When the apex angle of wedge δ is vanishingly small, the disturbances will be small, and we can consider these disturbance waves to be identical to sound pulses. In such a case, the deviation of streamlines will be small and there will be infinitesimally small increase of pressure across the Mach cone as shown in Figure 1.6.

1.9.2 Finite Disturbance

When the wedge angle δ is finite, the disturbances introduced are finite and then the wave is not called Mach wave but a shock or shock wave (see Figure 1.7). The angle of shock β is always smaller than the Mach angle. The deviation of the streamlines is finite and the pressure increase across a shock wave is finite.

1.10 Summary

High enthalpy flows are those with their specific heats ratio as a function of temperature. The word enthalpy is based on the Greek word enthalpein, which means to put heat into.

The enthalpy, H, of a homogeneous system is defined as

$$\boxed{H = U + p\mathbb{V}}$$

where U, p, and $\mathbb{V}$, respectively, are the internal energy, pressure, and volume of the system. The enthalpy is an *extensive property*.

For an inhomogeneous system, the enthalpy is the sum of the enthalpies of the subsystems composing the system.

$$H = \sum_k H_k$$

where the label k refers to the various subsystems. In a system with continuously varying p, T, and/or composition, the summation becomes an integral:

$$H = \int \rho \, h \, d\mathbb{V}$$

where ρ is the density.

The enthalpy can be expressed as

$$dH(S, p) = TdS + \mathbb{V}dp$$

This expression of dH in terms of entropy and pressure may be unfamiliar to many readers. However, there are expressions in terms of more familiar variables such as temperature and pressure [4]

$$dH = c_p \, dT + \mathbb{V}(1 - \alpha T) \, dp$$

where c_p is the heat capacity at constant pressure (that is, specific heat at constant pressure) and α is the *coefficient of (cubic) thermal expansion*

$$\alpha = \frac{1}{\mathbb{V}} \left(\frac{\partial \mathbb{V}}{\partial T} \right)_p$$

With this expression, one can, in principle, determine the enthalpy if c_p and $\mathbb{V}$ are known as functions of p and T.

The internal energy U can be interpreted as the energy required to create a system, and the $p\mathbb{V}$ term as the energy that would be required to "make room" for the system if the pressure of the environment remained constant. Enthalpy is the *working horse* of engineering thermodynamics.

The first law of thermodynamics for a closed system

$$dU = \delta Q - \delta W$$

But

$$\delta W = p \, d\mathbb{V} + \delta W'$$

Thus the first law becomes

$$dU = \delta Q - p \, d\mathbb{V} - \delta W'$$

Using this, Equation (1.1) can be expressed as

$$dH = \delta Q + \mathbb{V}dp - \delta W'$$

From this relation, we see that the increase in enthalpy of a system is equal to the added heat

$$dH = \delta Q$$

provided that the system is under constant pressure ($dp = 0$) and that the only work done by the system is expansion work ($\delta W' = 0$).

For systems at constant pressure, the change in enthalpy is the heat received by the system.

The total enthalpy of a system *cannot* be measured directly; the enthalpy change of a system is measured instead. Enthalpy change is defined by the following equation:

$$\Delta H = H_f - H_i$$

where ΔH is the "enthalpy change" and H_f is the final enthalpy of the system, expressed in joules. In a chemical reaction, H_f is the enthalpy of the products. H_i is the initial enthalpy of the system, expressed in joules. In a chemical reaction, H_i is the enthalpy of the reactants.

Although enthalpy is commonly used in engineering and science, it is impossible to measure directly, as enthalpy has no datum (reference point).

Gas dynamics is the science of fluid flow in which both density and temperature changes become significant. Gas dynamics is the flow field with speeds Mach 0.5 and above. Therefore, gas dynamic regime consists of both subsonic and supersonic Mach numbers.

The waves prevailing in supersonic flow fields can be grouped as *compression waves*, *expansion waves*, and *Mach waves*.

The essence of gas dynamics is that when the flow speed is supersonic, the entire flow field is dominated by Mach waves, expansion waves, and compression or shock waves. It is only through these waves, the change of flow properties from one state to another takes place.

Compressible flow is the science of fluid flow in which the density change associated with pressure change is appreciable. Fluid mechanics is the science of fluid flow in which the temperature change associated with the flow is insignificant. *Fluid mechanics* is essentially the science of *isenthalpic* flows, and thus the main equations governing a fluid dynamic stream are only the continuity and momentum equations and the second law of thermodynamics. The energy equation is *passive* as far as fluid dynamic streams are concerned.

In the theory of gas dynamics, change of state or flow properties is achieved by the following three means.

1. With area change, treating the fluid to be inviscid and passage to be frictionless.

2. With friction, treating the heat transfer between the surrounding and system to be negligible.
3. With heat transfer, assuming the fluid to be inviscid.

These three types of flows are called *isentropic flow*, in which the area change is the primary parameter causing change of state; *frictional* or *Fanno flow*, in which the friction is the primary parameter causing change of state; and *Rayleigh flow*, in which the change in the stagnation (total) temperature (that is, heat addition or heat removal) is the primary parameter causing change of state.

Fluids such as water are incompressible at normal conditions. But at very high pressures (for example, 1000 atm), they are compressible. The change in volume is the characteristic feature of a compressible medium under static condition. Under dynamic conditions, that is, when the medium is moving, the characteristic feature for incompressible and compressible flow situations are the volume flow rate, $\dot{Q} = AV =$ constant at any cross section of a streamtube for incompressible flow, and the mass flow rate, $\dot{m} = \rho AV =$ constant at any cross section of a streamtube for compressible flow.

In general, the flow of an incompressible medium is called *incompressible flow* and that of a compressible medium is called *compressible flow*.

A quantitative measure of compressibility is the *volume modulus of elasticity*, E, defined as

$$\Delta p = -E \frac{\Delta \mathbb{V}}{\mathbb{V}_i}$$

For ideal gases, the equation of state is

$$p\mathbb{V} = RT$$

For isothermal flows, this reduces to

$$p\mathbb{V} = p_i \mathbb{V}_i = \text{constant}$$

For incompressible flows, by Bernoulli's equation, we have

$$p + \frac{1}{2}\,\rho\, V^2 = \text{constant} = p_{\text{stag}}$$

where the subscript "stag" refers to stagnation condition.

The compressibility effects can be neglected if the density changes are very small, that is, if

$$\frac{\Delta \rho}{\rho_i} \ll 1$$

For gases, the speed of sound "a" may be expressed in terms of pressure and density changes as

$$a^2 = \frac{\Delta p}{\Delta \rho}$$

The ratio V/a is called the *Mach number* M. The condition of incompressibility for gases is

$$\frac{M^2}{2} \ll 1$$

Thus, the criterion determining the effect of compressibility for gases is the magnitude of M.

It is widely accepted that compressibility can be neglected when

$$\frac{\Delta\rho}{\rho_i} \leq 0.05$$

That is, when $M \leq 0.3$.

The Mach number M is defined as the ratio of the local flow speed V to the local speed of sound a

$$\boxed{M = \frac{V}{a}}$$

Thus M is a dimensionless quantity.

A flow with Mach number greater than unity is termed *supersonic flow*. In a supersonic flow, $V > a$ and the flow upstream of a given point remains unaffected by changes in conditions at that point.

Sound waves are infinitely small pressure disturbances. The speed with which sound propagates in a medium is called *speed of sound* and is denoted by a.

In the limiting case of Δp and $\Delta\rho$ approaching zero, the speed of sound becomes

$$\boxed{a^2 = \frac{dp}{d\rho}}$$

This is Laplace equation and is valid for any fluid.

The sound wave is a weak compression wave, across which only infinitesimal change in fluid properties occur.

For isentropic process of a gas,

$$\frac{p}{\rho^\gamma} = \text{constant}$$

where the isentropic index γ is the ratio of specific heats and is a constant for a perfect gas.

For a perfect gas, by the state equation,

$$p = \rho RT$$

For a perfect gas, the speed of sound can be expressed as

$$\boxed{a = \sqrt{\gamma RT}}$$

Perfect gas assumption is valid as long as the speed of gas stream is not too high. However, at hypersonic speeds, the assumption of perfect gas is not valid and we must consider Equation (1.12) to calculate the speed of sound.

For a perfect gas, the gas constant R can be expressed as

$$R = c_p - c_v$$

For an isentropic change of state, an equation not involving T can be written as

$$\frac{p}{\rho^{\gamma}} = \text{constant}$$

In a compressible medium, there will be change in density and temperature at the stagnation point 0. The temperature rise at the stagnation point can be obtained from the energy equation.

The energy equation for an isentropic flow is

$$h + \frac{V^2}{2} = \text{constant}$$

where h is the enthalpy and V is the flow velocity.

Equating the energy at far upstream, ∞, and the stagnation point 0, we get

$$h_{\infty} + \frac{V_{\infty}^2}{2} = h_0 + \frac{V_0^2}{2}$$

But $V_0 = 0$, thus

$$h_0 - h = \frac{V_{\infty}^2}{2}$$

The presence of a small disturbance is felt throughout the field by means of disturbance waves traveling at the local velocity of sound relative to the medium. In a subsonic flow, the disturbance waves reach a stationary observer before the source of disturbance could reach him. But in supersonic flows, it takes considerable amount of time for an observer to perceive the pressure disturbance, after the source has passed him. Therefore, in a subsonic flow, the streamlines sense the presence of any obstacle in the flow field and adjust themselves well ahead of the obstacles and flow around it smoothly.

For supersonic motion of an object, there is a well-defined conical zone in the flow field with the object located at the nose of the cone, and the disturbance created by the moving object is confined only to the field included inside the cone. The flow field zone outside the cone does not even feel the disturbance. For this reason, von Karman termed the region inside the cone as the *zone of action* and the region outside the cone as the *zone of silence*. The lines at which the pressure disturbance is concentrated and which generate the cone are called *Mach waves* or *Mach lines*. The angle between the Mach line and the direction of motion of the body is called the *Mach angle* μ.

Exercise Problems

1.1 Find the limiting flow speed above which air flow becomes a gas dynamic flow at sea level condition.
[Answer: 612.47 km/h]

1.2 Air is accelerated from 1 atm and 300 K to 0.2 atm. If the speed of sound associated with the acceleration process is 400 m/s, (a) determine the final temperature. (b) Is this process isentropic?
[Answer: (a) 105.325 K, (b) No.]

1.3 Methane gas at 140 kPa is compressed isothermally, and nitrogen gas at 100 kPa is compressed isentropically. What is the modulus of elasticity of each gas? Which is more compressible?
[Answer: $E = 140$ kPa, for both, and both are equally compressible.]

1.4 If the enthalpy of an air stream at 270 K becomes 10 times its value when the flow is isentropically brought to rest, determine the flow Mach number. Treat air as perfect gas even at the stagnation state.
[Answer: 6.708]

1.5 Determine the maximum Mach number up to which the flow over an object flying at sea level can be treated as perfect gas flow.
[Answer: 2.98]

1.6 A balloon filled with gas expands its volume by 2.0 L. If the pressure outside the balloon is 0.93 bar and the energy change of the gas is 450 J, how much heat did the surroundings give the balloon? [Hint: 100 J = 1 liter bar].
[Answer: 636 J]

1.7 A heater that operates at 4 V and at 35 ohms is used to heat up 15 g of copper wire. The specific heat capacity of copper is 24.440 J/(mol K). How much time is required to increase the temperature from 25 to 69°C? [Hint: power: $P = V^2/R$, which is derived from the equation $V = IR$].
[Answer: 555.47 s]

References

[1] Henderson D., *Physical Chemistry: An Advanced Treatise*, Vol. 2, Academic Press, New York, 1967, p. 29.
[2] Laidler K., *The World of Physical Chemistry*, Oxford University Press, 1995, p. 110.
[3] Guggenheim E. A., *Thermodynamics*, North-Holland Publishing Company, Amsterdam, 1959.
[4] Moran M. J., and Shapiro H. N., *Fundamentals of Engineering Thermodynamics*, 5th ed. John Wiley & Sons, Inc., 2006, p. 511.
[5] Rathakrishnan E., *Applied Gas Dynamics*, John Wiley & Sons, Inc., Hoboken, NJ, 2010.

2

Thermodynamics of Fluid Flow

2.1 Introduction

Entropy and temperature are the two fundamental concepts of thermodynamics. Unlike low-speed or incompressible flows, the energy change associated with a compressible flow is substantial enough to strongly interact with other properties of the flow. Hence, the energy concept plays an important role in the study of compressible flows. In other words, the study of thermodynamics which deals with energy (and entropy) is an essential component in the study of compressible flow.

The following are the broad divisions of fluid flow based on thermodynamic considerations.

1. *Fluid mechanics of perfect fluids* – fluids without viscosity and heat (transfer) conductivity – is an extension of equilibrium thermodynamics to moving fluids. The kinetic energy of the fluid has to be considered in addition to the internal energy which the fluid possesses even when at rest.
2. *Fluid mechanics of real fluids* (goes beyond the scope of classical thermodynamics). The transport processes of momentum and heat (energy) are of primary interest here. But, even though thermodynamics is not fully and directly applicable to all phases of real fluid flow, it is often extremely helpful in relating the initial and final conditions.

For low-speed flow (flow with Mach number less than 0.5) problems, thermodynamic considerations are not needed because the heat content of the fluid flow is so large, compared to the kinetic energy of the flow, that the temperature remains nearly constant even if the whole kinetic energy is transformed into heat. In other words, the difference between the static and stagnation temperatures is not significant in low-speed flows. But in high-speed flows, the kinetic energy content of the fluid can be so large compared to its heat content that the difference between the static and stagnation temperatures can become substantial. Hence, emphasis on the thermodynamic concepts assumes importance in high-speed flow analysis.

High Enthalpy Gas Dynamics, First Edition. Ethirajan Rathakrishnan.

www.wiley.com/go/rathakrishnan

2.2 First Law of Thermodynamics

Consider a closed system, consisting of a certain amount of gas at rest, across whose boundaries no transfer of mass is possible. Let δQ be an incremental amount of heat added to the system across the boundary (by thermal conduction or by direct radiation). Also, let δW denote the work done on the system by the surroundings (or by the system on the surroundings). The sign convention is positive when the work is done by the system and negative when the work is done on the system. Owing to the molecular motion of the gas, the system has an internal energy U. The first law of thermodynamics states that *"the heat added minus work done by the system is equal to the change in the internal energy of the system,"* that is,

$$\boxed{\delta Q - \delta W = dU} \tag{2.1}$$

This is an empirical result confirmed by laboratory experiments and practical experience. In Equation (2.1), the internal energy U is a state variable (thermodynamic property). Hence, the change in internal energy dU is an exact differential and its value depends only on the initial and final states of the system. In contrast (the non-thermodynamic properties), δQ and δW depend on the process by which the system attained its final state from the initial state.

In general, for any given dU, there are infinite number of ways (processes) by which heat can be added and work can be done on the system. In the present course of study, we will be mainly concerned with only the following three types of processes.

- *Adiabatic process* – a process in which no heat is added to or taken away from the system.
- *Reversible process* – a process that can be reversed without leaving any trace on the surroundings, that is, both the system and the surroundings are returned to their initial states at the end of the reverse process.
- *Isentropic process* – a process that is adiabatic and reversible.

For an open system (for example, pipe flow), there is always a term $(U + p\,\mathbb{V})$ instead of just U. This term is referred to as *enthalpy* or *heat function* H given by

$$H = U + p\,\mathbb{V} \tag{2.2}$$

$$H_2 - H_1 = U_2 - U_1 + p_2\mathbb{V}_2 - p_1\mathbb{V}_1 \tag{2.3}$$

where $(p_2\mathbb{V}_2 - p_1\mathbb{V}_1)$ is termed *flow work* and subscripts 1 and 2 represent states 1 and 2, respectively.

In general, we can say that the following are the major differences between the open and closed systems.

1. The mass that enters or leaves an open system has kinetic energy, whereas there is no mass transfer possible across the boundaries of a closed system.
2. The mass can enter and leave an open system at different levels of potential energy.

3. Open systems are capable of delivering work continuously, because in the system, the medium that transforms energy is continuously replaced. This useful work, which a machine continuously delivers, is called the *shaft work*.

2.2.1 Energy Equation for an Open System

Consider the system shown in Figure 2.1. The total energy E_1 at the inlet station 1 and E_2 at the outlet station 2 are given by

$$E_1 = U_1 + \frac{1}{2}\, m\, V_1^2 + m\, g\, z_1 \tag{2.4}$$

$$E_2 = U_2 + \frac{1}{2}\, m\, V_2^2 + m\, g\, z_2 \tag{2.5}$$

For an open system, the first-law expressions given by Equation (2.1) has to be rewritten with the total energy E in place of the internal energy U. Thus, we have

$$\boxed{Q_{12} - W_{12} = E_2 - E_1} \tag{2.6}$$

Substituting for E_1 and E_2 from Equations (2.4) and (2.5), respectively, we get

$$Q_{12} - W_{12} = \left(U_2 + \frac{m}{2}\, V_2^2 + m\, g\, z_2\right) - \left(U_1 + \frac{m}{2}\, V_1^2 + m\, g\, z_1\right) \tag{2.7}$$

For an open system, the shaft (useful) work is not just equal to W_{12}, but the work done to move the pistons at 1 and 2 must also be considered. Work done with respect to the system by the piston at state 1 is

$W_1' = -F_1 \Delta_1$ (F_1 = force and Δ_1 = displacement)

$W_1' = -p_1 A_1 \Delta_1$ (p_1 = pressure at 1; A_1 = cross-sectional area of piston)

$W_1' = -p_1 \mathbb{V}_1$

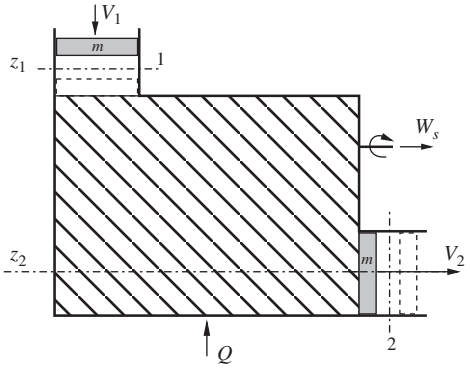

Figure 2.1 An open system.

Work delivered at 2 is $W_2^{'} = p_2 \mathbb{V}_2$. Therefore,

$$W_{12} = W_s + p_2 \mathbb{V}_2 - p_1 \mathbb{V}_1 \tag{2.8}$$

In Equation (2.8), W_s is the shaft work, which can be extracted from the system, and $(p_2 \mathbb{V}_2 - p_1 \mathbb{V}_1)$ is the flow work necessary to maintain the flow. Substituting Equation (2.8) into Equation (2.7), we get

$$Q_{12} - W_s = \left(U_2 + p_2 \mathbb{V}_2 + \frac{m}{2} V_2^2 + m\, g\, z_2\right) - \left(U_1 + p_1 \mathbb{V}_1 + \frac{m}{2} V_1^2 + m\, g\, z_1\right)$$

or

$$Q_{12} - W_s = \left(H_2 + \frac{m}{2} V_2^2 + m\, g\, z_2\right) - \left(H_1 + \frac{m}{2} V_1^2 + m\, g\, z_1\right)$$

where $H_1 = U_1 + p_1 \mathbb{V}_1$ and $H_2 = U_2 + p_2 \mathbb{V}_2$. This is the fundamental equation for an open system. If there are any other forms of energy, such as, electrical energy or magnetic energy, their initial and final values should be added properly to this equation. The energy equation for an open system is

$$\boxed{H_1 + \frac{m}{2} V_1^2 + m\, g\, z_1 = H_2 + \frac{m}{2} V_2^2 + m\, g\, z_2 + W_s - Q_{12}} \tag{2.9}$$

This equation is universally valid. This is the expression of the first law of thermodynamics for any open system. In most applications of gas dynamics, the gravitational energy is negligible compared to the kinetic energy. For working processes such as flow in turbines and compressors, the shaft work W_s in Equation (2.9) is finite, and for flow processes such as flow around an airplane, $W_s = 0$. Therefore, for a gas dynamic working process, Equation (2.9) becomes

$$H_1 + \frac{m}{2} V_1^2 = H_2 + \frac{m}{2} V_2^2 - Q_{12} \tag{2.10}$$

This is usually the case with systems such as turbo machines and internal combustion engines, where the process is assumed to be adiabatic (that is, $Q_{12} = 0$). For a gas dynamic adiabatic flow process, the energy equation (2.9) becomes

$$H_1 + \frac{m}{2} V_1^2 = H_2 + \frac{m}{2} V_2^2 \tag{2.11}$$

or

$$\boxed{H_1 + \frac{m}{2} V_1^2 = H_0 = \text{constant}} \tag{2.12}$$

where H_0 is the stagnation enthalpy and H_1 is the static enthalpy. That is, the sum of static enthalpy and kinetic energy is constant in an adiabatic flow.

2.2.2 Adiabatic Flow Process

For an adiabatic process, the heat transfer is associated with the process, $Q = 0$. Therefore, the energy equation is given by Equations (2.11) and (2.12). Dividing Equations (2.11) and (2.12) by m, we can rewrite them as

$$h_1 + \frac{V_1^2}{2} = h_2 + \frac{V_2^2}{2} \tag{2.13}$$

$$h_1 + \frac{V_1^2}{2} = h_0 \tag{2.14}$$

or, in general,

$$\boxed{h + \frac{V^2}{2} = h_0 = \text{constant}} \tag{2.15}$$

where $h = H/m$ is called *specific static enthalpy* and h_0 is the *specific stagnation enthalpy*. With $h = p/\rho$, Equation (2.15) represents Bernoulli's equation for incompressible flow,

$$p + \frac{1}{2}\,\rho\, V^2 = p_0 = \text{constant}$$

where p_0 is the stagnation pressure. That is, for incompressible flow of air, the energy equation happens to be the Bernoulli equation, because we are not interested in the internal energy and the temperature for such flows. In other words, Bernoulli's equation is the limiting case of the energy equation for incompressible flows. Here it is important to realize that even though Bernoulli's equation for incompressible flow of a gas is shown to be the limiting case of energy equation, it is *essentially a momentum equation*. For a closed system,

$$Q_{12} - W_{12} = U_2 - U_1$$

In terms of specific quantities, this becomes

$$q_{12} - w_{12} = u_2 - u_1$$

For the processes of a closed system, there is no shaft work involved, that is, no useful work can be extracted from the working medium. There will only be compression or expansion work. Therefore, w_{12} may be expressed as

$$w_{12} = \int_1^2 p\, dv$$

where v is the specific volume.

Thus, the change in internal energy becomes

$$du = \delta q - p\, dv \tag{2.16a}$$

Also, $h = u + pv$; $dh = du + p\, dv + v\, dp$. Using relation (2.16a), we can write the change in enthalpy as

$$dh = \delta q + v\, dp \tag{2.16b}$$

For adiabatic change of state, Equations (2.16a) and (2.16b) reduce to

$$du = -p\, dv, \quad dh = v\, dp \tag{2.16c}$$

where u, q, and v in Equations (2.16a)–(2.16c) stand for specific quantities of internal energy, heat energy, and volume, respectively.

2.3 The Second Law of Thermodynamics (Entropy Equation)

Consider a cold body coming into contact with a hot body. From experience, we can say that the cold body will get heated up and the hot body will cool down. However, Equation (2.1) does not necessarily imply that this will happen. In fact, the first law allows the cold body to become cooler and the hot body to become hotter as long as energy is conserved during the process. However, in practice, this does not happen; instead, the law of nature imposes another condition on the process, a condition that stipulates the direction in which a process should take place. To ascertain the proper direction of a process, let us define a new state variable, the entropy, as follows:

$$ds = \frac{\delta q_{\text{rev}}}{T} \tag{2.17}$$

where s is the entropy (amount of disorder) of the system, δq_{rev} is an incremental amount of heat added reversibly to the system, and T is the system temperature. The above definition gives the change in entropy in terms of a reversible addition of heat, δq_{rev}. As entropy is a state variable, it can be used in conjunction with any type of process, reversible or irreversible. The quantity δq_{rev} is just an artifice; an effective value of δq_{rev} can always be assigned to relate the initial and final states of an irreversible process, where the actual amount of heat added is δq. Indeed, an alternative and probably more lucid relation is

$$\boxed{ds = \frac{\delta q}{T} + ds_{\text{irrev}}} \tag{2.18}$$

Equation (2.18) applies in general to all processes. It states that the change in entropy during any process is equal to the actual heat added, δq; divided by the temperature, $\delta q/T$; plus a contribution from the irreversible dissipative phenomena of viscosity,

thermal conductivity, and mass diffusion occurring within the system, ds_{irrev}. These dissipative phenomena always cause increase of entropy, that is,

$$ds_{\text{irrev}} \geq 0 \tag{2.19}$$

The equal sign in the inequality (2.19) denotes a reversible process in which, by definition, the above dissipative phenomena are absent. Hence, a combination of Equations (2.18) and (2.19) yields

$$ds \geq \frac{\delta q}{T} \tag{2.20}$$

Further, if the process is adiabatic, $\delta q = 0$, and Equation (2.20) reduces to

$$ds \geq 0 \tag{2.21}$$

Equations (2.20) and (2.21) are two forms of the second law of thermodynamics. The second law gives the direction in which a process will take place. Equations (2.20) and (2.21) imply that a process will always proceed in a direction such that the entropy of the system plus surroundings always increases or at least remains unchanged. That is, in an adiabatic process, the entropy can never decrease. This aspect of the second law of thermodynamics is important because it distinguishes between reversible and irreversible processes.

If $ds > 0$, the process is called an *irreversible process*, and when $ds = 0$, the process is called a *reversible process*. A reversible and adiabatic process is called an *isentropic process*. However, in a nonadiabatic process, we can extract heat from the system and thus decrease the entropy of the system.

2.4 Thermal and Calorical Properties

The equation $pv = RT$ or $p/\rho = RT$ is called *thermal equation of state*, where p, T and $v(1/\rho)$ are *thermal properties* and R is the gas constant. A gas that obeys the thermal equation of state is called *thermally perfect gas*. Any relation between the calorical properties, u, h, and s, and any two thermal properties is called *calorical equation of state*. In general, the thermodynamic properties (the properties that do not depend on process) can be grouped into thermal properties (p, T, v) and calorical properties (u, h, s). From Equation (2.16), we have

$$u = u(T, v), \quad h = h(T, p)$$

In terms of exact differentials, the above relations become

$$du = \left(\frac{\partial u}{\partial T}\right)_v dT + \left(\frac{\partial u}{\partial v}\right)_T dv \tag{2.22}$$

$$dh = \left(\frac{\partial h}{\partial T}\right)_p dT + \left(\frac{\partial h}{\partial p}\right)_T dp \tag{2.23}$$

For a constant volume process, Equation (2.22) reduces to

$$du = \left(\frac{\partial u}{\partial T}\right)_v dT$$

where $\left(\frac{\partial u}{\partial T}\right)_v$ is the specific heat at constant volume represented as c_v; therefore,

$$du = c_v \, dT \tag{2.24}$$

For an isobaric process, Equation (2.23) reduces to

$$dh = \left(\frac{\partial h}{\partial T}\right)_p dT$$

where $\left(\frac{\partial h}{\partial T}\right)_p$ is the specific heat at constant pressure represented by c_p; therefore,

$$dh = c_p \, dT \tag{2.25}$$

From Equation (2.16a), for a constant volume (isochoric) process, we get

$$\delta q = du = c_v \, dT \tag{2.26a}$$

and for a constant pressure (isobaric) process,

$$\delta q = dh = c_p \, dT, \quad \delta q = dh = c_v \, dT + p \, dv \tag{2.26b}$$

For an adiabatic flow process ($q = 0$), therefore, from Equation (2.16c), we have

$$dh = v \, dp \tag{2.26c}$$

From Equations (2.26a)–(2.26c), the following can be inferred.

1. If heat is added at constant volume, it only raises the internal energy.
2. If heat is added at constant pressure, it not only increases the internal energy but also does some external work, that is, it increases the enthalpy.
3. If the change is adiabatic, the change in enthalpy is equal to external work $v \, dp$.

2.4.1 Thermally Perfect Gas

A gas is said to be thermally perfect when its internal energy and enthalpy are functions of temperature alone, that is, for a thermally perfect gas,

$$u = u(T), \quad h = h(T) \tag{2.27a}$$

Therefore, from Equations (2.24) and (2.25), we get

$$c_v = c_v(T), \quad c_p = c_p(T) \tag{2.27b}$$

Further, from Equations (2.22), (2.23), and (2.27a), we obtain

$$\left(\frac{\partial u}{\partial v}\right)_T = 0, \quad \left(\frac{\partial h}{\partial p}\right)_T = 0 \tag{2.27c}$$

The important relations of this section are

$$\boxed{du = c_v\, dT, \quad dh = c_p\, dT}$$

These equations are universally valid as long as the gas is thermally perfect. Otherwise, in order to have equations of universal validity, we must add $\left(\frac{\partial u}{\partial v}\right)_T dv$ to the first equation and $\left(\frac{\partial h}{\partial p}\right)_T dp$ to the second equation.

The state equation for a thermally perfect gas is

$$pv = RT$$

In the differential form, this equation becomes

$$p\, dv + v\, dp = R\, dT$$

Also,

$$h = u + pv$$

$$dh = du + p\, dv + v\, dp$$

Therefore,

$$dh - du = p\, dv + v\, dp = R\, dT$$

that is,

$$R\, dT = c_p\, dT - c_v\, dT$$

Thus,

$$R = c_p\,(T) - c_v(T) \tag{2.28}$$

For thermally perfect gases, Equation (2.28) shows that although c_p and c_v are functions of temperature, their difference is a constant with reference to temperature.

2.5 The Perfect Gas

This is even a greater specialization than thermally perfect gas. For a perfect gas, both c_p and c_v are constants and are independent of temperature, that is,

$$c_v = \text{constant} \neq c_v(T), \quad c_p = \text{constant} \neq c_p(T) \tag{2.29}$$

Such a gas with constant c_p and c_v is called a *calorically perfect gas*. Therefore, a perfect gas should be thermally as well as calorically perfect.

From the above discussions, the following are evident.

- A perfect gas must be both thermally and calorically perfect.
- A perfect gas must satisfy both the *thermal equation of state*, $p = \rho\, R\, T$, and the *caloric equations of state*, $c_p = (\partial h/\partial T)_p$, $c_v = (\partial u/\partial T)_v$.
- A calorically perfect gas must be thermally perfect, but a thermally perfect gas need not be calorically perfect. That is, thermal perfectness is a prerequisite for caloric perfectness.
- For a thermally perfect gas, $c_p = c_p(T)$ and $c_v = c_v(T)$; that is, both c_p and c_v are functions of temperature. But even though the specific heats c_p and c_v vary with temperature, their ratio, γ becomes a constant and independent of temperature, that is, $\gamma = \text{constant} \neq \gamma(T)$.
- For a calorically perfect gas, c_p, c_v, as well as γ are constants and independent of temperature.

2.5.1 Entropy Calculation

Entropy is defined by the relation (for a reversible process)

$$\delta q = T\, ds$$

Using Equations (2.16a)–(2.16c), we can write

$$T\, ds = du + p\, dv \tag{2.30}$$

$$T\, ds = dh - v\, dp \tag{2.31}$$

Equations (2.30) and (2.31) are as important and useful as the original form of the first law of thermodynamics, Equation (2.1).

For a thermally perfect gas, from Equation (2.25), we have $dh = c_p\, dT$. Substituting this relation into Equation (2.31), we obtain

$$ds = c_p\, \frac{dT}{T} - \frac{v\, dp}{T} \tag{2.32}$$

Substituting the perfect gas equation of state, $p\, v = R\, T$, into Equation (2.32), we get

$$ds = c_p\, \frac{dT}{T} - R\, \frac{dp}{p} \tag{2.33}$$

Integrating Equation (2.33) between states 1 and 2, we obtain

$$s_2 - s_1 = \int_{T_1}^{T_2} c_p\, \frac{dT}{T} - \int_{p_1}^{p_2} R\, \frac{dp}{p} \tag{2.34}$$

Equation (2.34) holds for a thermally perfect gas. The integral can be evaluated if c_p is known as a function of T. Further, assuming the gas to be calorically perfect, for which c_p is constant, Equation (2.34) reduces to

$$\boxed{s_2 - s_1 = c_p \ln\left(\frac{T_2}{T_1}\right) - R \ln\left(\frac{p_2}{p_1}\right)} \tag{2.35}$$

Using $du = c_v\, dT$ in Equation (2.30), the change in entropy can also be expressed as

$$\boxed{s_2 - s_1 = c_v \ln\left(\frac{T_2}{T_1}\right) + R \ln\left(\frac{v_2}{v_1}\right)} \tag{2.36}$$

From the above discussion, we can summarize that a perfect gas is both thermally and calorically perfect. Further, a calorically perfect gas must also be thermally perfect, whereas a thermally perfect gas need not be calorically perfect.

For a thermally perfect gas, $p = \rho RT$, $c_v = c_v(T)$, and $c_p = c_p(T)$, and for a perfect gas, $p = \rho RT$, $c_v =$ constant, and $c_p =$ constant. That is, for a calorically perfect gas, $p = \rho RT$ and c_p and c_v are constants and independent of temperature. Further, for a perfect gas, all equations get simplified, resulting in the following simple relations for u, h, and s.

$$u = u_1 + c_v\, T \tag{2.37a}$$

$$h = h_1 + c_p\, T \tag{2.37b}$$

$$s = s_1 + c_v \ln\left(\frac{p}{p_1}\right) - c_p \ln\left(\frac{\rho}{\rho_1}\right) \tag{2.37c}$$

where the subscript "1" refers to the initial state.

Equations (2.37a), (2.37b), and (2.28) combined with the thermal equation of state ($p = \rho RT$) result in

$$u = u_1 + \frac{1}{\gamma - 1}\frac{p}{\rho}, \quad h = h_1 + \frac{\gamma}{\gamma - 1}\frac{p}{\rho}$$

where γ is the ratio of specific heats, c_p/c_v. For the most simple molecular model, the kinetic theory of gases gives the specific heats ratio, γ as

$$\boxed{\gamma = \frac{n+2}{n}}$$

where n is the number of degrees of freedom of the gas molecules. Thus, for monatomic gases with $n = 3$, the specific heats ratio becomes

$$\boxed{\gamma = \frac{3+2}{3} = 1.67}$$

Diatomic gases, such as oxygen and nitrogen, have $n = 5$ (three translational degrees of freedom and two rotational degrees of freedom); thus

$$\gamma = \frac{5+2}{5} = 1.4$$

Gases with extremely complex molecules, such as freon and gaseous compounds of uranium, have large values of n, resulting in values of γ only slightly greater than unity. Thus, the value of specific heats ratio γ varies from 1 to 1.67, depending on the molecular nature of the gas, that is,

$$\boxed{1 \leq \gamma \leq 1.67}$$

The above relations for u and h are important, because they connect the quantities used in thermodynamics with those used in gas dynamics. With the aid of these relations, the energy equation can be written in two different forms as follows.

- The energy equation for an adiabatic process, as given by Equation (2.15), is

$$h + \frac{V^2}{2} = h_0 = \text{constant}$$

When the gas is perfect, it becomes

$$c_p T + \frac{V^2}{2} = c_p T_0 = \text{constant} \tag{2.38a}$$

- Equation (2.38a), when combined with the thermal state equation, yields

$$\boxed{\frac{\gamma}{\gamma - 1}\frac{p}{\rho} + \frac{V^2}{2} = \text{constant}} \tag{2.38b}$$

Equation (2.38b) is the form of energy equation commonly used in gas dynamics. This is popularly known as *compressible Bernoulli's equation* for isentropic flows.

From Equation (2.38a), we infer that for an adiabatic process of a perfect gas,

$$T_{01} = T_{02} = T_0 = \text{constant} \tag{2.39}$$

So far, we have not made any assumption about the reversibility or irreversibility of the process. Equation (2.39) implies that the stagnation temperature T_0 remains constant for an adiabatic process of a perfect gas, irrespective of the process being reversible or irreversible.

Consider the flow of gas in a tube with an orifice as shown in Figure 2.2. In such a flow process, there will be pressure loss. But if the stagnation temperature is measured before and after the orifice plate, and if it remains constant, then the gas can be treated as a perfect gas and all the simplified equations (Equation (2.37)) can be used. Otherwise, it cannot be treated as perfect gas, and Equation (2.37c) can be rewritten as

$$\frac{p_2}{p_1} = \left(\frac{\rho_2}{\rho_1}\right)^{\gamma} \exp\left[\frac{(s_2 - s_1)}{c_v}\right] \tag{2.40}$$

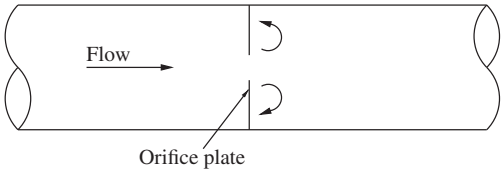

Figure 2.2 Flow through an orifice plate.

2.5.2 *Isentropic Relations*

An adiabatic and reversible process is called *isentropic process*. For an adiabatic process, $\delta q = 0$, and for a reversible process, $ds_{\text{irrev}} = 0$. Hence, from Equation (2.18), an isentropic process is one for which $ds = 0$, that is, the entropy is constant. Important relations for an isentropic process can be directly obtained from Equations (2.35), (2.36), and (2.40) by setting $s_2 = s_1$. For example, from Equation (2.35), we have

$$0 = c_p \ln\left(\frac{T_2}{T_1}\right) - R \ln\left(\frac{p_2}{p_1}\right)$$

$$\ln\left(\frac{p_2}{p_1}\right) = \frac{c_p}{R} \ln\left(\frac{T_2}{T_1}\right)$$

$$\frac{p_2}{p_1} = \left(\frac{T_2}{T_1}\right)^{c_p/R} \tag{2.41}$$

From Equation (2.38),

$$c_p - c_v = R$$

$$1 - \frac{c_v}{c_p} = \frac{R}{c_p}$$

$$\frac{\gamma - 1}{\gamma} = \frac{R}{c_p}$$

because $c_p/c_v = \gamma$. Therefore,

$$\frac{c_p}{R} = \frac{\gamma}{\gamma - 1}$$

Substituting this relation into Equation (2.41), we obtain

$$\frac{p_2}{p_1} = \left(\frac{T_2}{T_1}\right)^{\gamma/(\gamma-1)} \tag{2.42}$$

Similarly, from Equation (2.36),

$$0 = c_v \ln\left(\frac{T_2}{T_1}\right) + R \ln\left(\frac{v_2}{v_1}\right)$$

$$\ln\left(\frac{v_2}{v_1}\right) = -\frac{c_v}{R} \ln\left(\frac{T_2}{T_1}\right)$$

$$\frac{v_2}{v_1} = \left(\frac{T_2}{T_1}\right)^{-c_v/R} \tag{2.43}$$

But it can be shown that

$$\frac{c_v}{R} = \frac{1}{\gamma - 1}$$

Substituting the above relation into Equation (2.43), we get

$$\frac{v_2}{v_1} = \left(\frac{T_2}{T_1}\right)^{-1/(\gamma-1)} \tag{2.44}$$

As $\rho_2/\rho_1 = v_1/v_2$, Equation (2.44) becomes

$$\frac{\rho_2}{\rho_1} = \left(\frac{T_2}{T_1}\right)^{1/(\gamma-1)} \tag{2.45}$$

Substituting $s_1 = s_2$ into Equation (2.40), we obtain

$$\frac{p_2}{p_1} = \left(\frac{\rho_2}{\rho_1}\right)^{\gamma} \tag{2.46}$$

This relation is also called *Poisson's equation*. Summarizing Equations (2.42), (2.45), and (2.46), we can write

$$\boxed{\frac{p_2}{p_1} = \left(\frac{\rho_2}{\rho_1}\right)^{\gamma} = \left(\frac{T_2}{T_1}\right)^{\gamma/(\gamma-1)}} \tag{2.47}$$

Equation (2.47) is an important equation and used very frequently in the analysis of compressible flows.

Using the above-discussed isentropic relations, several useful equations of total (stagnation) conditions can be obtained as follows. From Equation (2.38a), we have

$$\frac{T_0}{T} = 1 + \frac{V^2}{2c_pT}$$

But for perfect gases,

$$c_p = \frac{\gamma}{\gamma - 1} R$$

Therefore,

$$\frac{T_0}{T} = 1 + \frac{V^2}{2\,\gamma RT/(\gamma - 1)}$$

By Equation (1.16), $\gamma RT = a^2$; thus

$$\frac{T_0}{T} = 1 + \frac{V^2}{2a^2/(\gamma - 1)}$$

where T is the static temperature, T_0 is the stagnation temperature, and V is the flow velocity. Hence,

$$\boxed{\frac{T_0}{T} = 1 + \frac{\gamma - 1}{2} M^2} \tag{2.48}$$

Equation (2.48) gives the ratio of total to static temperature at a point in an isentropic flow field as a function of the flow Mach number M at that point. Combining Equations (2.47) and (2.48), we get

$$\boxed{\frac{p_0}{p} = \left(1 + \frac{\gamma - 1}{2} M^2\right)^{\gamma/(\gamma-1)}} \tag{2.49}$$

$$\boxed{\frac{\rho_0}{\rho} = \left(1 + \frac{\gamma - 1}{2} M^2\right)^{1/(\gamma-1)}} \tag{2.50}$$

Equations (2.49) and (2.50) give the ratio of total to static pressure and total to static density, respectively, at a point in an isentropic flow field as a function of the flow Mach number M at that point. Equations (2.48)–(2.50) form a set of most important equations for total properties, which are often used in gas dynamic studies. Their value as a function of M for $\gamma = 1.4$ are tabulated in Table A.1 of Ref. [1].

At this stage, we may ask how Equation (2.47), which is derived on the basis of the concept of isentropic change of state (which is so restrictive – adiabatic as well as reversible – that it may find only limited applications), is so important and why it is frequently used. In compressible flow processes such as flow processes, through a rocket engine, and flow over an aerofoil, large regions of the flow fields are isentropic. In the region adjacent to the rocket nozzle walls and the aerofoil surface, a boundary layer is formed wherein the dissipative mechanisms of viscosity, thermal conduction, and diffusion are strong. Hence, the entropy increases within these boundary layers. On the other hand, for fluid elements outside the boundary layer, the dissipative effects are negligible. Further, no heat is being added to or removed from the fluid element at these points; hence, the flow is adiabatic. Therefore, the fluid elements outside the boundary layer experience reversible adiabatic process; hence, the flow is isentropic. Moreover, the boundary layers are usually thin; hence, large regime of flow fields are isentropic. Therefore, a study of isentropic flow is directly applicable to many types of practical flow problems. Equation (2.47) is a powerful relation connecting pressure, density, and temperature and is valid for calorically perfect gases.

Expressing all the quantities as stagnation quantities, Equation (2.37c) can be written as

$$s_{02} - s_{01} = c_v \ln\left(\frac{p_{02}}{p_{01}}\right) - c_p \ln\left(\frac{\rho_{02}}{\rho_{01}}\right) \tag{2.51}$$

Also, by Equation (2.28),

$$R = c_p - c_v$$

and from the state equation,

$$\frac{p_{01}}{p_{02}} = \frac{\rho_{01}}{\rho_{02}} \frac{T_{01}}{T_{02}}$$

Substitution of the above relations into Equation (2.51) yields

$$s_{02} - s_{01} = R \ln\left(\frac{p_{01}}{p_{02}}\right) + c_p \ln\left(\frac{T_{02}}{T_{01}}\right)$$

For an adiabatic process of a perfect gas,

$$T_{01} = T_{02}$$

Therefore,

$$\boxed{s_{02} - s_{01} = R \ln\left(\frac{p_{01}}{p_{02}}\right)} \tag{2.52}$$

From Equation (2.52), it is obvious that the entropy changes only when there are losses in pressure. It does not change with velocity, and hence, there is nothing like static and stagnation entropy. Also, by Equation (2.39), the stagnation temperature does not change even when there are pressure losses. There is always an increase in entropy associated with pressure loss. In other words, when there are losses, there will be an increase in entropy, leading to a drop in stagnation pressure. These losses can be due to friction, separation, shocks, etc.

Example 2.1 Argon is compressed adiabatically in a steady-flow compressor from 101 kPa and 25°C to 505 kPa. If the compression work required is 475 kJ/kg, show that the compression process is irreversible. Assume argon to be an ideal gas.

Solution

As we know, the work required for a process is minimum when the process is isentropic, that is, when the process is adiabatic and reversible. Also, any process requiring more work than that required for an isentropic process is irreversible.
For an isentropic process, work transfer can be expressed as [1]

$$w_{12} = \frac{\gamma}{\gamma - 1} R T_1 \left[1 - \left(\frac{p_2}{p_1}\right)^{\frac{\gamma-1}{\gamma}}\right]$$

where subscripts 1 and 2, respectively, refer to the initial and final states. Given that

$$T_1 = 25^\circ\text{C} = 298.15 \text{ K}, \quad p_1 = 101 \text{ kPa}, \quad p_2 = 505 \text{ kPa}$$

For argon, $\gamma = 1.67$ and $R = 8314/39.944 = 208.14$ J/(kg K), because the molecular weight of argon is 39.944 [2].

Substituting these values into the work transfer equation, we get

$$w_{12} = \frac{1.67}{0.67} \times 208.14 \times 298.15 \left[1 - \left(\frac{505}{101}\right)^{0.67/1.67}\right]$$
$$= \boxed{-140.34 \text{ kJ/kg}}$$

The actual work required, 475 kJ/kg, is more than the isentropic work transfer. Hence, the process is irreversible. ■

Example 2.2 The Mach number of an aircraft is the same at all altitudes. If its speed is 90 kmph slower at 7000 m altitude than at sea level, what is its Mach number?

Solution

From standard atmospheric table, at 7000 m altitude, we get the local temperature T_h as [2]

$$T_h = 242.65 \text{ K}$$

Therefore, the speed of sound at 7000 m altitude is

$$a_h = \sqrt{\gamma R T_h}$$
$$= \sqrt{1.4 \times 287 \times 242.65}$$
$$= 312.24 \text{ m/s}$$

At sea level,

$$T_0 = 15^\circ\text{C} = 288.15 \text{ K}$$

The speed of sound at sea level is

$$a_0 = \sqrt{\gamma R T_0}$$
$$= \sqrt{1.4 \times 287 \times 288.15}$$
$$= 340.26 \text{ m/s}$$

The Mach number is the same at these two altitudes. Thus,

$$\frac{V_0}{a_0} = \frac{V_h}{a_h} = \frac{\left(V_0 - \frac{90}{3.6}\right)}{a_h}$$
$$V_0 \frac{a_h}{a_0} = V_0 - \frac{90}{3.6}$$
$$V_0 \left(\frac{a_h}{a_0} - 1\right) = -\frac{90}{3.6}$$

$$V_0\left(\frac{312.24}{340.26}-1\right) = -25$$

$$V_0 = \frac{25}{0.08235}$$

$$= 303.58 \text{ m/s}$$

$$M = \frac{V_0}{a_0}$$

$$= \frac{303.58}{340.26}$$

$$= \boxed{0.892}$$

■

Example 2.3 Air enters a compressor at a stagnation state of 100 kPa and 27°C. If it has to be compressed to a stagnation pressure of 900 kPa, calculate the power input to the compressor when the mass flow rate is 0.02 kg/s. Assume the compression process to be isentropic.

Solution

Let subscripts 01 and 02 refer to the initial and final stagnation states, respectively.

Given

$$p_{01} = 100 \text{ kPa}, \quad T_{01} = 27^\circ\text{C} = 300.15 \text{ K}, \quad p_{02} = 900 \text{ kPa}, \quad \dot{m} = 0.02 \text{ kg/s}$$

The entropy change can be expressed as

$$s_2 - s_1 = c_p \ln\left(\frac{T_{02}}{T_{01}}\right) - R \ln\left(\frac{p_{02}}{p_{01}}\right)$$

For an isentropic compression, $s_2 - s_1 = 0$. Therefore,

$$c_p \ln\left(\frac{T_{02}}{T_{01}}\right) = R \ln\left(\frac{p_{02}}{p_{01}}\right)$$

$$\ln\left(\frac{T_{02}}{T_{01}}\right) = \frac{R}{c_p} \ln\left(\frac{p_{02}}{p_{01}}\right)$$

$$= \frac{287}{1004.5} \ln\left(\frac{900}{100}\right)$$

$$= 0.628$$

$$T_{02} = (e^{0.628})\, T_{01}$$

$$= (e^{0.628}) \times 300.15$$

$$= 562.44 \text{ K}$$

The power required is

$$\begin{aligned}\text{Power} &= \dot{m}\ \Delta h \\ &= \dot{m}\ c_p(T_{02} - T_{01}) \\ &= 0.02 \times 1004.5 \times (562.44 - 300.15) \\ &= \boxed{5.27\ \text{kW}}\end{aligned}$$

■

Example 2.4 Show that for air, the difference between stagnation and static temperature in the kelvin scale is approximately 5 × (speed in hundreds of meters per second)^2.

Solution

By energy equation, we have

$$h + \frac{V^2}{2} = h_0$$

where h and h_0, respectively, are the static and stagnation enthalpies and V is the flow speed. For a perfect gas, $h = c_p T$; thus the energy equation becomes

$$c_p\ T + \frac{V^2}{2} = c_p\ T_0$$

Therefore, the stagnation temperature rise is

$$\begin{aligned}T_0 - T &= \frac{V^2}{2\ c_p} \\ &= \frac{(\gamma - 1)}{\gamma}\ \frac{V^2}{2\ R}\end{aligned}$$

because $c_p = \frac{\gamma}{\gamma - 1} R$.
For air, $R = 287$ J/(kg K) and $\gamma = 1.4$, under normal temperatures. Substituting for R and γ in the above equation, we get

$$\begin{aligned}T_0 - T &= \frac{0.4}{2 \times 1.4 \times 287}\ V^2 \\ &= 4.9776 \times 10^{-4}\ V^2\ \text{K} \\ &\approx 5(V \times 10^{-2})^2\ \text{K} \\ &\approx \boxed{5\ \text{(speed in hundreds of meters per second)}^2}\end{aligned}$$

■

2.5.3 Limitations on Air as a Perfect Gas

The following are the limitations to treat air as a perfect gas, obeying both thermal state equation and calorical state equations.

- When the temperature is less than 500 K, air can be treated as a perfect gas and the ratio of specific heats, γ, takes a constant value of 1.4.
- When the temperature lies between 500 and 2000 K, air is only thermally perfect and the state equation $p = \rho RT$ is valid, but c_p and c_v become functions of temperature, $c_p = c_p(T)$ and $c_v = c_v(T)$. Even though c_p and c_v are functions of temperature, their ratio γ continues to be independent of temperature. That is, c_p and c_v vary with temperature in such a manner that their ratio continues to be the same constant as in temperatures below 500 K.
- For temperatures more than 2000 K, air becomes both thermally and calorically imperfect. That is, c_p, c_v, as well as γ become functions of temperature.

In supersonic flight with Mach number, say 2.0 at sea level, the temperature reached would already be about 245°C (more than 500 K). But, for 500 K $\leq T \leq$ 700 K, we can still use perfect gas equations and the error involved in doing so will be negligible, that is, for Mach number less than 2.68, perfect gas equations can be used with slight error. For temperatures more than 700 K, we must go for thermally perfect gas equations.

At this stage, we may have some doubt about the possible values of the isentropic index γ, when the flow medium is at a temperature that is quite high and the medium cannot be assumed as perfect. This doubt can be cleared if we consider the flow medium as an ideal gas, which satisfies perfect gas equations, and has γ as a constant and independent of temperature. For a monatomic gas (such as He, Ar, and Ne), the simplest possible molecular structure gives $\gamma = 5/3$. This prediction is well confirmed by experiment. At the other extreme of molecular complexity, very complicated molecules have large number of degrees of freedom and γ may approach unity, which represents the minimum possible value, because $c_p \geq c_v$ by virtue of a general thermodynamic argument (Ref. [3]). Then γ necessarily has a range of values

$$\boxed{\frac{5}{3} \geq \gamma \geq 1}$$

Experimental results show that most diatomic gases, nitrogen and oxygen in particular, have $\gamma = 7/5$ at room temperature, gradually tending to $\gamma = 9/7$ at a few thousand kelvin.

Example 2.5 Compute, tabulate, and plot the variation of c_p, c_v, specific enthalpy h, and specific heats ratio γ of the air as functions of temperature (300 K $\leq T \leq$ 30,000 K), assuming that chemical reactions are frozen and the air is composed

of N_2 and O_2 with their mass fractions of 0.7656 and 0.2344, respectively, at any temperature. Also assume that temperatures in all the energy modes (translational, vibrational, etc.) are the same at any temperature (see Chapter 5 for more details). Use curve-fit polynomial provided in the reference (NASA-TP-2792) and curve-fit database in the reference (NASA-TM-102602). Also, give the program listing.

Solution

According to empirical relations given in a literature (NASA-TM-102602), c_p for species "s" is obtained by $c_p^s(T) = \frac{R_u}{M_s} \sum_{k=1}^{5} A_k^s T^{k-1}$ and c_v is written as $c_v^s = c_p^s - \frac{R_u}{M_s}$. Curve-fit constants A_k^s are given in the above literature.
The computed values of c_p, c_v, h, and γ for some specific temperatures in the range from 300 to 30,000 K are listed in Table 2.1.

Table 2.1 Values of c_p, c_v, h, and γ for some specific temperatures.

T [K]	c_p [J/(kg K)]	c_v [J/(kg K)]	h [J/kg]	γ
0.30000000E+03	0.10111361E+04	0.72289337E+03	0.60611738E+04	0.13987348E+01
0.40000000E+03	0.10202679E+04	0.73202515E+03	0.10755926E+06	0.13937607E+01
0.50000000E+03	0.10367528E+04	0.74851007E+03	0.21035962E+06	0.13850887E+01
0.60000000E+03	0.10581094E+04	0.76986652E+03	0.31507197E+06	0.13744063E+01
0.70000000E+03	0.10820491E+04	0.79380615E+03	0.42206744E+06	0.13631150E+01
0.80000000E+03	0.11064762E+04	0.81823346E+03	0.53149781E+06	0.13522744E+01
0.90000000E+03	0.11294884E+04	0.84124561E+03	0.64331531E+06	0.13426381E+01
0.10000000E+04	0.11493759E+04	0.86113306E+03	0.75729119E+06	0.13347250E+01
0.11000000E+04	0.11694280E+04	0.88118518E+03	0.87870762E+06	0.13271081E+01
0.12000000E+04	0.11825452E+04	0.89430231E+03	0.99631406E+06	0.13223103E+01
0.13000000E+04	0.11947478E+04	0.90650500E+03	0.11151861E+07	0.13179716E+01
0.14000000E+04	0.12060857E+04	0.91784283E+03	0.12352346E+07	0.13140438E+01
0.15000000E+04	0.12166071E+04	0.92836426E+03	0.13563759E+07	0.13104846E+01
0.16000000E+04	0.12263589E+04	0.93811609E+03	0.14785305E+07	0.13072571E+01
0.17000000E+04	0.12353868E+04	0.94714404E+03	0.16016236E+07	0.13043283E+01
0.18000000E+04	0.12437350E+04	0.95549219E+03	0.17255852E+07	0.13016695E+01
0.19000000E+04	0.12514465E+04	0.96320374E+03	0.18503494E+07	0.12992542E+01
0.20000000E+04	0.12585631E+04	0.97032031E+03	0.19758548E+07	0.12970594E+01
0.21000000E+04	0.12651249E+04	0.97688208E+03	0.21020435E+07	0.12950641E+01
0.22000000E+04	0.12711708E+04	0.98292804E+03	0.22288625E+07	0.12932491E+01
0.23000000E+04	0.12767384E+04	0.98849561E+03	0.23562615E+07	0.12915975E+01
0.24000000E+04	0.12818643E+04	0.99362146E+03	0.24841952E+07	0.12900932E+01
0.25000000E+04	0.12865833E+04	0.99834052E+03	0.26126210E+07	0.12887219E+01
0.26000000E+04	0.12909290E+04	0.10026862E+04	0.27414998E+07	0.12874706E+01
0.27000000E+04	0.12949337E+04	0.10066909E+04	0.28707952E+07	0.12863270E+01
0.28000000E+04	0.12986284E+04	0.10103857E+04	0.30004762E+07	0.12852799E+01
0.29000000E+04	0.13020428E+04	0.10138001E+04	0.31305120E+07	0.12843190E+01
0.30000000E+04	0.13052053E+04	0.10169625E+04	0.32608762E+07	0.12834351E+01
0.31000000E+04	0.13081426E+04	0.10198997E+04	0.33915455E+07	0.12826189E+01

(*continued overleaf*)

Table 2.1 (*continued*)

T [K]	c_p [J/(kg K)]	c_v [J/(kg K)]	h [J/kg]	γ
0.32000000E+04	0.13108805E+04	0.10226377E+04	0.35224980E+07	0.12818621E+01
0.33000000E+04	0.13134434E+04	0.10252006E+04	0.36537155E+07	0.12811575E+01
0.34000000E+04	0.13158541E+04	0.10276113E+04	0.37851815E+07	0.12804979E+01
0.35000000E+04	0.13181345E+04	0.10298917E+04	0.39168820E+07	0.12798768E+01
0.36000000E+04	0.13203048E+04	0.10320620E+04	0.40488048E+07	0.12792883E+01
0.37000000E+04	0.13223840E+04	0.10341411E+04	0.41809402E+07	0.12787268E+01
0.38000000E+04	0.13243898E+04	0.10361470E+04	0.43132790E+07	0.12781872E+01
0.39000000E+04	0.13263384E+04	0.10380955E+04	0.44458165E+07	0.12776651E+01
0.40000000E+04	0.13282450E+04	0.10400022E+04	0.45785460E+07	0.12771560E+01
0.41000000E+04	0.13301230E+04	0.10418802E+04	0.47114640E+07	0.12766564E+01
0.42000000E+04	0.13319851E+04	0.10437423E+04	0.48445700E+07	0.12761627E+01
0.43000000E+04	0.13338420E+04	0.10455992E+04	0.49778610E+07	0.12756723E+01
0.44000000E+04	0.13357039E+04	0.10474611E+04	0.51113385E+07	0.12751824E+01
0.45000000E+04	0.13375784E+04	0.10493354E+04	0.52450025E+07	0.12746909E+01
0.46000000E+04	0.13394728E+04	0.10512300E+04	0.53788550E+07	0.12741958E+01
0.47000000E+04	0.13413928E+04	0.10531501E+04	0.55128970E+07	0.12736957E+01
0.48000000E+04	0.13433431E+04	0.10551003E+04	0.56471345E+07	0.12731899E+01
0.49000000E+04	0.13453267E+04	0.10570839E+04	0.57815675E+07	0.12726773E+01
0.50000000E+04	0.13473445E+04	0.10591016E+04	0.59162010E+07	0.12721579E+01
0.51000000E+04	0.13493975E+04	0.10611547E+04	0.60510365E+07	0.12716312E+01
0.52000000E+04	0.13514845E+04	0.10632417E+04	0.61860820E+07	0.12710981E+01
0.53000000E+04	0.13536036E+04	0.10653607E+04	0.63213350E+07	0.12705590E+01
0.54000000E+04	0.13557507E+04	0.10675081E+04	0.64568030E+07	0.12700145E+01
0.55000000E+04	0.13579213E+04	0.10696785E+04	0.65924865E+07	0.12694668E+01
0.56000000E+04	0.13601085E+04	0.10718657E+04	0.67283875E+07	0.12689168E+01
0.57000000E+04	0.13623052E+04	0.10740624E+04	0.68645080E+07	0.12683669E+01
0.58000000E+04	0.13645023E+04	0.10762595E+04	0.70008485E+07	0.12678190E+01
0.59000000E+04	0.13666895E+04	0.10784467E+04	0.71374085E+07	0.12672759E+01
0.60000000E+04	0.13688550E+04	0.10806123E+04	0.72741860E+07	0.12667401E+01
0.61000000E+04	0.13683191E+04	0.10800763E+04	0.74198470E+07	0.12668726E+01
0.62000000E+04	0.13695768E+04	0.10813340E+04	0.75567410E+07	0.12665622E+01
0.63000000E+04	0.13709114E+04	0.10826686E+04	0.76937645E+07	0.12662337E+01
0.64000000E+04	0.13723307E+04	0.10840879E+04	0.78309270E+07	0.12658851E+01
0.65000000E+04	0.13738422E+04	0.10855994E+04	0.79682330E+07	0.12655149E+01
0.66000000E+04	0.13754529E+04	0.10872101E+04	0.81056975E+07	0.12651216E+01
0.67000000E+04	0.13771699E+04	0.10889270E+04	0.82433280E+07	0.12647036E+01
0.68000000E+04	0.13789996E+04	0.10907568E+04	0.83811360E+07	0.12642595E+01
0.69000000E+04	0.13809489E+04	0.10927061E+04	0.85191320E+07	0.12637881E+01
0.70000000E+04	0.13830233E+04	0.10947805E+04	0.86573280E+07	0.12632883E+01
0.71000000E+04	0.13852292E+04	0.10969865E+04	0.87957410E+07	0.12627587E+01
0.72000000E+04	0.13875717E+04	0.10993289E+04	0.89343800E+07	0.12621989E+01
0.73000000E+04	0.13900564E+04	0.11018136E+04	0.90732610E+07	0.12616076E+01
0.74000000E+04	0.13926882E+04	0.11044453E+04	0.92123960E+07	0.12609843E+01
0.75000000E+04	0.13954719E+04	0.11072291E+04	0.93518020E+07	0.12603281E+01
0.76000000E+04	0.13984120E+04	0.11101693E+04	0.94914980E+07	0.12596384E+01
0.77000000E+04	0.14015126E+04	0.11132698E+04	0.96314900E+07	0.12589155E+01

Table 2.1 (*continued*)

T [K]	c_p [J/(kg K)]	c_v [J/(kg K)]	h [J/kg]	γ
0.78000000E+04	0.14047780E+04	0.11165352E+04	0.97718030E+07	0.12581583E+01
0.79000000E+04	0.14082112E+04	0.11199684E+04	0.99124520E+07	0.12573669E+01
0.80000000E+04	0.14118164E+04	0.11235736E+04	0.10053452E+08	0.12565411E+01
0.81000000E+04	0.14155959E+04	0.11273533E+04	0.10194822E+08	0.12556809E+01
0.82000000E+04	0.14195536E+04	0.11313108E+04	0.10336578E+08	0.12547866E+01
0.83000000E+04	0.14236910E+04	0.11354482E+04	0.10478738E+08	0.12538582E+01
0.84000000E+04	0.14280114E+04	0.11397686E+04	0.10621321E+08	0.12528960E+01
0.85000000E+04	0.14325161E+04	0.11442732E+04	0.10764346E+08	0.12519004E+01
0.86000000E+04	0.14372074E+04	0.11489646E+04	0.10907831E+08	0.12508718E+01
0.87000000E+04	0.14420868E+04	0.11538440E+04	0.11051795E+08	0.12498109E+01
0.88000000E+04	0.14471548E+04	0.11589120E+04	0.11196254E+08	0.12487185E+01
0.89000000E+04	0.14524135E+04	0.11641707E+04	0.11341230E+08	0.12475950E+01
0.90000000E+04	0.14578624E+04	0.11696196E+04	0.11486742E+08	0.12464415E+01
0.91000000E+04	0.14635032E+04	0.11752603E+04	0.11632807E+08	0.12452588E+01
0.92000000E+04	0.14693347E+04	0.11810919E+04	0.11779452E+08	0.12440478E+01
0.93000000E+04	0.14753582E+04	0.11871155E+04	0.11926686E+08	0.12428093E+01
0.94000000E+04	0.14815723E+04	0.11933295E+04	0.12074527E+08	0.12415451E+01
0.95000000E+04	0.14879768E+04	0.11997339E+04	0.12223003E+08	0.12402557E+01
0.96000000E+04	0.14945706E+04	0.12063276E+04	0.12372129E+08	0.12389425E+01
0.97000000E+04	0.15013527E+04	0.12131099E+04	0.12521924E+08	0.12376065E+01
0.98000000E+04	0.15083215E+04	0.12200786E+04	0.12672406E+08	0.12362494E+01
0.99000000E+04	0.15154751E+04	0.12272323E+04	0.12823595E+08	0.12348722E+01
0.10000000E+05	0.15228121E+04	0.12345693E+04	0.12975508E+08	0.12334764E+01
0.10100000E+05	0.15303293E+04	0.12420865E+04	0.13128163E+08	0.12320634E+01
0.10200000E+05	0.15380251E+04	0.12497822E+04	0.13281578E+08	0.12306346E+01
0.10300000E+05	0.15458960E+04	0.12576531E+04	0.13435772E+08	0.12291911E+01
0.10400000E+05	0.15539395E+04	0.12656968E+04	0.13590765E+08	0.12277343E+01
0.10500000E+05	0.15621516E+04	0.12739089E+04	0.13746569E+08	0.12262663E+01
0.10600000E+05	0.15705295E+04	0.12822867E+04	0.13903200E+08	0.12247881E+01
0.10700000E+05	0.15790687E+04	0.12908259E+04	0.14060678E+08	0.12233011E+01
0.10800000E+05	0.15877649E+04	0.12995220E+04	0.14219021E+08	0.12218069E+01
0.10900000E+05	0.15966143E+04	0.13083715E+04	0.14378239E+08	0.12203065E+01
0.11000000E+05	0.16056113E+04	0.13173685E+04	0.14538345E+08	0.12188020E+01
0.11100000E+05	0.16147520E+04	0.13265090E+04	0.14699365E+08	0.12172943E+01
0.11200000E+05	0.16240300E+04	0.13357872E+04	0.14861304E+08	0.12157849E+01
0.11300000E+05	0.16334413E+04	0.13451985E+04	0.15024174E+08	0.12142752E+01
0.11400000E+05	0.16429784E+04	0.13547356E+04	0.15187996E+08	0.12127669E+01
0.11500000E+05	0.16526365E+04	0.13643938E+04	0.15352769E+08	0.12112607E+01
0.11600000E+05	0.16624084E+04	0.13741655E+04	0.15518523E+08	0.12097585E+01
0.11700000E+05	0.16722888E+04	0.13840460E+04	0.15685258E+08	0.12082610E+01
0.11800000E+05	0.16822698E+04	0.13940269E+04	0.15852990E+08	0.12067699E+01
0.11900000E+05	0.16923438E+04	0.14041008E+04	0.16021715E+08	0.12052865E+01
0.12000000E+05	0.17025049E+04	0.14142621E+04	0.16191462E+08	0.12038114E+01
0.12100000E+05	0.17127434E+04	0.14245007E+04	0.16362220E+08	0.12023464E+01
0.12200000E+05	0.17230538E+04	0.14348109E+04	0.16534007E+08	0.12008926E+01

(*continued overleaf*)

Table 2.1 (*continued*)

T [K]	c_p [J/(kg K)]	c_v [J/(kg K)]	h [J/kg]	γ
0.12300000E+05	0.17334255E+04	0.14451826E+04	0.16706830E+08	0.11994509E+01
0.12400000E+05	0.17438518E+04	0.14556090E+04	0.16880696E+08	0.11980221E+01
0.12500000E+05	0.17543225E+04	0.14660797E+04	0.17055604E+08	0.11966078E+01
0.12600000E+05	0.17648302E+04	0.14765874E+04	0.17231558E+08	0.11952088E+01
0.12700000E+05	0.17753645E+04	0.14871216E+04	0.17408576E+08	0.11938261E+01
0.12800000E+05	0.17859159E+04	0.14976731E+04	0.17586636E+08	0.11924604E+01
0.12900000E+05	0.17964753E+04	0.15082324E+04	0.17765752E+08	0.11911131E+01
0.13000000E+05	0.18070315E+04	0.15187886E+04	0.17945930E+08	0.11897848E+01
0.13100000E+05	0.18175737E+04	0.15293311E+04	0.18127160E+08	0.11884763E+01
0.13200000E+05	0.18280938E+04	0.15398510E+04	0.18309448E+08	0.11871887E+01
0.13300000E+05	0.18385791E+04	0.15503362E+04	0.18492778E+08	0.11859229E+01
0.13400000E+05	0.18490181E+04	0.15607751E+04	0.18677158E+08	0.11846794E+01
0.13500000E+05	0.18593989E+04	0.15711560E+04	0.18862580E+08	0.11834592E+01
0.13600000E+05	0.18697114E+04	0.15814688E+04	0.19049038E+08	0.11822627E+01
0.13700000E+05	0.18799435E+04	0.15917007E+04	0.19236516E+08	0.11810911E+01
0.13800000E+05	0.18900818E+04	0.16018389E+04	0.19425020E+08	0.11799450E+01
0.13900000E+05	0.19001152E+04	0.16118726E+04	0.19614534E+08	0.11788248E+01
0.14000000E+05	0.19100284E+04	0.16217856E+04	0.19805040E+08	0.11777318E+01
0.14100000E+05	0.19198105E+04	0.16315676E+04	0.19996532E+08	0.11766663E+01
0.14200000E+05	0.19294475E+04	0.16412047E+04	0.20188996E+08	0.11756288E+01
0.14300000E+05	0.19389266E+04	0.16506838E+04	0.20382418E+08	0.11746203E+01
0.14400000E+05	0.19482312E+04	0.16599884E+04	0.20576780E+08	0.11736414E+01
0.14500000E+05	0.19573505E+04	0.16691077E+04	0.20772060E+08	0.11726928E+01
0.14600000E+05	0.19662683E+04	0.16780254E+04	0.20968244E+08	0.11717751E+01
0.14700000E+05	0.19749709E+04	0.16867283E+04	0.21165320E+08	0.11708887E+01
0.14800000E+05	0.19834408E+04	0.16951980E+04	0.21363240E+08	0.11700349E+01
0.14900000E+05	0.19916663E+04	0.17034233E+04	0.21561980E+08	0.11692139E+01
0.15000000E+05	0.19996300E+04	0.17113872E+04	0.21761556E+08	0.11684264E+01
0.15100000E+05	0.20081250E+04	0.17198821E+04	0.22037132E+08	0.11675946E+01
0.15200000E+05	0.20167510E+04	0.17285082E+04	0.22238388E+08	0.11667582E+01
0.15300000E+05	0.20251853E+04	0.17369426E+04	0.22440492E+08	0.11659483E+01
0.15400000E+05	0.20334258E+04	0.17451830E+04	0.22643420E+08	0.11651648E+01
0.15500000E+05	0.20414703E+04	0.17532275E+04	0.22847146E+08	0.11644069E+01
0.15600000E+05	0.20493164E+04	0.17610736E+04	0.23051700E+08	0.11636745E+01
0.15700000E+05	0.20569612E+04	0.17687184E+04	0.23257032E+08	0.11629671E+01
0.15800000E+05	0.20644036E+04	0.17761608E+04	0.23463090E+08	0.11622841E+01
0.15900000E+05	0.20716414E+04	0.17833987E+04	0.23669884E+08	0.11616255E+01
0.16000000E+05	0.20786724E+04	0.17904294E+04	0.23877400E+08	0.11609910E+01
0.16100000E+05	0.20854956E+04	0.17972529E+04	0.24085604E+08	0.11603795E+01
0.16200000E+05	0.20921089E+04	0.18038661E+04	0.24294480E+08	0.11597917E+01
0.16300000E+05	0.20985127E+04	0.18102698E+04	0.24504040E+08	0.11592265E+01
0.16400000E+05	0.21047021E+04	0.18164594E+04	0.24714196E+08	0.11586839E+01
0.16500000E+05	0.21106785E+04	0.18224358E+04	0.24924952E+08	0.11581634E+01
0.16600000E+05	0.21164409E+04	0.18281982E+04	0.25136332E+08	0.11576649E+01
0.16700000E+05	0.21219875E+04	0.18337449E+04	0.25348252E+08	0.11571879E+01
0.16800000E+05	0.21273167E+04	0.18390740E+04	0.25560700E+08	0.11567326E+01
0.16900000E+05	0.21324282E+04	0.18441854E+04	0.25773700E+08	0.11562982E+01

Table 2.1 (*continued*)

T [K]	c_p [J/(kg K)]	c_v [J/(kg K)]	h [J/kg]	γ
0.17000000E+05	0.21373223E+04	0.18490796E+04	0.25987168E+08	0.11558844E+01
0.17100000E+05	0.21419978E+04	0.18537551E+04	0.26201162E+08	0.11554912E+01
0.17200000E+05	0.21464529E+04	0.18582102E+04	0.26415596E+08	0.11551185E+01
0.17300000E+05	0.21506904E+04	0.18624478E+04	0.26630454E+08	0.11547655E+01
0.17400000E+05	0.21547083E+04	0.18664655E+04	0.26845708E+08	0.11544324E+01
0.17500000E+05	0.21585037E+04	0.18702610E+04	0.27061388E+08	0.11541190E+01
0.17600000E+05	0.21620813E+04	0.18738386E+04	0.27277426E+08	0.11538247E+01
0.17700000E+05	0.21654365E+04	0.18771938E+04	0.27493770E+08	0.11535498E+01
0.17800000E+05	0.21685754E+04	0.18803329E+04	0.27710502E+08	0.11532934E+01
0.17900000E+05	0.21714922E+04	0.18832495E+04	0.27927490E+08	0.11530560E+01
0.18000000E+05	0.21741934E+04	0.18859506E+04	0.28144780E+08	0.11528369E+01
0.18100000E+05	0.21766743E+04	0.18884316E+04	0.28362320E+08	0.11526361E+01
0.18200000E+05	0.21789365E+04	0.18906940E+04	0.28580112E+08	0.11524533E+01
0.18300000E+05	0.21809834E+04	0.18927407E+04	0.28798110E+08	0.11522886E+01
0.18400000E+05	0.21828127E+04	0.18945701E+04	0.29016292E+08	0.11521415E+01
0.18500000E+05	0.21844272E+04	0.18961846E+04	0.29234684E+08	0.11520119E+01
0.18600000E+05	0.21858271E+04	0.18975846E+04	0.29453160E+08	0.11518997E+01
0.18700000E+05	0.21870146E+04	0.18987720E+04	0.29671824E+08	0.11518048E+01
0.18800000E+05	0.21879932E+04	0.18997505E+04	0.29890568E+08	0.11517266E+01
0.18900000E+05	0.21887563E+04	0.19005137E+04	0.30109412E+08	0.11516657E+01
0.19000000E+05	0.21893145E+04	0.19010717E+04	0.30328316E+08	0.11516212E+01
0.19100000E+05	0.21896631E+04	0.19014204E+04	0.30547272E+08	0.11515933E+01
0.19200000E+05	0.21898088E+04	0.19015660E+04	0.30766260E+08	0.11515818E+01
0.19300000E+05	0.21897476E+04	0.19015049E+04	0.30985212E+08	0.11515867E+01
0.19400000E+05	0.21894888E+04	0.19012460E+04	0.31204188E+08	0.11516073E+01
0.19500000E+05	0.21890288E+04	0.19007861E+04	0.31423120E+08	0.11516439E+01
0.19600000E+05	0.21883704E+04	0.19001274E+04	0.31641994E+08	0.11516967E+01
0.19700000E+05	0.21875173E+04	0.18992747E+04	0.31860764E+08	0.11517646E+01
0.19800000E+05	0.21864709E+04	0.18982284E+04	0.32079480E+08	0.11518482E+01
0.19900000E+05	0.21852354E+04	0.18969928E+04	0.32298066E+08	0.11519471E+01
0.20000000E+05	0.21838110E+04	0.18955684E+04	0.32516512E+08	0.11520613E+01
0.20100000E+05	0.21822029E+04	0.18939602E+04	0.32734780E+08	0.11521904E+01
0.20200000E+05	0.21804136E+04	0.18921710E+04	0.32952954E+08	0.11523343E+01
0.20300000E+05	0.21784438E+04	0.18902009E+04	0.33170900E+08	0.11524932E+01
0.20400000E+05	0.21762983E+04	0.18880557E+04	0.33388640E+08	0.11526664E+01
0.20500000E+05	0.21739783E+04	0.18857356E+04	0.33606184E+08	0.11528542E+01
0.20600000E+05	0.21714915E+04	0.18832488E+04	0.33823392E+08	0.11530560E+01
0.20700000E+05	0.21688357E+04	0.18805930E+04	0.34040496E+08	0.11532723E+01
0.20800000E+05	0.21660203E+04	0.18777775E+04	0.34257176E+08	0.11535021E+01
0.20900000E+05	0.21630437E+04	0.18748009E+04	0.34473632E+08	0.11537458E+01
0.21000000E+05	0.21599111E+04	0.18716683E+04	0.34689768E+08	0.11540031E+01
0.21100000E+05	0.21566282E+04	0.18683856E+04	0.34905612E+08	0.11542736E+01
0.21200000E+05	0.21531956E+04	0.18649530E+04	0.35121148E+08	0.11545576E+01
0.21300000E+05	0.21496204E+04	0.18613776E+04	0.35336280E+08	0.11548545E+01
0.21400000E+05	0.21459045E+04	0.18576617E+04	0.35551028E+08	0.11551644E+01

(*continued overleaf*)

Table 2.1 (*continued*)

T [K]	c_p [J/(kg K)]	c_v [J/(kg K)]	h [J/kg]	γ
0.21500000E+05	0.21420549E+04	0.18538123E+04	0.35765400E+08	0.11554865E+01
0.21600000E+05	0.21380745E+04	0.18498318E+04	0.35979468E+08	0.11558210E+01
0.21700000E+05	0.21339656E+04	0.18457229E+04	0.36193064E+08	0.11561679E+01
0.21800000E+05	0.21297363E+04	0.18414935E+04	0.36406268E+08	0.11565267E+01
0.21900000E+05	0.21253875E+04	0.18371448E+04	0.36619016E+08	0.11568971E+01
0.22000000E+05	0.21209304E+04	0.18326879E+04	0.36831300E+08	0.11572785E+01
0.22100000E+05	0.21163604E+04	0.18281177E+04	0.37043148E+08	0.11576718E+01
0.22200000E+05	0.21116919E+04	0.18234492E+04	0.37254544E+08	0.11580756E+01
0.22300000E+05	0.21069277E+04	0.18186849E+04	0.37465520E+08	0.11584897E+01
0.22400000E+05	0.21020669E+04	0.18138240E+04	0.37675940E+08	0.11589144E+01
0.22500000E+05	0.20971216E+04	0.18088790E+04	0.37885924E+08	0.11593487E+01
0.22600000E+05	0.20920935E+04	0.18038506E+04	0.38095368E+08	0.11597931E+01
0.22700000E+05	0.20869905E+04	0.17987477E+04	0.38304320E+08	0.11602464E+01
0.22800000E+05	0.20818206E+04	0.17935779E+04	0.38512788E+08	0.11607082E+01
0.22900000E+05	0.20765798E+04	0.17883370E+04	0.38720696E+08	0.11611792E+01
0.23000000E+05	0.20712876E+04	0.17830447E+04	0.38928104E+08	0.11616577E+01
0.23100000E+05	0.20659355E+04	0.17776926E+04	0.39134928E+08	0.11621444E+01
0.23200000E+05	0.20605430E+04	0.17723000E+04	0.39341276E+08	0.11626377E+01
0.23300000E+05	0.20551060E+04	0.17668632E+04	0.39547056E+08	0.11631382E+01
0.23400000E+05	0.20496389E+04	0.17613960E+04	0.39752264E+08	0.11636446E+01
0.23500000E+05	0.20441437E+04	0.17559009E+04	0.39957044E+08	0.11641567E+01
0.23600000E+05	0.20386259E+04	0.17503831E+04	0.40161096E+08	0.11646742E+01
0.23700000E+05	0.20330973E+04	0.17448544E+04	0.40364712E+08	0.11651959E+01
0.23800000E+05	0.20275564E+04	0.17393137E+04	0.40567708E+08	0.11657221E+01
0.23900000E+05	0.20220193E+04	0.17337765E+04	0.40770240E+08	0.11662514E+01
0.24000000E+05	0.20164855E+04	0.17282427E+04	0.40972092E+08	0.11667838E+01
0.24100000E+05	0.20109689E+04	0.17227261E+04	0.41173504E+08	0.11673179E+01
0.24200000E+05	0.20054752E+04	0.17172323E+04	0.41374348E+08	0.11678532E+01
0.24300000E+05	0.20000022E+04	0.17117595E+04	0.41574560E+08	0.11683897E+01
0.24400000E+05	0.19945696E+04	0.17063268E+04	0.41774304E+08	0.11689259E+01
0.24500000E+05	0.19891770E+04	0.17009343E+04	0.41973496E+08	0.11694614E+01
0.24600000E+05	0.19838419E+04	0.16955991E+04	0.42172156E+08	0.11699947E+01
0.24700000E+05	0.19785577E+04	0.16903149E+04	0.42370280E+08	0.11705261E+01
0.24800000E+05	0.19733450E+04	0.16851022E+04	0.42567908E+08	0.11710536E+01
0.24900000E+05	0.19682056E+04	0.16799626E+04	0.42764992E+08	0.11715770E+01
0.25000000E+05	0.19631481E+04	0.16749052E+04	0.42961508E+08	0.11720951E+01
0.25100000E+05	0.19515212E+04	0.16632784E+04	0.43156200E+08	0.11732980E+01
0.25200000E+05	0.19452184E+04	0.16569756E+04	0.43351040E+08	0.11739572E+01
0.25300000E+05	0.19389169E+04	0.16506740E+04	0.43545276E+08	0.11746213E+01
0.25400000E+05	0.19326165E+04	0.16443738E+04	0.43738840E+08	0.11752902E+01
0.25500000E+05	0.19263218E+04	0.16380790E+04	0.43931752E+08	0.11759639E+01
0.25600000E+05	0.19200292E+04	0.16317864E+04	0.44124096E+08	0.11766425E+01
0.25700000E+05	0.19137419E+04	0.16254991E+04	0.44315772E+08	0.11773257E+01
0.25800000E+05	0.19074607E+04	0.16192179E+04	0.44506836E+08	0.11780136E+01
0.25900000E+05	0.19011854E+04	0.16129426E+04	0.44697252E+08	0.11787062E+01
0.26000000E+05	0.18949189E+04	0.16066763E+04	0.44887096E+08	0.11794031E+01

Table 2.1 (*continued*)

T [K]	c_p [J/(kg K)]	c_v [J/(kg K)]	h [J/kg]	γ
0.26100000E+05	0.18886595E+04	0.16004167E+04	0.45076232E+08	0.11801049E+01
0.26200000E+05	0.18824092E+04	0.15941665E+04	0.45264788E+08	0.11808109E+01
0.26300000E+05	0.18761699E+04	0.15879272E+04	0.45452740E+08	0.11815213E+01
0.26400000E+05	0.18699392E+04	0.15816964E+04	0.45640052E+08	0.11822364E+01
0.26500000E+05	0.18637207E+04	0.15754779E+04	0.45826704E+08	0.11829557E+01
0.26600000E+05	0.18575154E+04	0.15692726E+04	0.46012812E+08	0.11836792E+01
0.26700000E+05	0.18513214E+04	0.15630786E+04	0.46198256E+08	0.11844071E+01
0.26800000E+05	0.18451412E+04	0.15568983E+04	0.46383056E+08	0.11851392E+01
0.26900000E+05	0.18389761E+04	0.15507333E+04	0.46567256E+08	0.11858752E+01
0.27000000E+05	0.18328248E+04	0.15445819E+04	0.46750836E+08	0.11866155E+01
0.27100000E+05	0.18266890E+04	0.15384462E+04	0.46933836E+08	0.11873597E+01
0.27200000E+05	0.18205708E+04	0.15323280E+04	0.47116172E+08	0.11881077E+01
0.27300000E+05	0.18144691E+04	0.15262263E+04	0.47297956E+08	0.11888598E+01
0.27400000E+05	0.18083838E+04	0.15201411E+04	0.47479084E+08	0.11896157E+01
0.27500000E+05	0.18023179E+04	0.15140752E+04	0.47659608E+08	0.11903754E+01
0.27600000E+05	0.17962703E+04	0.15080275E+04	0.47839564E+08	0.11911390E+01
0.27700000E+05	0.17902415E+04	0.15019988E+04	0.48018860E+08	0.11919061E+01
0.27800000E+05	0.17842339E+04	0.14959911E+04	0.48197604E+08	0.11926768E+01
0.27900000E+05	0.17782458E+04	0.14900032E+04	0.48375700E+08	0.11934510E+01
0.28000000E+05	0.17722803E+04	0.14840375E+04	0.48553232E+08	0.11942288E+01
0.28100000E+05	0.17663357E+04	0.14780929E+04	0.48730196E+08	0.11950099E+01
0.28200000E+05	0.17604122E+04	0.14721693E+04	0.48906508E+08	0.11957947E+01
0.28300000E+05	0.17545134E+04	0.14662706E+04	0.49082272E+08	0.11965823E+01
0.28400000E+05	0.17486359E+04	0.14603929E+04	0.49257392E+08	0.11973735E+01
0.28500000E+05	0.17427826E+04	0.14545398E+04	0.49431964E+08	0.11981677E+01
0.28600000E+05	0.17369551E+04	0.14487123E+04	0.49605976E+08	0.11989648E+01
0.28700000E+05	0.17311506E+04	0.14429078E+04	0.49779376E+08	0.11997652E+01
0.28800000E+05	0.17253717E+04	0.14371289E+04	0.49952188E+08	0.12005686E+01
0.28900000E+05	0.17196196E+04	0.14313768E+04	0.50124440E+08	0.12013745E+01
0.29000000E+05	0.17138918E+04	0.14256492E+04	0.50296120E+08	0.12021835E+01
0.29100000E+05	0.17081918E+04	0.14199489E+04	0.50467240E+08	0.12029953E+01
0.29200000E+05	0.17025183E+04	0.14142755E+04	0.50637756E+08	0.12038095E+01
0.29300000E+05	0.16968719E+04	0.14086292E+04	0.50807736E+08	0.12046264E+01
0.29400000E+05	0.16912532E+04	0.14030103E+04	0.50977128E+08	0.12054460E+01
0.29500000E+05	0.16856633E+04	0.13974207E+04	0.51145996E+08	0.12062676E+01
0.29600000E+05	0.16801012E+04	0.13918584E+04	0.51314256E+08	0.12070920E+01
0.29700000E+05	0.16745691E+04	0.13863262E+04	0.51482020E+08	0.12079185E+01
0.29800000E+05	0.16690642E+04	0.13808215E+04	0.51649192E+08	0.12087473E+01
0.29900000E+05	0.16635901E+04	0.13753473E+04	0.51815848E+08	0.12095782E+01
0.30000000E+05	0.16581455E+04	0.13699026E+04	0.51981904E+08	0.12104113E+01

The plots showing the variations of specific heat at constant pressure, c_p; specific heat at constant volume, c_v; the enthalpy h; and the ratio of specific heats γ with temperature are given in Figures 2.3–2.6, respectively.

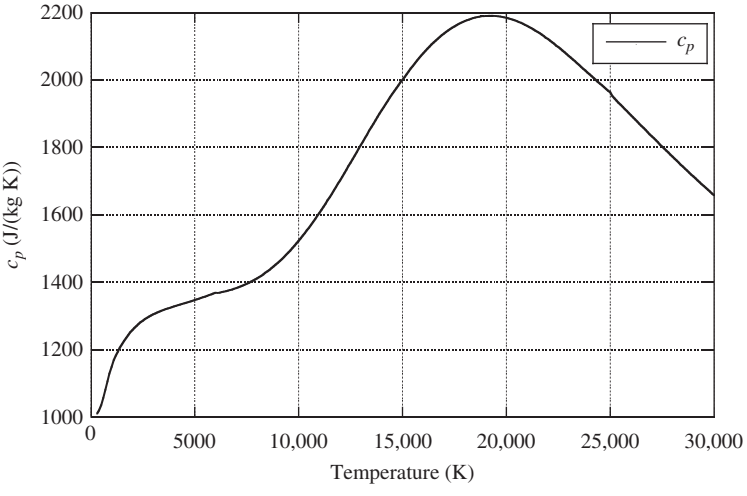

Figure 2.3 Variation of c_p with temperature.

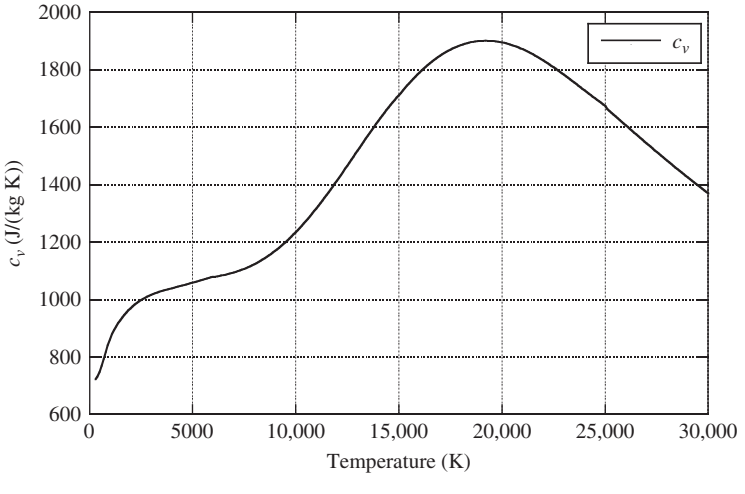

Figure 2.4 Variation of c_v with temperature.

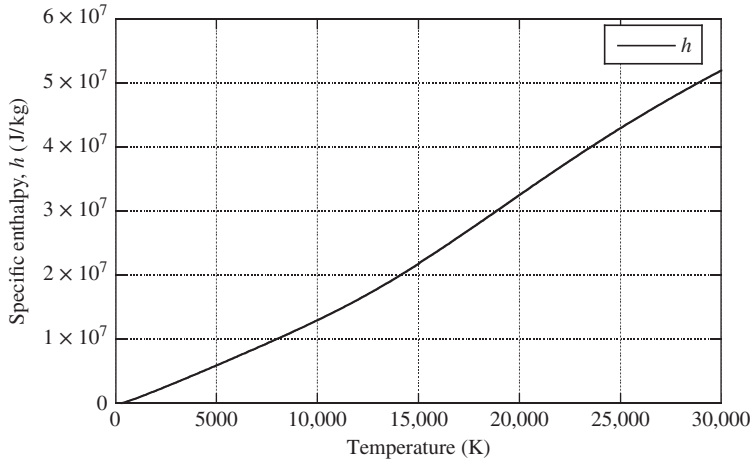

Figure 2.5 Variation of h with temperature.

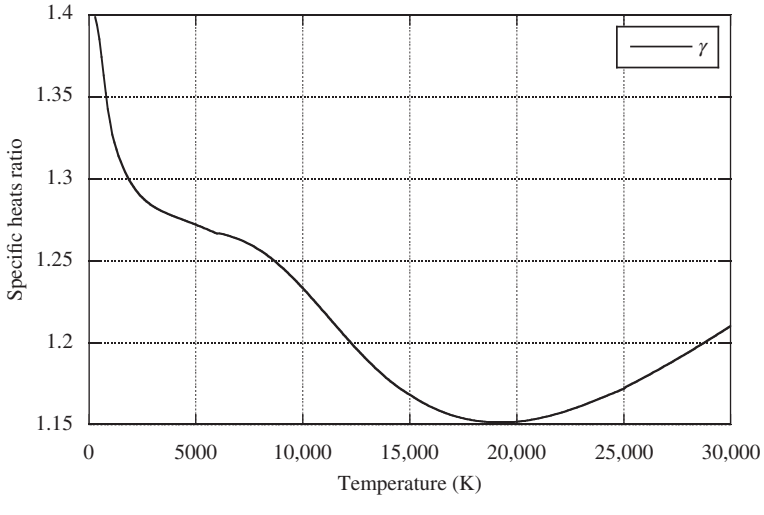

Figure 2.6 Variation of γ with temperature.

Program listing

```
      program cpcvg
      open(unit=80,file='cpcvg.txt',form='formatted')
      write(80,*) '#Temperature(K) cp(J/kg.K) cv(J/kg.K) h(J/kg) gamma'
c     atmosphere condition
      cn20 = 0.7656
      co20 = 0.2344
c
      do i=3,300
         tkel=float(i*100)
         call equair(tkel,cn20,co20,hmx,cpmx,cvmx,gamma)
         write(80,100) tkel,cpmx,cvmx,hmx,gamma
      end do
 100  format(5E16.8)
      close(unit=80)
      stop
      end
c
      subroutine equair(tkel,cn20,co20,hmx,cpmx,cvmx,gamma)
c=====================================================================
c     s-index  :   1   2   3  4  5   6    7   8   9   10   11
c     species  :   N2  O2  N  O  NO  NO+  e-  N+  O+  N2+  O2+
c---------------------------------------------------------------------
c     inputs   :   tkel = temp.(K)
c                  cn20, co20 = free-stream composition (mass fraction)
c---------------------------------------------------------------------
c    outputs   :   hmx = enthalpy of mixture(j/kg)
c                 cpmx = enthalpy of mixture(j/kg)
c                ci(i) = mass fraction     of i-th species (i=1-11)
c                hi(i) = enthalpy           of i-th species (i=1-11)
c               cpi(i) = specific enthalpy of i-th species (i=1-11)
c---------------------------------------------------------------------
c     original code nasa tp2792
c     database for curve fit constants from NASA-TM-102602
c     modified on 14feb2014 for High Enthalpy Book Example
c=====================================================================
      dimension ci(11),cpi(11),hi(11)
      dimension aa(11,7,5),wm(11)
c                           (0) set functions and species constants.
c---------------------------------------------------------------------
c     functions. (cp,h)
c---------------------------------------------------------------------
      cpbyr(i,k,t)= aa(i,1,k)             +aa(i,2,k)*t
     1             +aa(i,3,k)*t**2        +aa(i,4,k)*t**3
     2             +aa(i,5,k)*t**4
      hbyrt(i,k,t)= aa(i,1,k)             +aa(i,2,k)*t   /2.
     1             +aa(i,3,k)*t**2/3.     +aa(i,4,k)*t**3/4.
     2             +aa(i,5,k)*t**4/5.     +aa(i,6,k)/t
c---------------------------------------------------------------------
c          coefficients of the approximating polynomials
c        for the thermodynamic functions (11 species model)
c     divided into five ranges :  300- 1000k, 1000- 6000k,  6000-15000k
c                               ,15000-25000k,25000-30000k.
c---------------------------------------------------------------------
```

```
 data ((aa(i,1,l),l=1,5),i=1,11)/
1  0.36748e+01, 0.32125e+01, 0.31811e+01, 0.96377e+01,-0.51681e+01,
2  0.36146e+01, 0.35949e+01, 0.38599e+01, 0.34867e+01, 0.39620e+01,
3  0.25031e+01, 0.24820e+01, 0.27480e+01,-0.12280e+01, 0.15520e+02,
4  0.28236e+01, 0.25421e+01, 0.25460e+01,-0.97871e-02, 0.16428e+02,
5  0.35887e+01, 0.32047e+01, 0.38543e+01, 0.43309e+01, 0.23507e+01,
6  0.35294e+01, 0.32152e+01, 0.26896e+01, 0.59346e+01,-0.51595e+01,
7  0.25000e+01, 0.25000e+01, 0.25000e+01, 0.25000e+01, 0.25000e+01,
8  0.27270e+01, 0.27270e+01, 0.24990e+01, 0.23856e+01, 0.22286e+01,
9  0.24985e+01, 0.25060e+01, 0.29440e+01, 0.12784e+01, 0.12889e+01,
0  0.35498e+01, 0.33970e+01, 0.33780e+01, 0.43942e+01, 0.39493e+01,
1  0.32430e+01, 0.32430e+01, 0.51690e+01,-0.28017e+00, 0.20445e+01/
 data ((aa(i,2,l),l=1,5),i=1,11)/
1 -0.12081e-02, 0.10137e-02, 0.89745e-03,-0.25728e-02, 0.23337e-02,
2 -0.18598e-02, 0.75213e-03, 0.32510e-03, 0.52384e-03, 0.39446e-03,
3 -0.21800e-04, 0.69258e-04,-0.39090e-03, 0.19268e-02,-0.38858e-02,
4 -0.89478e-03,-0.27551e-04,-0.59520e-04, 0.12450e-02,-0.39313e-02,
5 -0.12479e-02, 0.12705e-02, 0.23409e-03,-0.58086e-04, 0.58643e-03,
6 -0.30342e-03, 0.99742e-03, 0.13796e-02,-0.13178e-02, 0.26290e-02,
7  0.00000e+00, 0.00000e+00, 0.00000e+00, 0.00000e+00, 0.00000e+00,
8 -0.28200e-03,-0.28200e-03,-0.37250e-05, 0.83495e-04, 0.12458e-03,
9  0.11411e-04,-0.14464e-04,-0.41080e-03, 0.40866e-03, 0.43343e-03,
0 -0.60810e-03, 0.45250e-03, 0.86290e-03, 0.18868e-03, 0.36795e-03,
1  0.11740e-02, 0.11740e-02,-0.86200e-03, 0.16674e-02, 0.10313e-02/
 data ((aa(i,3,l),l=1,5),i=1,11)/
1  0.23240e-05,-0.30467e-06,-0.20216e-06, 0.33020e-06,-0.12953e-06,
2  0.70814e-05,-0.18732e-06,-0.92131e-08,-0.39123e-07,-0.29506e-07,
3  0.54205e-07,-0.63065e-07, 0.13380e-06,-0.24370e-06, 0.32288e-06,
4  0.83060e-06,-0.31028e-08, 0.27010e-07,-0.16154e-06, 0.29840e-06,
5  0.39786e-05,-0.46603e-06,-0.21354e-07, 0.28059e-07,-0.31316e-07,
6  0.38544e-06,-0.29030e-06,-0.33985e-06, 0.23297e-06,-0.16254e-06,
7  0.00000e+00, 0.00000e+00, 0.00000e+00, 0.00000e+00, 0.00000e+00,
8  0.11050e-06, 0.11050e-06, 0.11470e-07,-0.58815e-08,-0.87636e-08,
9 -0.29761e-07, 0.12446e-07, 0.91560e-07,-0.21731e-07,-0.26758e-07,
0  0.14690e-05, 0.12720e-06,-0.12760e-06,-0.71272e-08,-0.26910e-07,
1 -0.39000e-06,-0.39000e-06, 0.20410e-06,-0.12107e-06,-0.74046e-07/
 data ((aa(i,4,l),l=1,5),i=1,11)/
1 -0.63218e-09, 0.41091e-10, 0.18266e-10,-0.14315e-10, 0.27872e-11,
2 -0.68070e-08, 0.27913e-10,-0.78684e-12, 0.10094e-11, 0.73975e-12,
3 -0.56476e-10, 0.18387e-10,-0.11910e-10, 0.12193e-10,-0.96053e-11,
4 -0.16837e-09, 0.45511e-11,-0.27980e-11, 0.80380e-11,-0.81613e-11,
5 -0.28651e-08, 0.75007e-10, 0.16689e-11,-0.15694e-11, 0.60495e-12,
6  0.10519e-08, 0.36925e-10, 0.33776e-10,-0.11733e-10, 0.39381e-11,
7  0.00000e+00, 0.00000e+00, 0.00000e+00, 0.00000e+00, 0.00000e+00,
8 -0.15510e-10,-0.15510e-10,-0.11020e-11, 0.18850e-12, 0.26204e-12,
9  0.32247e-10,-0.46858e-11,-0.58480e-11, 0.33252e-12, 0.62159e-12,
0 -0.65091e-10,-0.38790e-10, 0.80870e-11,-0.17511e-12, 0.67110e-12,
1  0.54370e-10, 0.54370e-10,-0.13000e-10, 0.32113e-11, 0.19257e-11/
 data ((aa(i,5,l),l=1,5),i=1,11)/
1 -0.22577e-12,-0.20170e-14,-0.50334e-15, 0.20333e-15,-0.21360e-16,
2  0.21628e-11,-0.15774e-14, 0.29426e-16,-0.88718e-17,-0.64209e-17,
3  0.20999e-13,-0.11747e-14, 0.33690e-15,-0.19918e-15, 0.95472e-16,
4 -0.73205e-13,-0.43681e-15, 0.93800e-16,-0.12624e-15, 0.75004e-16,
```

```
     5  0.63015e-12,-0.42314e-14,-0.49070e-16, 0.24104e-16,-0.40557e-17,
     6 -0.72777e-12,-0.15994e-14,-0.10427e-14, 0.18402e-15,-0.34311e-16,
     7  0.00000e+00, 0.00000e+00, 0.00000e+00, 0.00000e+00, 0.00000e+00,
     8  0.78470e-15, 0.78470e-15, 0.30780e-16,-0.16120e-17,-0.21674e-17,
     9 -0.12376e-13, 0.65549e-15, 0.11900e-15, 0.63160e-18,-0.45131e-17,
     0 -0.35649e-12, 0.24590e-14,-0.18800e-15, 0.67176e-17,-0.58244e-17,
     1 -0.23920e-14,-0.23920e-14, 0.24940e-15,-0.28349e-16,-0.17461e-16/
      data ((aa(i,6,l),l=1,5),i=1,11)/
     1 -0.10430e+04,-0.10430e+04,-0.10430e+04,-0.10430e+04,-0.10430e+04,
     2 -0.10440e+04,-0.10440e+04,-0.10440e+04,-0.10440e+04,-0.10440e+04,
     3  0.56130e+05, 0.56130e+05, 0.56130e+05, 0.56130e+05, 0.56130e+05,
     4  0.29150e+05, 0.29150e+05, 0.29150e+05, 0.29150e+05, 0.29150e+05,
     5  0.97640e+04, 0.97640e+04, 0.97640e+04, 0.97640e+04, 0.97640e+04,
     6  0.11840e+06, 0.11840e+06, 0.11840e+06, 0.11840e+06, 0.11840e+06,
     7 -0.74542e+03,-0.74542e+03,-0.74542e+03,-0.74542e+03,-0.74542e+03,
     8  0.22540e+06, 0.22540e+06, 0.22540e+06, 0.22540e+06, 0.22540e+06,
     9  0.18790e+06, 0.18790e+06, 0.18790e+06, 0.18790e+06, 0.18790e+06,
     0  0.18260e+06, 0.18260e+06, 0.18260e+06, 0.18260e+06, 0.18260e+06,
     1  0.14000e+06, 0.14000e+06, 0.14000e+06, 0.14000e+06, 0.14000e+06/
      data ((aa(i,7,l),l=1,5),i=1,11)/
     1  0.23580e+01, 0.43661e+01, 0.46264e+01,-0.37587e+02, 0.66217e+02,
     2  0.43628e+01, 0.38353e+01, 0.23789e+01, 0.48179e+01, 0.13985e+01,
     3  0.41676e+01, 0.42618e+01, 0.28720e+01, 0.28469e+02,-0.88120e+02,
     4  0.35027e+01, 0.49203e+01, 0.50490e+01, 0.21711e+02,-0.94358e+02,
     5  0.51497e+01, 0.66867e+01, 0.31541e+01, 0.10735e+00, 0.14026e+02,
     6  0.37852e+01, 0.51508e+01, 0.83904e+01,-0.11079e+02, 0.65896e+02,
     7 -0.11734e+02,-0.11734e+02,-0.11733e+02,-0.11733e+02,-0.11733e+02,
     8  0.36450e+01, 0.36450e+01, 0.49500e+01, 0.56462e+01, 0.67811e+01,
     9  0.43864e+01, 0.43480e+01, 0.17500e+01, 0.12761e+02, 0.12604e+02,
     0  0.36535e+01, 0.42050e+01, 0.40730e+01,-0.23693e+01, 0.65472e+00,
     1  0.59250e+01, 0.59250e+01,-0.59260e+01, 0.31013e+02, 0.14310e+02/
c-----------------------------------------------------------------------
c                                                  * molecular weight
      data wm / 28.,32.,14.,16.,30.,30.,0.0005486,14.,16.,28.,32./
c-----------------------------------------------------------------------
c                            (1) set constants.
      runiv = 8.31441
c                            (2) choose range for thermodynamic func.
      k=1
      if(tkel .gt.  1000.) k=2
      if(tkel .gt.  6000.) k=3
      if(tkel .gt. 15000.) k=4
      if(tkel .gt. 25000.) k=5
c                            (3) compute cp(i),h(i)
      do 300 i=1,11
       cpi(i)= cpbyr(i,k,tkel)*(runiv*1000./wm(i))
        hi(i)= hbyrt(i,k,tkel)*(runiv*1000./wm(i))*tkel
  300 continue
c                            (4) mol/mass fraction
      do 400 i=1,11
         ci(i) = 0.
  400  continue
      ci(1) = cn20
      ci(2) = co20
```

```
c                              (5) cp & h of mixture
        hmx=0.0
       cpmx=0.0
       cvmx=0.0
      do 500 i=1,11
        cpmx=cpmx+cpi(i)*ci(i)
        cvmx=cvmx+(cpi(i)-runiv*1000./wm(i))*ci(i)
         hmx= hmx+ hi(i)*ci(i)
  500 continue
      gamma = cpmx/cvmx
c
      return
      end
```

■

2.6 Summary

The energy concept plays an important role in the study of compressible flows. In other words, the study of thermodynamics that deals with energy (and entropy) is an essential component in the study of compressible flow.

Fluid mechanics of perfect fluids is an extension of equilibrium thermodynamics to moving fluids. The kinetic energy of the fluid has to be considered in addition to the internal energy that the fluid possesses even when at rest.

Fluid mechanics of real fluids is the science of fluid flow where the transport processes of momentum and heat (energy) are of primary interest.

The difference between the static and stagnation temperatures is not significant in low-speed flows. But in high-speed flows, the difference between the static and stagnation temperature can become substantial.

The first law of thermodynamics states that *"the heat added minus work done by the system is equal to the change in the internal energy of the system,"* that is,

$$\boxed{\delta Q - \delta W = dU}$$

Adiabatic process – a process in which no heat is added to or taken away from the system.

Reversible process – a process that can be reversed without leaving any trace on the surroundings, that is, both the system and the surroundings are returned to their initial states at the end of the reverse process.

Isentropic process – a process that is adiabatic and reversible.

For an open system (for example, pipe flow), there is always a term $(U + p\,\mathbb{V})$ instead of just U. This term is referred to as *enthalpy* or *heat function H* given by

$$H = U + p\,\mathbb{V}$$

The mass that enters or leaves an open system has kinetic energy, whereas there is no mass transfer possible across the boundaries of a closed system.

The mass can enter and leave an open system at different levels of potential energy.

Open systems are capable of delivering work continuously, because, in the system, the medium that transforms energy is continuously replaced. This useful work, which a machine continuously delivers, is called the *shaft work*.

The energy equation for an open system is

$$\boxed{H_1 + \frac{m}{2} V_1^2 + m\, g\, z_1 = H_2 + \frac{m}{2} V_2^2 + m\, g\, z_2 + W_s - Q_{12}}$$

This equation is universally valid. This is the expression of the first law of thermodynamics for any open system.

In general,

$$\boxed{h + \frac{V^2}{2} = h_0 = \text{constant}}$$

For a closed system,

$$Q_{12} - W_{12} = U_2 - U_1$$

The entropy is defined as

$$ds = \frac{\delta q_{\text{rev}}}{T}$$

An alternative and probably more lucid relation is

$$\boxed{ds = \frac{\delta q}{T} + ds_{\text{irrev}}}$$

This applies in general to all processes. It states that the change in entropy during any process is equal to the actual heat added, δq; divided by the temperature, $\delta q/T$; plus a contribution from the irreversible dissipative phenomena of viscosity, thermal conductivity, and mass diffusion occurring within the system, ds_{irrev}. These dissipative phenomena always cause increase of entropy, that is,

$$ds_{\text{irrev}} \geq 0$$

The equal sign in the inequality denotes a reversible process where, by definition, the above dissipative phenomena are absent.

For adiabatic process, $\delta q = 0$, and hence,

$$ds \geq 0$$

If $ds > 0$, the process is called an *irreversible process*, and when $ds = 0$, the process is called a *reversible process*. A reversible and adiabatic process is called an *isentropic process*.

The equation $pv = RT$ or $p/\rho = RT$ is called *thermal equation of state*, where p, T, and $v(1/\rho)$ are *thermal properties* and R is the gas constant. Any relation between

the calorical properties, u, h, and s, and any two thermal properties is called *calorical equation of state*.

If heat is added at constant volume, it only raises the internal energy.

If heat is added at constant pressure, it not only increases the internal energy but also does some external work, that is, it increases the enthalpy.

If the change is adiabatic, the change in enthalpy is equal to external work $v\ dp$.

A gas is said to be thermally perfect when its internal energy and enthalpy are functions of temperature alone.

A gas with constant c_p and c_v is called a *calorically perfect gas*. Therefore, a perfect gas should be thermally as well as calorically perfect.

Entropy is defined by the relation (for a reversible process)

$$\delta q = T\ ds$$

For the most simple molecular model, the kinetic theory of gases gives the specific heats ratio, γ, as

$$\boxed{\gamma = \frac{n+2}{n}}$$

where n is the number of degrees of freedom of the gas molecules.

For monatomic gases with $n = 3$,

$$\gamma = \frac{3+2}{3} = 1.67$$

Diatomic gases, such as oxygen and nitrogen, have $n = 5$; thus

$$\gamma = \frac{5+2}{5} = 1.4$$

Gases with extremely complex molecules, such as freon and gaseous compounds of uranium, have large values of n, resulting in values of γ only slightly greater than unity. Thus, the value of specific heats ratio γ varies from 1 to 1.67, depending on the molecular nature of the gas, that is,

$$\boxed{1 \leq \gamma \leq 1.67}$$

$$\boxed{\frac{\gamma}{\gamma - 1}\frac{p}{\rho} + \frac{V^2}{2} = \text{constant}}$$

is the form of energy equation commonly used in gas dynamics. This is popularly known as *compressible Bernoulli's equation* for isentropic flows.

An adiabatic and reversible process is called *isentropic process*.

The ratio of total to static temperature at a point in an isentropic flow field as a function of the flow Mach number M is

$$\boxed{\frac{T_0}{T} = 1 + \frac{\gamma - 1}{2} M^2}$$

The ratio of total to static pressure in terms of M is

$$\boxed{\frac{p_0}{p} = \left(1 + \frac{\gamma - 1}{2} M^2\right)^{\gamma/(\gamma-1)}}$$

The ratio of total to static density in terms of M is

$$\boxed{\frac{\rho_0}{\rho} = \left(1 + \frac{\gamma - 1}{2} M^2\right)^{1/(\gamma-1)}}$$

The entropy change can be expressed as

$$\boxed{s_{02} - s_{01} = R \ \ln\left(\frac{p_{01}}{p_{02}}\right)}$$

This implies that the entropy changes only when there are losses in pressure. It does not change with velocity, and hence, there is nothing like static and stagnation entropy.

The following are the limitations to treat air as a perfect gas, obeying both thermal state equation and calorical state equations.

- When the temperature is less than 500 K, air can be treated as a perfect gas and the ratio of specific heats, γ, takes a constant value of 1.4.
- When the temperature lies between 500 and 2000 K, air is only thermally perfect, and the state equation $p = \rho RT$ is valid, but c_p and c_v become functions of temperature, $c_p = c_p(T)$ and $c_v = c_v(T)$. Even though c_p and c_v are functions of temperature, their ratio γ continues to be independent of temperature. That is, c_p and c_v vary with temperature in such a manner that their ratio continues to be the same constant as in temperatures below 500 K.
- For temperatures more than 2000 K, air becomes both thermally and calorically imperfect. That is, c_p, c_v, as well as γ become functions of temperature.

Exercise Problems

2.1 Oxygen gas is heated from 25 to 125°C. Determine the increase in its internal energy and enthalpy.

[Answer: $\Delta u = 64{,}950$ J/(kg K), $\Delta h = 90{,}930$ J/(kg K)]

2.2 Air enters a compressor at 100 kPa and 1.175 kg/m^3 and exits at 500 kPa and 5.875 kg/m^3. Determine the enthalpy difference between the outlet and inlet states.
[Answer: 0]

2.3 Air undergoes a change of state isentropically from 300 K and 110 kPa to a final pressure of 550 kPa. Assuming ideal gas behavior, determine the change in enthalpy.
[Answer: 176.19 kJ/kg]

2.4 If the entropy of a gas of volume 5.0 L, initially at 400 K and 1.12 bar, goes up by 0.787 J/(K mol), what is the final volume of the gas?
[Answer: 8.772 L]

2.5 At a temperature of 30°C, 0.5 mol of an ideal gas is expanded isothermally and reversibly from 10 to 20 L. Determine the heat transfer and work associated with this process.
[Answer: 873.5 J, −873.5 J]

2.6 Find the work required to lift a mass of 80 kg by 15 m above the ground level.
[Answer: 11,772 J]

2.7 Describe the internal energy change and work done when a spring is (a) compressed and (b) expanded.
[Answer: (a) $W > 0$, (b) $W < 0$]

2.8 Calculate the internal energy of 1 mol of argon at 300 K. Assume the atoms behave as an ideal gas.
[Answer: 3741.3 J/mol]

2.9 Calculate the internal energy of 1 mol of hydrogen at 300 K. Assume the molecules behave as an ideal gas.
[Answer: 6235.5 J/mol]

2.10 A gas expands against a constant external pressure and does 25 kJ of expansion work on the surroundings. During the process, 60 kJ of heat is absorbed by the system. Determine the changes in enthalpy and internal energy of the gas.
[Answer: $\Delta H = 60$ kJ, $\Delta U = 35$ kJ]

2.11 A 100 L vessel, containing 6 mol of hydrogen gas at 2 atm, is cooled to 203 K. Assuming the gas behaves ideally, calculate the changes in internal energy and enthalpy associated with this cooling process.
[Answer: $\Delta U = -25.346$ kJ, $\Delta H = -35.484$ kJ]

2.12 Argon gas of volume 200 L, at 140 kPa and 10°C, undergoes a polytropic process leading to 700 kPa and 180°C. Find the heat transfer associated with this process.

[Answer: −15.637 kJ]

2.13 Unit mass of nitrogen is heated in an isobaric process from $T_1 = 300$ K to $T_2 = 1000$ K. Calculate the enthalpy change during this process, treating nitrogen as a perfect gas.

[Answer: 727.475 kJ]

2.14 Air in a cylinder changes state from 101 kPa and 310 K to a pressure of 1100 kPa according to the process

$$pv^{1.32} = \text{constant}$$

Determine the entropy change associated with this process. Assume air to be an ideal gas with $c_p = 1004$ J/(kg K) and $\gamma = 1.4$.

[Answer: −103.8 J/(kg K)]

References

[1] Rathakrishnan E., *Applied Gas Dynamics*, John Wiley & Sons, Inc., Hoboken, NJ, 2010.
[2] Rathakrishnan E., *Gas Tables*, 3rd ed. Universities Press, Hyderabad, India, 2012.
[3] Rathakrishnan E., *Fundamentals of Engineering Thermodynamics*, 2nd ed. PHI Learning, Delhi, India, 2005.

3

Wave Propagation

3.1 Introduction

We know that in incompressible flows, the fluid particles will be able to sense the presence of a body before actually reaching it. This fact suggests that a signaling mechanism exists, whereby the fluid particles can be informed, in advance, about the presence of a body ahead of them. The velocity of propagation of this signal must be apparently greater than the fluid velocity, because the flow is able to adjust to the presence of a body before reaching it. On the other hand, if the fluid particles were moving faster than the signal waves as in the case of supersonic flows, the fluid would not be able to sense the body before actually reaching it and abrupt changes in velocity and other properties would take place.

An understanding of the mechanism by which the signal waves are propagating through fluid medium along with an expression for the velocity of propagation of the waves will be extremely useful in deriving significant conclusions concerning the fundamental differences between incompressible and compressible flows.

When a fluid medium is allowed to vary its density, the consequence is that the fluid elements will be able to occupy varying volumes in space. This possibility means that a set of fluid elements can spread into a larger region of space without requiring a simultaneous shift to be made to all fluid elements in the flow field, as would be required in the case of incompressible flow, in order to keep the density constant. From studies on physics, we know that a small shift of fluid elements in compressible media will induce in due course similar small movements in adjacent elements, and in this way, a disturbance, referred to as an *acoustic wave*, propagates at a relatively high speed through the medium. Furthermore, in incompressible flows, these waves propagate with infinitely large velocity; in other words, adjustments take place instantaneously throughout the flow, and so in the conventional sense, there are no acoustic or elastic waves to be considered. With the introduction of compressibility, we thus permit the possibility of elastic waves having a finite velocity, and the magnitude of this wave velocity is of great importance in compressible flow theory.

High Enthalpy Gas Dynamics, First Edition. Ethirajan Rathakrishnan.

www.wiley.com/go/rathakrishnan

3.2 Velocity of Sound

A *sound wave* is a weak compression wave across which only infinitesimal changes in flow properties occur, that is, across these waves there will be only infinitesimal pressure variations. In the ensuing chapters, we shall study waves where comparatively large pressure variation occurs over a very narrow front. Such waves are called *shock waves*, the flow process across them is nonisentropic and move relative to the fluid at speeds that exceed the speed of sound. At this stage, one may think of the sound waves as limiting cases of shock waves where the change in pressure across the wave becomes infinitesimal.

From Equation (1.16), we have the speed of sound as $a = \sqrt{\gamma RT}$, where T is the static temperature of the medium in absolute unit. The speed of sound in perfect gas may be computed by employing Equation (1.16) and for the other fluids by employing Equation (1.12).

3.3 Subsonic and Supersonic Flows

The velocity of sound is used as the limiting value for differentiating the subsonic flow from the supersonic flow. Flows with velocity more than the speed of sound are called *supersonic flows*, and those with velocities less than the speed of sound are called *subsonic flows*. Flows with velocity close to the speed of sound are classified under a special category called *transonic flows*.

We saw the propagation of disturbance waves in flow fields with velocities from zero level to a level greater than the speed of sound and that these disturbances will propagate along a 'Mach-cone'. For supersonic flow over two-dimensional objects, we will have a 'Mach-wedge' instead of Mach-cone. The angle μ for such waves is measured in a counterclockwise manner from an axis taken parallel to the direction of freestream as shown in Figure 3.1.

For an observer looking in the direction of flow toward the disturbance, the wave to his\her left is called *left-running wave* and the wave to his\her right is called *right-running wave* (Figure 3.1). Usually, the disturbance arises at a solid boundary where the fluid, having arrived supersonically without prior warning

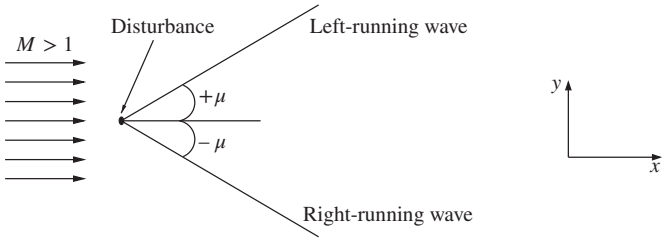

Figure 3.1 Waves in supersonic flows.

through pressure or sound signals, is made to undergo a change in direction, thus initiating a disturbance at the boundary that propagates along the Mach waves.

For historical interest, we should mention that Newton was the first to calculate the propagation speed of pressure waves. On the basis of the assumed isothermal process in a perfect gas, he found the speed of propagation of sound to be equal to the square root of the ratio of the pressure to the corresponding density involved in the process, that is,

$$a = \sqrt{\frac{p}{\rho}}$$

Because the science of thermodynamics was not known at Newton's time, the 117% difference between his theory and experiment was never justified.

Nearly a century later, Marquis de Laplace rectified Newton's calculation. The basic difference between Laplace's theory and Newton's theory is that the former considered an adiabatic process for propagation of pressure waves. This is fully justified because the compressions taking place in the propagation of pressure waves produce a very small temperature gradient, and hence, it is not possible for heat due to compression to be transferred to the surrounding region. The correction by Laplace from adiabatic process model multiplied Newton's formula by $\sqrt{\gamma}$. The correct expression for speed of sound is $a = \sqrt{\gamma RT}$, which is the same as Equation (1.16).

Example 3.1 Find the error in the speed of sound in air calculated with Newton's formula instead of the correct relation (Equation (1.16)), when (a) $p = 1$ atm, $T = 15°\text{C}$; (b) $p = 1$ atm, $T = 30°\text{C}$; and (c) $p = 10$ atm, $T = 300$ K.

Solution

(a) Given $p = 101{,}325$ Pa and $T = 15 + 273.15 = 288.15$ K.
The density is

$$\begin{aligned}\rho &= \frac{p}{RT} \\ &= \frac{101{,}325}{287 \times 288.15} \\ &= 1.225 \text{ kg/m}^3\end{aligned}$$

The speed of sound by Newton's relation is

$$\begin{aligned}a_{\text{Newton}} &= \sqrt{\frac{p}{\rho}} \\ &= \sqrt{\frac{101{,}325}{1.225}} \\ &= 287.60 \text{ m/s}\end{aligned}$$

By Equation (1.16),

$$\begin{aligned} a_{\text{isentropic}} &= \sqrt{\gamma RT} \\ &= \sqrt{1.4 \times 287 \times 288.15} \\ &= 340.26 \text{ m/s} \end{aligned}$$

The error is

$$\begin{aligned} \text{Error} &= \frac{a_{\text{isentropic}} - a_{\text{Newton}}}{a_{\text{isentropic}}} \\ &= \frac{340.26 - 287.60}{340.26} \\ &= 0.1548 \\ &= \boxed{15.48\%} \end{aligned}$$

(b) Given $p = 101{,}325$ Pa and $T = 30 + 273.15 = 303.15$ K. Therefore,

$$\begin{aligned} \rho &= \frac{p}{RT} \\ &= \frac{101{,}325}{287 \times 303.15} \\ &= 1.165 \text{ kg/m}^3 \end{aligned}$$

The speed of sound by Newton's relation is

$$\begin{aligned} a_{\text{Newton}} &= \sqrt{\frac{p}{\rho}} \\ &= \sqrt{\frac{101{,}325}{1.165}} \\ &= 294.91 \text{ m/s} \end{aligned}$$

By Equation (1.16),

$$\begin{aligned} a_{\text{isentropic}} &= \sqrt{\gamma RT} \\ &= \sqrt{1.4 \times 287 \times 303.15} \\ &= 349.01 \text{ m/s} \end{aligned}$$

The error is

$$\begin{aligned} \text{Error} &= \frac{a_{\text{isentropic}} - a_{\text{Newton}}}{a_{\text{isentropic}}} \\ &= \frac{349.01 - 294.91}{349.01} \\ &= 0.1550 \\ &= \boxed{15.5\%} \end{aligned}$$

(c) Given $p = 10 \times 101{,}325$ Pa and $T = 300$ K. Therefore,

$$\begin{aligned}\rho &= \frac{p}{RT} \\ &= \frac{10 \times 101{,}325}{287 \times 300} \\ &= 11.77 \text{ kg/m}^3\end{aligned}$$

The speed of sound by Newton's relation is

$$\begin{aligned}a_{\text{Newton}} &= \sqrt{\frac{p}{\rho}} \\ &= \sqrt{\frac{10 \times 101{,}325}{11.77}} \\ &= 293.41 \text{ m/s}\end{aligned}$$

By Equation (1.16)

$$\begin{aligned}a_{\text{isentropic}} &= \sqrt{\gamma RT} \\ &= \sqrt{1.4 \times 287 \times 300} \\ &= 347.19 \text{ m/s}\end{aligned}$$

The error is

$$\begin{aligned}\text{Error} &= \frac{a_{\text{isentropic}} - a_{\text{Newton}}}{a_{\text{isentropic}}} \\ &= \frac{347.19 - 293.41}{347.19} \\ &= 0.1549 \\ &= \boxed{15.49\%}\end{aligned}$$

■

Example 3.2 Devise a direct procedure to obtain the error in the speed of sound in air calculated with Newton's formula instead of the correct relation (Equation (1.16)), demonstrated in Example 3.1.

Solution

The speed of sound by Newton's formula is

$$\begin{aligned}a_{\text{Newton}} &= \sqrt{\frac{p}{\rho}} \\ &= \sqrt{\frac{\rho RT}{\rho}} \\ &= \sqrt{RT}\end{aligned}$$

The speed of sound by Equation (1.16) is

$$a_{\text{isentropic}} = \sqrt{\gamma RT}$$

Thus the error between a_{Newton} and $a_{\text{isentropic}}$ is

$$\text{Error} = \frac{a_{\text{isentropic}} - a_{\text{Newton}}}{a_{\text{isentropic}}}$$

$$= \frac{\sqrt{\gamma RT} - \sqrt{RT}}{\sqrt{\gamma RT}}$$

$$= 1 - \frac{1}{\sqrt{\gamma}}$$

Thus, for $\gamma = 1.4$, the error is

$$\text{Error} = 1 - \frac{1}{\sqrt{1.4}}$$

$$= 0.1548457$$

$$= \boxed{15.48457\%}$$

Note that the value of the error in a is the same in all the three cases in Example 3.1, because the error is a function of γ only. However, due to the truncation error, there is some difference in the error for the three cases. ■

3.4 Similarity Parameters

In our discussions in the previous chapters, we saw the Mach number M as a primary parameter that dictates the flow pattern in the compressible regime of flow. In the chapters to follow, it will be seen that M is also a parameter that appears almost in all equations of motion. Here the aim is to show that M is an important parameter for experimental studies too.

Let us consider a prototype and a model that are geometrically similar. Now, it is our interest to find the condition that must be met in order to have the flow pattern around the model to be similar to that around the prototype. Examining the energy equation and taking into account the effect of viscosity and heat conductivity, it can be shown that the specific heats ratio, γ, must be the same for both the model and prototype flow fields. Thus, it can be concluded that the Mach number, M, must be the same for the model and prototype if the flows are to be similar. When viscous effects are finite, an analysis applied to the inertia and viscous terms in the momentum equation leads to the criterion that the Reynolds number must be the same for ensuring similarity of flow pattern around the model and the prototype.

Thus, by considering all the physical equations that govern the flow, namely, the continuity, momentum, and energy equation and the equations of state (the thermal and calorical state equations), it is possible to arrive at the following four dimensionless parameters that must be the same for dynamic similarity of the model and prototype flow fields.

- Mach number, $M = \frac{V}{a}$
- Reynolds number, $Re_L = \frac{\rho VL}{\mu}$
- Ratio of specific heats, $\gamma = \frac{c_p}{c_v}$
- Prandtl number, $Pr = \frac{\mu c_p}{k}$

where V is the flow velocity, a is speed of sound, ρ is the flow density, L is a characteristic dimension of the body in the flow, μ is the viscosity coefficient, c_p is specific heat at constant pressure, c_v is specific heat at constant volume, and k is the thermal conductivity of the fluid.

In the potential flow region outside the boundary layer, where the viscous and heat conduction effects are relatively unimportant, it is usually necessary that only M and γ are to be the same between the model and prototype flow fields to establish similarity. Of the two, similarity in M is more important than γ, because γ has a relatively weak influence on the flow pattern.

Within the boundary layer, or in the interior of shock waves, viscous and heat conduction effects are significant. Hence, the Reynolds number and Prandtl number must also be included in the similarity conditions. But the Prandtl number is nearly the same for all gases and varies only slowly with temperature.

3.5 Continuum Hypothesis

From the kinetic theory of gases, we know that matter is made up of a large number of molecules that are in constant motion and collision. But in the problems of engineering interest, we are concerned only with the gross behavior of the fluid, thought of as a continuous material and not in the motion of the individual molecules of the fluid. Even though the postulation of continuous fluid (continuum) is only a convenient assumption, it is a valid approach to many practical problems where only the macroscopic or phenomenological information is of interest. The assumption of fluids as continua is valid only when the smallest volume of fluid of interest contains large number of molecules so that the statistical averages are meaningful. The advantage of continuum treatment is that instead of dealing with the instantaneous states of large number of molecules, we have to deal with only certain properties describing the gross behavior of the substance. In compressible flows, the relevant properties are the density, pressure, temperature, velocity, shear stress, coefficient of viscosity, internal energy, entropy, and coefficient of thermal conductivity. The macroscopic approach with continuum hypothesis will fail whenever the mean free path of the molecules is of the same order of the smallest significant dimension of the problem

under consideration. The flow in which the mean free path of the molecules is of the same order or more than the characteristic dimension of the problem is termed *rarefied flow*. To deal with highly rarefied gases, we should resort to microscopic approach of kinetic theory, because the continuum approach of classical fluid mechanics and thermodynamics is not valid there.

In order to determine whether the condition of continuum is valid, let us consider a steady flow and perform some approximate calculations of order-of-magnitude nature.

With kinetic theory, it can be shown using an order-of-magnitude approach that the viscosity coefficient μ can be expressed as

$$\mu \approx \rho\, \bar{c}\, \lambda$$

and

$$\bar{c} \approx a$$

where $\bar{c}$ is the mean molecular velocity, λ is the mean free path, and a is the speed of sound.

The Reynolds number of a flying vehicle can be expressed as

$$\begin{aligned} Re_L &= \frac{\rho V L}{\mu} \\ &= \frac{\rho \bar{c} \lambda}{\mu}\ \frac{V}{a}\ \frac{a}{\bar{c}}\ \frac{L}{\lambda} \\ &\approx \frac{V}{a}\ \frac{L}{\lambda} \end{aligned}$$

where L is a characteristic length of the vehicle. But $V/a = M$; therefore,

$$\frac{L}{\lambda} \approx \frac{Re_L}{M} \tag{3.1}$$

Equation (3.1) shows that the ratio of Reynolds number to Mach number is a dimensionless parameter indicative of whether a given problem is amenable to the continuum approach or not. From this ratio, it is seen that the continuum hypothesis is likely to fail when the Mach number is very large or the Reynolds number is extremely low. But we have to exercise caution while using Equation (3.1), because Re_L and M depend on the nature of the problem considered. For example, when Re_L is very low owing to low density, the continuum hypothesis is not valid, whereas when it is very low due to high viscosity, the continuum concept is perfectly valid and such a flow is termed *stratified flow*. However, the rules for determining the validity of the continuum concept in terms of Re_L and M can be illustrative by supposing that in a given problem, the smallest *significant* body dimension is of the order of the boundary layer thickness, δ. If Re_L is large compared to unity and if the boundary layer flow is also laminar, then the boundary layer relations for a flat plate gives that

$$\frac{\delta}{L} \approx \frac{1}{\sqrt{Re_L}}$$

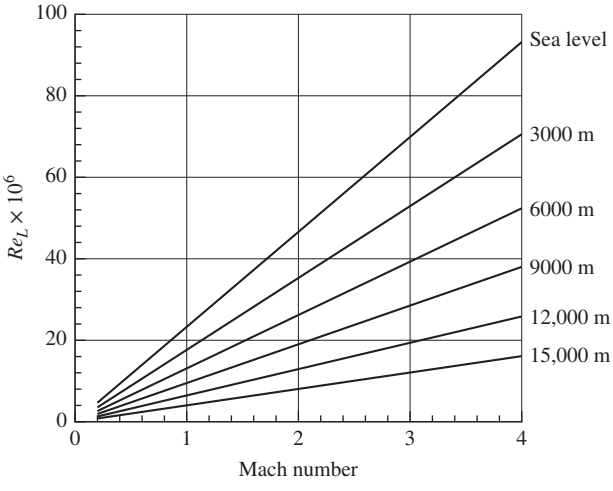

Figure 3.2 Reynolds number per meter versus Mach number, based on standard atmosphere [2].

Using Equation (3.1), this can be expressed as

$$\frac{\delta}{\lambda} \approx \frac{\sqrt{Re_L}}{M}$$

For this case, Tsien [1] suggests that the realm of continuum gas dynamics be limited to instances where the boundary layer thickness is at least 100 times the mean free path. That is,

$$\frac{\sqrt{Re_L}}{M} > 100$$

Figure 3.2 shows the Reynolds number per unit length as a function of flight Mach number for various altitudes, based on the standard atmosphere.

3.6 Compressible Flow Regimes

The compressible flow regime can be subdivided into different zones based on the local flow velocity and the local speed of sound. To do this classification, we can make use of the energy equation as follows.

Consider a streamtube in a steady compressible flow in which the flow does not exchange heat with the fluid in neighboring streamtubes, that is, the flow process is adiabatic. The steady-flow energy equation for the adiabatic flow through such a streamtube is

$$h + \frac{V^2}{2} = h_0$$

where h and h_0 are the static and stagnation enthalpies, respectively, and V is the flow velocity. For a perfect gas, $h = c_p T$; therefore,

$$c_p T + \frac{V^2}{2} = c_p T_0$$

But $c_p = \frac{\gamma}{\gamma - 1} R$ for perfect gases; thus,

$$\frac{\gamma}{\gamma - 1} RT + \frac{V^2}{2} = \frac{\gamma}{\gamma - 1} RT_0$$

This simplifies to

$$\boxed{V^2 + \frac{2}{\gamma - 1} a^2 = \frac{2}{\gamma - 1} a_0^2 = V_{\max}^2} \tag{3.2}$$

because $a = \sqrt{\gamma RT}$, the local speed of sound; $a_0 = \sqrt{\gamma RT_0}$, the speed of sound at the stagnation state (where $V = 0$); and $V_{\max}$ is the maximum possible flow velocity in the fluid (where the absolute temperature is zero).

Equation (3.2) represents an ellipse and is called as *adiabatic steady-flow ellipse*. The adiabatic ellipse can be plotted as in Figure 3.3.

Different realms of compressible flow having significantly different physical characteristics are represented schematically on the adiabatic ellipse. The zones highlighted on the adiabatic ellipse are the following.

- *Incompressible flow* is the flow in which the flow velocity, V, is small compared to the speed of sound, a, in the flow medium. The changes in a are very small compared to the changes in V.
- *Compressible subsonic flow* is the flow in which the flow velocity and the speed of sound are of comparable magnitude, but $V < a$. The changes in flow Mach number M are mainly due to the changes in V.
- *Transonic flow* is the flow in which the difference between the flow velocity and the speed of sound is small compared to either V or a. The changes in V and a are of comparable magnitude.

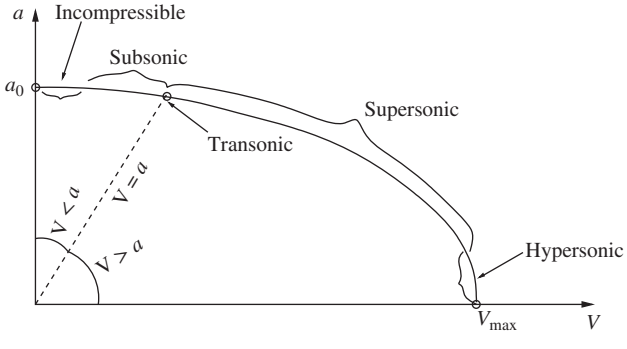

Figure 3.3 Steady-flow adiabatic ellipse.

- *Supersonic flow* is the flow in which the flow velocity and the speed of sound are of comparable magnitude, but $V > a$. The changes in Mach number M take place through substantial variation in both V and a.
- *Hypersonic flow* is the flow in which the flow velocity is very large compared with the speed of sound. The changes in flow velocity are very small, and thus variations in Mach number M are almost exclusively due to the changes in the speed of sound a.

3.7 Summary

In incompressible flows, the fluid particles will be able to sense the presence of a body before actually reaching it. On the other hand, if the fluid particles were moving faster than the signal waves as in the case of supersonic flows, the fluid would not be able to sense the body before actually reaching it and abrupt changes in velocity and other properties would take place.

When a fluid medium is allowed to vary its density, the consequence is that the fluid elements will be able to occupy varying volumes in space.

A small shift of fluid elements in compressible media will induce in due course similar small movements in adjacent elements, and in this way, a disturbance, referred to as an *acoustic wave*, propagates at a relatively high speed through the medium.

A *sound wave* is a weak compression wave across which only infinitesimal changes in flow properties occur.

Waves where comparatively large pressure variation occurs over a very narrow front. Such waves are called *shock waves*, the flow process across them is nonisentropic, and move relative to the fluid at speeds that exceed the speed of sound.

The speed of sound is given by $a = \sqrt{\gamma RT}$, where T is the static temperature of the medium in absolute unit.

Flows with velocity more than the speed of sound are called *supersonic flows*, and those with velocities less than the speed of sound are called *subsonic flows*. Flows with velocity close to the speed of sound are classified under a special category called *transonic flows*.

For an observer looking in the direction of flow toward the disturbance, the wave to his\her left is called *left-running wave* and the wave to his\her right is called *right-running wave*.

The Mach number M is a primary parameter that dictates the flow pattern in the compressible regime of flow.

The four dimensionless parameters that must be the same for dynamic similarity of the model and prototype flow fields are

- Mach number, $M = \frac{V}{a}$
- Reynolds number, $Re_L = \frac{\rho VL}{\mu}$
- Ratio of specific heats, $\gamma = \frac{c_p}{c_v}$
- Prandtl number, $Pr = \frac{\mu c_p}{k}$

The assumption of fluids as continua is valid only when the smallest volume of fluid of interest contains large number of molecules so that the statistical averages are meaningful.

In compressible flows, the relevant properties are the density, pressure, temperature, velocity, shear stress, coefficient of viscosity, internal energy, entropy, and coefficient of thermal conductivity.

The flow in which the mean free path of the molecules is of the same order or more than the characteristic dimension of the problem is termed *rarefied flow*.

The steady-flow energy equation for the adiabatic flow through such a streamtube is

$$h + \frac{V^2}{2} = h_0$$

For perfect gases, this simplifies to

$$\boxed{V^2 + \frac{2}{\gamma - 1} a^2 = \frac{2}{\gamma - 1} a_0^2 = V_{\max}^2} \tag{3.3}$$

- *Incompressible flow* is the flow in which the flow velocity, V, is small compared to the speed of sound, a, in the flow medium. The changes in a are very small compared to the changes in V.
- *Compressible subsonic flow* is the flow in which the flow velocity and the speed of sound are of comparable magnitude, but $V < a$. The changes in flow Mach number M are mainly due to changes in V.
- *Transonic flow* is the flow in which the difference between the flow velocity and the speed of sound is small compared to either V or a. The changes in V and a are of comparable magnitude.
- *Supersonic flow* is the flow in which the flow velocity and the speed of sound are of comparable magnitude, but $V > a$. The changes in Mach number M take place through substantial variation in both V and a.
- *Hypersonic flow* is the flow in which the flow velocity is very large compared with the speed of sound. The changes in the flow velocity are very small, and thus variations in Mach number M are almost exclusively due to the changes in the speed of sound a.

Exercise Problems

3.1 Determine the mean free path for air at sea level state.
[Answer: 4.292×10^{-8} m]

3.2 Determine the Prandtl number of air at sea level state.
[Answer: 0.7]

3.3 What will be the limiting Mach number up to which a flow with Reynolds number 10^6 can be treated as continuum?

[Answer: 10]

3.4 If the maximum velocity obtained by expanding air in a storage tank is 600 m/s, determine the temperature of air in the tank.

[Answer: 179.2 K]

References

[1] Tsien H. S., "Super-aerodynamics, mechanics of rarefied gases", *Journal of the Aeronautical Sciences*, Vol. 13, No. 2, 1946, p. 653.

[2] Rathakrishnan E., *Gas Tables*, 3rd ed. Universities Press, Hyderabad, India, 2012.

4

High-Temperature Flows

4.1 Introduction

In Chapter 1, it was mentioned that a gas can be treated as perfect, with the specific heats independent of temperature, only when the temperature is below a specified limit. Also, a perfect gas has to be thermally as well as calorically perfect. For example, air can be treated as both thermally and calorically perfect for temperatures less than 800 K, and for temperatures from 800 to 2000 K, it is only thermally perfect but calorically imperfect. For temperatures above 2000 K, the air is thermally as well as calorically imperfect. For flows of imperfect gases, none of the gas dynamic relations obtained with perfect gas assumption are valid.

In many engineering problems of practical interest, the temperature of the flow is appreciably above the limiting value for which the gas can be treated as perfect. For example, the flow through rocket engines, arc-driven hypersonic wind tunnels, flow in shock tubes, high-energy gas dynamic and chemical lasers, and internal combustion engines are some of the engineering devices with operating temperatures well above the perfect gas limiting temperature of about 800 K. Hence, flows with temperature above 800 K need to be analyzed considering the functional dependence of the specific heats c_p and c_v on temperature. In this kind of flows with temperature more than 800 K, if the temperature is in the range from 800 to 2000 K, the flowing gas is termed *thermally perfect*. This is because, even though c_p and c_v are functions of temperature, their ratio continues to be independent of temperature, as in the case of perfect gases. That is, the specific heats ratio γ continues to be independent of temperature even for the case of high-enthalpy flows with temperature less than 2000 K. This implies that the property relations, such as the ratio of static to stagnation pressures, temperatures, and densities, as a function of flow Mach number, derived based on perfect gas and inviscid assumptions can be used for solving high-enthalpy flows that are thermally perfect. However, for high-enthalpy flows with temperature above 2000 K, even the specific heats ratio γ becomes a function of temperature. This makes the isentropic, shock, Fanno, and Rayleigh flow relations, derived based on perfect gas assumption invalid.

High Enthalpy Gas Dynamics, First Edition. Ethirajan Rathakrishnan.

www.wiley.com/go/rathakrishnan

Therefore, for solving high-enthalpy flows that are both calorically as well as thermally imperfect, each problem has to be dealt with the actual equations governing the transport of mass, momentum, and energy and the second law of thermodynamics. Our aim in this chapter is to study some of the fundamental aspects of the high-temperature effects on compressible flows.

Example 4.1 Determine the specific heats ratio of oxygen gas at 400 K.

Solution

At 400 K, the oxygen can be treated as a perfect gas. For oxygen, the molecular weight is 32. Therefore, the gas constant becomes

$$\begin{aligned} R &= \frac{R_u}{M_m} \\ &= \frac{8314}{32} \\ &= 259.75 \text{ m}^2/(\text{s}^2 \text{ K}) \end{aligned}$$

From classical thermodynamics, for a perfect gas [1], the specific heat at constant pressure is

$$\begin{aligned} c_p &= \frac{\gamma}{\gamma - 1} R \\ &= \frac{1.4}{1.4 - 1} \times 259.75 \\ &= 909.125 \text{ m}^2/(\text{s}^2 \text{ K}) \end{aligned}$$

The specific heat at constant volume is

$$\begin{aligned} c_v &= \frac{1}{\gamma - 1} R \\ &= \frac{1}{1.4 - 1} \times 259.75 \\ &= 649.375 \text{ m}^2/(\text{s}^2 \text{ K}) \end{aligned}$$

Therefore, the ratio of specific heats is

$$\begin{aligned} \gamma &= \frac{c_p}{c_v} \\ &= \frac{909.125}{649.375} \\ &= \boxed{1.4} \end{aligned}$$

■

4.2 Importance of High-Enthalpy Flows

To gain an insight into the importance of high enthalpy flow at high speeds, referred to as *hypervelocity flows*, let us examine the reentry of a spacecraft into earth's atmosphere. Let its velocity at 50 km altitude be 11 km/s (equal to escape velocity from the gravitational attraction of earth). Let the nose shape of the vehicle be blunt, as shown in Figure 4.1. At this high Mach number, there will be a very strong detached shock positioned ahead of the blunt nose. The portion of the shock, on either side of the stagnation streamline, near the nose can be approximated as a normal shock. The vehicle Mach number at that altitude can be obtained as follows.

The Mach number is defined as

$$M_\infty = \frac{V_\infty}{a_\infty}$$

where V_∞ is the flight speed of the vehicle and a_∞ is speed of sound at that altitude. At 50,000 m altitude, the temperature of the atmosphere is about −25°C, that is, 248 K. Therefore, the speed of sound, assuming the air as a perfect gas, is

$$\begin{aligned} a_\infty &= \sqrt{\gamma R T_\infty} \\ &= \sqrt{1.4 \times 287 \times 248} \\ &= 315.67 \text{ m/s} \end{aligned}$$

Thus the Mach number is

$$\begin{aligned} M_\infty &= \frac{V_\infty}{a_\infty} \\ &= \frac{11{,}000}{315.67} \\ &= 34.85 \end{aligned}$$

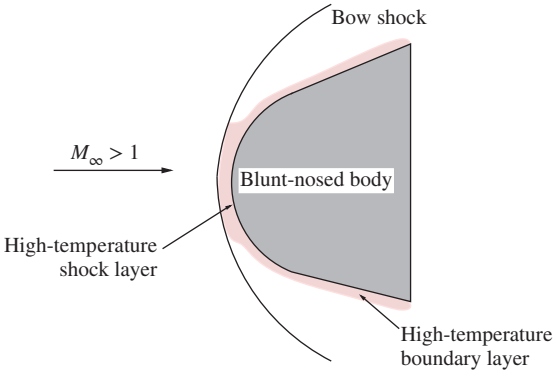

Figure 4.1 Flow field around a blunt-nosed body at reentry.

From gas dynamics of perfect gases, we know that when $M_\infty \to \infty$, the temperature behind the shock tends to infinity. This theoretical limit indicates that for the present shock with $M_1 = 33.4$, the temperature T_2 behind the shock will be very high. That is, the massive amount of flow kinetic energy in the hypersonic freestream is converted to internal energy of the gas across the shock, thereby creating very high temperatures in the shock layer near the nose.

Downstream of the nose region, the gas in the shock layer expands and forms a cooler zone around the body. Also, there is a boundary layer with high Mach number at its outer edge. Hence, there is an intense frictional dissipation within the hypersonic boundary layer, resulting in high temperature. This high temperature can cause the boundary layer to become chemically reacting. Another challenge associated with reentry problem occurs when ionization is present in the shock layer, thereby resulting in the production of a large number of free electrons throughout the shock layer. Because of the above complications, associated with high-temperature gas streams, the results of gas dynamics based on perfect gas assumption become invalid for the analysis of high-enthalpy gas dynamic problems. However, analysis of such problems become essential because in many flow processes of engineering importance, we come across high-temperature effects.

Example 4.2 What will be the stagnation temperature at the nose of a reentry vehicle entering with 11,000 m/s, at an altitude where the atmospheric temperature is 270 K, based on perfect gas theory?

Solution

Given $T_\infty = 270$ K and $V_\infty = 11{,}000$ m/s. The corresponding speed of sound and Mach number are

$$\begin{aligned} a_\infty &= \sqrt{\gamma R T_\infty} \\ &= \sqrt{1.4 \times 287 \times 270} \\ &= 329.37 \text{ m/s} \\ M_\infty &= \frac{V_\infty}{a_\infty} \\ &= \frac{11{,}000}{329.37} \\ &= 33.4 \end{aligned}$$

From perfect gas theory, the ratio of static temperature, T, to stagnation temperature, T_0, is

$$\frac{T_0}{T_\infty} = 1 + \frac{\gamma - 1}{2} M_\infty^2$$

For perfect air, $\gamma = 1.4$; therefore,

$$\begin{aligned} T_0 &= \left(1 + \frac{\gamma - 1}{2} M_\infty^2\right) T_\infty \\ &= \left(1 + \frac{1.4 - 1}{2} \times 33.4^2\right) \times 270 \\ &= \boxed{60{,}510.24 \text{ K}} \end{aligned}$$

■

4.3 Nature of High-Enthalpy Flows

There are two major physical characteristics that cause a high-enthalpy flow to deviate from calorically perfect gas behavior. These are the following:

- At high temperatures, the vibrational excitation of the gas molecules becomes important, absorbing some of the energy which, at normal temperatures, would go into the translational and rotational motion. The excitation of vibrational energy causes the specific heats of the gas to become a function of temperature, causing the gas to become calorically imperfect.
- With further increase in temperature, the molecules begin to dissociate and even ionize. Under these conditions, the gas becomes chemically reacting, and the specific heats become functions of both temperature and pressure.

Because of the above effects, the high-enthalpy gas flows have the following differences as compared to flow of gas with constant specific heats (perfect gas).

- The specific heats ratio, $\gamma = c_p/c_v$, is a variable.
- The thermodynamic properties (the thermal and calorical properties) are totally different.
- For high-enthalpy flows, heat transfer rate is predominant.
- Usually, some numerical procedure, rather than analytical approach, is required for solving high-enthalpy problems.
- Because of these reasons, analysis of high-enthalpy flows are different from that of gas dynamic flows obeying perfect gas assumption.

4.4 Most Probable Macrostate

It is the macrostate that occurs when the system is in thermodynamic equilibrium. This plays a dominant role in the study of high-enthalpy gas dynamics, because at temperatures above 800 K, the vibration excitation of the molecules becomes active; beyond 2000 K, the molecules in a gas dissociate to become atoms; and beyond 3000 K, the atoms themselves become active and get ionized, heading towards

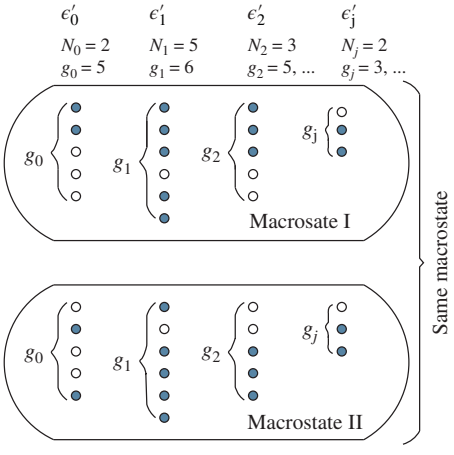

Figure 4.2 Microstates in a macrostate.

plasma state. Therefore, it is essential to have a thorough understanding of the kinetic theory of gases and statistical thermodynamics if we have to deal with high-enthalpy or high-temperature flows. To make a beginning in this direction, let us start with the following question:

Find the most probable macrostate of a system with a fixed number of identical particles,

$$N = \sum_j N_j \tag{4.1}$$

and fixed energy

$$E = \sum_j \epsilon'_j N_j \tag{4.2}$$

where $\epsilon'_0, \epsilon'_1, \epsilon'_2, \ldots, \epsilon'_j$, respectively, are the energy of molecules $N_0, N_1, N_2, \ldots, N_j$.

To solve this problem, consider the gaseous system shown in Figure 4.2, consisting different groups of molecules at energy levels $\epsilon'_0, \epsilon'_1, \epsilon'_2, \ldots, \epsilon'_j$. The g_js in the figure show the possible positions that the N_j molecules of energy levels ϵ'_j can occupy. That is, there are two molecules at energy level ϵ'_0 and they can take any two positions out of five possible locations (that is, out of $g_0 = 5$). A particular distribution in which the molecules in each set of molecules $N_0, N_1, N_2, \ldots, N_j$ can be arranged forms a macrostate. Two typical macrostates are illustrated in Figure 4.2.

From kinetic theory of gases, we know the following.

- In any given system of molecules, the microstates are constantly changing because of molecular collisions.
- The most probable macrostate is that *macrostate that has the maximum number of microstates*.

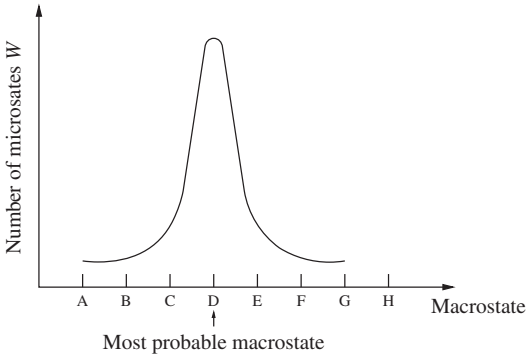

Figure 4.3 Most probable macrostate.

- If each microstate appears in the system with equal probability and there is one particular macrostate that has considerably more microstates than any other, then that is the macrostate that will prevail in the system most of the time. A typical variation of macrostate with number of microstates, W, will be as shown in Figure 4.3. The macrostate D with the maximum number of microstates is the most probable macrostate.
- Therefore, if we can count the number of microstates in any given macrostate, we can easily identify the most probable macrostate.

4.5 Counting the Number of Microstates for a given Macrostate

Molecules and atoms are constituted by the elementary particles, namely, the electrons, protons, and neutrons. Quantum mechanics makes a distinction between two different class of molecules and atoms, depending on the number of elementary particles in them as follows.

- Molecules and atoms with *even number* of elementary particles obey a certain statistical distribution called *Bose–Einstein* statistics. Let us call them *bosons*.
- Molecules and atoms with *odd number* of elementary particles obey a different statistical distribution called *Fermi–Dirac* statistics. Let us call such molecules and atoms as *fermions*.

The following is an important distinction between the above two classes.

- For bosons, the number of molecules that can be in any one degenerate state (in any one of the boxes in Figure 4.4) is unlimited (except, of course, that it must be less than or equal to N_j).
- For fermions, only one molecule may be in any given degenerate state at any instant.

This distinction has a major impact on the counting of microstates in a macrostate.

4.5.1 Bose–Einstein Statistics

For the time being, let us consider one energy level, say ϵ'_j. This energy level has g_j degenerate states and N_j molecules. Consider g_j states as the g_j containers, as shown in Figure 4.4.

Distribute the N_j molecules among the containers, such that three molecules are present in the first container, two in the second, etc., where the molecules are denoted by x. The distribution of molecules over these containers represents a distinct macrostate. If a molecule is moved from container one to container two, a different macrostate is formed. To count the total number of different microstates possible, first note that the number of permutations between the symbols x and | is

$$[N_j + (g_j - 1)]!$$

This gives the number of distinct ways in which the N_j molecules and the $(g_j - 1)$ partitions can be arranged. However, the partitions are indistinguishable. The $(g_j - 1)$ partitions can be permuted in $(g_j - 1)!$ different ways. The molecules are also indistinguishable; therefore, they can be permuted in $N_j!$ different ways without changing the picture drawn in Figure 4.4. Therefore, there are $(g_j - 1)!\, N_j!$ different permutations that yield the identical picture drawn in Figure 4.4, that is, the same macrostate. Thus, the number of different ways in which the N_j indistinguishable molecules can be distributed over g_j states is

$$\frac{(N_j + g_j - 1)!}{(g_j - 1)! N_j!}$$

This expression applies to one energy level ϵ'_j with population N_j and gives the number of different microstates just because of the different arrangements within the energy level ϵ'_j.

Now, consider the whole set of N_js distributed over the complete set of energy levels (note that N_js define a particular macrostate). Let W denote the total number of microstates for a given macrostate, the above expression, multiplied over all the energy levels, yields

$$W = \prod_j \frac{(N_j + g_j - 1)!}{(g_j - 1)! N_j!} \tag{4.3}$$

Note that W is a function of all the N_j values, that is,

$$W = W(N_1, N_2, \ldots, N_j, \ldots)$$

Figure 4.4 Illustration of degenerate states.

The quantity W is called the *thermodynamic probability*. The thermodynamic probability is a measure of the "disorder" of the system. Equation (4.3) can be used to count the number of microstates in a given macrostate as long as the molecules are bosons.

4.5.2 Fermi–Dirac Statistics

For fermions, only one molecule can be present in any given degenerate state at any instant, that is, there can be no more than one molecule per box. This implicitly requires that $g_j \geq N_j$.

Consider g_j boxes. Take one of the molecules and put it in one of the containers. There will be g_j choices or ways of doing this. Take the next molecule and put it in one of the boxes. However, there are now only $(g_j - 1)$ choices, because one of the containers is already occupied. Likewise, we find the number of ways N_j molecules can be distributed over g_j containers, with only one molecule (or less) per box, is

$$g_j(g_j - 1)(g_j - 2)\cdot\cdots[g_j - (N_j - 1)] \equiv \frac{g_j!}{(g_j - N_j)!}$$

However, the N_j molecules are indistinguishable; they can be permuted in $N_j!$ different ways without changing the degenerate states, illustrated in Figure 4.4. Therefore, the number of different microstates just because of different arrangements with ϵ'_j energy levels is

$$\frac{g_j!}{(g_j - N_j)!N_j!}$$

Considering all energy levels, the total number of microstates for a given macrostate for fermions is

$$W = \prod_j \frac{g_j!}{(g_j - N_j)!N_j!} \tag{4.4}$$

4.5.3 The Most Probable Macrostate

We saw that the most probable macrostate is defined as that macrostate that contains the maximum number of microstates. That is, it is the macrostate that has $W_{\max}$. Let us find the specific set of N_js that allows the maximum W. First consider the case of bosons. From Equation (4.3), we have

$$W = \prod_j \frac{(N_j + g_j - 1)!}{(g_j - 1)!N_j!}$$

Taking log on both sides, we have

$$\ln W = \sum_j [\ln(N_j + g_j - 1)! - \ln(g_j - 1)! - \ln N_j!] \tag{4.5}$$

At this stage, it is extremely important to note that the total energy of a molecule consists of translational, rotational, vibrational, and electronic energies. That is, for a *molecule*, the total energy is given by

$$\varepsilon = \varepsilon_{\text{trans}} + \varepsilon_{\text{rot}} + \varepsilon_{\text{vib}} + \varepsilon_{\text{el}}$$

However, for a single atom, only the translational and electronic energies exist, that is, for *atoms*, the total energy is given by

$$\varepsilon = \varepsilon_{\text{trans}} + \varepsilon_{\text{el}}$$

To have a better understanding about the above energy components, let us have a close look at the microscopic picture of a gas. Let us assume that the gas consists of a large number of individual molecules. We know that a molecule is a collection of atoms bound together by a rather complex intramolecular force. A simple concept of a diatomic molecule (molecule with two atoms) is the "dumbbell" model shown in Figure 4.5(a).

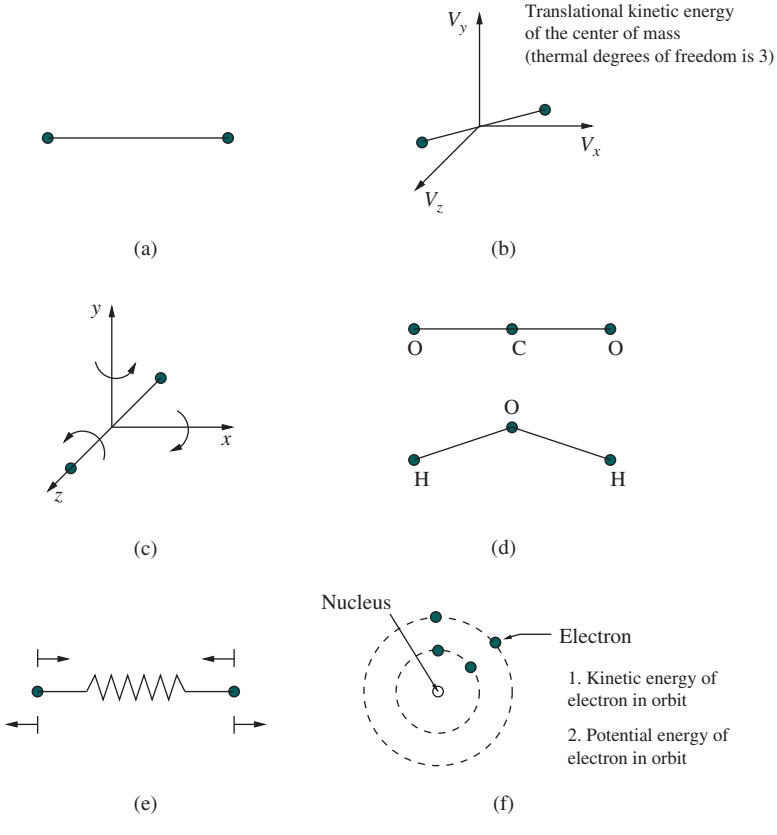

Figure 4.5 Molecular energy modes. (a) Diatomic molecule; (b) Translational energy, $\varepsilon_{\text{trans}}$; (c) Rotational energy, ε_{rot}; (d) polyatomic molecule; (e) vibrational energy, ε_{vib}; (f) electrical energy, ε_{el}.

The molecules have the following forms (modes) of energy.

- *Translational energy*, ε_{trans} – the translational kinetic energy of the center of mass of the molecule is the source of this energy. As shown in Figure 4.5(b), a molecule has three *geometric degrees of freedom* in translation. As motion along *x*-, *y*-, and *z*-coordinate directions constitutes to the total kinetic energy, the molecule is also said to have three *thermal degrees of freedom*.
- *Rotational energy*, ε_{rot} – the rotational energy is due to the rotation of the molecule about the three orthogonal axes in space, as shown in Figure 4.5(c). The sources of the rotational energy, ε_{rot}, are (i) the rotational kinetic energy associated with the molecules rotational velocity and (ii) its moment of inertia. But, for the diatomic molecule sketched in Figure 4.5(c), the moment of inertia about the internucleus axis (the *z*-axis) is very small and, therefore, the rotational kinetic energy about the *z*-axis is negligible in comparison to the rotation about the *x*- and *y*-axes. Thus, the diatomic molecule has only two *geometric* and two *thermal* degrees of freedom. The same is true for a linear polyatomic molecule such as CO_2 shown in Figure 4.5(d). However, for a nonlinear polyatomic molecule, such as H_2O shown in Figure 4.5(d), the number of *geometric* as well as *thermal* degrees of freedom in rotation are three.
- *Vibrational energy*, ε_{vib} – the molecules and atoms are vibrating with respect to an equilibrium location within the molecule. For a diatomic molecule, this vibration may be modeled by a spring connecting the two atoms, as shown in Figure 4.5(e). Thus, the molecule has *vibrational energy*, ε_{vib}. The sources of this vibrational energy are (i) the kinetic energy of the linear motion of the atoms as they vibrate back and forth and (ii) the potential energy associated with the intramolecular force. Therefore, although a diatomic molecule vibrates along one direction, namely, the internucleus axis only, and has only one geometric degree of freedom, it has *two thermal degrees* of freedom because of the contribution of kinetic and potential energies. For polyatomic molecules, the vibrational motion is more complex and numerous fundamental vibrational modes can exist, with a consequent large number of degrees of freedom.
- *Electronic energy*, ε_{el} – the electronic energy is due to the motion of electrons about the nucleus of each atom constituting the molecule, as shown in Figure 4.5(f). The sources of electronic energy are (i) the kinetic energy because of its translational motion throughout its orbit about the nucleus and (ii) the potential energy because of its location in the electromagnetic force field established principally by the nucleus. The concepts of geometric and thermal degrees of freedom are usually not useful for describing electronic energy, because the overall electron motion is complex.

Quantum mechanics results show that each of the above energies are *quantized*, that is, they can exist only at certain discrete values, as illustrated in Figure 4.6. From the representation of quantized levels of different modes of energy, it is clear that we are dealing with the combined translational, rotational, vibrational, and electronic

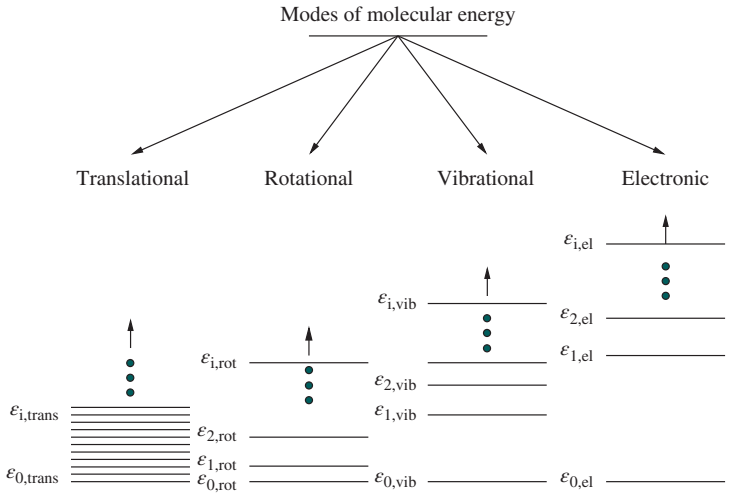

Figure 4.6 Quantized levels of different energy modes of molecules.

energies of a molecule and that the closely spaced translational levels can be grouped into a number of degenerate states with essentially the same energy.

Therefore, in Equation (4.5), we can assume that $N_j \gg 1$ and $g_j \gg 1$, leading to

$$(N_j + g_j - 1) \approx (N_j + g_j)$$

and

$$(g_j - 1) \approx g_j$$

Moreover, we can employ Sterling's formula

$$\ln a! = a \ln a - a \tag{4.6}$$

for the factorial terms in Equation (4.5). Thus,

$$\ln W = \sum_j [(N_j + g_j) \ln(N_j + g_j) - (N_j + g_j) - g_j \ln g_j + g_j - N_j \ln N_j + N_j]$$

This gives

$$\ln W = \sum_j \left[N_j \ln \left(1 + \frac{g_j}{N_j} \right) + g_j \ln \left(\frac{N_j}{g_j} + 1 \right) \right] \tag{4.7}$$

Recall that

$$\ln W = f(N_j s) = f(N_0, N_1, N_2, \ldots, N_j, \ldots)$$

Also, for the maximum value of the thermodynamic probability W, we have

$$d\ (\ln W) = 0 \tag{4.8}$$

Thus,

$$d\ (\ln W) = \frac{\partial(\ln W)}{\partial\ N_0}\ dN_0 + \frac{\partial(\ln W)}{\partial\ N_1}\ dN_1 + \cdots + \frac{\partial(\ln W)}{\partial\ N_j}\ dN_j + \cdots + \cdots \quad (4.9)$$

Combining Equations (4.8) and (4.9), we get

$$d\ (\ln W) = \sum_j \frac{\partial(\ln W)}{\partial\ N_j}\ dN_j = 0 \quad (4.10)$$

Differentiating Equation (4.7), with respect to N_j, we get

$$\frac{\partial(\ln W)}{\partial\ N_j} = \ln\left(1 + \frac{g_j}{N_j}\right) \quad (4.11)$$

Substituting Equation (4.11) into Equation (4.10), we get

$$d\ (\ln W) = \sum_j \left[\ln\left(1 + \frac{g_j}{N_j}\right)\right]\ dN_j = 0 \quad (4.12)$$

In Equation (4.12), the variation of N_j is not totally independent; dN_j is subject to two physical constraints, namely,

1. $N = \sum_j N_j$ = constant, and hence,

$$\sum_j dN_j = 0 \quad (4.13)$$

2. $E = \sum_j \epsilon_j' N_j$ = constant, and hence,

$$\sum_j \epsilon_j'\ dN_j = 0 \quad (4.14)$$

Assuming α and β to be two Lagrange multipliers (two constants to be determined), Equations (4.13) and (4.14) can be written as

$$-\sum_j \alpha\ dN_j = 0 \quad (4.15)$$

$$-\sum_j \beta\ \epsilon_j'\ dN_j = 0 \quad (4.16)$$

Adding Equations (4.12), (4.15), and (4.16), we get

$$\sum_j \left[\ln\left(1 + \frac{g_j}{N_j}\right) - \alpha - \beta\ \epsilon_j'\right]\ dN_j = 0 \quad (4.17)$$

From the standard method of Lagrange multipliers, α and β are defined such that each term in brackets in Equation (4.17) is zero, that is,

$$\ln\left(1+\frac{g_j}{N_j}\right)-\alpha-\beta\ \epsilon_j'=0$$

or

$$1+\frac{g_j}{N_j}=e^{\alpha}\ e^{\beta\epsilon_j'}$$

This gives the N_j corresponding to the maximum value of the thermodynamic probability W as

$$\boxed{N_j^*=\frac{g_j}{e^{\alpha}\ e^{\beta\epsilon_j'}-1}} \tag{4.18}$$

The superscript "*" is added to N_j to emphasize that N_j^* corresponds to the maximum value of W (via) Equation (4.8), that is, N_j^* corresponds to the most probable distribution of molecules over the energy levels ϵ_j'. Equation (4.18) gives the most probable macrostate for bosons. That is, the set of values obtained from Equation (4.18) for all levels

$$N_0^*, N_1^*, N_2^*, \ \ldots\ , N_j^*, \ \ldots$$

is the *most probable macrostate*.

Similarly, the most probable macrostate for fermions can be obtained, starting from Equation (4.4), as

$$\boxed{N_j^*=\frac{g_j}{e^{\alpha}\ e^{\beta\epsilon_j'}+1}} \tag{4.19}$$

4.5.4 The Limiting Case: Boltzmann's Distribution

At very low temperatures, $T\to 0$ K, as shown in Figure 4.6, the molecules of the system are jammed together at or near the ground energy levels, and therefore, the degenerate states of these low-lying energy levels are highly populated. As a result, the difference between the Bose–Einstein and Fermi–Dirac statistics are important. In contrast, at high temperatures, the molecules are distributed over many energy levels, and therefore, the states are generally sparsely populated, that is, $N_j \ll g_j$. For this case, the denominators of Equations (4.18) and (4.19) must be very large, that is,

$$e^{\alpha}e^{\beta\epsilon_j}-1\gg 1$$

or

$$e^{\alpha}e^{\beta\epsilon_j}+1\gg 1$$

Hence, in the high-temperature limit, the unity terms in these denominators can be neglected, and both Equations (4.18) and (4.19) reduce to

$$\boxed{N_j^*=g_j e^{-\alpha}e^{-\beta\epsilon_j'}} \tag{4.20}$$

This limiting case is called the *Boltzmann limit*, and Equation (4.20) is termed the *Boltzmann distribution*.

As all gas dynamic problems generally deal with temperatures above 5 K, the Boltzmann distribution is appropriate for all our future considerations. That is, we will be dealing with Equation (4.20) rather than Equation (4.18) or (4.19).

In Equation (4.20), the Lagrange constants α and β are unknowns. The link between the classical and statistical thermodynamics is the constant β. It can be shown that

$$\beta = \frac{1}{kT}$$

where k is the Boltzmann constant and T is the temperature of the system. With $\beta = \frac{1}{kT}$, Equation (4.20) can be written as

$$N_j^* = g_j \, e^{-\alpha} \, e^{-\epsilon_j'/kT} \tag{4.21}$$

To obtain an expression for α, recall that

$$N = \sum_j N_j^*$$

Hence, from Equation (4.21), we have

$$\begin{aligned} N &= \sum_j g_j \, e^{-\alpha} \, e^{-\epsilon_j'/kT} \\ &= e^{-\alpha} \sum_j g_j \, e^{-\epsilon_j'/kT} \end{aligned}$$

or

$$e^{-\alpha} = \frac{N}{\sum\limits_j g_j \, e^{-\epsilon_j'/kT}} \tag{4.22}$$

Substituting Equation (4.22) into Equation (4.21), we get

$$\boxed{N_j^* = N \, \frac{g_j \, e^{-\epsilon_j'/kT}}{\sum\limits_j g_j \, e^{-\epsilon_j'/kT}}} \tag{4.23}$$

The Boltzmann distribution given by Equation (4.23) is important. It is the *most probable distribution* of the molecules over all the energy levels ϵ_j' of the system. Also, ϵ_j' is the total energy, including the zero-point energy. However, Equation (4.23) can also be written in terms of ϵ_j, the energy measured above the zero-point energy, as follows. As $\epsilon_j' = \epsilon_j + \epsilon_0$, we have

$$\frac{e^{-\epsilon_j'/kT}}{\sum\limits_j g_j \, e^{-\epsilon_j'/kT}} = \frac{e^{-(\epsilon_j+\epsilon_0)/kT}}{\sum\limits_j g_j \, e^{-(\epsilon_j+\epsilon_0)/kT}}$$

$$= \frac{e^{-\epsilon_0/kT}\ e^{-\epsilon_j/kT}}{e^{-\epsilon_0/kT}\ \sum_j\ g_j\ e^{-\epsilon_j/kT}}$$

$$= \frac{e^{-\epsilon_j/kT}}{\sum_j\ g_j\ e^{-\epsilon_j/kT}}$$

Hence, from Equation (4.23), we get

$$\boxed{N_j^* = N\ \frac{g_j\ e^{-\epsilon_j/kT}}{\sum_j\ g_j\ e^{-\epsilon_j/kT}}} \tag{4.24}$$

where the energies are measured above the zero-point energy.

Finally, the partition function Q, also called the *state sum*, is defined as

$$Q \equiv \sum_j\ g_j\ e^{-\epsilon_j/kT}$$

and the Boltzmann distribution, from Equation (4.24), can be written in terms of the partition function Q as

$$\boxed{N_j^* = N\ \frac{g_j\ e^{-\epsilon_j/kT}}{Q}} \tag{4.25}$$

It can be shown that the partition function Q is a function of the volume, $\mathbb{V}$, as well as the temperature, T, of the system, that is,

$$Q = f\ (T, \mathbb{V})$$

Equation (4.25) implies that, for molecules and atoms of a given species, quantum mechanics says that a set of well-defined energy levels, ϵ_j, exist, over which the molecules or atoms can be distributed at any given instant, and that each energy level has a certain number of degenerate states g_j.

For a system of N molecules or atoms at a given temperature T and volume $\mathbb{V}$, Equation (4.25) gives total number of such molecules or atoms N_j^* in each energy level ϵ_j when the system is in thermodynamic equilibrium.

4.6 Evaluation of Thermodynamic Properties

The thermodynamic properties such as the internal energy, enthalpy, entropy, and pressure can be expressed in terms of the partition function Q.

4.6.1 Internal Energy E

From the microscopic view point, for a system in equilibrium, the energy of the system is given by

$$E = \sum_j \epsilon_j N_j^* \tag{4.26}$$

Note that Equation (4.26) gives the energy E, measured above the zero-point energy.

Combining Equations (4.26) and (4.25), we have

$$E = \sum_j \epsilon_j N \frac{g_j e^{-\epsilon_j/kT}}{Q} = \frac{N}{Q} \sum_j g_j \epsilon_j e^{-\epsilon_j/kT} \tag{4.27}$$

Recall that the partition function

$$Q \equiv \sum_j g_j \epsilon_j e^{-\epsilon_j/kT}$$
$$= f(\mathbb{V}, T)$$

Differentiating Q with respect to temperature, T, we have

$$\left(\frac{\partial Q}{\partial T}\right)_v = \frac{1}{kT^2} \sum_j g_j \epsilon_j e^{-\epsilon_j/kT}$$

that is,

$$\sum_j g_j \epsilon_j e^{-\epsilon_j/kT} = kT^2 \left(\frac{\partial Q}{\partial T}\right)_v \tag{4.28}$$

Substituting Equation (4.28) into Equation (4.27), we get

$$E = \frac{N}{Q} kT^2 \left(\frac{\partial Q}{\partial T}\right)_v$$

or

$$\boxed{E = NkT^2 \left(\frac{\partial \ln Q}{\partial T}\right)_v} \tag{4.29}$$

If we have 1 mol of atoms or molecules, then $N = N_A$, the Avogadro number $(6.02214179 \times 10^{23})$[1].

[1] The mole, abbreviated mol, is an SI unit that measures the number of particles in a specific substance. One mole is equal to $6.02214179 \times 10^{23}$ atoms or other elementary units such as molecules. For example, if we have 1 mol of oxygen atoms, then we have $6.02214179 \times 10^{23}$ oxygen atoms. The number $6.02214179 \times 10^{23}$ alone is called *Avogadro's number* (N_A) or *Avogadro's constant*, after the nineteenth-century scientist Amedeo Avogadro. Each Carbon-12 atom weighs about 1.99265×10^{-23} g; therefore, $(1.99265 \times 10^{-23}\ \text{g}) \times (6.02214179 \times 10^{23}\ \text{atoms}) = 12$ g of Carbon-12.

Also, $N_A\ k = R_u$, the universal gas constant. Consequently, for the internal energy per mole, Equation (4.29) gives

$$E = R_u T^2 \left(\frac{\partial \ln Q}{\partial T} \right)_v \tag{4.30}$$

In the science of gas dynamics, a unit mass is more fundamental quantity than a unit mole. Let M be the mass of the system of N molecules and m be mass of an individual molecule. Then $M = Nm$. From Equation (4.29), the internal energy per unit mass, e, is

$$e = \frac{E}{M} = \frac{NkT^2}{Nm} \left(\frac{\partial \ln Q}{\partial\ T} \right)_v \tag{4.31}$$

But $k/m = R$ is the specific gas constant. Therefore, Equation (4.31) becomes

$$\boxed{e = RT^2 \left(\frac{\partial \ln Q}{\partial\ T} \right)_v} \tag{4.32}$$

The specific enthalpy is defined as the sum of the specific internal energy and flow work,

$$h = e + pv$$

But by state equation,

$$pv = RT$$

Thus the specific enthalpy becomes

$$h = e + RT$$

Substituting for e from Equation (4.32), we have the enthalpy in terms of the partition function Q as

$$\boxed{h = RT + RT^2 \left(\frac{\partial \ln Q}{\partial\ T} \right)_v} \tag{4.33}$$

Note that Equations (4.32) and (4.33) are *hybrid equations*, that is, they contain a mixture of thermodynamic variables, such as e, h, and T, and a statistical variable Q.

We know that the entropy or the amount of disorder in a system is a function of the thermodynamic probability, that is,

$$S = S\ (W_{\max}) \tag{4.34}$$

where S is the entropy and $W_{\max}$ is the *thermodynamic probability*.

If we have two systems with S_1, W_1 and S_2, W_2, respectively, and add these systems, the entropy of the combined system is additive, $S_1 + S_2$. But the thermodynamic probability of the combined system is the product of the thermodynamic probabilities of the individual systems $W_1 W_2$ (because each microstate of the first system can exist in

the combined system along with each one of the microstates of the second system). This suggests that Equation (4.34) should be of the form

$$S = (\text{constant}) \ln W_{\max} \tag{4.35}$$

Equation (4.35) was first postulated by Ludwig Boltzmann, and the constant is named in his honor. Thus

$$\boxed{S = k \ln W_{\max}} \tag{4.36}$$

where k is the familiar *Boltzmann constant*. Equation (4.36) is the bridge between classical (represented by entropy S) and statistical thermodynamics (represented by the thermodynamic probability W).

For the case where $N_j \ll g_j$, using the approximation that $\ln (1 + x) \approx x$ for $x \ll 1$, Equation (4.7) (in the Boltzmann limit) becomes

$$\ln W = \sum_j \left[N_j \ln \frac{g_j}{N_j} + N_j \right]$$

or

$$\ln W = \sum_j N_j \left[\ln \frac{g_j}{N_j} + 1 \right] \tag{4.37}$$

For $W = W_{\max}$, N_j becomes N_j^*. From Equation (4.25), we have

$$N_j^* = \frac{N}{Q} g_j \, e^{-\beta \epsilon_j}$$

since

$$\beta = \frac{1}{kT}$$

Rearranging, we have

$$\frac{g_j}{N_j^*} = \frac{Q}{N} e^{\beta \epsilon_j} \tag{4.38}$$

Substituting Equation (4.38) into Equation (4.37), we have

$$\ln W_{\max} = \sum_j N_j^* \ln \frac{Q}{N} + \sum_j N_j^* + \sum_j N_j^* \, \beta \, \epsilon_j$$

$$= N \ln \frac{Q}{N} + N + \beta \, E$$

or,

$$\ln W_{\max} = N \left(\ln \frac{Q}{N} + 1 \right) + \beta \, E \tag{4.39}$$

Substituting Equation (4.39) into Equation (4.36), we get the entropy as

$$S = k \, N \left(\ln \frac{Q}{N} + 1 \right) + k \, \beta \, E \tag{4.40}$$

Note that we are treating β as unknown and then $\beta = \frac{1}{kT}$. To show that $\beta = \frac{1}{kT}$, consider the following expression for entropy in terms of the energy, pressure, and volume

$$T\, dS = dE + p d\,\mathbb{V} \tag{4.41}$$

or

$$\left(\frac{\partial\, S}{\partial\, E}\right)_v = \frac{1}{T} \tag{4.42}$$

From Equation (4.40), we have

$$\left(\frac{\partial\, S}{\partial\, E}\right)_v = k\,\beta \tag{4.43}$$

Equation (4.42) is from *classical thermodynamics*, and Equation (4.43) is from *statistical thermodynamics*. From Equations (4.42) and (4.43), we get

$$\boxed{\beta = \frac{1}{kT}} \tag{4.44}$$

With this result, Equation (4.40) can be written as

$$S = k\, N\, \left(\ln \frac{Q}{N} + 1\right) + \frac{E}{T} \tag{4.45}$$

Combining Equations (4.45) and (4.29), we have

$$\boxed{S = N\, k\, \left(\ln \frac{Q}{N} + 1\right) + N\, k\, T\, \left(\frac{\partial \ln Q}{\partial T}\right)_v} \tag{4.46}$$

This is the statistical thermodynamics result for entropy in terms of the partition function Q.

From Equation (4.41), we can write

$$T\, \left(\frac{\partial\, S}{\partial\, \mathbb{V}}\right)_T = \left(\frac{\partial\, E}{\partial\, \mathbb{V}}\right)_T + p \tag{4.47}$$

Noting that we are dealing with a single chemical species and that the gas is thermally perfect. For a thermally perfect gas, the internal energy is a function of only temperature; thus

$$\left(\frac{\partial\, E}{\partial\, \mathbb{V}}\right)_T = 0$$

Therefore, from Equation (4.47), we have the pressure as

$$p = T\, \left(\frac{\partial\, S}{\partial\, \mathbb{V}}\right)_T \tag{4.48}$$

From Equation (4.45), we have

$$\left(\frac{\partial\, S}{\partial\, \mathbb{V}}\right)_T = N\, k\, \left(\frac{\partial \ln Q}{\partial \mathbb{V}}\right)_T + \frac{1}{T}\left(\frac{\partial\, E}{\partial\, \mathbb{V}}\right)_T$$

For a calorically perfect gas, the internal energy is a constant and independent of temperature; therefore,

$$\left(\frac{\partial E}{\partial \mathbb{V}}\right)_T = 0$$

Hence,

$$\left(\frac{\partial S}{\partial \mathbb{V}}\right)_T = N\,k\left(\frac{\partial \ln Q}{\partial \mathbb{V}}\right)_T \tag{4.49}$$

Combining Equations (4.48) and (4.49), we get the pressure in terms of partition function as

$$\boxed{p = N\,k\,T\left(\frac{\partial \ln Q}{\partial \mathbb{V}}\right)_T} \tag{4.50}$$

This is the statistical thermodynamics result for pressure in terms of partition function Q.

Note that Q is the key factor in all the above equations. Once Q can be evaluated as a function of volume, $\mathbb{V}$, and temperature, T, the thermodynamic state variables can be calculated.

4.7 Evaluation of Partition Function in terms of T and $\mathbb{V}$

The partition function Q, by definition, is

$$Q \equiv \sum_j g_j e^{-\epsilon_j/kT}$$

Now expressions for the energy level ϵ_j is needed for evaluating Q. Recall that the total energy of a state is the sum of translational, rotational, vibrational, and electronic energies, that is,

$$\epsilon' = \epsilon'_{\text{trans}} + \epsilon'_{\text{rot}} + \epsilon'_{\text{vib}} + \epsilon'_{\text{el}}$$

The quantized levels for translational, rotational, vibrational, and electronic energies are given by quantum mechanics [2, 3]. Let us state the results here without proof.

From quantum mechanics, we have translational energy as

$$\epsilon'_{\text{trans}} = \frac{h_P^2}{8\,m}\left(\frac{n_1^2}{a_1^2} + \frac{n_2^2}{a_2^2} + \frac{n_3^2}{a_3^2}\right)$$

where n_1, n_2, n_3 are quantum numbers that can take the integer values 1, 2, 3, etc., a_1, a_2, a_3 are linear dimensions that describe the size of the system, and h_P ($= 6.62606957 \times 10^{-34}$ (m^2 kg)/s) is the Planck constant.

The rotational energy is given by

$$\epsilon'_{\text{rot}} = \frac{h_P^2}{8\,\pi^2 I}\,J(J+1)$$

where J is the rotational quantum number, $J = 0,1,2, \ldots$, and I is the moment of inertia of the molecule.

The expression for vibrational energy is

$$\epsilon'_{\text{vib}} = h_P \, \nu \left(n + \frac{1}{2} \right)$$

where n is the vibrational quantum number, $n = 0,1,2, \ldots$, and ν is the fundamental vibrational frequency of the molecule.

For electronic energy, no simple expression can be written, and hence, it will continue to be expressed simply as ϵ'_{el}.

- In the above expressions for the rotational and vibrational energies, I and ν for a given molecule are usually obtained from spectroscopic measurements.
- The translational energy ϵ'_{trans} depends on the size of the system, whereas, ϵ'_{rot}, ϵ'_{vib} and ϵ'_{el} are not. Because of this special dependence of ϵ'_{trans} on the size of the system, the partition function Q depends on the volume of the system, $\mathbb{V}$, and its temperature, T.
- The lowest quantum number defines the zero-point energy for each mode, and from the above expression, the zero-point energy for rotation is precisely zero (that is, for $J = 0$, $\epsilon'_{\text{rot}} = 0$), whereas it is a finite value for the other modes.

Consider the energy measured above zero-point energy level. For this, we can write

$$\begin{aligned} \epsilon_{\text{trans}} &= \epsilon'_{\text{trans}} - \epsilon_{\text{trans}\,0} \\ &\approx \frac{h_P^2}{8\, m} \left(\frac{n_1^2}{a_1^2} + \frac{n_2^2}{a_2^2} + \frac{n_3^2}{a_3^2} \right) \end{aligned}$$

Here, we are neglecting the small but finite value of $\epsilon_{\text{trans}\,0}$. Also,

$$\begin{aligned} \epsilon_{\text{rot}} &= \epsilon'_{\text{rot}} - \epsilon_{\text{rot}\,0} \\ &= \frac{h_P^2}{8\, \pi^2\, I} \, J(J+1) \\ \epsilon_{\text{vib}} &= \epsilon'_{\text{vib}} - \epsilon_{\text{vib}\,0} \\ &= n \, h_P \, \nu \\ \epsilon_{\text{el}} &= \epsilon'_{\text{el}} - \epsilon_{\text{el}\,0} \end{aligned}$$

Therefore, the total energy is

$$\epsilon' = \epsilon_{\text{trans}} + \epsilon_{\text{rot}} + \epsilon_{\text{vib}} + \epsilon_{\text{el}} + \epsilon_0$$

Now, let us consider the error in the total energy ϵ measured above the zero-point energy ϵ_0, where

$$\epsilon = \epsilon' - \epsilon_0$$

sensible energy, that is, energy measured above zero point

$$= \epsilon_{\text{trans}} + \epsilon_{\text{rot}} + \epsilon_{\text{vib}} + \epsilon_{\text{el}}$$

all measured above the zero-point energy. Thus, all are equal to zero at $T = 0$ K

Recall from Equations (4.24) and (4.25) that the partition function Q is defined in terms of the sensible energy, that is, the energy measured above the zero-point energy.

The partition function is

$$Q \equiv \sum_j g_j \, e^{-\epsilon_j / kT}$$

where

$$\epsilon_j = \epsilon_{i,\text{trans}} + \epsilon_{j,\text{rot}} + \epsilon_{n,\text{vib}} + \epsilon_{l,\text{el}}$$

Hence,

$$Q = \sum_i \sum_j \sum_n \sum_l g_i \, g_j \, g_n \, g_l \, \exp\left[-\frac{1}{kT}\left(\epsilon_{i,\text{trans}} + \epsilon_{j,\text{rot}} + \epsilon_{n,\text{vib}} + \epsilon_{l,\text{el}}\right)\right]$$

or

$$Q = \left[\sum_i g_i \, \exp\left(-\frac{\epsilon_{i,\text{trans}}}{kT}\right)\right] \times \left[\sum_j g_j \, \exp\left(-\frac{\epsilon_{j,\text{rot}}}{kT}\right)\right] \times \left[\sum_n g_n \, \exp\left(-\frac{\epsilon_{n,\text{vib}}}{kT}\right)\right] \times \left[\sum_l g_l \, \exp\left(-\frac{\epsilon_{l,\text{el}}}{kT}\right)\right] \tag{4.51}$$

Note that the "sum" in each parenthesis in Equation (4.51) are the partition functions of each mode of energy. Thus, Equation (4.51) can be written as

$$Q = Q_{\text{trans}} \, Q_{\text{rot}} \, Q_{\text{vib}} \, Q_{\text{el}}$$

Now, the evaluation of Q becomes essentially the evaluation of Q_{trans}, Q_{rot}, Q_{vib}, and Q_{el}.

First, let us consider the translational partition function

$$Q_{\text{trans}} = \sum_i g_{i,\text{trans}} \, \exp\left(\frac{-\epsilon_{i,\text{trans}}}{kT}\right)$$

In this equation, the summation is over all energy levels, each with g_i states. Therefore, the sum can just as well be taken over all energy states and be written as

$$Q_{\text{trans}} = \sum_i \exp\left(\frac{-\epsilon_{i,\text{trans}}}{kT}\right)$$
$$= \sum_{n_1=1}^{\infty}\sum_{n_2=1}^{\infty}\sum_{n_3=1}^{\infty} \exp\left[-\frac{h_P^2}{8\ mkT}\left(\frac{n_1^2}{a_1^2}+\frac{n_2^2}{a_2^2}+\frac{n_3^2}{a_3^2}\right)\right]$$

or

$$Q_{\text{trans}} = \left[\sum_{n_1=1}^{\infty}\exp\left(-\frac{h_P^2}{8\ mkT}\ \frac{n_1^2}{a_1^2}\right)\right] \times \left[\sum_{n_2=1}^{\infty}\exp\left(-\frac{h_P^2}{8\ mkT}\ \frac{n_2^2}{a_2^2}\right)\right]$$
$$\times \left[\sum_{n_3=1}^{\infty}\exp\left(-\frac{h_P^2}{8\ mkT}\ \frac{n_3^2}{a_3^2}\right)\right] \tag{4.52}$$

If each of the terms in each summation above were plotted versus n, an almost continuous curve would be obtained because of the close spacings between the translational energies. As a result, each summation can be replaced by an integral, resulting in

$$Q_{\text{trans}} = a_1\frac{\sqrt{2\pi\ mkT}}{h_P}\ a_2\frac{\sqrt{2\pi\ mkT}}{h_P}\ a_3\frac{\sqrt{2\pi\ mkT}}{h_P}$$

or

$$\boxed{Q_{\text{trans}} = \left(\frac{2\pi\ mkT}{h_P^2}\right)^{3/2}\ \mathbb{V}} \tag{4.53}$$

where $\mathbb{V} = (a_1\ a_2\ a_3)$ is the volume of the system.

To evaluate the rotational partition function, we use the quantum mechanics result $g_j = 2J + 1$.

Therefore,

$$Q_{\text{rot}} = \sum_j\ g_j\ \exp\left(\frac{-\epsilon_j}{kT}\right)$$

But

$$\epsilon_j = \frac{h_P^2}{8\pi^2 I}\ J\ (J+1)$$

Therefore,

$$Q_{\text{rot}} = \sum_{J=0}^{\infty}(2J+1)\ \exp\left[\frac{-h_P^2}{8\pi^2 IkT}\ J\ (J+1)\right]$$

Again replacing the summation by an integral, we can obtain

$$\boxed{Q_{\text{rot}} = \frac{8\pi^2 IkT}{h_P^2}} \tag{4.54}$$

For vibration partition function, from quantum mechanics, $g_n = 1$ for all levels of a diatomic molecule. Hence,

$$Q_{\text{vib}} = \sum_n g_n e^{-\epsilon_n/kT}$$

$$= \sum_{n=0}^{\infty} e^{-nh_P\nu/kT}$$

This is a simple geometric series, with a closed-form expression for the sum, resulting in

$$\boxed{Q_{\text{vib}} = \frac{1}{1 - e^{-nh_P\nu/kT}}} \tag{4.55}$$

For Q_{el}, no closed-form solution is possible. It is expressed as

$$Q_{\text{el}} \equiv \sum_{l=0}^{\infty} g_l \, e^{-\epsilon_l/kT}$$

or

$$Q_{\text{el}} = g_0 + g_1 \, e^{-\epsilon_1/kT} + e^{-\epsilon_2/kT} + \cdots \tag{4.56}$$

4.8 High-Temperature Thermodynamic Properties of a Single-Species Gas

The partition function, by Equation (4.53), is

$$Q_{\text{trans}} = \left(\frac{2\pi \, mkT}{h_P^2} \right)^{3/2} \mathbb{V}$$

Taking log on both sides, we have

$$\ln Q_{\text{trans}} = \frac{3}{2} \ln T + \frac{3}{2} \ln \left(\frac{2\pi mk}{h_P^2} \right) + \ln \mathbb{V}$$

Differentiating this with respect to temperature T, we have

$$\left(\frac{\partial \ln Q_{\text{trans}}}{\partial T} \right)_{\mathbb{V}} = \frac{3}{2} \frac{1}{T}$$

Substituting this into Equation (4.32), we have

$$e_{\text{trans}} = RT^2 \ \frac{3}{2} \ \frac{1}{T}$$

or

$$\boxed{e_{\text{trans}} = \frac{3}{2} \ RT} \tag{4.57}$$

From Equation (4.54), we have Q_{rot} as

$$Q_{\text{rot}} = \frac{8\pi^2 IkT}{h_P^2}$$

Taking log on both sides, we have

$$\ln Q_{\text{rot}} = \ln T + \ln\left(\frac{8\pi^2 Ik}{h_P^2}\right)$$

Thus,

$$\frac{\partial \ln Q_{\text{rot}}}{\partial T} = \frac{1}{T} \tag{4.58}$$

From Equations (4.58) and (4.32), we get

$$\boxed{e_{\text{rot}} = RT} \tag{4.59}$$

Similarly, from Equation (4.55), we have

$$\ln Q_{\text{vib}} = -\ln(1 - e^{-h_P \nu/kT})$$

Differentiating with respect to T, we have

$$\frac{\partial \ln Q_{\text{vib}}}{\partial T} = \frac{h_P \nu/kT^2}{e^{h_P \nu/kT} - 1} \tag{4.60}$$

From Equations (4.60) and (4.32), we get

$$\boxed{e_{\text{vib}} = \frac{h_P \nu/kT}{e^{h_P \nu/kT} - 1} \ RT} \tag{4.61}$$

Let us examine the above results with the *theorem of equipartition of energy* of kinetic theory of gases [4], which states that

"*each thermal degree of freedom of the molecule contributes* $\frac{1}{2}$ *kT to the energy of each molecule, or* $\frac{1}{2}$ *RT to the energy per unit mass of gas*."

We know that the translational motion of a molecule or atom contributes three thermal degrees of freedom. Hence, because of the equipartition of energy, the translational energy per unit mass should be

$$e_{\text{trans}} = 3\left(\frac{1}{2} \ RT\right) = \frac{3}{2} \ RT$$

This is same as Equation (4.57) obtained from the modern principles of statistical thermodynamics.

Similarly, for a diatomic molecule, the rotational motion contributes two thermal degrees of freedom. Therefore,

$$e_{\text{rot}} = 2\left(\frac{1}{2}\,RT\right) = RT$$

which is same as Equation (4.59).

For vibrational freedom, two degrees of freedom should result in

$$e_{\text{vib}} = 2\left(\frac{1}{2}\,RT\right) = RT$$

But this is not confirmed by Equation (4.61). Indeed, the factor

$$\frac{h_P\nu/kT}{(e^{-h_P\nu/kT} - 1)}$$

is less than unity, except when $T \to \infty$, when it approaches unity, thus in general, $e_{\text{vib}} < RT$, in conflict with classical theory. This implies the following.

- The classical results based on macroscopic observations do not necessarily describe phenomena in the microscopic world of molecules.
- As a result, the equipartition of energy principle is misleading.

Equation (4.61), obtained from quantum mechanics considerations, is the proper expression for vibrational energy.

Thus, we have for atoms

$$e = \frac{3}{2}\,RT + e_{\text{el}} \tag{4.62}$$

This implies that, for atoms,

Specific internal energy measured above zero-point energy (sensible energy)
= Translational energy + Electronic energy obtained directly from spectroscopic measurement

For molecules, we have the internal energy as

$$e = \frac{3}{2}\,RT + RT + \frac{h_P\nu/kT}{e^{h_P\nu/kT} - 1}\,RT + e_{\text{el}} \tag{4.63}$$

Also, we know that the specific heat at constant volume is

$$c_v \equiv \left(\frac{\partial e}{\partial T}\right)_v$$

Thus, from Equation (4.62), we have the c_v for atoms as

$$\boxed{c_v = \frac{3}{2} + \frac{\partial e_{\text{el}}}{\partial T}} \tag{4.64}$$

For molecules, from Equation (4.63), we have the c_v as

$$\boxed{c_v = \frac{3}{2}R + R + \frac{(h_P\nu/kT)^2\, e^{h_P\nu/kT}}{(e^{h_P\nu/kT}-1)^2}R + \frac{\partial e_{\text{el}}}{\partial T}} \tag{4.65}$$

From Equations (4.62)–(4.65), we see that both internal energy, e, and specific heat at constant volume, c_v, are functions of temperature, T, only. This is the case for a thermally perfect nonreacting gas. That is,

$$e = f_1(T)$$
$$c_v = f_2(T)$$

This is a consequence of our assumption that molecules are independent (no intermolecular forces) during the counting of microstates.

For a gas with only translational and rotational energy, we have the following.

For atoms,

$$c_v = \frac{3}{2}R$$

and for diatomic molecules,

$$c_v = \frac{5}{2}R$$

That is, c_v is a constant and independent of temperature. This is the case of a *calorically perfect gas*. For air around room temperature, being a perfect gas, we have

$$c_p - c_v = R$$

Therefore,

$$c_p = c_v + R$$

Substituting $c_v = \frac{5}{2}R$, we have

$$c_p = \frac{7}{2}R$$

Hence, the specific heats ratio γ becomes

$$\gamma = \frac{c_p}{c_v} = \frac{7}{5}$$
$$= 1.4$$

The theoretical variation of c_v for air as a function of temperature T is shown Figure 4.7.

Consider the perfect gas equation of state. In classical thermodynamics, the equation is obtained from state postulate (the state postulate is a term used in thermodynamics that defines the given number of properties to a thermodynamic system

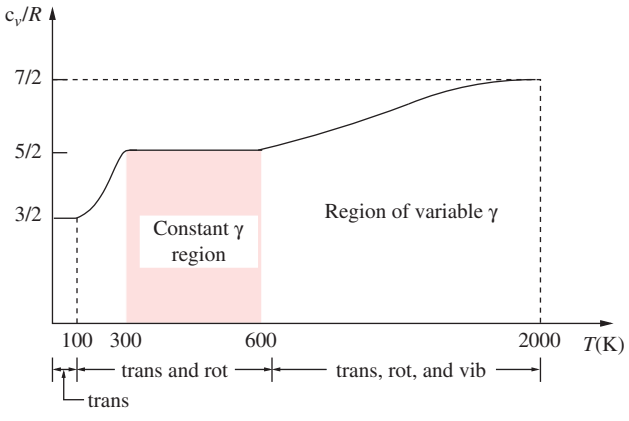

Figure 4.7 Variation of c_v/R with temperature.

in a state of equilibrium. The state postulate allows a finite number of properties to be specified in order to fully describe a state of thermodynamic equilibrium. Once the state postulate is given, the other unspecified properties must assume certain values. The state postulate says "*the state of a simple compressible system is completely specified by two independent, intensive properties*," but not from first principle. With statistical thermodynamics, the equation of state can be obtained from first principles as follows. From Equation (4.50), we have the pressure, in terms of partition function, as

$$p = NkT \left(\frac{\partial \ln Q}{\partial \mathbb{V}} \right)_T$$

Now, examine the partition function. The only one that depends on volume, $\mathbb{V}$, is the translational partition function Q_{trans}. Equation (4.53) gives the partition function as

$$Q_{\text{trans}} = \left(\frac{2\pi mkT}{h_P^2} \right)^{3/2} \mathbb{V}$$

Taking log on both sides and differentiating with respect to $\mathbb{V}$, we have

$$\left(\frac{\partial \ln Q}{\partial \mathbb{V}} \right)_T = \left(\frac{\partial \ln Q_{\text{trans}}}{\partial \mathbb{V}} \right)_T = \frac{1}{\mathbb{V}}$$

Hence, the pressure becomes

$$p = NkT \left(\frac{1}{\mathbb{V}} \right)$$

or

$$\boxed{p\,\mathbb{V} = NkT}$$

But $Nk = R$, the gas constant. Thus

$$p\,\mathbb{V} = RT$$

Note that this is the same as the classical thermodynamic relation obtained from state postulation.

4.9 Equilibrium Properties of High-Temperature Air

For high-temperature air,

- the equations from statistical thermodynamics can be used directly in the flow calculations and the thermodynamic properties can be generated internally in the calculation.
- tables of thermodynamic properties of high-temperature air is presented by Hilsenrath and Klein [5]. These tables were calculated using the statistical methods.
- graphical plots of high-temperature air properties are also available. Indeed, a large *Mollier diagram* is helpful in such cases.
- the tabulated data can be cast in the form of polynomial correlations that are easy and convenient to apply within the framework of flow calculations.

4.10 Kinetic Theory of Gases

Some important characteristics of gases are dominated by translational motion. A study of such matters is the purview of the science of kinetic theory. Consider a gas in a cubical box as shown in Figure 4.8.

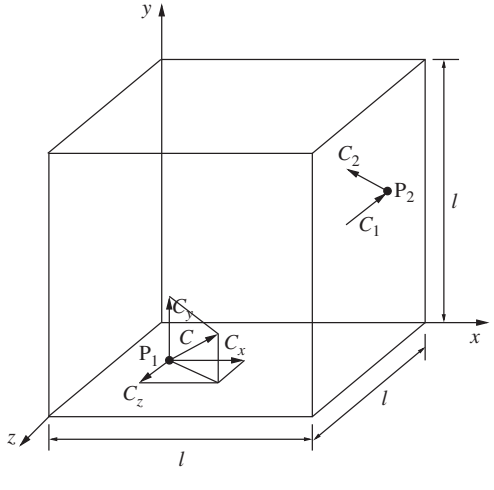

Figure 4.8 Illustration of particle velocity components.

Identify a gas molecule at some instant in time and at some location P_1. The particle has a translational velocity denoted by C. The components of the velocity along x-, y-, and z-directions are C_x, C_y, and C_z, respectively. Let us assume the gas molecule to be a structureless "billiard ball," translating in space and frequently colliding with the neighboring molecules. Such molecular collisions, given enough time, would establish a state of equilibrium in the system. Assume that the gas in the box is in equilibrium. When the molecule under study reaches the rightface of the box, it is assumed to specularly reflect from the surface at point P_2. Then $|C_1| = |C_2|$, that is, the magnitudes of the incident and reflected velocities are equal in magnitude and opposite in direction, and

$$C_{x_2} = -C_{x_1},\ C_{y_2} = C_{y_1},\ C_{z_2} = C_{z_1}$$

where C_{x_1} and C_{x_2}, respectively, are the components of incident and reflected velocities of the molecules in the x-direction, C_{y_1} and C_{y_2}, respectively, are the components of incident and reflected velocities of the molecules in the y-direction, and C_{z_1} and C_{z_2}, respectively, are the components of incident and reflected velocities of the molecules in the z-direction. The incident velocity C_1 and reflected velocity C_2 are equal in magnitude but opposite in direction.

During the impact, the molecule experiences a change in momentum in the x-direction given by $2\,mC_x$, where m is the mass of the molecule. The molecule makes a number of traverses back and forth across the box in the x-direction over a unit time (say 1 s). The number of complete traverses per unit time is $C_x/2\,l$, where l is the length of the box along the x-axis. Hence, the time rate of change of momentum experienced by the molecule, when impacting the right-hand face of the cube shown in Figure 4.8, is given by

$$(2\,mC_x)\left(\frac{C_x}{2\,l}\right) = \frac{mC_x^2}{l}$$

This is equal to force by Newton's second law.

As the pressure is force per unit area, pressure exerted by a particle on the right-hand face is given by

$$\frac{mC_x^2}{l^3} = \frac{mC_x^2}{\mathbb{V}}$$

where $\mathbb{V}$ is the volume of the system.

Now assume that we have a large number of molecules in the box, each with a different mass m_i and different velocity C_i. Then, the pressure exerted by the molecules in the system on the right-hand face is

$$p = \frac{1}{\mathbb{V}} \sum_i m_i\, C_{i,x}^2 \tag{4.66}$$

Similarly, the pressure exerted on the faces perpendicular to y- and z-directions, respectively, can be expressed as

$$p = \frac{1}{\mathbb{V}} \sum_i m_i\, C_{i,y}^2 \tag{4.67}$$

and

$$p = \frac{1}{\mathbb{V}} \sum_i m_i \, C_{i,z}^2 \tag{4.68}$$

The pressure is given by the average of Equations (4.66)–(4.68). Thus

$$p = \frac{1}{3\mathbb{V}} \sum_i m_i \, (C_{i,x}^2 + C_{i,y}^2 + C_{i,z}^2)$$

that is,

$$p = \frac{1}{3\mathbb{V}} \sum_i m_i \, C_i^2 \tag{4.69}$$

The total kinetic energy for the system, E'_{trans}, is given by

$$E'_{\text{trans}} = \frac{1}{2} \sum_i m_i \, C_i^2 \tag{4.70}$$

Combining Equations (4.69) and (4.70), we have

$$\boxed{p\mathbb{V} = \frac{2}{3} E'_{\text{trans}}} \tag{4.71}$$

This is the *kinetic theory equivalent* of the perfect gas state equation.

Assume that we have 1 mol of molecules in the system. Then the volume $\mathbb{V}$ in Equation (4.71) becomes the molar volume $\mathbb{V}_{\text{mol}}$, and E_{trans} is the kinetic energy per mole. Thus

$$\boxed{p\mathbb{V}_{\text{mol}} = \frac{2}{3} E_{\text{trans}}} \tag{4.72}$$

By state equation, we have

$$p\mathbb{V}_{\text{mol}} = R_u T \tag{4.73}$$

where R_u (= 8314 $\text{m}^2/(\text{s}^2\ \text{K})$) is the universal gas constant. Thus, the total kinetic energy of the system becomes

$$\boxed{E_{\text{trans}} = \frac{3}{2} R_u T} \tag{4.74}$$

This result is the same as that in Equation (4.57), we already know. Hence, our simple kinetic theory model leads to the same result as obtained by statistical mechanics for the translational energy.

Dividing Equation (4.74) by Avogadro's number N_A (= $6.02214 \times 10^{23}\ \text{mol}^{-1}$), we obtain

$$\frac{E_{\text{trans}}}{N_A} = \frac{3}{2} \frac{R_u}{N_A} T$$

$$\boxed{e_{\text{trans}} = \frac{3}{2}\, kT} \tag{4.74a}$$

where $k = R_u/N_A$ ($= 1.3806488 \times 10^{-23}$ m^2 kg/(s^2 K) is the Boltzmann constant. Equation (4.74a) gives the kinetic energy per mole.

Now, divide Equation (4.69) by the total mass of the system M, where $M = \sum_i m_i$,

$$\frac{p\mathbb{V}}{M} = \frac{1}{3}\frac{\sum_i m_i\, C_i^2}{\sum_i m_i} \tag{4.75}$$

Note that $M/\mathbb{V} = \rho$, and define a mean square velocity $\overline{C^2}$ as

$$\overline{C^2} \equiv \frac{\sum_i m_i\, C_i^2}{\sum_i m_i} \tag{4.76}$$

Then Equation (4.75) becomes

$$\boxed{\frac{p}{\rho} = \frac{1}{3}\,\overline{C^2}} \tag{4.77}$$

This is *another form* of the kinetic theory equivalent of the perfect gas state equation.

Using Equation (4.68), we find from Equation (4.77) that

$$\overline{C^2} = 3RT \tag{4.77a}$$

The root-mean-square (RMS) velocity is given by

$$\sqrt{\overline{C^2}} = \sqrt{3RT} \tag{4.78}$$

From the expression for the mean velocity in Equation (4.77a), the following can be inferred.

- The translational kinetic energy for a molecule, e_{trans}, is given by $\frac{1}{2}m_i\, C_i^2$.
- From Equation (4.74a), e_{trans} is also given by $\frac{3}{2}\, kT$, independent of the mass of the molecule.
- Hence, for a gas mixture at temperature T, the heavy molecule will be moving more slowly, on an average, than the light molecules.

4.11 Collision Frequency and Mean Free Path

Consider a molecule of diameter d moving at the mean molecular velocity, $\overline{C}$, shown in Figure 4.9.

As shown in the figure, any colliding molecule whose center comes within a distance d of the given molecule is going to cause a collision. As a given molecule moves

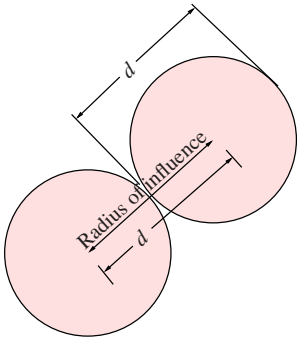

Figure 4.9 Illustration of radius of influence.

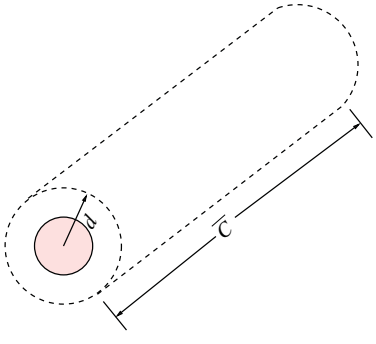

Figure 4.10 Cylindrical volume swept by a molecule of diameter d in 1 s.

through space, its radius of influence will sweep out a cylindrical volume per unit time equal to $\pi d^2 \overline{C}$ as shown in Figure 4.10.

If n is the number density, that is, the number of molecule per unit volume, then the molecule under consideration will experience $n\pi d^2 \overline{C}$ collisions per second. This is defined as the *single particle collision frequency*, Z',

$$\boxed{Z' = n\ \pi\ d^2\ \overline{C}} \tag{4.79}$$

The *mean free path*, λ, is defined as *the mean distance traveled by a molecule between two successive collisions*. As, in unit time, the molecule travels a distance $\overline{C}$ and experiences Z' collisions during this time, we can write

$$\boxed{\lambda = \frac{\overline{C}}{Z'} = \frac{1}{n\pi d^2}} \tag{4.80}$$

In the above results of collision frequency, Z', and mean free path, λ, the mean velocity, $\overline{C}$, which is very much simplified, is taken for analysis. For accurate results, we should consider the *relative velocity* rather than the mean velocity. This requires

a more sophisticated analysis; without going into the details, let us see the results of collision frequency and mean free path, in terms of the average velocity.

The single particle collision frequency between a single molecule of species A and the molecules of species B is given by

$$Z_{AB} = n_B \, \pi \, d^2 \, \overline{C}_{AB} \tag{4.81}$$

where n_B is the number density (that is, the number of molecules per unit volume) of space B and $\overline{C}_{AB}$ is the *mean relative velocity* between A and B molecules given by

$$\overline{C}_{AB} = \sqrt{\frac{8kT}{\pi \, m^*_{AB}}} \tag{4.82}$$

where k is the Boltzmann constant. Hence, we have the single particle collision frequency between a single molecule of species A and the molecules of species B as

$$\boxed{Z_{AB} = n_B \, \pi \, d^2_{AB} \sqrt{\frac{8kT}{\pi \, m^*_{AB}}}} \tag{4.83}$$

where m^*_{AB} is the *reduced mass*, defined as

$$m^*_{AB} \equiv \frac{m_A \, m_B}{m_A + m_B} \tag{4.84}$$

where m_A and m_B are the mass of the molecules of species A and B, respectively.

For a single species gas, the single particle collision frequency is obtained as follows.

For a single species gas, the reduced mass, given by Equation (4.84), with $m_A = m_B = m$, is

$$m^* = \frac{m^2}{2m} = \frac{m}{2}$$

Substituting this into Equation (4.82), we get the average velocity as

$$\overline{C} = \sqrt{\frac{8kT}{\pi(m/2)}}$$

that is,

$$\begin{aligned} \overline{C} &= \sqrt{2} \sqrt{\frac{8kT}{\pi \, m}} \\ &= \sqrt{2} \, \overline{C}_{AB} \end{aligned}$$

The average relative speed is $\sqrt{2}$ times (that is, slightly larger than) the average speed of one of the particles. Note that this is in accordance with our expectation that the relative average speed should be between $\overline{C}$ and $2\overline{C}$.

Substituting this $\overline{C}$ into Equation (4.83), we get the single particle collision frequency as

$$Z = n\pi d^2 \sqrt{2} \sqrt{\frac{8kT}{\pi m}}$$

But it is essential to note that the total collision frequency Z_{tot} will be n times the single particle collision frequency, divided by a factor 2 to avoid double counting. Thus the single particle collision frequency becomes

$$\boxed{Z = \frac{n}{\sqrt{2}} \pi d^2 \overline{C} = \frac{n}{\sqrt{2}} \pi d^2 \sqrt{\frac{8kT}{\pi m}}} \tag{4.85}$$

Note that the collision theory is based on collisions and the average total collision frequency per unit volume given by Equation (4.85) is the key quantity.

The difference between Equations (4.79) and (4.85) is that in Equation (4.85) more accurate result is achieved by the factor $\sqrt{2}$, which takes into account the relative velocity between molecules. Also, note that Equation (4.85) for a single species gas cannot be obtained directly by simply inserting $m_A = m_B$ in Equations (4.83) and (4.84). To specialize Equation (4.83) for a single species gas, it must be divided by an additional factor of 2 because of the collision counting procedure used to drive Equation (4.83).

For the mean free path of the single species gas, taking into account the relative velocities of the molecules, it can be shown that

$$\boxed{\lambda = \frac{1}{\sqrt{2} \pi d^2 n}} \tag{4.86}$$

Note that, in the above equation, πd^2 is called the *collision cross section* denoted by σ.

4.11.1 Variation of Z and λ with p and T of the Gas

From state equation, we have

$$p = \rho RT$$

where the gas constant $R = nk$, where n is the number density and k is the Boltzmann constant. Therefore,

$$p = nk\rho T$$

This gives the number density as

$$n = \frac{p}{kT}$$

Using this in Equation (4.85), we get the single particle collision frequency as

$$Z = \frac{n}{\sqrt{2}}\ \pi\ d^2\ \overline{C}$$

$$= \frac{n}{\sqrt{2}}\ \pi\ d^2\ \sqrt{\frac{8kT}{\pi\ m}}$$

that is,

$$Z = C\frac{p}{\sqrt{T}}$$

where

$$C = \sqrt{\frac{\pi}{km}}\ 2d^2$$

Thus

$$\boxed{Z\ \propto\ \frac{p}{\sqrt{T}}} \tag{4.87}$$

From Equation (4.86), we get the mean free path as

$$\lambda = \frac{1}{\sqrt{2}\ \pi\ d^2\ n}$$

Substituting $n = (p/kT)$, we get

$$\lambda = \frac{1}{\sqrt{2}\ \pi\ d^2}\ \frac{kT}{p}$$

or

$$\lambda = C_1\frac{T}{p}$$

where

$$C_1 = \frac{k}{\sqrt{2}\ \pi\ d^2}$$

Thus

$$\boxed{\lambda\ \propto\ \frac{T}{p}} \tag{4.88}$$

Note that the collision frequency is *directly proportional* to pressure and the mean free path is *inversely proportional* to pressure.

4.12 Velocity and Speed Distribution Functions

Consider N molecules of a gas distributed in some manner (not necessarily uniformly) throughout physical space, shown in Figure 4.11(a). The instantaneous location of a

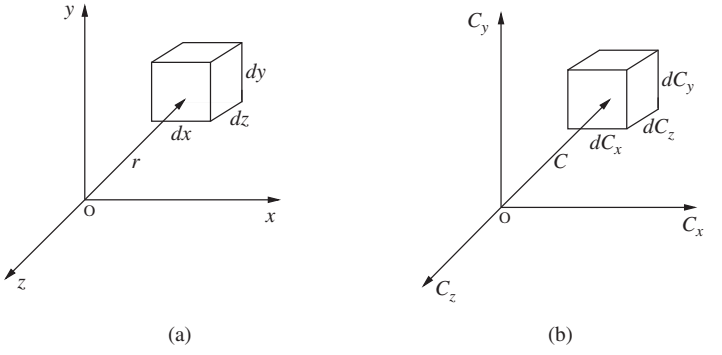

Figure 4.11 Volume element in (a) physical and (b) velocity spaces.

molecule is given by the position vector r. The system of N molecules is then represented by a cloud of N points in the physical space. Also, at the same instant, a given molecules has a velocity C. For each molecule, there is a corresponding point in the velocity space, shown in Figure 4.11(b). The *velocity distribution function* $f(r, C)$ is defined as the number of molecules per unit volume of physical space at r, with velocities per unit volume of velocity space at C. That is,

$$f(x, y, z, C_x, C_y, C_z)\, dx\, dy\, dz\, dC_x\, dC_y\, dC_z$$

represents the number of particles located between x and $x + dx$, y and $y + dy$, and z and $z + dz$, with velocities that range from C_x to $C_x + d\,C_x$, C_y to $C_y + d\,C_y$, and C_z to $C_z + d\,C_z$.

Note that the gaseous system is composed of molecules of constant motion in space and that they collide with the neighboring molecules, thus changing their velocities (in both magnitude and direction). Therefore, in the most general case of nonequilibrium gas, the molecules will be distributed nonuniformly throughout the space and time. That is, the number of points within the space volume element $dx\, dy\, dz$, in Figure 4.11(a), will be a function of r and t, and the number of points at any instant within the element $dC_x\, dC_y\, dC_z$, in Figure 4.11(b), may be changing with time.

Integrating over all space and all velocities, we get

$$\int_{-\infty}^{\infty}\int_{-\infty}^{\infty}\int_{-\infty}^{\infty}\int_{-\infty}^{\infty}\int_{-\infty}^{\infty}\int_{-\infty}^{\infty} f(x, y, z, C_x, C_y, C_z) d_x d_y d_z\, dC_x dC_y dC_z = N \tag{4.89}$$

One of the intrinsic values of the velocity distribution function f is that the average value of any physical quantity Q, which is a function of space and/or velocity, $Q = Q(x, y, z, C_x, C_y, C_z)$, can be obtained from

$$\overline{Q} = \frac{1}{N}\int_{-\infty}^{\infty}\int_{-\infty}^{\infty}\int_{-\infty}^{\infty}\int_{-\infty}^{\infty}\int_{-\infty}^{\infty}\int_{-\infty}^{\infty} Q f\, d_x\, d_y\, d_z\, dC_x\, dC_y\, dC_z \tag{4.90}$$

where $\overline{Q}$ is the average value of the property Q.

Now consider the case of a gas in translational equilibrium, that is, the number density n is constant, independent of x, y, and z, and the number of molecular collisions that tend to decrease the number of points in the volume $dC_x\ dC_y\ dC_z$ in velocity space is exactly balanced by other molecular collisions that increase the number of points in the elemental space volume $dxdydz$. For this case, the velocity distribution function, f, becomes essentially a velocity distribution function $f = f(C_x,\ C_y,\ C_z)$, given by [6]

$$\boxed{f(C_x,\ C_y,\ C_z) = N\left(\frac{m}{2\pi kT}\right)^{3/2} \exp\left[\frac{-m}{2kT}\left(C_x^2\ C_y^2\ C_z^2\right)\right]} \tag{4.91}$$

This is called the *Maxwellian distribution*. This gives the number of molecules per unit volume of velocity space located by the velocity vector C. Note that both f and *vdf* denote magnitude and direction.

In a system in equilibrium, velocity distribution function f is a symmetric function, that is,

$$f(C_x,\ C_y,\ C_z) = f(-C_x,\ C_y,\ C_z) = f(C_x, -C_y,\ C_z),\ \ldots$$

Thus, for a system under equilibrium, we are concerned only with the magnitude of the molecular velocity, that is, the speed of the molecules. Hence, we can introduce *speed distribution function* $\chi\ (C)$ as follows. Consider the velocity space shown in Figure 4.12.

All molecules on the surface of the sphere of radius C have the same speed. Now consider the space between the spheres of radius C and $C + dC$. The volume of the sphere is $4\pi C^2 dC$.

The number of molecules per unit volume of velocity space is given by Equation (4.91). Thus the number of particles in the space between the two spheres becomes

$$4\pi\ N\left(\frac{m}{2\pi\ kT}\right)^{3/2} C^2\ \exp\left(-\frac{mC^2}{2\ kT}\right)\ dC$$

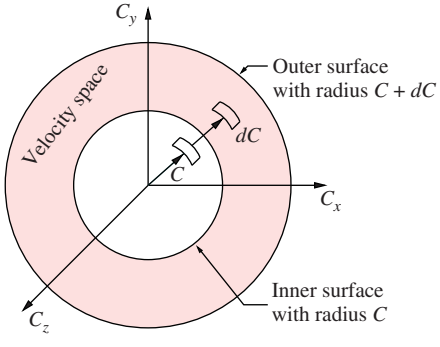

Figure 4.12 Velocity space between spherical surfaces of radius C and $C + dC$.

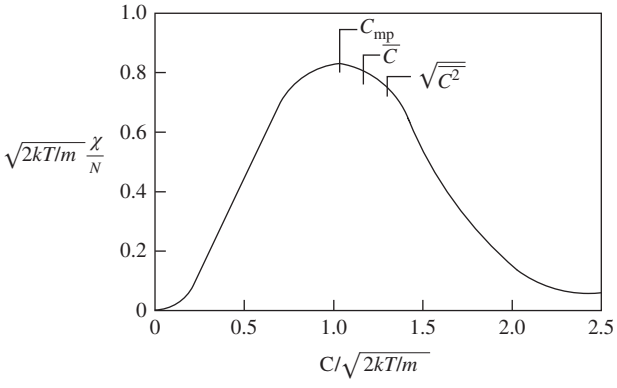

Figure 4.13 Variation of speed distribution function with molecular speed.

This gives the number of particles with speed between C and $C + dC$. In turn, the number of particles with speed C per unit velocity change, which is defined as the speed distribution function χ, is given by

$$\boxed{\chi = 4\pi\, N \left(\frac{m}{2\pi\, kT}\right)^{3/2} C^2\, e^{-(mC^2/2kT)}} \tag{4.92}$$

Variation of $\sqrt{2\pi\, kT/m}\,\frac{\chi}{N}$ with $C/\sqrt{2\pi\, kT/m}$ is shown in Figure 4.13. Values of most probable speed, C_{mp}; mean speed, $\overline{C}$; and root-mean-square speed, $\sqrt{\overline{C^2}}$, are marked on the plot.

Most probable speed is the speed corresponding to maximum value of χ, and it can be obtained by differentiating Equation (4.92) as

$$\boxed{C_{mp} = \sqrt{2RT}} \tag{4.93a}$$

where R is the specific gas constant. The constant R can be expressed as

$$R = \frac{R_u}{m}$$

where R_u is the universal gas constant and m is the molecular mass. The gas constant R can also be expressed as

$$R = \frac{k}{m}$$

where k ($= 1.38 \times 10^{-23}$ J/K) is the Boltzmann constant and m is the molecular mass of the gas.

Average speed is obtained from Equation (4.90) by replacing Q by C. The result is

$$\boxed{\overline{C} = \sqrt{\frac{8RT}{\pi}}} \tag{4.93b}$$

Root-mean-square speed is obtained from Equation (4.90) with $Q = C^2$. Root-mean-square speed is the measure of the speed of particles in a gas that is most convenient for problem solving within the kinetic theory of gases. It is defined as the square root of the average velocity of the molecules in a gas. The root-mean-square (RMS) speed can be expressed as

$$\boxed{\sqrt{\overline{C}^2} = \sqrt{\frac{3R_uT}{M_m}}} \tag{4.93c}$$

where M_m is the molar mass of the gas in kilograms per mole, R is the molar gas constant, and T is the temperature in kelvin. Although the molecules in a sample of gas have an average kinetic energy (and, therefore, an average speed), the individual molecules move at various speeds and they stop and change direction according to the law of density measurements and isolation, that is, they exhibit a distribution of speeds. Some move fast, others relatively slow. Collisions change individual molecular speeds, but the distribution of speeds remains the same. This equation is derived from kinetic theory of gases using Maxwell–Boltzmann distribution function. The higher the temperature is, the greater the mean velocity will be. This works well for both nearly ideal atomic gases such as helium and molecular gases such as diatomic oxygen. This is because despite the larger internal energy in many molecules (compared to that for an atom), $3RT/2$ is still the mean translational kinetic energy. This can also be written in terms of the Boltzmann constant ($k = 1.38 \times 10^{-23}$ J/K) as

$$\sqrt{\overline{C}^2} = \sqrt{\frac{3kT}{m}}$$

where m is the mass of one molecule of the gas. But $k/m = R$; thus

$$\boxed{\overline{C}^2 = \sqrt{3RT}} \tag{4.93d}$$

This can also be derived with energy methods:

$$E_{\text{ke}} = \frac{3}{2}nRT = \frac{3}{2}NkT$$

where E_{ke} is the kinetic energy and N is the number of gas molecules.

$$E_{\text{ke,molecule}} = \frac{1}{2}mv^2$$

Given that v^2 ignores direction, it is logical to assume that the formula can be extended to the entire sample, replacing m with the entire sample's mass, equal to the molar mass times the number of moles n yielding

$$\frac{1}{2}nMv^2 = E_{\text{ke}}$$

Therefore,

$$\sqrt{\overline{C}^2} = \sqrt{\frac{2E_{\text{ke}}}{m}}$$

which is equivalent.

The same result is obtained by solving the Gaussian integral containing the Maxwell speed distribution, χ:

$$\begin{aligned}
\sqrt{\overline{C}^2} &= \sqrt{\int_0^\infty C^2 \chi \, d\chi} \\
&= \sqrt{\int_0^\infty 4\pi \left(\frac{m}{2\pi kT}\right)^{3/2} C^4 \quad e^{-mC^2/2kT} dC} \\
&= \sqrt{4\pi \left(\frac{m}{2\pi kT}\right)^{3/2} \frac{3}{8}\pi^{1/2} \left(\frac{2kT}{m}\right)^{5/2}} \\
&= \sqrt{\frac{3kT}{m}}
\end{aligned}$$

Example 4.3 Calculate the most probable, mean, and RMS speeds of air at standard sea level state.

Solution

Given $T = 15°\text{C} = 288.15$ K.
The most probable velocity, by Equation (4.93a), is

$$\begin{aligned}
C_{\text{mp}} &= \sqrt{2RT} \\
&= \sqrt{2 \times 287 \times 288.15} \\
&= \boxed{406.69 \text{ m/s}}
\end{aligned}$$

The mean or average speed, by Equation (4.93b), is

$$\begin{aligned}
\overline{C} &= \sqrt{\frac{8RT}{\pi}} \\
&= \sqrt{\frac{8 \times 287 \times 288.15}{\pi}} \\
&= \boxed{458.90 \text{ m/s}}
\end{aligned}$$

The root-mean-square speed, by Equation (4.93d), is

$$\begin{aligned}\sqrt{\overline{C}^2} &= \sqrt{3RT} \\ &= \sqrt{3 \times 287 \times 288.15} \\ &= \boxed{498.09 \text{ m/s}}\end{aligned}$$

■

4.13 Inviscid High-Temperature Equilibrium Flows

A flow is said to be in *local thermodynamic equilibrium* if a local Boltzmann distribution, which is given by

$$N_j^* = N \frac{e^{-\epsilon_j/kT}}{Q}$$

exists at each point in the flow at the local temperature T.

A flow is said to be in *local chemical equilibrium* if the local chemical composition at each point in the flow is the same as that determined by the chemical equilibrium calculations.

In our present discussions, we will simply assume that the local equilibrium conditions hold at each point in the flow field.

4.14 Governing Equations

Consider the following equations of continuity, momentum, and energy for an inviscid compressible flow.

Continuity equation:

$$\frac{\partial \rho}{\partial t} + \frac{\partial(\rho u)}{\partial x} + \frac{\partial(\rho v)}{\partial y} + \frac{\partial(\rho w)}{\partial z} = 0$$

Momentum equation (x-, y-, and z-components, respectively):

$$\rho \frac{\partial u}{\partial t} + \rho u \frac{\partial u}{\partial x} + \rho v \frac{\partial u}{\partial y} + \rho w \frac{\partial u}{\partial z} = -\frac{\partial p}{\partial x}$$

$$\rho \frac{\partial v}{\partial t} + \rho u \frac{\partial v}{\partial x} + \rho v \frac{\partial v}{\partial y} + \rho w \frac{\partial v}{\partial z} = -\frac{\partial p}{\partial y}$$

$$\rho \frac{\partial w}{\partial t} + \rho u \frac{\partial w}{\partial x} + \rho v \frac{\partial w}{\partial y} + \rho w \frac{\partial w}{\partial z} = -\frac{\partial p}{\partial z}$$

Energy equation:

$$\frac{\partial s}{\partial t} + u \frac{\partial s}{\partial x} + v \frac{\partial s}{\partial y} + w \frac{\partial s}{\partial z} = 0$$

This is a *specialized energy equation* for an adiabatic, inviscid flow.

- Continuity equation is a statement that the mass flow rate is conserved.
- Momentum equations are statements of Newton's second law, $F = ma$.
- Energy equation is a statement that entropy is constant along a streamline for an inviscid, adiabatic flow.

If entropy is constant along a streamline, then for an isentropic process of a calorically perfect gas, the quantity p/ρ^{γ} is also constant along a streamline, and we can write the above specialized energy equation in terms of the entropy in the following form.

$$\frac{\partial}{\partial t}\left(\frac{p}{\rho^{\gamma}}\right) + u\,\frac{\partial}{\partial x}\left(\frac{p}{\rho^{\gamma}}\right) + v\,\frac{\partial}{\partial y}\left(\frac{p}{\rho^{\gamma}}\right) + w\,\frac{\partial}{\partial z}\left(\frac{p}{\rho^{\gamma}}\right) = 0$$

Thus, the continuity, momentum, and energy equations in terms of entropy s are valid for a high-temperature, chemically reacting, inviscid, equilibrium flow.

Note that the above equation in terms of p/ρ^{γ} is not valid for such a flow, because it is a specialized form assuming constant γ and, hence, applied only to *calorically perfect gases*.

The energy equation in terms of entropy s is a statement that the entropy of a moving fluid element is constant in an adiabatic, inviscid flow. For a high-temperature gas, this remains true as long as the flow is in local equilibrium.

However, for a nonequilibrium flow, we know that there is entropy increase due to the irreversible effect of the nonequilibrium process, and hence, the energy equation *does not hold* for a nonequilibrium inviscid flow.

For such flows, and essentially for all high-temperature flows, it is preferable to deal with another variable rather than the entropy in the energy equation.

Let us choose the total enthalpy, h_0, as the *independent variable* and write the energy equation for an adiabatic inviscid flow as

$$\boxed{\rho\,\frac{Dh_0}{Dt} = \rho\,\frac{\partial h_0}{\partial t} + \rho u\,\frac{\partial h_0}{\partial x} + \rho v\,\frac{\partial h_0}{\partial y} + \rho w\,\frac{\partial h_0}{\partial z} = \frac{\partial p}{\partial t}} \tag{4.94}$$

This equation is valid for *both equilibrium* and *nonequilibrium flows*.

Therefore, the governing equations for an inviscid, high-temperature, equilibrium flows are the following.

Continuity equation:

$$\frac{\partial \rho}{\partial t} + \nabla \cdot (\rho V) = 0 \tag{4.95}$$

Momentum equation:

$$\rho \frac{DV}{Dt} = -\nabla p \tag{4.96}$$

Energy equation:

$$\rho \frac{Dh_0}{Dt} = \frac{\partial p}{\partial t} \tag{4.97}$$

where the stagnation enthalpy h_0 is given by

$$h_0 = h + \frac{V^2}{2} \tag{4.98}$$

where h is the static enthalpy and V is the flow velocity. The governing equations (4.95)–(4.97) constitute three equations for the four unknowns, namely, the density, ρ; velocity, V; pressure, p; and enthalpy, h.

Therefore, this system of three equations must be completed by the addition of the equilibrium thermodynamic properties for the gas, in order to solve for ρ, V, p, and h. Conceptually, we can write these properties in the form

$$T = T\ (\rho, h) \tag{4.99}$$

$$p = p\ (\rho, h) \tag{4.100}$$

Therefore, Equations (4.95)–(4.97), (4.99), and (4.100) constitute five equations for the five unknowns, p, V, ρ, h, and T.

In a given calculation, Equations (4.99) and (4.100) can take the form of any of the following.

- A direct calculation of the equilibrium thermodynamic properties from the equations of statistical thermodynamics carried out in parallel with the solution of the flow equations.
- A tabulation of the equilibrium thermodynamic properties.
- Correlations of the equilibrium thermodynamic properties.
- Graphical plots of the equilibrium thermodynamic properties.

It is important to note that the analytical, closed-form solutions of Equations (4.95)–(4.100) have not yet been obtained in the literature, even for the simplest type of high-temperature flow problems.

4.15 Normal and Oblique Shocks

Consider a stationary normal shock, as shown in Figure 4.14, with known flow field ahead of it. Let us assume that the shock is strong enough to compress the flow resulting in the downstream temperature, T_2, which is high enough to cause vibrational excitation and chemical reactions behind the shock. Also let us assume that local thermodynamic and chemical equilibria hold behind the shock. The conditions ahead of the shock are known, and the problem now is to calculate the properties behind the shock.

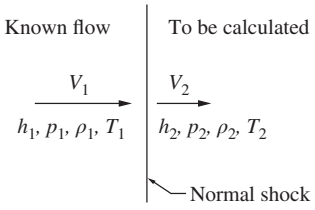

Figure 4.14 Flow through a stationary normal shock.

The governing equations for the flow across a normal shock (one-dimensional flow) are

Continuity equation:

$$\rho_1 V_1 = \rho_2 V_2 \tag{4.101}$$

Momentum equation:

$$p_1 + \rho_1 V_1^2 = p_2 + \rho_2 V_2^2 \tag{4.102}$$

Energy equation:

$$h_1 + \frac{V_1^2}{2} = h_2 + \frac{V_2^2}{2} \tag{4.103}$$

Note that the Equations (4.101) and (4.102) are general and *valid* for both reacting and nonreacting gases.

Assume that the equilibrium thermodynamic properties for high-temperature gas are known from the techniques discussed, for example, as tables or graphs.

Let us consider these properties in terms of the following functional relations:

$$p_2 = p\ (\rho_2, h_2) \tag{4.104}$$

$$T_2 = T\ (\rho_2, h_2) \tag{4.105}$$

Recall that for calculation in perfect gases, Equations (4.101)–(4.105) yield a series of closed-form algebraic relations for p_2/p_1, T_2/T_1, M_2, etc. as functions of M_1. Derivation of these equations and the physical significance of the flow process through normal shock in perfect gas are presented in detail by Rathakrishnan [7]. But no such simple formulae can be obtained when the gas is vibrationally excited and/or chemically reacting. For such high-temperature flows, Equations (4.101)–(4.105) must be solved numerically.

To set up such a numerical scheme to solve for flow properties behind the normal shock, let us first rearrange Equations (4.101)–(4.103).

From Equation (4.101), we can write the velocity, V_2, downstream of the shock as

$$V_2 = \frac{\rho_1 V_1}{\rho_2} \tag{4.106}$$

Substituting Equation (4.106) into Equation (4.102), we get

$$p_1 + \rho_1 V_1^2 = p_2 + \rho_2 \left(\frac{\rho_1 V_1}{\rho_2} \right)^2 \tag{4.107}$$

Solving Equation (4.107) for p_2, we get

$$\boxed{p_2 = p_1 + \rho_1 V_1^2 \left(1 - \frac{\rho_1}{\rho_2} \right)} \tag{4.108}$$

Substituting Equation (4.106) into Equation (4.103), we get

$$h_1 + \frac{V_1^2}{2} = h_2 + \frac{(\rho_1 V_1 / \rho_2)^2}{2} \tag{4.109}$$

Solving Equation (4.109), we obtain the enthalpy h_2 behind the shock as

$$\boxed{h_2 = h_1 + \frac{V_1^2}{2} \left[1 - \left(\frac{\rho_1}{\rho_2} \right)^2 \right]} \tag{4.110}$$

As the flow properties ρ_1, V_1, p_1, h_1, etc. ahead of the shock are known, Equations (4.108) and (4.110) express p_2 and h_2, respectively, in terms of only one unknown, namely, the density ratio ρ_1/ρ_2. This establishes the basis for an interactive numerical solution as follows.

1. Assume a value for ρ_1/ρ_2 (a value of 0.1 is usually good for a start).
2. Calculate p_2 from Equation (4.108) and h_2 from Equation (4.110).
3. With these p_2 and h_2, calculate ρ_2 from Equation (4.104).
4. Form a new value of ρ_1/ρ_2, using the value of ρ_2 obtained with step 3.
5. Use this new value of ρ_1/ρ_2 in Equations (4.108) and (4.110) to obtain new value of p_2 and h_2, respectively. Repeat steps 3–5 until convergence is obtained.
6. Now we have the correct values of p_2, h_2, and ρ_2. Obtain the correct value of T_2 from Equation (4.105).
7. Obtain the correct value of velocity V_2 from Equation (4.106).

Example 4.4 Determine the static pressure and temperature rise caused by a normal shock in a Mach 6 air stream with pressure and temperature ahead of the shock as 80 kPa and 270 K. Also, find the pressure loss caused by the shock.

Solution

Given $M_1 = 6$, $p_1 = 80$ kPa, and $T_1 = 270$ K.

From normal shock table [8], for $M_1 = 6$,

$$\frac{p_2}{p_1} = 41.833, \qquad \frac{T_2}{T_1} = 7.9406, \qquad \frac{p_{02}}{p_{01}} = 0.029651$$

From isentropic table, for $M_1 = 6$,

$$\frac{p_1}{p_{01}} = 0.63336 \times 10^{-3}$$

Therefore,

$$\begin{aligned} p_2 &= 41.833\ p_1 \\ &= 41.833 \times 80 \\ &= 3346.64 \text{ kPa} \\ T_2 &= 7.9406\ T_1 \\ &= 7.9406 \times 270 \\ &= 2143.962 \text{ K} \\ p_{01} &= \frac{p_1}{0.63336 \times 10^{-3}} \\ &= \frac{80}{0.63336 \times 10^{-3}} \\ &= 126.31 \times 10^3 \text{ kPa} \end{aligned}$$

Thus the static pressure and the temperature are

$$\begin{aligned} \Delta p &= p_2 - p_1 \\ &= 3346.64 - 80 \\ &= \boxed{3266.64 \text{ kPa}} \\ \Delta T &= T_2 - T_1 \\ &= 2143.962 - 270 \\ &= \boxed{1873.962} \end{aligned}$$

The total pressure behind the shock is

$$\begin{aligned} p_{02} &= 0.029651\ p_{01} \\ &= 0.029651 \times (126.31 \times 10^3) \\ &= 3.745 \times 10^3 \text{ kPa} \end{aligned}$$

Thus the pressure loss caused by the shock is

$$p_{01} - p_{02} = 126.31 \times 10^3 - 3.745 \times 10^3$$
$$= \boxed{122.56 \times 10^3 \text{ kPa}}$$ ■

There is a basic practical difference between the shock results for a calorically perfect gas and those for a chemically reacting gas.

For a calorically perfect gas, we have the pressure, density, and enthalpy ratios across a shock as [7]

$$\frac{p_2}{p_1} = f_1\,(M_1)$$
$$= 1 + \frac{2\gamma}{\gamma + 1}(M_1^2 - 1)$$
$$\frac{\rho_2}{\rho_1} = f_2\,(M_1)$$
$$= \frac{(\gamma + 1)M_1^2}{(\gamma - 1)M_1^2 + 2}$$
$$\frac{h_2}{h_1} = f_3\,(M_1)$$
$$= 1 + \frac{2(\gamma - 1)}{(\gamma + 1)^2}\frac{(\gamma M_1^2 + 1)}{M_1^2}(M_1^2 - 1)$$

Note that only the Mach number upstream of the shock, M_1, is required to obtain the ratio of flow properties across a normal shock wave.

But, for an equilibrium chemically reacting gas, we have seen that

$$\frac{p_2}{p_1} = g_1\,(V_1, p_1, T_1)$$
$$\frac{\rho_2}{\rho_1} = g_2\,(V_1, p_1, T_1)$$
$$\frac{h_2}{h_1} = g_3\,(V_1, p_1, T_1)$$

Note that, in this case, three freestream properties, namely, the velocity, pressure, and temperature, are necessary to obtain the properties downstream of a normal shock wave.

In contrast to a calorically perfect gas, the upstream Mach number M_1 no longer plays a dominant role in the results of normal shock wave in a high-temperature gas. In fact, for most high-temperature flows, in general, the Mach number is not a particularly useful quantity.

Consider a *reentry vehicle* at 5000 m (about 17,000 ft) standard altitude with a velocity of 10,000 m/s (about 36,000 ft/s). The properties across a normal shock wave

Table 4.1 The pressure, density, enthalpy, and temperature ratio across a normal shock at the face of a reentry vehicle[a]

Property	For calorically perfect gas $\gamma = 1.4$	For equilibrium chemically reacting gas (CAL report AG-1729-A-2)
p_2/p_1	1233	1387
ρ_2/ρ_1	5.972	15.19
h_2/h_1	206.35	212.8
T_2/T_1	206.35	41.64

[a]Cornell Aeronautical Laboratory, Inc., Buffalo, NY 14221.

for this case, considering the gas as calorically perfect and chemically reacting, are listed in Table 4.1.

Note that the chemical reactions have the strongest effect on the temperature T. This is generally true for all types of chemically reacting flows – the temperature T is the most sensitive variable. In contrast, the pressure ratio is affected only by a small amount. Pressure is a "mechanically" oriented variable and is governed mainly by the fluid mechanics of the flow, and not so much by the thermodynamic. This is substantiated by examining the momentum Equation (4.102). For high-speed flows, $V_2 \ll V_1$, and $p_2 \gg p_1$. Hence, from Equation (4.102), we have

$$\boxed{p_2 \approx \rho_1 V_1^2}$$

This is a common hypersonic approximation; note that p_2 is mainly governed by the freestream velocity, and the thermodynamic effects are secondary.

In an equilibrium dissociating and ionizing gas, increasing the pressure at constant temperature tends to decrease the atom and ion mass fractions; this effect on equilibrium normal shock wave properties are shown in Figure 4.15.

Note that the temperature ratio, T_2/T_1, is high at high levels of freestream pressure, p_1, and decreases with decrease of freestream pressure. The gas is less dissociated and ionized at higher pressures, and hence, more energy goes into the translational molecular motion behind the shock rather than into the zero-point energy of the products of dissociation.

The ratio of density, ρ_2/ρ_1, across the shock has an important effect on the *shock detachment distance* in front of a blunt-nosed body in a hypersonic flow. An approximate expression for the shock detachment distance, δ, ahead of the nose of a blunt-nosed body, with spherical nose of radius R, in terms of the density ratio across the detached shock is [9]

$$\boxed{\frac{\delta}{R} = \frac{\rho_1/\rho_2}{1 + \sqrt{2\,(\rho_1/\rho_2)}}} \tag{4.111}$$

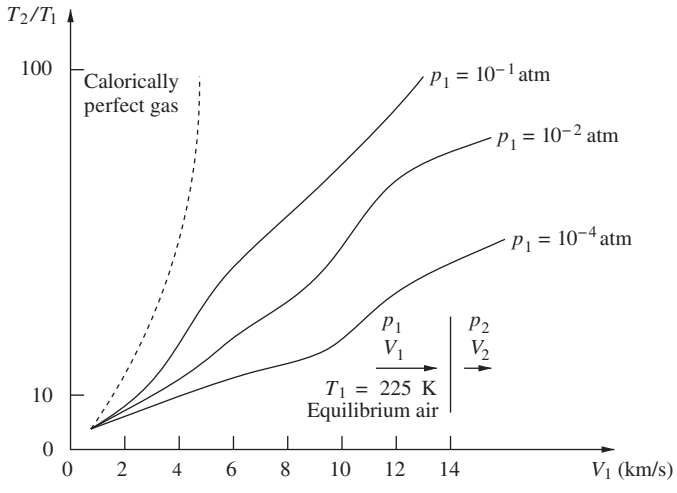

Figure 4.15 Effect of freestream pressure on the temperature ratio across a normal shock in equilibrium air.

In the limit of high velocities, ρ_1/ρ_2 becomes small compared to unity, and Equation (4.111) is approximated by

$$\frac{\delta}{R} \approx \frac{\rho_1}{\rho_2} = \frac{1}{(\rho_2/\rho_1)} \tag{4.112}$$

Therefore, the value of the density ratio across a normal shock has a major impact on shock detachment distance; the higher the density ratio, ρ_2/ρ_1, is, the smaller is the shock detachment distance, δ.

The effect of chemical reactions is to increase density ratio, ρ_2/ρ_1, which in turn decreases the shock detachment distance.

Therefore, in comparison to a calorically perfect gas, the shock wave for a chemically reacting gas (at the same velocity and altitude conditions) will lie closer to the body, as illustrated in Figure 4.16.

Example 4.5 Mach 4.6 air stream at 0.1 atm and 200 K flows past a blunt nose of radius of curvature of 33 mm. Determine the shock detachment distance along the stagnation streamline.

Solution

Let subscripts 1 and 2 refer to the flow state ahead of and behind the shock, respectively. Given $M_1 = 4.6$, $p_1 = 0.1$ atm, $T_1 = 200$ K, and $R = 33$ mm.
At the given conditions, the freestream can be treated as perfect with specific heats ratio $\gamma = 1.4$. For $M_1 = 4.6$, from normal shock table, for $\gamma = 1.4$,

$$\frac{\rho_2}{\rho_1} = 4.8532$$

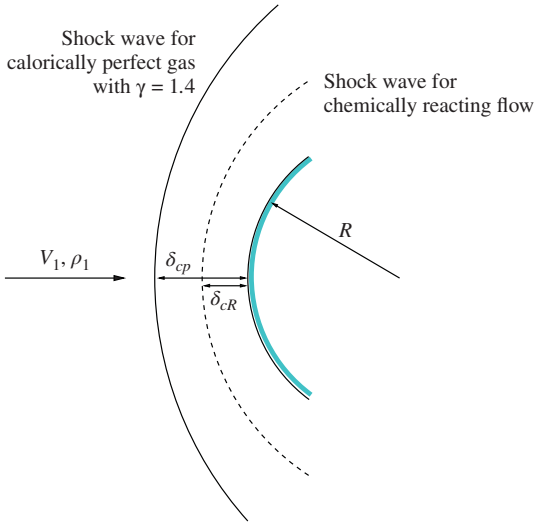

Figure 4.16 Relative locations of bow shock for a perfect and chemically reacting gases.

By Equation (4.111), the shock detachment distance from the blunt nose is

$$\begin{aligned}\delta &= R\left[\frac{\rho_1/\rho_2}{1+\sqrt{2\,(\rho_1/\rho_2)}}\right] \\ &= 33\times\left[\frac{1/4.8532}{1+\sqrt{2\times 1/4.8532}}\right] \\ &= \boxed{4.14 \text{ mm}}\end{aligned}$$

■

4.16 Oblique Shock Wave in an Equilibrium Gas

Consider the flow across an oblique shock, as shown in Figure 4.17, at an angle β to the freestream flow. It can be shown that $V_{t_1} = V_{t_2}$. This is a basic mechanical

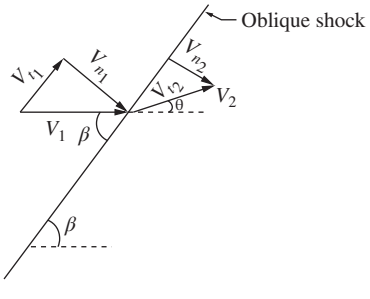

Figure 4.17 Oblique shock in an equilibrium gas.

result obtained from the momentum equation, and hence, it is not influenced by high-temperature effects. The thermodynamic changes across the oblique shock are dictated only by the component of the upstream velocity, V_{n_1}, perpendicular to the shock. Therefore, for the high-temperature equilibrium flow across an oblique shock wave, we have the same basic, familiar results as those for a chemically reacting flow through a normal shock. Thus,

$$\tan(\beta - \theta) = \frac{V_{n_2}}{V_{t_2}} \tag{4.113}$$

By multiplying and dividing the right-hand side by V_{n_1}, we have

$$\tan(\beta - \theta) = \frac{V_{n_2}}{V_{t_1}} = \frac{V_{n_2}}{V_{n_1}} \frac{V_{n_1}}{V_{t_1}}$$

But $\frac{V_{n_1}}{V_{t_1}} = \tan\ \beta$; thus

$$\boxed{\tan(\beta - \theta) = \frac{V_{n_2}}{V_{n_1}}\ \tan\beta} \tag{4.114}$$

This relation in terms of θ, β, V_{n_2}, and V_{n_1} for the equilibrium high-temperature gases is the analog of the $\theta-\beta-M$ relation for calorically perfect gases. An equivalent $\theta-\beta-V$ diagram for high-temperature air is given in Figure 4.18. A plot of shock angle, β,

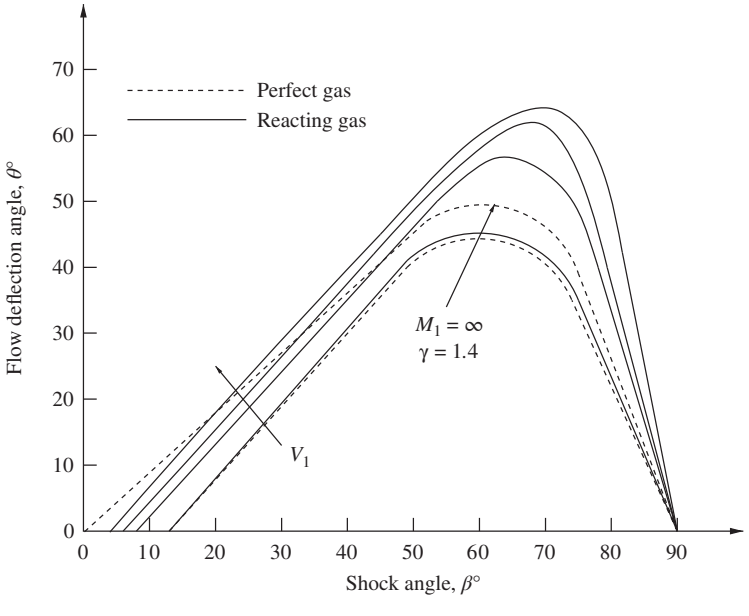

Figure 4.18 Flow deflection angle–shock angle–velocity diagram for oblique shocks in high-temperature air at 10,000 ft altitude.

variation with the flow turning angle, θ, as a function of upstream velocity V_1 is given in Figure 4.18. A similar plot of β variation with θ as a function of upstream Mach number ($\theta-\beta-M$ plot) for perfect gases is given in Figure 4.3 of Reference 7.

From Figure 4.18, it is seen that

- The $\theta-\beta-M$ behavior for equilibrium chemically reacting air is qualitatively similar to calorically perfect air.
- For the equilibrium chemically reacting results, the flow Mach number, M_1, upstream of the shock is not an important parameter. The results of an oblique shock wave in a chemically reacting flow depend on the upstream velocity, V_1, as well as the pressure, p_1, and the temperature, T_1, ahead of the shock.
- It is seen that, for a given flow turning angle θ, (for the weak solution) the equilibrium shock angle β (solid curves) is less than that for a calorically perfect gas with $\gamma = 1.4$ (dashed curves). This implies that the oblique shock wave will lie closer to the surface for the chemically reacting equilibrium case as shown in Figure 4.19.

The reason why the shock in a chemically reacting flow lies closer to the body surface is because of the increased density ratio ρ_2/ρ_1 across the wave, in the chemically reacting flow, compared to the density ratio across the wave in a perfect gas.

For the "strong-shock" solutions, given by the upper portion of $\theta-\beta-M$ curve, the solution is just the reverse of weak-shock case.

Note that, as reported by Rathakrishnan [7], all naturally occurring oblique shocks are weak; thus, in the vast majority of applications, the "weak-shock solution" is used.

The maximum flow deflection angle, θ, allowed for the solution of a straight oblique shock wave is increased by the effects of chemical reaction.

4.17 Equilibrium Quasi-One-Dimensional Nozzle Flows

Consider the inviscid, adiabatic high-temperature flow through a convergent–divergent (C-D) nozzle, shown in Figure 4.20. Flow through this kind of passages, with streamlines having large radius of curvature and without any abrupt change in the cross-sectional area of the passage, can be regarded as one dimensional.

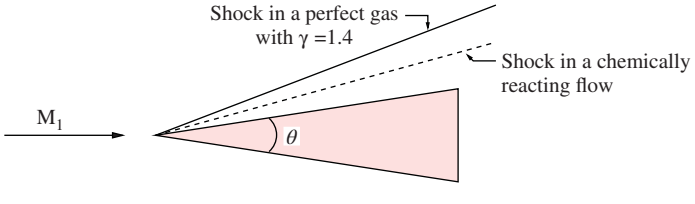

Figure 4.19 Comparative locations of oblique shock in a perfect and an equilibrium chemically reacting gases.

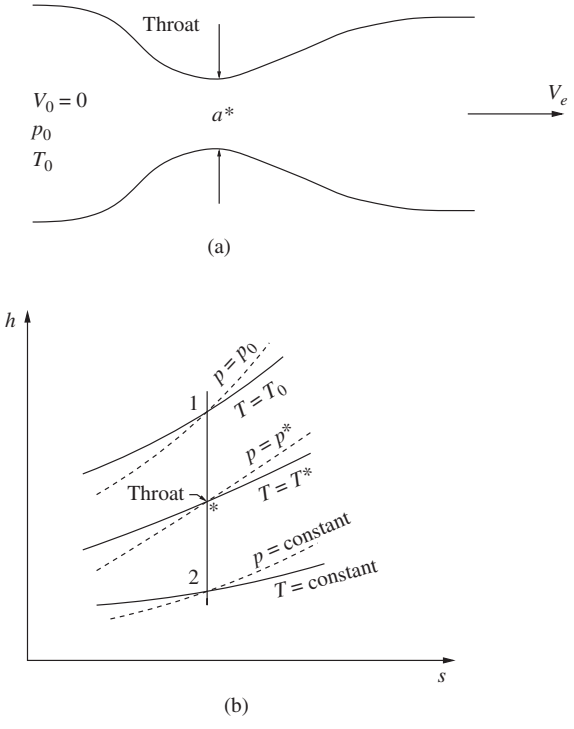

Figure 4.20 (a) An equilibrium nozzle flow, (b) its Mollier diagram.

First, let us examine whether the chemically reacting flow is isentropic? Given that the flow is both inviscid and adiabatic. For an equilibrium chemically reacting flow, by the first and second laws of thermodynamics, we have

$$Tds = dh - vdp \tag{4.115}$$

where T is the temperature, s is the entropy, h is the enthalpy, v is the specific volume, and p is the pressure.

For an adiabatic steady flow, with constant stagnation enthalpy h_0, by energy equation, we have

$$h + \frac{V^2}{2} = h_0$$

where h and h_0, respectively, are the static and stagnation enthalpies and V is the flow velocity. Thus in the differential form, the above relation for enthalpy becomes

$$dh + VdV = 0 \tag{4.116}$$

Along a streamline, by Euler's equation [by Equation (2.4) of Rathakrishnan [7]], we have the pressure–velocity relation as

$$\frac{dp}{\rho} + VdV = 0$$

that is,

$$VdV = -\frac{dp}{\rho} \tag{4.117}$$

This can be expressed as

$$VdV = -\frac{dp}{\rho} = -vdp \tag{4.118}$$

where v $(= 1/\rho)$ is the specific volume.

Thus Equation (4.118) becomes

$$dh - vdp = 0 \tag{4.119}$$

Substituting this into Equation (4.115), we have

$$Tds = 0 \tag{4.120}$$

Hence, the equilibrium chemically reacting flow through a nozzle is *isentropic*. It is a general result implying that the equilibrium chemical reactions do not introduce irreversibilities into the system. Thus, any shock-free, inviscid, adiabatic, equilibrium chemically reacting flow is isentropic.

4.17.1 Quasi One-Dimensional Flow

One-dimensional flow is that in which the radius of curvature of the streamlines are very large and the cross-sectional area of the passage (streamtube) does not change abruptly. Thus, it is a flow where the cross-sectional area of the streamtube is a variable and a function of one space variable, say x; $A = A(x)$. Also, the flow properties across any given cross section can be assumed to be uniform and depends only on x. That is, $p = p(x)$, $v = u = u(x)$, $T = T(x)$, $\rho = \rho(x)$ (the coordinate in the stream direction), and so on.

Let us investigate whether for an equilibrium, chemically reacting quasi-one-dimensional nozzle flow, sonic flow exists at the throat of the nozzle?

We know that, for an isentropic flow, choking will take place only at the throat and not at any other location [7]. The area–velocity relation can be expressed as follows.

For any streamtube of cross-sectional area A, the continuity equation is given by

$$\rho Au = \text{constant}$$

where ρ is the density and u is the velocity. Differentiating with respect to u, we obtain

$$\frac{d(\rho Au)}{du} = \rho u\frac{dA}{du} + A\frac{d(\rho u)}{du} = 0$$

The term

$$A\ \frac{d(\rho u)}{du} = A\left[\rho + u\frac{d\rho}{du}\right]$$

This can be expressed as

$$A\,\frac{d(\rho u)}{du} = A\left(\rho + u\frac{d\rho}{dp}\,\frac{dp}{du}\right)$$

By Equation (4.117),

$$\frac{dp}{du} = -\rho u$$

and by Laplace equation, we have

$$\frac{dp}{d\rho} = a^2$$

Substituting for $\frac{dp}{du}$ and $\frac{dp}{d\rho}$, we have

$$\begin{aligned} A\frac{d(\rho u)}{du} &= A\left[\rho + \frac{u}{a^2}(-\rho u)\right] \\ &= A\left(\rho - \rho\,\frac{u^2}{a^2}\right) \\ &= A\rho\,(1 - M^2) \end{aligned}$$

Therefore,

$$\rho u\frac{dA}{du} + A\rho\,(1 - M^2) = 0$$

This gives

$$\boxed{\frac{dA}{du} = -\frac{A}{u}(1 - M^2)} \tag{4.121}$$

Equation (4.121) is an important result. It is called the *area–velocity relation*. This is valid for any gas, irrespective of whether it is perfect or chemically reacting. Further, when $M = 1$, $dA/A = 0$, and therefore, sonic flow does exist at the throat of an equilibrium chemically reacting nozzle flow.

Examine the h–s (Mollier) diagram for the nozzle flow, shown in Figure 4.20(b). It is seen that a given point on the Mollier diagram not only gives the enthalpy, h, and entropy, s, but the pressure, p, and temperature, T, at that point as well (and any other equilibrium thermodynamic property, because the state of an equilibrium system is completely specified by any two independent state variables).

Let point 1 on the h–s diagram (Figure 4.20(b)) denotes the known reservoir condition, with stagnation pressure p_0 and stagnation temperature T_0, for the nozzle flow. As the flow is isentropic, conditions at all other locations throughout the nozzle must fall somewhere on the vertical line passing through point 1 on the h–s diagram.

In particular, let us choose a value of $u = u_2 \neq 0$. The velocity corresponds to this point can be found from Equations (4.97) and (4.98) as follows.

$$h_0 = \text{constant}$$

Hence,

$$h_1 + \frac{u_1^2}{2} = h_2 + \frac{u_2^2}{2} = h_0 \tag{4.122}$$

Thus,

$$\Delta h = h_0 - h_2 = \frac{u_2^2}{2} \tag{4.123}$$

Therefore, for a given velocity u_2, Equation (4.123) locates the appropriate points on the Mollier diagram.

In turn, the constant pressure and the constant temperature lines that run through point 2 define the pressure p_2 and the temperature T_2 associated with the chosen velocity u_2.

In this way, the variation of the thermodynamic properties of the flow expanding through the nozzle can be calculated as a function of velocity u, for a given reservoir condition (that is, for a given p_0 and T_0).

For an equilibrium gas, the speed of sound, $a^2 \equiv (\partial p/\partial \rho)_s$, is also a unique function of the thermodynamic state. For example,

$$a = a\,(h, s) \tag{4.124}$$

where h and s, respectively, are the enthalpy and entropy. Thus, at each point on the Mollier diagram, there exists a definite value of a.

Moreover, at some point along the vertical line through point 1 (Figure 4.20), the speed of sound a will be equal to the flow velocity u at that point. Such a point is marked by an asterisk in Figure 4.20. At this point,

$$u = a = u^* = a^*$$

Earlier, it was demonstrated that the location of sonic flow in a nozzle is the throat. Thus the location where $u = a^*$, marked by asterisk in Figure 4.20, must also correspond to the throat.

By continuity equation, we have

$$\rho u A = \rho^* u^* A^* \tag{4.125}$$

where ρ, u, and A, respectively, are the local density, velocity, and cross-sectional area at any location in the streamtube and ρ^*, u^*, and A^*, respectively, are the density, velocity, and cross-sectional area at the sonic state.

From Equation (4.125), we have

$$\frac{A}{A^*} = \frac{\rho^*\ u^*}{\rho\ u} \tag{4.126}$$

But ρ^* and u^* are constant for a given stagnation state with pressure p_0 and temperature T_0. Therefore, Equation (4.126) allows the calculation of the nozzle area ratio as a function of flow velocity, u, through the nozzle.

The appropriate values of u, p, T, and A/A^* at different axial locations of the nozzle for an equilibrium nozzle flow, for a given reservoir condition, can be obtained from isentropic and area–Mach number relations.

Note that the familiar closed-form algebraic relations that can be obtained for a calorically perfect gas are not possible for a chemically reacting flow through a nozzle. This is analogous to the case of chemically reacting flow through a shock wave. That is, closed-form algebraic relations cannot be obtained for any high-temperature chemically reacting flow of interest. Numerical or graphical solutions are necessary for such cases.

For a calorically perfect gas, the nozzle flow characteristics are given by the local flow Mach number, M, only. We have the area ratio, temperature ratio, and pressure ratio as [7]

$$\begin{aligned}
\frac{A}{A^*} &= f_1\,(M) \\
&= \frac{1}{M^2}\left(\frac{2}{\gamma+1}\left(1+\frac{\gamma-1}{2}\,M^2\right)\right)^{(\gamma+1)/(\gamma-1)} \\
\frac{T}{T_0} &= f_2\,(M) \\
&= \left(1+\frac{\gamma-1}{2}\,M^2\right)^{-1} \\
\frac{p}{p_0} &= f_3\,(M) \\
&= \left(1+\frac{\gamma-1}{2}\,M^2\right)^{-\gamma/(\gamma-1)}
\end{aligned}$$

where subscript 0 refers to the stagnation state. In contrast, for an equilibrium chemically reacting gas, the area ratio, temperature ratio, and pressure ratio are given by

$$\begin{aligned}
\frac{A}{A^*} &= g_1\,(p_0, T_0, u) \\
\frac{T}{T_0} &= g_2\,(p_0, T_0, u) \\
\frac{p}{p_0} &= g_3\,(p_0, T_0, u)
\end{aligned}$$

Note that, as in the case of normal shock, the nozzle flow properties also depend on three parameters. Also, again we see that unlike in the case of calorically perfect gas, the Mach number is not the pivotal parameter for a chemically reacting flow.

Some results for the equilibrium supersonic expansion of high-temperature air are shown Figure 4.21. The mole–mass ratios for N_2, O_2, N, O, and NO are given as a function of area ratio, for $T_0 = 8000\,\mathrm{K}$ and $p_0 = 100$ atm. At the given stagnation

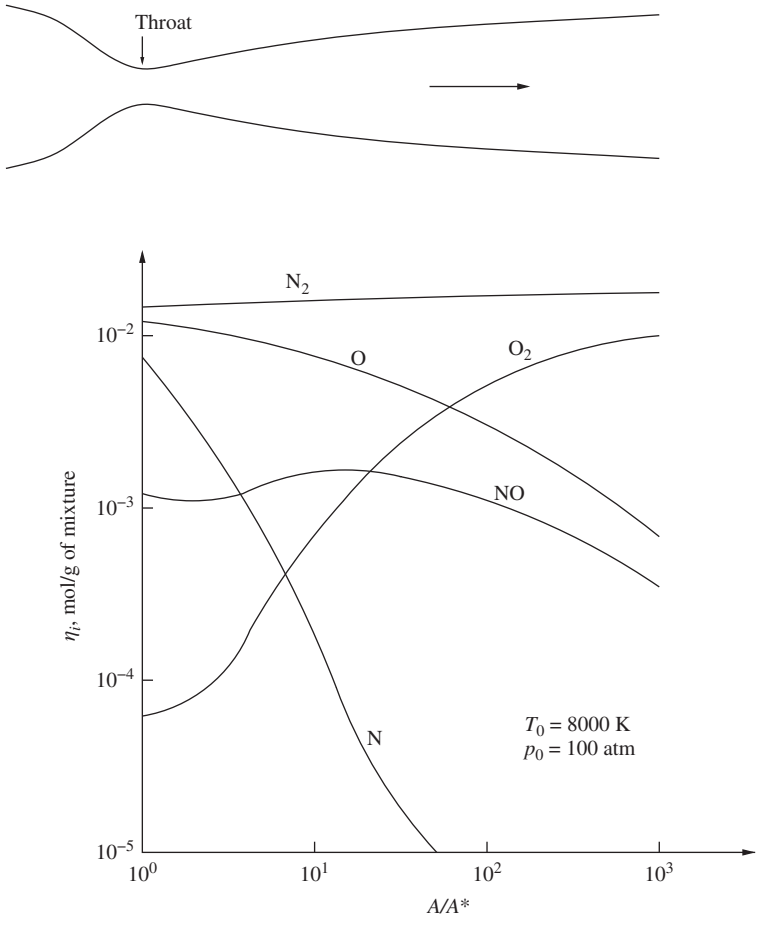

Figure 4.21 Chemical composition of an equilibrium high-temperature air flow through a nozzle.

temperature of $T_0 = 8000\,\text{K}$, the air is highly dissociated in the reservoir. As the gas expands through the nozzle, the temperature decreases, leading to the recombination of oxygen (O) and nitrogen (N) atoms. This is reflected as decrease of the mole fractions η_O and η_N of oxygen and nitrogen atoms and increase of the mole fractions η_{O_2} and η_{N_2} of oxygen and nitrogen molecules, as the gas expands supersonically from $A/A^* = 1$ to 1000.

A typical result of temperature distribution along the nozzle for equilibrium chemically reacting flow through a rocket nozzle is shown in Figure 4.22. The reservoir conditions are produced by the equilibrium combustion of an oxidizer (say N_2O_2, the hyponitrite) with a fuel (say half-N_2H_4 and half-unsymmetrical dimethyl hydrazine) at an oxidizer-to-fuel ratio of 2.25 and a chamber pressure of 4 atm. The calorically perfect gas is assumed to have a constant specific heats ratio of $\gamma = 1.20$.

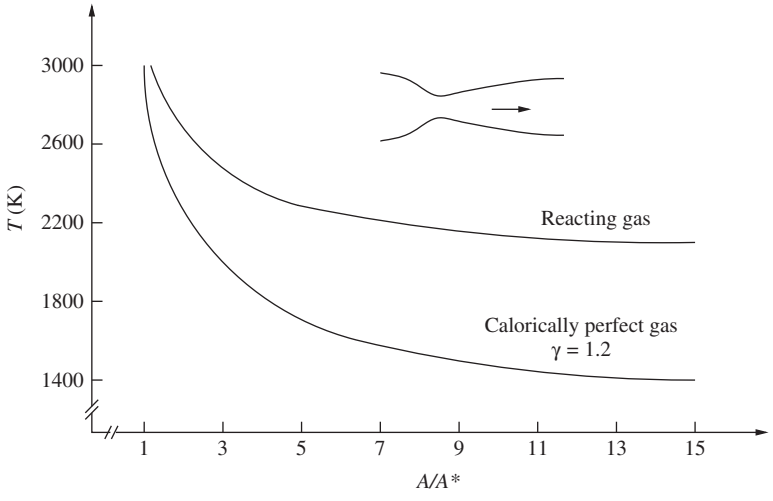

Figure 4.22 Temperature variation of perfect and reacting equilibrium flow through a rocket nozzle.

Note that, all along the nozzle, the temperature of a reacting equilibrium flow is higher than that of the calorically perfect gas flow. This is because as the gas expands and becomes cooler, the chemical composition changes from a high percentage of atomic species (O and H), in the reservoir with an attendant high zero-point energy, to a high percentage of molecular products (H_2O, CO, etc.) in the nozzle expansion, with an attendant lower zero-point energy. That is, the gas atoms recombine, giving up chemical energy that serves to increase the translational energy of the molecules and, hence, resulting in a higher static temperature than that would exist in the nonreacting case.

Also, note that for nozzle flow, the equilibrium temperature is always higher than that for a calorically perfect gas. But for flow behind a shock wave, the equilibrium temperature is always lower than that for a calorically perfect gas. In the nozzle flow case, the reactions are *exothermic* and energy is dumped into the translational molecular motion, but in the case of normal shock flow, the reactions are *endothermic* and energy is taken from the translational mode.

4.18 Frozen and Equilibrium Flows

So far we have discussed flows that were in local thermodynamic and chemical equilibrium. In reality, such flows never occur precisely in nature. This is because all chemical reactions and vibrational energy exchanges require a certain number of molecular collisions to occur; because the gas particles experience a finite collision frequency, such reactions and energy exchanges require a finite time to occur. Therefore, in the hypothetical case of local equilibrium flow, the equilibrium properties of a moving

fluid element demand instantaneous adjustment of local temperature, T, and pressure, p, as the element moves through the flow field. For this, the *reaction rates* have to be infinitely large. Therefore, equilibrium flow implies *infinite chemical* and *vibrational rates*. The opposite to this flow is that where the reaction rates are practically zero. Such a flow with no reaction is termed *frozen flow*. As a result, the chemical composition of frozen flow remains constant throughout the space and time.

Consider the flow through a C-D nozzle is shown in Figure 4.23. Fully dissociated oxygen, at 5000 K and 1 atm, from a reservoir is expanded through the C-D nozzle, shown in Figure 4.23(a). Qualitative variation of flow temperature for equilibrium and frozen chemically reacting flows, from entry to the exit of the nozzle, are shown in Figure 4.23(b). Qualitative variation of species concentration for equilibrium and frozen chemically reacting flows, from entry to the exit, are shown in Figure 4.23(c). For the case of equilibrium flow, at the nozzle inlet, the mole fraction of oxygen atom $C_O = 1$ and the mole fraction of oxygen molecule $C_{O_2} = 0$. As the

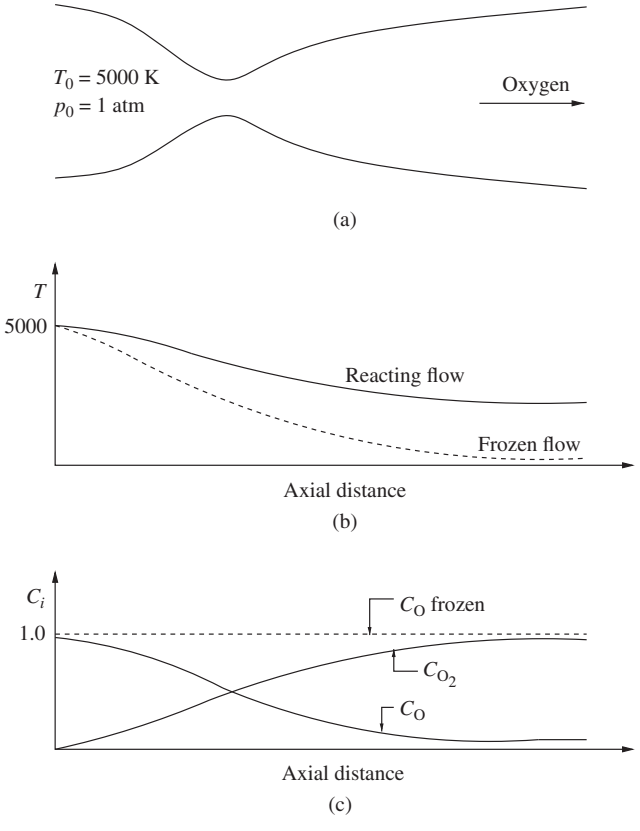

Figure 4.23 (a) Fully dissociated oxygen flow through a nozzle, qualitative comparison of (b) temperature, T, and (c) species concentration, C_i, variation for equilibrium and frozen chemically reacting flows through the nozzle.

temperature decreases owing to the expansion of the flow from the nozzle inlet to exit, the oxygen atoms would recombine; hence, the mole fraction of O (that is, C_O) would decrease and that of O_2 (that is, C_{O_2}) would increase, as a function of distance through the nozzle. If the expansion is such that the equilibrium temperature is equal to the atmospheric temperature, $T_e = T_{atm}$, equilibrium conditions demand that virtually all the oxygen atoms recombine, leading to $C_{O_2} = 1$ and $C_O = 0$ at the nozzle exit.

For frozen flow, the mass fractions of O and O_2 are constant through the nozzle. Recombination is an exothermic reaction. Therefore, the equilibrium expansion results in the chemical zero-point energy of the atomic species being transferred into the transitional, rotational, and vibrational modes of molecular energy. That is, the zero-point energy of two oxygen atoms is much higher than that of one O_2 molecule. When two oxygen atoms recombine, forming one O_2 molecule, the decrease in zero-point energy results in an increase in the internal molecular energy modes. As a result, the temperature distribution for reacting equilibrium flow is higher than that of frozen flow as shown in Figure 4.23(b).

Examine the nonreacting, vibrationally excited flow expanding through a nozzle, shown in Figure 4.24(a).

For vibrationally frozen flow, vibrational energy remains constant throughout the flow. In the reservoir, there is diatomic oxygen at a temperature high enough to excite the vibrational energy but less than the limiting value at which dissociation begins. If the flow is in local thermodynamic equilibrium, the translational, rotational, and vibrational energies decrease throughout the nozzle as shown by the solid curves in Figure 4.24(c). However, if the flow is vibrationally frozen, then e_{vib} is constant throughout the nozzle and equal to its value at the stagnation state in the reservoir. In turn, because energy is permanently sealed in the frozen vibrational mode, less energy is available for translational and rotational modes.

Thus, because the temperature T is proportional to the translational energy, the frozen flow temperature distribution is less than that for equilibrium flow as shown in Figure 4.24(b). In turn, the distribution of translational energy, e_{trans}, and rotational energy, e_{rot}, will be lower for vibrationally frozen flow as shown in Figure 4.24(c).

Note that a flow that is both chemically and vibrationally frozen has *constant specific heats*. This situation is the same as the calorically perfect gas. But no flow in reality is precisely an equilibrium flow or a frozen flow. However, there are a large number of flow applications that come very close to such a limiting situation of equilibrium frozen flow and thus can be analyzed using these assumptions. The judgment about this depends on the comparison between reaction time and flow speed.

4.19 Equilibrium and Frozen Specific Heats

For an equilibrium chemically reacting gas, the enthalpy of a chemically reacting mixture can be obtained from the equation

$$h = \sum_i c_i \, h_i \tag{4.127}$$

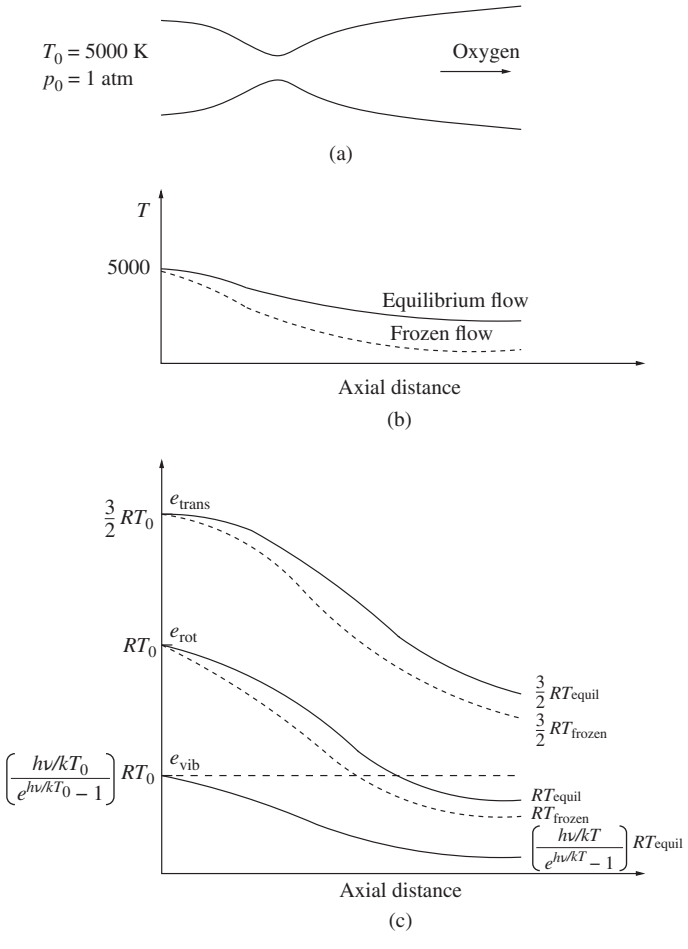

Figure 4.24 (a) Nonreacting, vibrationally excited flow through a C-D nozzle, comparison of (b) the temperatures of equilibrium and frozen vibrationally relaxing flow through the nozzle and (c) the translational, rotational, and vibrational energy of equilibrium and frozen vibrationally relaxing flow through the nozzle.

where h is the static enthalpy of the mixture and c_i and h_i, respectively, are the mass fraction and specific enthalpy of the species constituting the system.

By definition, the specific heat at constant pressure is

$$c_p \equiv \left(\frac{\partial h}{\partial T}\right)_p \tag{4.128}$$

Thus, for a chemically reacting mixture, Equations (4.127) and (4.128) give

$$c_p = \left[\frac{\partial}{\partial T}\left(\sum_i c_i\, h_i\right)\right]_p$$

or

$$c_p = \sum_i c_i \left(\frac{\partial h_i}{\partial T}\right)_p + \sum_i h_i \left(\frac{\partial c_i}{\partial T}\right)_p \tag{4.129}$$

In Equation (4.129), $(\partial h_i/\partial T)_p$ is the specific heat per unit mass for the pure species i, c_{p_i}. Hence, Equation (4.129) becomes

$$\boxed{c_p = \sum_i c_i \, c_{p_i} + \sum_i h_i \left(\frac{\partial c_i}{\partial T}\right)_p} \tag{4.130}$$

This gives c_p for a *chemically reacting mixture*.

If the flow is frozen, by definition, there is no chemical reaction, and therefore, in Equation (4.130), the term $(\partial c_i/\partial T)_p = 0$. Thus, for *frozen flow*, the specific heat Equation (4.130) becomes

$$c_p = c_{p_f} = \sum_i c_i \, c_{p_i} \tag{4.131}$$

With this, Equation (4.130) can be written as

$$\boxed{\underset{\substack{\text{(Specific heat at}\\ \text{constant } p \text{ for}\\ \text{reacting mixture)}}}{c_p} = \underset{\substack{\text{(Frozen}\\ \text{specific heat)}}}{c_{p_f}} + \underset{\substack{\text{(Contribution because of}\\ \text{chemical reaction)}}}{\sum_i h_i \left(\frac{\partial c_i}{\partial T}\right)_p}} \tag{4.132}$$

Considering the internal energy of the chemically reacting gas given by

$$e = \sum_i c_i \, e_i$$

and using the definition of specific heat at constant volume,

$$c_v \equiv \left(\frac{\partial e}{\partial T}\right)_v$$

Thus, for a chemically reacting mixture, we have

$$c_v = \left[\frac{\partial}{\partial T}\left(\sum_i c_i \, e_i\right)\right]_v$$

or

$$c_v = \sum_i c_i \left(\frac{\partial e_i}{\partial T}\right)_v + \sum_i e_i \left(\frac{\partial c_i}{\partial T}\right)_v$$

The term $(\partial e_i/\partial T)_v$ is the specific heat per unit mass for the pure species i, c_{v_i}. Hence,

$$\boxed{c_v = \sum_i c_i \, c_{v_i} + \sum_i e_i \left(\frac{\partial c_i}{\partial T}\right)_v} \tag{4.133}$$

This gives c_v for a *chemically reacting mixture*.

If the flow is frozen, by definition, there is no chemical reaction, and therefore, in Equation (4.133), the term $(\partial\, c_i/\partial T)_v = 0$. Thus, for *frozen flow*, the specific heat Equation (4.133) becomes

$$c_v = c_{v_f} = \sum_i c_i\, c_{v_i} \tag{4.134}$$

With this, Equation (4.133) can be written as

$$\underset{\substack{\text{(Specific heat at}\\ \text{constant } v \text{ for}\\ \text{reacting mixture)}}}{c_v} = \underset{\substack{\text{(Frozen}\\ \text{specific heat)}}}{c_{v_f}} + \underset{\substack{\text{(Contribution because of}\\ \text{chemical reaction)}}}{\sum_i e_i \left(\frac{\partial c_i}{\partial T}\right)_v} \tag{4.133a}$$

In Equations (4.132) and (4.133), the extra contribution (compared to perfect gas) is purely due to reactions. The magnitude of this extra contribution can be very large and usually dominates the value of c_p and c_v.

Example 4.6 Determine the specific heat at constant pressure for air, assuming it as a mixture of 78% of nitrogen, 21% of oxygen, and 0.3% of carbon dioxide, neglecting the contribution to the remaining species, at sea level state.

Solution

At sea level state, the air can be treated as a perfect gas. The specific heats ratio for O_2 and N_2 are 1.4 and for CO_2, $\gamma = 1.3$. The molecular weight for oxygen, nitrogen, and carbon dioxide, respectively, are 32, 28, and 44.
For a perfect gas,

$$c_p = \frac{\gamma}{\gamma - 1} R$$

The c_p for O_2, N_2, and CO_2, being perfect gas, by Equation (4.132), are

$$\begin{aligned}
c_{p_{O_2}} &= \frac{\gamma}{\gamma - 1} \frac{R_u}{M} \\
&= \frac{1.4}{1.4 - 1} \times \frac{8314}{32} \\
&= 909.34 \text{ J/(kg K)} \\
c_{p_{N_2}} &= \frac{\gamma}{\gamma - 1} \frac{8314}{28} \\
&= \frac{1.4}{1.4 - 1} \times \frac{8314}{28} \\
&= 1039.25 \text{ J/(kg K)} \\
c_{p_{CO_2}} &= \frac{1.3}{1.3 - 1} \times \frac{8314}{44} \\
&= 818.803 \text{ J/(kg K)}
\end{aligned}$$

Thus, the c_p for air becomes

$$\begin{aligned} c_{p_{\text{air}}} &= 0.78 \times c_{p_{\text{N}_2}} + 0.21 \times c_{p_{\text{O}_2}} + 0.003 \times c_{p_{\text{CO}_2}} \\ &= 0.78 \times 1039.25 + 0.21 \times 909.34 + 0.003 \times 818.803 \\ &= 810.615 + 190.96 + 2.4564 \\ &= \boxed{1004.031 \text{ J/(kg K)}} \end{aligned}$$

■

4.19.1 Equilibrium Speed of Sound

The general expression for the speed of sound is

$$a = \sqrt{\left(\frac{\partial p}{\partial \rho}\right)_s}$$

This is a physical fact and is not changed by the presence of chemical Reactions; hence, this relation for the speed of sound, a, is valid for both perfect gas flow and reacting gas flow.

We know that for a calorically perfect gas, the thermal state equation is

$$p = \rho RT$$

Also, the sound wave being an isentropic wave, the process through the wave can be represented by

$$\frac{p}{\rho^\gamma} = \text{constant}$$

By differentiating, we get

$$dp = \text{constant } \gamma \rho^{\gamma-1} d\rho$$

that is,

$$\begin{aligned} \frac{dp}{d\rho} &= \text{constant } \gamma \rho^{\gamma-1} \\ &= \frac{p}{\rho^\gamma} \gamma \rho^{\gamma-1} \\ &= \frac{\gamma p}{\rho} \end{aligned}$$

Substituting this into the above expression for a, we get

$$a = \sqrt{\frac{\gamma p}{\rho}}$$

But from state equation,

$$\frac{p}{\rho} = RT$$

Hence, the speed of sound in a perfect gas is given by

$$\boxed{a = \sqrt{\gamma RT}}$$

But this expression for the speed of sound is so restrictive and valid only for calorically perfect gases.

Now, to find the relation for the speed of sound in an equilibrium reacting mixture, let us consider an equilibrium chemically reacting mixture at a fixed pressure p and temperature T. Therefore, the chemical composition is uniquely fixed by pressure and temperature. Imagine a sound wave passing through this equilibrium mixture. Inside the wave, the pressure and temperature will change slightly. In other words, the change of pressure and temperature due to the motion of a sound wave will be infinitesimally small. This is because the sound wave is a weak isentropic wave.

If the gas remains in local chemical equilibrium through the internal structure of the sound wave, the gas composition is changed locally within the wave according to the local variations of pressure and temperature. For this situation, the speed of sound wave is called *equilibrium speed of sound*, denoted by a_e. In turn, if the gas is in motion at the velocity V, then V/a_e is termed the *equilibrium Mach number*, M_e.

4.19.2 Quantitative Relation for the Equilibrium Speed of Sound

We know from the first and second laws of thermodynamics that the enthalpy in differential form can be expressed as

$$Tds = de + pdv \tag{4.135}$$

$$Tds = dh - vdp \tag{4.136}$$

The process through the sound wave is isentropic, thus Equations (4.135) and (4.136) become

$$de + pdv = 0 \tag{4.137}$$

$$dh - vdp = 0 \tag{4.138}$$

For equilibrium chemically reacting gas, the internal energy can be expressed as

$$e = e\ (v, T)$$

In differential form, this becomes

$$de = \left(\frac{\partial e}{\partial v}\right)_T dv + \left(\frac{\partial e}{\partial T}\right)_v dT$$

or

$$de = \left(\frac{\partial e}{\partial v}\right)_T dv + c_v\, dT \tag{4.139}$$

because $(\partial e/\partial T)_v = c_v$.

Similarly, the enthalpy can be expressed as

$$h = h\,(p, T)$$

In differential form, this becomes

$$dh = \left(\frac{\partial h}{\partial p}\right)_T dp + \left(\frac{\partial h}{\partial T}\right)_p dT$$

$$dh = \left(\frac{\partial h}{\partial p}\right)_T dp + c_p\, dT \tag{4.140}$$

because $(\partial h/\partial T)_p = c_p$. Substituting Equation (4.139) into Equation (4.137), we obtain

$$\left(\frac{\partial e}{\partial v}\right)_T dv + c_v\, dT + p dv = 0$$

that is,

$$c_v\, dT + \left[p + \left(\frac{\partial e}{\partial v}\right)_T\right] dv = 0 \tag{4.141}$$

Substituting Equation (4.140) into Equation (4.138), we get

$$dh = \left(\frac{\partial h}{\partial p}\right)_T dp + c_p\, dT - v dp = 0$$

that is,

$$c_p\, dT + \left[\left(\frac{\partial h}{\partial p}\right)_T - v\right] dp = 0 \tag{4.142}$$

Dividing Equation (4.142) by Equation (4.141), we get

$$\frac{c_p}{c_v} = \frac{[(\partial h/\partial p)_T - v]}{[(\partial e/\partial v)_T + p]} \frac{dp}{dv} \tag{4.143}$$

But $v = 1/\rho$; hence, $dv = -\,d\rho/\rho^2$. Thus, Equation (4.143) becomes

$$\frac{c_p}{c_v} = \frac{[(\partial h/\partial p)_T - 1/\rho]}{[(\partial e/\partial v)_T + p]} (-\rho^2) \frac{dp}{d\rho} \tag{4.144}$$

As the condition within the sound wave is isentropic, the changes in pressure dp and density $d\rho$ within the wave must take place isentropically. Thus,

$$\frac{dp}{d\rho} \equiv \left(\frac{\partial p}{\partial \rho}\right)_s \equiv a_e^2$$

Hence, Equation (4.144) becomes

$$\left(\frac{\partial p}{\partial \rho}\right)_s = \frac{c_p}{c_v} \frac{1}{\rho^2} \frac{[(\partial e/\partial v)_T + p]}{\left[\frac{1}{\rho} - (\partial h/\partial p)_T\right]}$$

But $(\partial p/\partial \rho)_s = a_e^2$ by definition. Thus,

$$a_e^2 = \frac{c_p}{c_v}\,\frac{p}{\rho}\,\frac{\left[1+\left(\frac{1}{p}\right)\,(\partial e/\partial v)_T\right]}{[1-\rho\,(\partial h/\partial p)_T]} \tag{4.145}$$

Let $\gamma \equiv c_p/c_v$; also note from the equation of state, $p/\rho = RT$. Thus, Equation (4.145) becomes

$$\boxed{a_e^2 = \gamma RT\,\frac{[1+(1/p)(\partial e/\partial v)_T]}{[1-\rho\,(\partial h/\partial p)_T]}} \tag{4.146}$$

This is the expression for the *equilibrium speed of sound* in a chemically reacting mixture.

Note that the speed of sound "a_e" in an equilibrium reacting mixture is not equal to $\sqrt{\gamma RT}$. However, if the gas is calorically perfect, then $h = c_p T$ and $e = c_v T$. In turn, $(\partial h/\partial p)_T = 0$ and $(\partial e/\partial v)_T = 0$, and Equation (4.146) reduces to the familiar result for the speed of sound in a perfect gas

$$\boxed{a_f = \sqrt{\gamma RT}} \tag{4.147}$$

The symbol a_f is used to denote the *frozen speed of sound*, because a calorically perfect gas assumes no reactions.

Equation (4.147) is the speed at which a sound wave will propagate when no chemical reactions take place internally within the wave, that is, when the flow inside the wave is frozen.

For a thermally perfect gas, $h = h\,(T)$ and $e = e\,(T)$. Hence, for this case, also Equation (4.146) reduces to Equation (4.147).

The full form of Equation (4.146) must be used whenever $(\partial e/\partial v)_T$ and $(\partial h/\partial p)_T$ are finite. This occurs

- when the gas is chemically reacting;
- when intermolecular forces are important (that is, for real gases).

In both of the above cases, $h = h\,(T, p)$ and $e = e\,(T, v)$. That is, for both reacting and real gas, the enthalpy and internal energy are functions of two thermodynamic variables. Hence, Equation (4.146) must be used for calculating the speed of sound.

Note that the equilibrium speed of sound given by Equation (4.146) is a function of both temperature, T, and pressure, p, unlike the case for calorically or thermally perfect gas where it depends on temperature only.

4.20 Inviscid High-Temperature Nonequilibrium Flows

We know that a frozen flow is one with the reaction rate constants $k_f = k_b = 0$ and the vibrational relaxation time $\tau \to \infty$, where k_f is the forward reaction rate constant and k_b is the backward reaction rate constant.

An equilibrium flow is one where both the forward and backward reaction rates tend to infinity ($k_f \to \infty$, $k_b \to \infty$) and $\tau = 0$. But in reality, neither of the above flows occurs exactly.

Let

- τ_f be the characteristic time for a fluid element to traverse the flow field of interest, given by l/V_∞, where l is a characteristic length of the flow field and V_∞ is the velocity of the fluid element;
- τ_c be the characteristic time for the chemical reactions and/or vibrational energy to approach equilibrium.

Then

1. the flow can be approximated as local equilibrium flow if $\tau_f \gg \tau_c$.
2. the flow can be approximated as frozen if $\tau_f \ll \tau_c$.

4.20.1 Governing Equations for Inviscid, Nonequilibrium Flows

The governing equation for inviscid, nonequilibrium flows are the following.

Continuity equation:

$$\frac{\partial \rho}{\partial t} + \nabla \cdot (\rho V) = 0$$

Momentum equation:

$$\rho \frac{DV}{Dt} = -\nabla p$$

Energy equation:

$$\rho \frac{Dh_0}{Dt} = \frac{\partial p}{\partial t}$$

where

$$h_0 = h + \frac{V^2}{2}$$

These equations are valid for both equilibrium and nonequilibrium flows.

In addition to the above continuity equation, which is referred to as the *global continuity equation*, we must consider the species continuity equation for each individual chemical species in the mixture.

Consider a fixed, finite-control volume in a nonequilibrium, inviscid, flow of a chemically reacting gas as shown in Figure 4.25.

Let ρ_i be the mass of species i per unit volume of the mixture. Hence, the density of the mixture becomes

$$\rho = \sum_i \rho_i$$

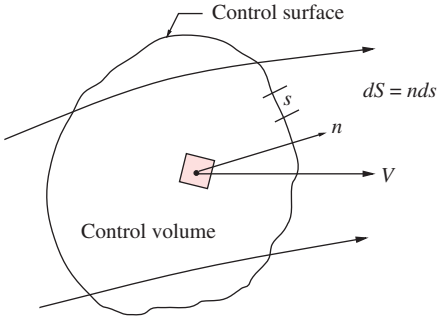

Figure 4.25 Flow through a control volume fixed in space.

The net mass flow of species i flowing out of the control volume is

$$\int\int_s \rho_i \, V \cdot dS$$

where V is the velocity and dS is the surface area of the element.

The mass of species i inside the control volume is

$$\int\int\int_{\mathbb{V}} \rho_i \, d\,\mathbb{V}$$

Let $\dot{w}_i$ be the local rate of change of density ρ_i due to chemical reactions inside the control volume. Therefore, the net time rate of change of the mass of species i inside the control volume is due to the following:

1. The net flux of species i through the surface.
2. The creation or extinction of species i inside the control volume due to chemical reaction.

Thus, in terms of integrals over the control volume, we have

$$\boxed{\int\int\int_{\mathbb{V}} \rho_i \, d\,\mathbb{V} = -\int\int_s \rho_i \, V \cdot dS + \int\int\int_{\mathbb{V}} \dot{w}_i \, d\,\mathbb{V}} \tag{4.148}$$

Equation (4.148) is the *integral form* of species continuity equation.

Using the divergence theorem, the *differential form* of the species continuity equation is obtained directly from Equation (4.148) as

$$\boxed{\frac{\partial \rho_i}{\partial t} + \nabla \cdot (\rho_i \, V) = \dot{w}_i} \tag{4.149}$$

For a nonequilibrium chemically reacting mixture with n different species, we need $(n-1)$ species continuity equations of the form of Equation (4.149). These along with the additional result that

$$\sum_i \rho_i = \rho$$

provide n equations for the solution of the instantaneous composition of a nonequilibrium mixture of n chemical species.

An alternative form of the species continuity equation can be obtained as follows.

The mass fraction of species i, C_i, is defined as

$$C_i = \frac{\rho_i}{\rho}$$

Substituting this relation into Equation (4.149), we get

$$\frac{\partial(\rho C_i)}{\partial t} + \nabla \cdot (\rho C_i \, V) = \dot{w}_i \tag{4.150}$$

Expansion of this equation gives

$$\rho \left[\frac{\partial C_i}{\partial t} + V \cdot \nabla \, C_i\right] + C_i \left[\frac{\partial \rho}{\partial t} + \nabla \cdot (\rho V)\right] = \dot{w}_i \tag{4.151}$$

The term

$$\rho \left[\frac{\partial C_i}{\partial t}\right]$$

is the substantial derivative of C_i, and

$$C_i \left[\frac{\partial \rho}{\partial t} + \nabla \cdot (\rho V)\right] = 0$$

by global continuity equation. Thus, Equation (4.151) becomes

$$\boxed{\frac{DC_i}{Dt} = \frac{\dot{w}_i}{\rho}} \tag{4.152}$$

In terms of mole-to-mass ratio,

$$\eta_i = \frac{C_i}{M_i}$$

where C_i is the number of moles of species i and M_i is the molar mass of species i in the mixture, Equation (4.152) becomes

$$\boxed{\frac{D\eta_i}{Dt} = \frac{\dot{w}_i}{M_i \rho}} \tag{4.153}$$

Equations (4.152) and (4.153) are *alternative forms* of species continuity equation in terms of substantial derivative.

Note that the substantial derivative of a quantity is physically the time rate of change of that quantity as we follow a fluid element moving with the flow. Therefore, from Equations (4.152) and (4.153), as we follow a fluid element of fixed mass moving through the flow field, we see that changes in the mass fraction, C_i, or mole-to-mass ratio, η_i, of the fluid element are only due to the finite rate chemical kinetic changes taking place within the element. This makes common sense and in hindsight; therefore, Equations (4.152) and (4.153) could have been written directly by inspection.

It is essential to note that in Equations (4.152) and (4.153), the flow variables C_i and η_i inside the substantial derivative are written per unit mass. As long as the nonequilibrium variable inside the substantial derivative is per unit mass of mixture, the right-hand side of the conservation equation is simply due to finite-rate chemical kinetics, such as that shown in Equations (4.152) and (4.153).

In contrast, Equation (4.149) can also be written as

$$\frac{D\,\rho_i}{D\,t} = \dot{w}_i - \rho_i\,(\nabla \cdot V) \tag{4.154}$$

If vibrational nonequilibrium is present, in addition to the species continuity equation, another equation must be added to the system given by Equations (4.149)–(4.152). If we follow a moving fluid element of fixed mass, the rate of change of vibrational energy e_{vib} for this element is equal to the rate of molecular energy exchange inside the element. Therefore, we can write the *vibrational rate equation* for a moving fluid element as

$$\boxed{\frac{De_{\text{vib}}}{Dt} = \frac{1}{\tau}(e_{\text{vib}}^{\text{eq}} - e_{\text{vib}})} \tag{4.155}$$

where $e_{\text{vib}}^{\text{eq}}$ is the equilibrium value of vibrational energy per unit mass of gas and e_{vib} is the local nonequilibrium value of vibrational energy per unit mass of gas. Equation (4.155) is referred to as *vibrational rate equation*.

Thus, in an inviscid, nonequilibrium, high-temperature flow, we wish to solve the flow for $p,\ \rho,\ T,\ V,\ h,\ e_{\text{vib}}$, and C_i, as a function of space and time. The governing equations that allow for the solution of these variables are the following.

Global continuity equation:

$$\frac{\partial \rho}{\partial t} + \nabla \cdot (\rho V) = 0 \tag{4.156}$$

Species continuity equation:

$$\frac{\partial \rho_i}{\partial t} + \nabla \cdot (\rho_i V) = \dot{w}_i \tag{4.157}$$

or

$$\frac{DC_i}{Dt} = \frac{\dot{w}_i}{\rho} \tag{4.158}$$

or

$$\frac{D\eta_i}{Dt} = \frac{\dot{w}_i}{M_i \rho} \tag{4.159}$$

Momentum equation:

$$\rho \frac{DV}{Dt} = -\nabla p \tag{4.160}$$

Energy equation:

$$\rho \frac{Dh_0}{Dt} = \frac{\partial p}{\partial t} + \dot{q} \tag{4.161}$$

where

$$h_0 = h + \frac{V^2}{2} \tag{4.162}$$

In Equation (4.161), $\dot{q}$ denotes a heat-addition term because of *volumetric heating* (say by the radiation absorbed by the gas or lost from the gas). The $\dot{q}$ term has nothing to do with the chemical reactions.

The energy exchange due to chemical reactions are naturally accounted for by the heat of formation appearing in enthalpy h in Equations (4.161) and (4.162). In addition to the above equations, we also have

State equation

$$p = \rho RT \tag{4.163}$$

where $R = R_u/\mu$, $\mu = \left(\sum_i (C^i/M)\right)^{-1}$

Enthalpy expression is

$$h = \sum_i C_i \, h_i \tag{4.164}$$

where

$$h_i = (e_{\text{trans}} + e_{\text{rot}} + e_{\text{vib}} + e_{\text{el}}) + R_i T + (\Delta \, h_f^\circ)_i \tag{4.165}$$

The term e_{vib} in Equation (4.165) is obtained with the assumption that local thermodynamic equilibrium prevails even though chemical nonequilibrium prevails. In some cases, this assumption is appropriate. However, when both thermodynamic and chemical nonequilibrium prevail, e_{vib} is a nonequilibrium value that must be obtained from the vibrational rate Equation (4.155) written for species i as

$$\frac{D(C_i \, e_{\text{vib}_i})}{\text{Dt}} = \frac{C_i}{\tau_i}(e^{eq}_{\text{vib}_i} - e_{\text{vib}_i}) \tag{4.166}$$

4.21 Nonequilibrium Normal Shock and Oblique Shock Flows

Consider a strong normal shock wave in a gas. Assume that the temperature within the shock wave is high enough to cause chemical reactions within the gas.

The thin region where large gradients in temperature, pressure, and velocity occur, and where the transport phenomena of momentum (μ) and energy (K) are important,

is called the *shock*. Essentially, a shock is a compression front across which the flow properties *jump*.

For shocks in a calorically perfect gas flow or a chemically reacting equilibrium flow, the flow properties ahead of and behind the shock are uniform, and the gradients (that is, the jump) in flow properties take place almost discontinuously (that is, abruptly) within a thin region of not more than a few mean free path thickness ($\lambda \approx 6.6317 \times 10^{-8}$ m, for air at sea level).

However, in nonequilibrium flows, all chemical reactions and/or vibrational excitations take place at a finite rate. As the thickness of a shock wave is of the order of only a few mean free path, the molecules in a fluid element can experience only a few collisions, as the fluid element traverses the shock front. Consequently, the flow through the shock front is essentially *frozen*. In turn, the flow properties immediately behind the shock front are frozen flow properties as illustrated in Figure 4.26.

The temperature and density of nitrogen (N_2) gas ahead of the shock are T_1 and ρ_1, respectively. Also, the species concentration of nitrogen atom, C_N, is zero, ahead of the shock. As the fluid element moves downstream, the finite rate reactions take place, and the flow properties relax towards their equilibrium values. Thus, the flow properties just behind the shock can be fixed with the perfect gas theory. In addition, the species concentration of nitrogen atom, C_N, immediately behind the shock is still zero (because the flow is frozen). Downstream of the shock front, the nonequilibrium flow must be treated with appropriate equations. In this region, the nitrogen molecules, N_2, become either partially or totally dissociated and the species concentration of nitrogen atom, C_N, increases as illustrated in Figure 4.26.

As the reaction is endothermic, the temperature, T, behind the shock decreases, whereas the density, ρ, increases. A procedure of numerical calculation of the

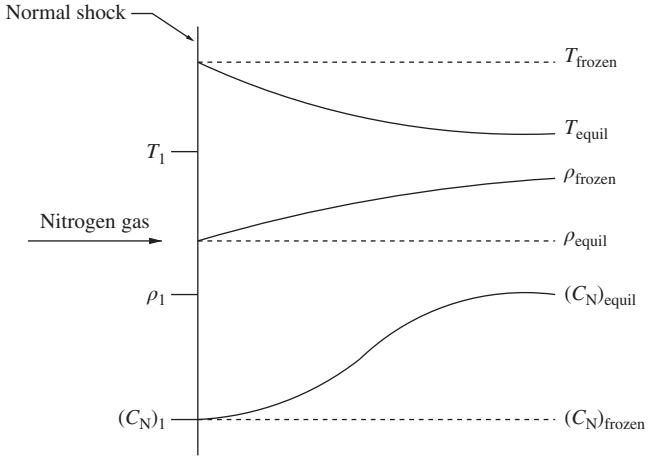

Figure 4.26 Properties of reacting nonequilibrium flow behind a normal shock.

nonequilibrium region behind the shock front can be established as follows. As the flow is one dimensional and steady, the governing equations become the following.

Global continuity equation:

$$\rho\, du + u\, d\rho = 0 \tag{4.167}$$

Momentum equation:

$$dp = -\rho\, u\, du \tag{4.168}$$

Energy equation:

$$dh_0 = 0 \tag{4.169}$$

Species continuity equation:

$$u\, dC_i = \frac{\dot{w}_i}{\rho}\, dx \tag{4.170}$$

In Equation (4.170), the distance x is measured from the shock front. Equation (4.170) explicitly involves the finite-rate chemical reaction term $\dot{w}_i$ and a distance dx multiplies this term. Hence, Equation (4.170) introduces a scale effect into the solution of the flow field. In turn, all flow field properties become a function of distance behind the shock front as illustrated in Figure 4.27.

Equations (4.167)–(4.170) can be solved by using a standard numerical technique for integrating ordinary differential equations (ODE), such as the well-known Runge–Kutta (R-K) technique, starting right from the shock front (point 1) and integrating downstream in steps Δx. The initial conditions at point 1 are obtained by assuming frozen flow across the shock front.

Note that if we are dealing with atmospheric flow, involving cool, nonreacting air, then the chemical composition at point 1 is the same as the known composition ahead of the shock, and the local velocity V, pressure p, temperature T, etc. at point 1 are the same as calculated for normal shock wave in a calorically perfect gas with specific heats ratio $\gamma = 1.4$.

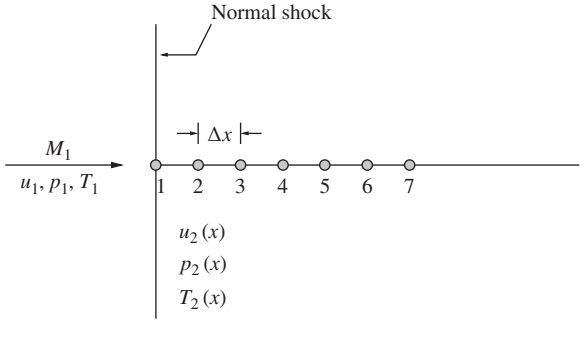

Figure 4.27 Grid points for numerical solution of nonequilibrium flow through a normal shock.

It is essential to realize that in carrying out such a numerical solution of nonequilibrium flow, a major problem can be encountered. If one or more of the finite-rate chemical reactions are very fast (that is, if $\dot{w}_i$ in Equation (4.170) is very large), then Δx must be chosen very small even when a higher-order numerical method is used.

The species continuity equations for such very fast reactions are called *stiff* equations and readily lead to instabilities in the solution.

A sample result for nonequilibrium flow field behind a normal shock wave in air, with Mach number, pressure, and temperature ahead of the shock as 12, 130 Pa, and 300 K, respectively, showing the variations of temperature and density behind the shock front, is shown in Figure 4.28.

The chemical reactions in the air behind a shock front are predominantly dissociation reactions of oxygen and nitrogen, which are endothermic. Hence, temperature T decreases and pressure p increases with distance behind the shock front – both by almost by a factor of 2.

4.21.1 Nonequilibrium Flow behind an Oblique Shock Wave

Consider a straight oblique shock wave as shown in Figure 4.29. Let x denote the distance downstream of the wave, measured normal to the shock front. From normal shock wave results, we see that density increases with distance for nonequilibrium case.

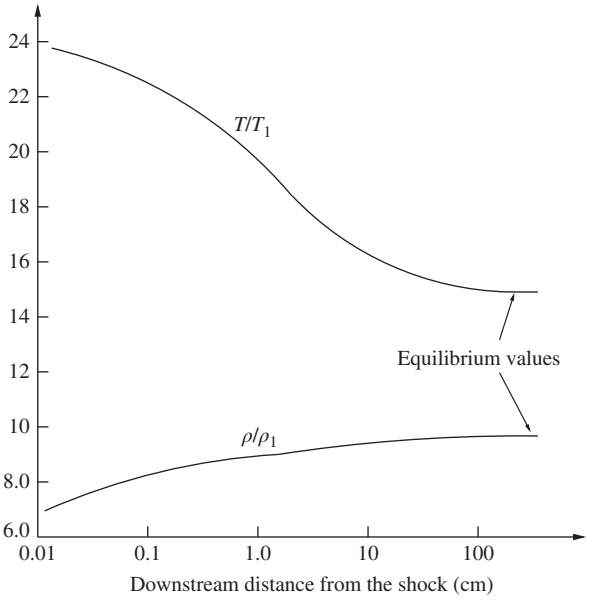

Figure 4.28 Temperature and density variation of a nonequilibrium flow through a normal shock wave in air, with $M_1 = 12$, $p_1 = 130$ Pa, and $T_1 = 300$ K.

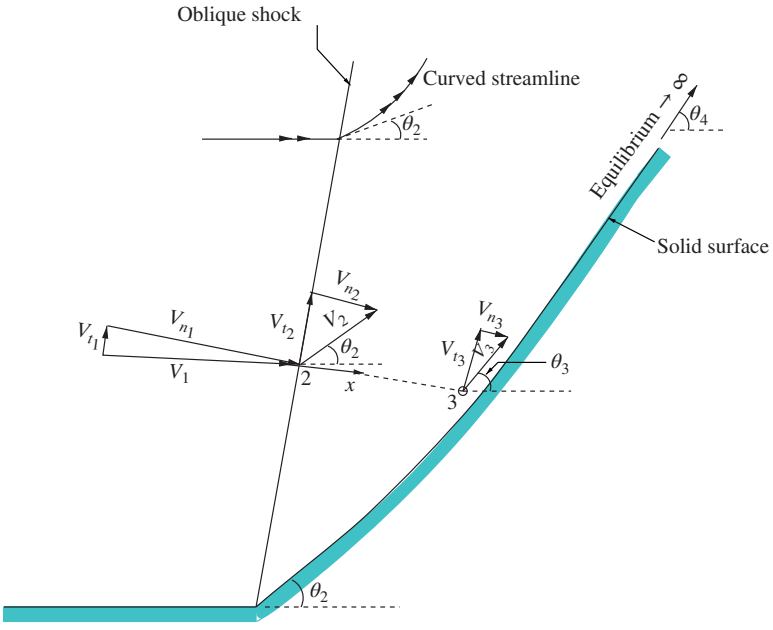

Figure 4.29 Geometry of nonequilibrium flow behind a straight oblique shock wave.

As the mass flow rate per unit area, ρV_n, is a constant for flow across a normal shock wave, the velocity component V_n must decrease with x, that is, $V_{n_3} < V_{n_2}$. However, as we know from the analysis of flow through oblique shock in perfect gas, the tangential velocities V_{t_1}, V_{t_2}, and V_{t_3} are all equal in the nonequilibrium flow behind the oblique shock also. Thus, because $V_{t_3} = V_{t_2}$, the flow deflection angle θ_3 is greater than θ_2. Therefore, the streamlines in the nonequilibrium flow behind a straight oblique shock front are curved and continually increase their deflection angle until equilibrium conditions are reached far downstream. This implies that in order to create a straight oblique shock front in a nonequilibrium flow, it is essential to have a compression corner that is shaped similar to the solid surface shown in Figure 4.29.

The compression surface, after its initial discontinuous deflection of θ_2 corresponding to frozen flow, must curve upward until equilibrium deflection angle is reached, as illustrated in Figure 4.29, to make the oblique shock straight, as shown in the figure. This curved, nonuniform flow field in the nonequilibrium region behind a straight oblique shock front, illustrated in Figure 4.29, is an important difference from the familiar uniform flows obtained for calorically perfect and equilibrium oblique shock results.

On the basis of the above reasoning, it can be visualized that for the supersonic or hypersonic nonequilibrium flow over a straight compression corner, the shock wave will be curved as shown in Figure 4.30.

The wave angle at the corner β_f, shown in Figure 4.30, corresponds to frozen flow. Far downstream, the wave angle approaches the equilibrium flow value β_e.

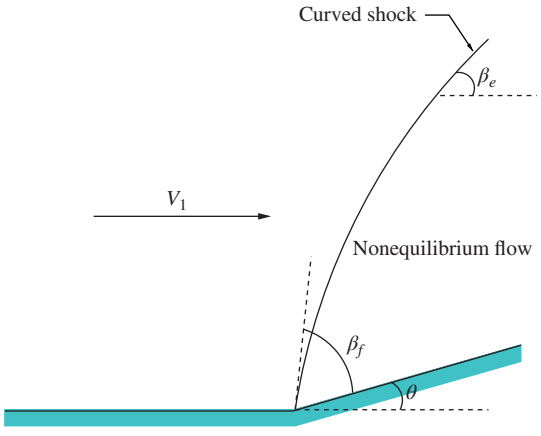

Figure 4.30 Oblique shock in a nonequilibrium flow.

Note that, for a given flow turning angle θ, the equilibrium shock angle β_e is always less than the frozen wave angle β_f (for $\gamma = 1.4$).

4.21.2 Nonequilibrium Quasi-One-Dimensional Nozzle Flows

Theses kind of flows find application in high-temperature flows through rocket nozzle, high-enthalpy aerodynamic testing facilities, etc. Because of these applications, intensive efforts were made after 1950 to obtain relatively exact numerical solutions for the expansion of high-temperature gas through a nozzle, when vibration and/or chemical nonequilibrium conditions prevail within the gas.

- In a rocket nozzle, nonequilibrium effects decrease the thrust and specific impulse.
- In a high-enthalpy (high-temperature) wind tunnel, the nonequilibrium effects make the flow conditions in the test section somewhat uncertain. Both of these are adverse effects.
- In contrast, a gas dynamic laser creates a laser medium by intensively promoting vibrational nonequilibrium in a supersonic expansion. Therefore, this application aims at obtaining the highest degree of nonequilibrium possible.

Consider the nozzle and grid-points distribution shown in Figure 4.31.

Widely accepted technique for solving nonequilibrium nozzle flows is the time-marching technique. The following are the steps used for solving such problems.

1. At the first grid point (reservoir conditions), the equilibrium conditions for e_{vib} and C_i, at the given stagnation pressure p_0 and temperature T_0, are calculated and held fixed, invariant with time.
2. Guessed value of e_{vib} and C_i are then arbitrarily specified at all other grid points (along with guessed values of all other flow variables); these guessed values represent the initial conditions for the time-marching solution.

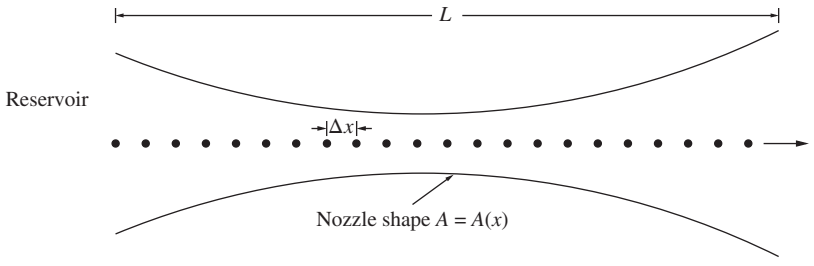

Figure 4.31 Grid points for the time marching of quasi-one-dimensional flow through a nozzle.

3. For initial values of e_{vib} and C_i, it is recommended that equilibrium values be assumed from the reservoir to the throat and then frozen values be prescribed downstream of the throat.

The governing equations for unsteady quasi-one-dimensional flow are the following.

Continuity equation:

$$\frac{\partial p}{\partial t} = -\frac{1}{A}\,\frac{\partial(\rho u A)}{\partial x} \tag{4.171}$$

Momentum equation:

$$\frac{\partial u}{\partial t} = -\frac{1}{\rho}\left(\frac{\partial p}{\partial x} + \rho u\,\frac{\partial u}{\partial x}\right) \tag{4.172}$$

Energy equation:

$$\frac{\partial e}{\partial t} = -\frac{1}{\rho}\left(p\,\frac{\partial u}{\partial x} + \rho u\,\frac{\partial e}{\partial x} + p u\,\frac{\partial \ln A}{\partial x}\right) \tag{4.173}$$

where A is the local cross-sectional area of the nozzle, p is the local pressure, and u is the local velocity.

In addition to these equations, for a nonequilibrium flow, the appropriate vibrational rate equation and species continuity equation are

$$\frac{\partial e_{\text{vib}}}{\partial t} = \frac{1}{\tau}(e_{\text{vib}}^{eq} - e_{\text{vib}}) - u\,\frac{\partial e_{\text{vib}}}{\partial x} \tag{4.174}$$

and

$$\frac{\partial C_i}{\partial t} = -u\,\frac{\partial C_i}{\partial x} + \frac{\dot{w}_i}{\rho} \tag{4.175}$$

Equations (4.171)–(4.175) are solved step by step in time, using the finite-difference predictor–corrector approach. Along with other flow variables, e_{vib} and C_i at each grid point will vary with time; but after many time steps, all flow variables will approach a steady state. It is this steady flow field we are interested in as our solution.

The nonequilibrium phenomena introduce an important new stability criterion for the time step Δt, in addition to the Courant Frederic Lewis (CFL) criterion. The value chosen for Δt must be geared to the speed of the nonequilibrium relaxation process and must not exceed the characteristic time for the fastest finite reaction rate taking place in the system. That is,

$$\Delta t < B\Gamma \tag{4.176}$$

where $\Gamma = \tau$ for vibrational nonequilibrium, $\Gamma = \rho(\partial \dot{w}_i / \partial C_i)^{-1}$ for chemical nonequilibrium, and B is a dimensionless proportionality constant found by experience to be less than unity, sometimes as low as 0.1. The value chosen for Δt in a nonequilibrium flow must satisfy both Equation (4.176) and the usual CFL criterion, given here as

$$\Delta t < \frac{\Delta x}{u + a} \tag{4.177}$$

which of the two stability criteria is the smaller, and, hence, governs the time step, depending on the nature of the case being calculated. That is, the stability criterion with small Δt governs the time step. In other words, the smaller among the time step Δt based on the governance of Equations (4.176) and (4.177) will be taken as the time step in the computation. If the local pressure and temperature are low enough everywhere in the flow, the rates will be slow and Equation (4.177) generally dictates the value of Δt.

On the other hand, if some of the rates have high-transition probabilities and/or the local p and T are very high, Equation (4.176) generally dictates Δt. This is almost always encountered in rocket nozzles with flow of hydrocarbon gases, where some of the chemical reactions involving hydrogen are very fast and combustion chamber pressures and temperatures are reasonably high.

Example 4.7 Calculate the number of microstates possible in the macrostate shown in Figure 4.2, using Bose–Einstein statistics.

Solution

Given there are four energy levels. In energy level ϵ_0', there are two molecules and five states. Thus, the thermodynamic probability for energy ϵ_0', with $N = 2$ and $g = 5$, by Equation (4.3), is

$$\begin{aligned} W_0 &= \frac{(N + g - 1)!}{(g - 1)!\, N!} \\ &= \frac{[2 + (5 - 1)]!}{(5 - 1)!\, 2!} \\ &= \frac{6!}{4!\, 2!} \\ &= \frac{720}{24 \times 2} \\ &= 15 \end{aligned}$$

For energy level ϵ_1', $N = 5$ and $g = 6$; therefore,

$$\begin{aligned} W_1 &= \frac{[5 + (6 - 1)]!}{(6 - 1)!\ 5!} \\ &= \frac{10!}{5!\ 5!} \\ &= \frac{3{,}628{,}800}{120 \times 120} \\ &= 252 \end{aligned}$$

For energy level ϵ_2', $N = 3$ and $g = 5$; therefore,

$$\begin{aligned} W_2 &= \frac{[3 + (5 - 1)]!}{(5 - 1)!\ 3!} \\ &= \frac{7!}{4!\ 3!} \\ &= \frac{5040}{24 \times 6} \\ &= 35 \end{aligned}$$

For energy level ϵ_3', $N = 2$ and $g = 3$; therefore,

$$\begin{aligned} W_3 &= \frac{[2 + (3 - 1)]!}{(3 - 1)!\ 2!} \\ &= \frac{4!}{2!\ 2!} \\ &= \frac{24}{2 \times 2} \\ &= 6 \end{aligned}$$

Thus the thermodynamic probability for the given macrostate, by Equation (4.3), is

$$\begin{aligned} W &= W_0\ W_1\ W_2\ W_3 \\ &= 15 \times 252 \times 35 \times 6 \\ &= \boxed{793{,}800} \end{aligned}$$

■

4.22 Nonequilibrium Flow over Blunt-Nosed Bodies

Nonequilibrium flow over a blunt nose not only resembles some of the characteristics of the equilibrium flow and perfect gas flow but also takes on some of the aspects of

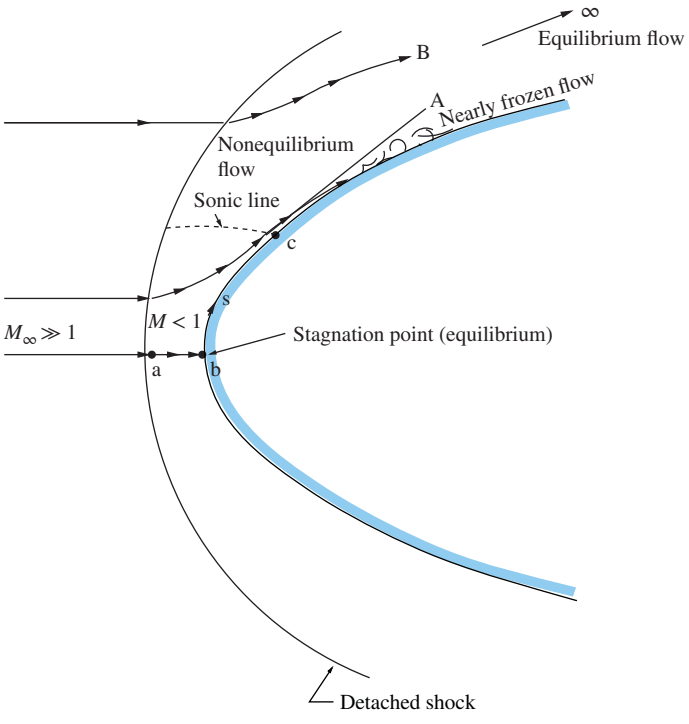

Figure 4.32 Different zones in a high-temperature flow past a blunt-nosed body.

nonequilibrium flow behind shock waves. Examine the nonequilibrium flow past a blunt-nosed body shown in Figure 4.32.

In the nose region, the chemical composition resembles that in a nonequilibrium region behind a normal shock wave. But for the streamline that goes through the stagnation point (abc), between a and b, the flow is compressed and decelerated; it reaches zero velocity at the stagnation point b. In doing so, it can be shown that a fluid element takes an infinite time to traverse the distance ab. This means that local equilibrium conditions must exist at the stagnation point b with its attendant highly *dissociated* and *ionized state*.

The flow then expands rapidly downstream of the stagnation point; indeed, the surface streamline bc encounters very large pressure and temperature gradients in the region near the sonic point c, that is, dp/ds and dT/ds are large negative quantities. This is similar to the nonequilibrium flow through a C-D nozzle, where it was pointed out that sudden freezing of the flow can occur downstream of the throat. The same type of sudden freezing of the flow can be experienced near point c. The streamline begins to experience a large amount of dissociation and ionization at point b. Because of this, the frozen flow is characterized by a thin region of highly dissociated and ionized gas that flows downstream over the body. Slightly ahead of the body nose, streamline A

also passes through a strong portion of the bow shock and exhibits similar behavior as the stagnation streamline abc; that is, there is a region of highly dissociated and ionized nonequilibrium flow along the streamline A, behind the shock, and fairly rapidly proceeding to freezing state in the vicinity of the sonic line. Much farther away from the body, streamline B passes through a weaker, more oblique portion of the bow shock. Consequently, the amount of dissociation and ionization are considerably smaller, but the nonequilibrium region extends much further downstream along streamline B.

4.23 Transport Properties in High-Temperature Gases

From kinetic theory of gases, we know that the atoms and molecules of a gaseous system are in continuous random motion. The random motion of atoms and molecules is the essence of molecular transport phenomena. The motion of molecules cause the transport of mass, momentum, and energy, popularly termed *transport phenomena*. The properties characterizing these transports are *diffusion coefficient*, D; *viscosity coefficient*, μ; and the *thermal conduction coefficient*, K, referring to the transport of mass, momentum, and energy, respectively. When a particle (molecule) moves from one location to another in space, it carries with it a certain momentum, energy, and mass associated with the particle itself. The transport of this particle motion gives rise to the transport phenomena of viscosity, thermal conduction, and diffusion.

Consider a gas in a two-dimensional space, showing two particles crossing the horizontal line $y = y_1$, because of the random motion as shown in Figure 4.33(a). Let ϕ be some mean property carried by the particle, say its momentum or energy or mass-related property. Also, assume that ϕ has a variation as shown in Figure 4.33(b). Let Δy be the distance above y_1 at which, on an average, particle 1 experienced its last collision before crossing y_1.

Similarly, particle 2 crosses y_1 from below. Let Δy be the average distance below y_1 at which particle 2 experienced its last collision before crossing y_1. In crossing y_1,

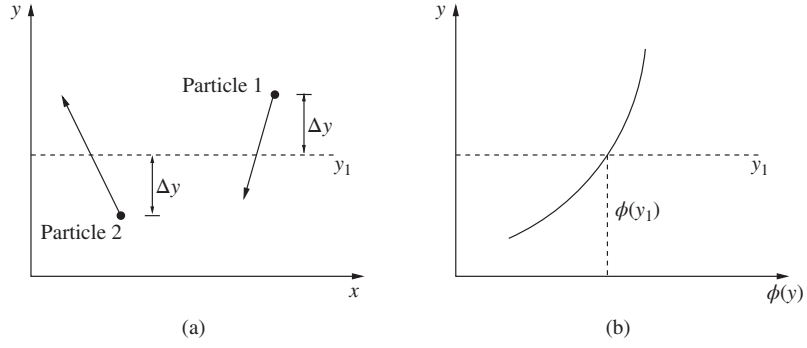

Figure 4.33 Model for transport phenomena. (a) Two particles crossing the horizontal line $y = y_1$, because of random motion, and (b) variation of a mean property carried by the particle.

particle 1 will carry with it a mean value of ϕ equal to $\phi\ (y + \Delta y)$, and particle 2 will carry a mean value of ϕ equal to $\phi\ (y - \Delta y)$. A reasonable value for Δy would be the mean free path, λ.

The flux of particles (that is, the number of particles per second per unit area) crossing y_1 from either above or below is proportional to $n\overline{C}$, where n is the number density and $\overline{C}$ is the mean speed of the particles. Therefore, the flux of ϕ across y_1 due to both directions is

$$\Lambda = an\overline{C}[\phi(y_1 - \lambda) - \phi\ (y_1 + \lambda)] \tag{4.178}$$

where the net flux Λ is positive in the upward direction, and a is a proportionality constant.

Expanding ϕ as Taylor's series about $y = y_1$, we have

$$\phi\ (y_1 + \lambda) = \phi\ (y_1) + \frac{d\phi}{dy}\ \lambda + \frac{d^2\phi}{dy^2}\ \frac{\lambda^2}{2} + \cdots$$

and

$$\phi\ (y_1 - \lambda) = \phi\ (y_1) - \frac{d\phi}{dy}\ \lambda + \frac{d^2\phi}{dy^2}\ \frac{\lambda^2}{2} - \cdots$$

Substituting this into Equation (4.178) and neglecting λ^2 and higher-order terms, we get

$$\boxed{\Lambda = -2\ a\ n\ \overline{C}\ \lambda\ \frac{d\phi}{dy}} \tag{4.179}$$

Equation (4.179) is a *general transport equation* for ϕ.

4.23.1 Momentum Transport

Let the property ϕ in Equation (4.179) be the mean momentum of the particles. Further, let $m\overline{C_x}$ be the x-component of the momentum vector, where m is the mass of the particle and $\overline{C_x}$ is the mean velocity in the x-direction. From Equation (4.179), we have

$$\Lambda = -2\ a\ n\ \overline{C}\ \lambda\ m\ \frac{d\overline{C_x}}{dy} \tag{4.180}$$

We know from mechanics that, in a flow, the flux of the x-component of momentum in the y-direction is simply the *shear stress* τ_{xy}. Thus, Equation (4.180), with $\tau_{xy} = -\Lambda$, becomes

$$\tau_{xy} = 2\ a\ n\ \overline{C}\ \lambda\ m\ \frac{d\overline{C_x}}{dy} \tag{4.181}$$

Further, from fluid mechanics, we know that

$$\tau_{xy} = \mu\ \frac{\partial u}{\partial y} = \mu\ \frac{\partial C_x}{\partial y} \tag{4.182}$$

where $\overline{C_x}$ is the x-component of the flow velocity and μ is the viscosity coefficient. Also, $\overline{C_x} = u$; thus, from Equations (4.181) and (4.182), we have

$$\boxed{\mu = 2\, a\, m\, n\, \overline{C}\, \lambda} \tag{4.182a}$$

This constant μ is termed *dynamic viscosity coefficient*.

4.23.2 Energy Transport

Let ϕ be the mean energy of the particle, given as $\frac{3}{2}\, k_1 T$, where k_1 is the Boltzmann constant and T is the temperature.

The flux of energy across y_1 is less than that obtained from Equation (4.179) as

$$\Lambda = -3\, a\, k_1 n\, \overline{C}\, \lambda\, \frac{dT}{dy}$$

Grouping the constants $3ak_1$ by k, the flux becomes

$$\Lambda = -k\, n\, \overline{C}\, \lambda\, \frac{dT}{dy} \tag{4.183}$$

From classical heat transfer, we know that the *energy flux* (that is, the heat transferred per second per unit area) is given by

$$\dot{q} = -K\, \frac{\partial T}{\partial y} \tag{4.184}$$

where K is the *thermal conductivity*.

From kinetic theory, we know that Λ in Equation (4.183) is the thermal flux $\dot{q}$; therefore, from Equations (4.183) and (4.184), we have the thermal conductivity as

$$\boxed{K = k\, n\, \overline{C}\lambda} \tag{4.185}$$

4.23.3 Mass Transport

Consider the transport of molecular mass in a binary gas mixture made up of A and B particles, with number densities n_A and n_B, respectively.

In Equation (4.179), let Λ be the flux of a particles across y_1, namely, the number of A particles crossing y_1 per second per unit area. In Equation (4.179), n is the total number density, $n = n_A + n_B$. Therefore, the quantity ϕ being transported across y_1 must be a probability that the particle crossing y_1 is indeed an A particle. This probability is the mole fraction, χ_A; thus $\phi = \chi_A = n_A/n$. For this case, Equation (4.179) can be written as

$$\Lambda = -2\, a\, n\, \overline{C}\lambda\, \frac{d(n_A/n)}{dy} = -2\, a\, \overline{C}\lambda \frac{d\, n_A}{dy} \tag{4.186}$$

We can define the flow of A particles per second per unit area as Γ_A and express it as

$$\Gamma_A = -D_{AB} \frac{d\, n_A}{dy} \tag{4.187}$$

where D_{AB} is the *binary diffusion coefficient* for species A into B. Comparing Equations (4.186) and (4.187), where $\Lambda = \Gamma_A$, we have

$$\boxed{D_{AB} = 2\, a\, \overline{C} \lambda} \tag{4.188}$$

We know that the *mean free path* is given by

$$\lambda = \frac{1}{\sqrt{2}\pi d^2 n} = \frac{1}{\sqrt{2}\sigma n}$$

and the *mean speed* is given by

$$\overline{C} = \sqrt{\frac{8RT}{\pi}}$$

where σ is the *collision cross section*. Thus, Equations (4.182a), (4.185), and (4.188) can be written as

$$\mu = K_\mu \frac{\sqrt{T}}{\sigma} \tag{4.189}$$

$$k = K_K \frac{\sqrt{T}}{\sigma} \tag{4.190}$$

$$D_{AB} = K_D \frac{\sqrt{T}}{\sigma n} \tag{4.191}$$

where K_μ, K_K, and K_D are constants.

From Equations (4.189)–(4.191), it is seen that μ and K for pure gases depend only on T, whereas D_{AB} depends on both T and n, that is, on temperature and density.

It is important to note that what is presented in this chapter is only the essential features of high-temperature flows. An elaborate information on this topic, with large number of appropriate references, can be found in References 10 and 11.

Example 4.8 As an example of vibrational–translational nonequilibrium phenomenon in hypersonic flow past a normal shock shown in Figure 4.34, solve and see the variation of e_{tr}, e_{vib}, T_{tr}, T_{vib}, ρ, p, and u in one-dimensional inviscid flow with the following procedure. List the code written for this example.
Assume an energy exchange phenomenon in one-dimensional hypersonic flow. Flow conditions are listed as follows.

- Flow gas composed only of nitrogen molecules N_2, with no chemical reactions.
- Freestream condition with typical orbital reentry speed: $M_1 = 25$, $T_1 = 195$ K, and $p_1 = 1$ Pa.

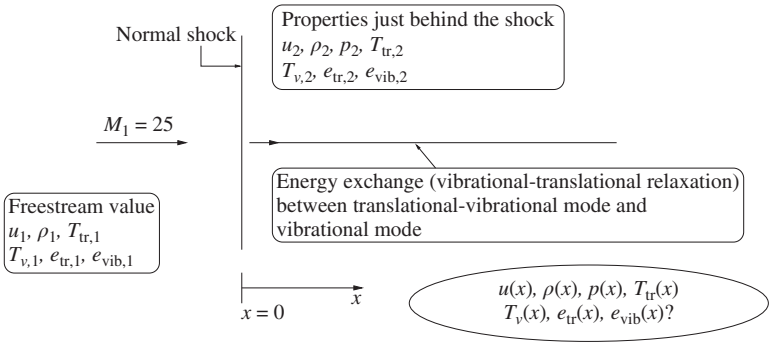

Figure 4.34 One-dimensional flow past a normal shock wave.

- One-dimensional, inviscid, steady flow problem.
- The thermodynamics state just behind the shock is thermally frozen, that is, $e_{\mathrm{vib}} = e_{\mathrm{vib},1}$.

Under the above assumptions, governing equations are written as follows.

$$\frac{d}{dx}\begin{pmatrix} \rho u \\ \rho u^2 + p \\ (E_t + p)u \\ \rho e_{\mathrm{vib}} u \end{pmatrix} = \begin{pmatrix} 0 \\ 0 \\ 0 \\ \frac{\rho(e_{\mathrm{vib}}^{\mathrm{eq}} - e_{\mathrm{vib}})}{\tau} \end{pmatrix} \tag{1}$$

These conservation equations are the one-dimensional Euler equations coupled with a vibrational relaxation equation. Here, we assume that the total energy of the gas E_t can be expressed as in perfect gas, that is,

$$E_t = \rho e + \rho \frac{u^2}{2} \tag{2}$$

where

$$e = e_{\mathrm{tr}} + e_{\mathrm{vib}} \tag{3}$$

$$e_{\mathrm{tr}} = \frac{5}{2} R T_{\mathrm{tr}} \tag{4}$$

The vibrational energy term e_{vib} of N_2 is given as

$$e_{\mathrm{vib}}(T_v) = \frac{\theta_{\mathrm{vib}}/R}{e^{\theta_{\mathrm{vib}}/T_v} - 1} \tag{5}$$

where θ_{vib} is the characteristic temperature of the oscillator $h\nu/k$ and for N_2,

$$\theta_{\mathrm{vib}} = 3395 \text{ K} \tag{6}$$

Vibrational relaxation time τ can be written as

$$p \text{ (atm)} \cdot \tau \text{ (s)} = \exp\ [A(T^{-1/3} - 0.015\mu^{1/4}) - 18.42] \tag{7}$$

where $A = 220$, $\mu = 14$ for N_2. Equations (6) and (7) are given in a literature by Millikan and White [12].
e_{vib}^{eq} is vibrational energy at equilibrium state and given as

$$e_{vib}^{eq} = e_{vib}(T_{tr}) \tag{8}$$

The equation of state $p = \rho RT$ can be combined with Equation (4) and yields

$$p = \frac{2}{5}\rho e_{tr} \tag{9}$$

Differentiating Equation (9) with x, we have

$$\frac{dp}{dx} = \frac{2}{5}e_{tr}\frac{d\rho}{dx} + \frac{2}{5}\rho\frac{de_{tr}}{dx} \tag{10}$$

Then, the governing equation (1) can be transformed into nonconservative form as

$$u\frac{d\rho}{dx} + \rho\frac{du}{dx} = 0 \tag{11}$$

$$\rho u\frac{du}{dx} + \frac{dp}{dx} = 0 \tag{12}$$

$$\rho u\frac{de_{tr}}{dx} + \rho u\frac{de_{vib}}{dx} + p\frac{du}{dx} = 0 \tag{13}$$

$$\rho u\frac{de_{vib}}{dx} = \frac{\rho(e_{vib}^{eq} - e_{vib})}{\tau} \tag{14}$$

Equations (11)–(14) can be simplified using Equation (10) and yield the final form as ordinary differential equations.

$$\frac{du}{dx} = \frac{\rho(e_{vib}^{eq} - e_{vib})/\tau}{\frac{5}{2}\rho u^2 - \rho e_{tr} - p} \tag{15}$$

$$\frac{d\rho}{dx} = -\frac{\rho}{u}\frac{du}{dx} \tag{16}$$

$$\frac{de_{tr}}{dx} = \left(-\frac{5}{2}u + \frac{e_{tr}}{u}\right)\frac{du}{dx} \tag{17}$$

$$\frac{de_{vib}}{dx} = \frac{e_{vib}^{eq} - e_{vib}}{\tau u} \tag{18}$$

Properties before the shock wave $x < 0$ is the freestream condition and initial properties at just after the shock $x = 0$ can be obtained assuming thermally frozen flow and using normal shock relations. The properties at downstream side $x > 0$ can be solved by integrating Equations (15)–(18).

Solution

From Figures 4.35–4.39, the variation of properties induced by the relaxation phenomenon can be clearly seen.

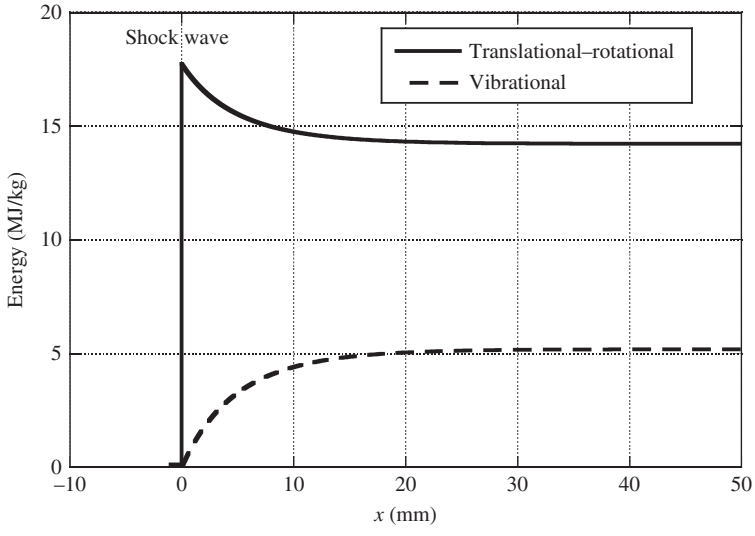

Figure 4.35 Energy variation behind the shock.

Variation of the translational–rotational energy and vibrational energy behind the shock is shown in Figure 4.35.
Variation of translational temperature, T_{tr}; vibrational temperature, T_v; and the difference between translational temperature and vibrational temperature, $(T_{tr} - T_v)$, in the reacting flow behind the shock is shown in Figure 4.36.

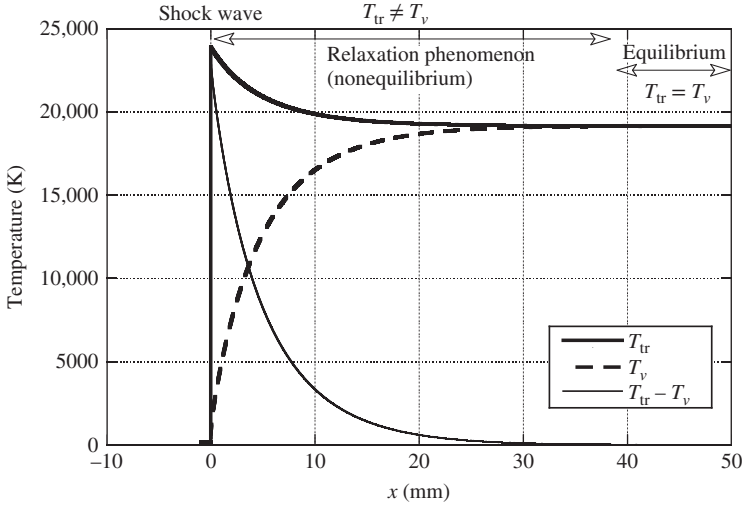

Figure 4.36 Variation of T_{tr}, T_v, and $(T_{tr} - T_v)$, in the reacting flow behind the shock.

From this temperature variation figure (Figure 4.36), we can clearly see that difference between translational temperature and vibrational temperature ($T_{tr} - T_v$) converges to be zero before reaching $x = 40$ mm. As "nonequilibrium" refers the state that these temperatures are different (that is, $T_{tr} \neq T_v$), it is clear that the relaxation progresses mainly in the region $0 < x < 40$ mm after the shock. The variation of properties induced by the relaxation phenomenon can be clearly seen in this region.
Variation of density, pressure, and velocity behind the shock are shown in Figures 4.37–4.39, respectively.

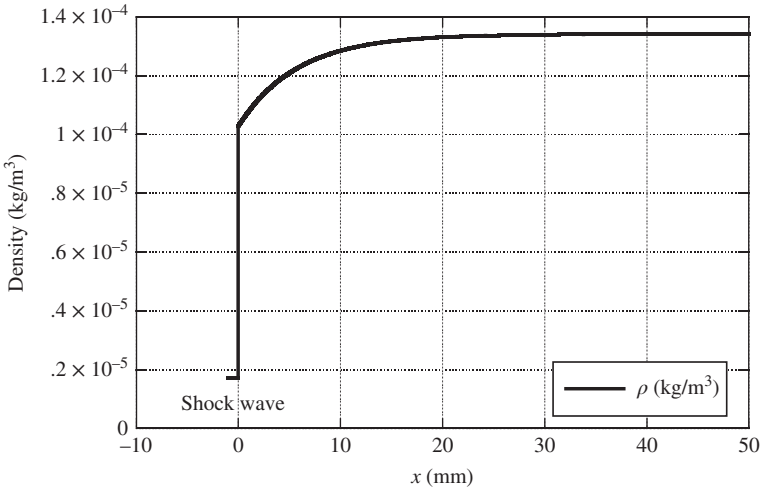

Figure 4.37 Density variation behind the shock.

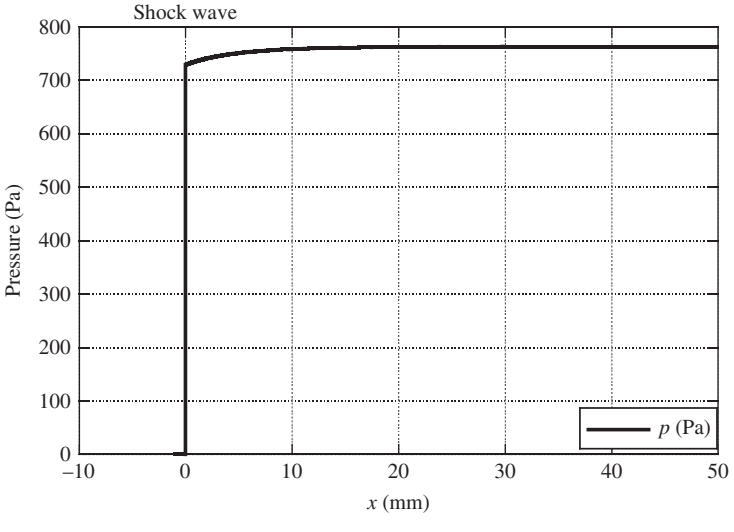

Figure 4.38 Pressure variation behind the shock.

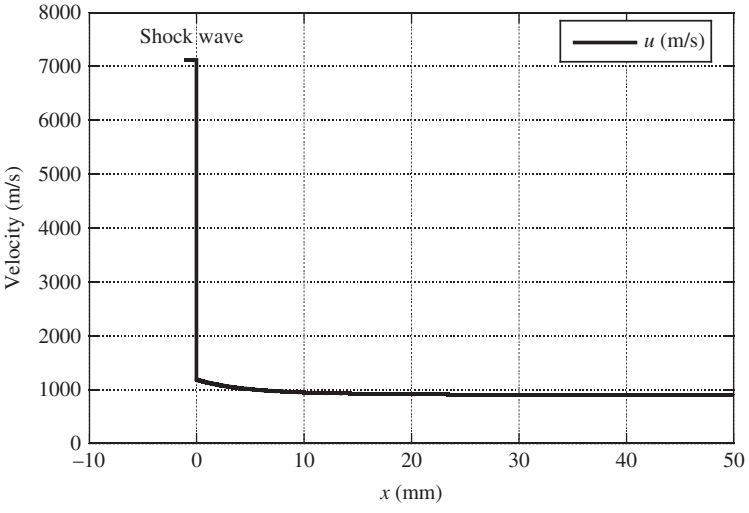

Figure 4.39 Velocity variation behind the shock.

```
      program tvrel
c=====================================================================
c     1-D relaxation problem for exercise 4.4
c     >> Solve ordinary differential equations with Runge-Kutta method
c     *** variables ***
c     rgas : gas constant for N2
c     gamma: specific heats ratio
c     fmach: Mach number
c     u    : flow velocity, m/s
c     ttr  : translational temperature, K
c     tv   : vibrational temperature, K
c     p    : pressure, Pa
c     rho  : density, kg/m3
c     etr  : translational-rotational energy, J/kg
c     ev,evib: vibrational energy, J/kg
c=====================================================================
      open(unit=60,file='result.txt',form='formatted')
c
c     (1) Initial Conditions
      rgas =8314./28.
      gamma=1.4
      xmin = -1.e-3
      xmax = 50.e-3
      np   = 10201
      dx   = (xmax-xmin)/float(np-1)
c     (1-1) Freestream values
      fmach1 = 25.
      ttr1   = 195.
      u1     = fmach1*sqrt(gamma*rgas*ttr1)
      tv1    = ttr1
```

```
      p1     = 1.
      rho1   = p1/(rgas*ttr1)
      evib1  = evib(tv1)
      etr1   = 5./2. * rgas*ttr1
      write(6,*) '*** freestream properties ***'
      write(6,*) 'Mach Number :    M  =',fmach1
      write(6,*) 'Flow speed : u(m/s) =',u1
      write(6,*) 'Temperature: Ttr(K) =',ttr1
      write(6,*) 'Temperature: Tv(K)  =',tv1
      write(6,*) 'Pressure   : P(Pa)  =',p1
      write(6,*) 'Density : rho(kg/m3)=',rho1
      write(6,*) 'Energy  :  etr(J/kg)=',etr1
      write(6,*) 'Energy  : evib(J/kg)=',evib1
c     (1-2) post-shock properties (initial condition at x=0)
      p2     = p1*(1.+2.*gamma/(gamma+1.)*(fmach1**2-1.))
      u2     =u1/( (gamma+1.)*fmach1**2/((gamma-1.)*fmach1**2+2.) )
      rho2   = rho1*u1/u2
      ttr2   = p2/(rgas*rho2)
      tv2    = tv1
      evib2  = evib(tv2)
      etr2   = 5./2. * rgas*ttr2
      fmach2 = u2/sqrt(gamma*rgas*ttr2)
      write(6,*) '*** initial properties at x=0 ***'
      write(6,*) 'Mach Number :    M  =',fmach2
      write(6,*) 'Flow speed : u(m/s) =',u2
      write(6,*) 'Temperature: Ttr(K) =',ttr2
      write(6,*) 'Temperature: Tv(K)  =',tv2
      write(6,*) 'Pressure   : P(Pa)  =',p2
      write(6,*) 'Density : rho(kg/m3)=',rho2
      write(6,*) 'Energy  :  etr(J/kg)=',etr2
      write(6,*) 'Energy  : evib(J/kg)=',evib2
c
      write(60,*)'#x(m) u(m/s) p(Pa) rho(kg/m3) T(K) Tv(K) etr evib'
c     (3) main loop
      do 1000 itr=1,np
c     (4) set x position
         x =xmin+dx*float(itr-1)
         n0=(np-1)/51+1
c     (5) x<0 : freestream condition
         if(itr.lt.n0) then
            rho=rho1
            u  =u1
            etr=etr1
            ev =evib1
            ttr=ttr1
            tv =tv1
            p  =rho*rgas*ttr
            write(60,1001) x,u,p,rho,ttr,tv,etr,ev
 1001       format(8E16.8)
c     (6) x=0 : initial condition
         else if(itr.eq.n0) then
            rho=rho2
            u  =u2
```

```
            etr=etr2
            ev =evib2
            ttr=ttr2
            tv =tv2
            p  =rho*rgas*ttr
            write(60,1001) x,u,p,rho,ttr,tv,etr,ev
c     (7) integrate into +x direction with 3-step TVD Runge-Kutta method
          else
c     (7-1) store previous values
            rhoold=rho
            uold  =u
            etrold=etr
            evold =ev
            ttrold=ttr
            tvold =tv
            pold  =p
c     (7-2) 1st step
            call rhs(rho,u,etr,ev,ttr,tv,p,dr,du,detr,dev)
c     (7-3) 2nd step
            rho=rho+dx*dr
            u  =u  +dx*du
            etr=etr+dx*detr
            ev =ev +dx*dev
            tv =evinv(ev)
            ttr=etr*2./(5.*rgas)
            p  =rho*rgas*ttr
            call rhs(rho,u,etr,ev,ttr,tv,p,dr,du,detr,dev)
c     (7-4) 3rd step
            rho=.75*rhoold+.25*(rho+dx*dr)
            u  =.75*uold  +.25*(u  +dx*du)
            etr=.75*etrold+.25*(etr+dx*detr)
            ev =.75*evold +.25*(ev +dx*dev)
            tv =evinv(ev)
            ttr=etr*2./(5.*rgas)
            p  =rho*rgas*ttr
            call rhs(rho,u,etr,ev,ttr,tv,p,dr,du,detr,dev)
c     (7-5) update properties
            rho=(rhoold+2.*(rho+dx*dr)  )/3.
            u  =(uold  +2.*(u  +dx*du)  )/3.
            etr=(etrold+2.*(etr+dx*detr))/3.
            ev =(evold +2.*(ev +dx*dev) )/3.
            tv =evinv(ev)
            ttr=etr*2./(5.*rgas)
            p  =rho*rgas*ttr
            write(60,1001) x,u,p,rho,ttr,tv,etr,ev
          end if
 1000 continue
      write(6,*) '*** final properties at x=',xmax*1000.,'(mm) ***'
      write(6,*) 'Mach Number :    M  =',u/sqrt(gamma*rgas*ttr)
      write(6,*) 'Flow speed : u(m/s) =',u
      write(6,*) 'Temperature: Ttr(K) =',ttr
      write(6,*) 'Temperature: Tv(K)  =',tv
      write(6,*) 'Pressure   : P(Pa)  =',p
```

```
      write(6,*) 'Density : rho(kg/m3)=',rho
      write(6,*) 'Energy  :  etr(J/kg)=',etr
      write(6,*) 'Energy  : evib(J/kg)=',ev
      close(unit=60)
      stop
      end
c=====================================================================
      subroutine rhs(rho,u,etr,ev,ttr,tv,p,dr,du,detr,dev)
      du=rho*(evib(ttr)-evib(tv))/tau(ttr,p)/(5./2.*rho*u**2-rho*etr-p)
      detr=du*(-5./2.*u+etr/u)
      dr=-rho/u*du
      dev=(evib(ttr)-evib(tv))/(tau(ttr,p)*u)
      return
      end
c
c=====================================================================
c     vibrational relaxation time
      function tau(tkel, ppa)
      wmu  =14.
      a    =220.
      ev   =exp(a*(tkel**(-1./3.)-.015*wmu**.25)-18.42)/(ppa/101325.)
      return
      end
c
c=====================================================================
c     vibrational energy
      function evib(tkel)
      rgas =8314./28.
      theta=3395.
      ev   =theta*rgas/(exp(theta/tkel)-1.)
      return
      end
c
c=====================================================================
c     inverse function of evib(tkel)
      function evinv(ev)
      rgas =8314./28.
      theta=3395.
      tkel =theta/alog(theta*rgas/ev +1.)
      evinv=tkel
      return
      end
```

■

4.24 Summary

Air can be treated as both thermally and calorically perfect for temperatures less than 800 K, and for temperatures from 800 to 2000 K, it is only thermally perfect but calorically imperfect. For temperatures above 2000 K, the air is thermally as well as calorically imperfect.

In many engineering problems of practical interest, the temperature of the flow is appreciably above the limiting value for which the gas can be treated as perfect.

Flows with temperature above 800 K need to be analyzed considering the functional dependence of the specific heats c_p and c_v on temperature. In this kind of flows with temperature more than 800 K, if the temperature is in the range from 800 to 2000 K, the flowing gas is termed *thermally perfect*. For high-enthalpy flows with temperature above 2000 K, even the specific heats ratio γ becomes a function of temperature. This makes the isentropic, shock, Fanno, and Rayleigh flow relations, derived based on perfect gas assumption invalid. Therefore, for solving high-enthalpy flows that are both calorically as well as thermally imperfect, each problem has to be dealt with the actual equations governing the transport of mass, momentum, and energy and the second law of thermodynamics.

The following are the two major physical characteristics that cause a high-enthalpy flow to deviate from calorically perfect gas behavior.

- At high temperatures, the vibrational excitation of the gas molecules becomes important, absorbing some of the energy that, at normal temperatures, would go into the translational and rotational motion. The excitation of vibrational energy causes the specific heats of the gas to become a function of temperature, causing the gas to become calorically imperfect.
- With further increase in temperature, the molecules begin to dissociate and even ionize. Under these conditions, the gas becomes chemically reacting, and the specific heats become functions of both temperature and pressure.

Because of the above effects, the high-enthalpy gas flows have the following differences as compared to the flow of gas with constant specific heats (perfect gas).

- The specific heats ratio, $\gamma = c_p/c_v$, is a variable.
- The thermodynamic properties (the thermal and calorical properties) are totally different.
- For high-enthalpy flows, heat transfer rate is predominant.
- Usually, some numerical procedure, rather than analytical approach, is required for solving high-enthalpy problems.
- Because of these reasons, analysis of high-enthalpy flows are different from that of gas dynamic flows obeying perfect gas assumption.

The macrostate that occurs when the system is in thermodynamic equilibrium, referred to as the *most probable macrostate*, plays a dominant role in the study of high-enthalpy gas dynamics, because at temperatures above 800 K, the vibration excitation of the molecules becomes active; beyond 2000 K, the molecules in a gas dissociate to become atoms; and beyond 3000 K, the atoms themselves become active and get ionized, heading towards plasma state.

From kinetic theory of gases, the following can be known.

- In any given system of molecules, the microstates are constantly changing because of molecular collisions.

- The most probable macrostate is that the *macrostate that has the maximum number of microstates*.
- If each microstate appears in the system with equal probability and there is one particular macrostate that has considerably more microstates than any other, then that is the macrostate that will prevail in the system most of the time.

Molecules and atoms are constituted by the elementary particles, namely, the electrons, protons, and neutrons. Quantum mechanics makes a distinction between two different class of molecules and atoms, depending on the number of elementary particles in them, as follows.

- Molecules and atoms with *even number* of elementary particles obey a certain statistical distribution called *Bose–Einstein* statistics. Let us call them *bosons*.
- Molecules and atoms with *odd number* of elementary particles obey a different statistical distribution called *Fermi–Dirac* statistics. Let us call such molecules and atoms as *fermions*.

The following is an important distinction between the above two classes.

- For bosons, the number of molecules that can be in any one degenerate state (in any one of the boxes in Figure 4.4) is unlimited (except, of course, that it must be less than or equal to N_j).
- For fermions, only one molecule may be in any given degenerate state at any instant.

The total number of microstates for a given macrostate with Bose–Einstien statistics is

$$W = \prod_j \frac{(N_j + g_j - 1)!}{(g_j - 1)! N_j!}$$

The quantity W is called the *thermodynamic probability*. The thermodynamic probability is a measure of the "disorder" of the system. This can be used to count the number of microstates in a given macrostate as long as the molecules are bosons.

The total number of microstates for a given macrostate for fermions is

$$W = \prod_j \frac{g_j!}{(g_j - N_j)! N_j!}$$

The most probable macrostate is the macrostate that has $W_{\max}$.

The total energy of a molecule consists of translational, rotational, vibrational, and electronic energies. That is, for a *molecule*, the total energy is given by

$$\varepsilon = \varepsilon_{\text{trans}} + \varepsilon_{\text{rot}} + \varepsilon_{\text{vib}} + \varepsilon_{\text{el}}$$

However, for a single atom, only the translational and electronic energies exist, that is, for *atoms* the total energy is given by

$$\varepsilon = \varepsilon_{\text{trans}} + \varepsilon_{\text{el}}$$

The molecules have the following forms (modes) of energy.

- *Translational energy*, $\varepsilon_{\text{trans}}$ – the translational kinetic energy of the center of mass of the molecule is the source of this energy.
- *Rotational energy*, ε_{rot} – the rotational energy is due to the rotation of the molecule about the three orthogonal axes in space.
- *Vibrational energy*, ε_{vib} – the molecules and atoms are vibrating with respect to an equilibrium location within the molecule.
- *Electronic energy*, ε_{el} – the electronic energy is due to the motion of electrons about the nucleus of each atom constituting the molecule.

Quantum mechanics results show that each of the above energies are *quantized*, that is, they can exist only at certain discrete values.

The N_j corresponding to the maximum value of the thermodynamic probability W is

$$\boxed{N_j^* = \frac{g_j}{e^{\alpha}\, e^{\beta\epsilon_j'} - 1}}$$

The superscript "*" is added to N_j to emphasize that N_j^* corresponds to the maximum value of W, that is, N_j^* corresponds to the most probable distribution of molecules over the energy levels ϵ_j'. The above equation gives the most probable macrostate for bosons.

The most probable macrostate for fermions is

$$\boxed{N_j^* = \frac{g_j}{e^{\alpha}\, e^{\beta\epsilon_j'} + 1}}$$

At very low temperatures, $T \to 0$ K, the molecules of the system are jammed together at or near the ground energy levels, and therefore, the degenerate states of these low-lying energy levels are highly populated. As a result, the difference between the Bose–Einstein and Fermi–Dirac statistics are important. In contrast, at high temperatures, the molecules are distributed over many energy levels, and therefore, the states are generally sparsely populated, that is, $N_j \ll g_j$.

In the high-temperature limit,

$$\boxed{N_j^* = g_j e^{-\alpha} e^{-\beta\epsilon_j'}}$$

This limiting case is called the *Boltzmann limit*, and this equation is termed the *Boltzmann distribution*.

In the above equation, the Lagrange constants α and β are unknowns. The link between the classical and statistical thermodynamics is the constant β. It can be shown that

$$\beta = \frac{1}{kT}$$

where k is the Boltzmann constant and T is the temperature of the system. With $\beta = \frac{1}{kT}$, Equation (4.20) can be written as

$$N_j^* = g_j \, e^{-\alpha} \, e^{-\epsilon_j'/kT}$$

The partition function Q, also called the *state sum*, is defined as

$$Q \equiv \sum_j g_j \, e^{-\epsilon_j/kT}$$

and the Boltzmann distribution, from Equation (4.24), can be written in terms of the partition function Q as

$$\boxed{N_j^* = N \, \frac{g_j \, e^{-\epsilon_j/kT}}{Q}}$$

It can be shown that the partition function Q is a function of the volume, $\mathbb{V}$, as well as the temperature, T, of the system, that is,

$$Q = f \, (T, \mathbb{V})$$

The thermodynamic properties such as the internal energy, enthalpy, entropy, and pressure can be expressed in terms of the partition function Q.

From the microscopic view point, for a system in equilibrium, the energy of the system is given by

$$\boxed{E = NkT^2 \left(\frac{\partial \ln Q}{\partial T} \right)_v}$$

If we have 1 mol of atoms or molecules, then $N = N_A$, the Avogadro number ($6.02214179 \times 10^{23}$).

Also, $N_A \, k = R_u$, the universal gas constant. Consequently, for the internal energy per mole, Equation (4.29) gives

$$E = R_u T^2 \left(\frac{\partial \ln Q}{\partial T} \right)_v$$

In the science of gas dynamics, a unit mass is more fundamental quantity than a unit mole. Let M be the mass of the system of N molecules and m be mass of an

individual molecule. Then $M = Nm$. From Equation (4.29), the internal energy per unit mass, e, is

$$e = \frac{E}{M} = \frac{NkT^2}{Nm} \left(\frac{\partial \ln Q}{\partial T} \right)_v$$

But $k/m = R$ is the specific gas constant. Therefore, Equation (4.31) becomes

$$\boxed{e = RT^2 \left(\frac{\partial \ln Q}{\partial T} \right)_v}$$

The specific enthalpy is defined as the sum of the specific internal energy and flow work,

$$h = e + pv$$

The enthalpy in terms of the partition function Q is

$$\boxed{h = RT + RT^2 \left(\frac{\partial \ln Q}{\partial T} \right)_v}$$

The entropy or the amount of disorder in a system is a function of the thermodynamic probability, that is,

$$S = S\,(W_{\max})$$

where S is entropy and $W_{\max}$ is the *thermodynamic probability*.

If we have two systems with S_1, W_1 and S_2, W_2, respectively, and add these systems, the entropy of the combined system is additive, $S_1 + S_2$. But the thermodynamic probability of the combined system is the product of the thermodynamic probabilities of the individual systems $W_1 W_2$ (because each microstate of the first system can exist in the combined system along with each one of the microstates of the second system). This suggests that Equation (4.34) should be of the form

$$S = (\text{constant}) \ln W_{\max}$$

Equation (4.35) was first postulated by Ludwig Boltzmann, and the constant is named in his honor. Thus

$$\boxed{S = k \ln W_{\max}}$$

where k is the familiar *Boltzmann constant*.

The pressure in terms of partition function is

$$\boxed{p = N\ k\ T \left(\frac{\partial \ln Q}{\partial \mathbb{V}} \right)_T}$$

The partition function Q, by definition, is

$$Q \equiv \sum_j g_j e^{-\epsilon_j/kT}$$

The total energy of a state is the sum of translational, rotational, vibrational, and electronic energies, that is,

$$\epsilon' = \epsilon'_{\text{trans}} + \epsilon'_{\text{rot}} + \epsilon'_{\text{vib}} + \epsilon'_{\text{el}}$$

From quantum mechanics, we have

$$\epsilon'_{\text{trans}} = \frac{h_P^2}{8\ m} \left(\frac{n_1^2}{a_1^2} + \frac{n_2^2}{a_2^2} + \frac{n_3^2}{a_3^2} \right)$$

$$\epsilon'_{\text{rot}} = \frac{h_P^2}{8\ \pi^2 I}\ J(J+1)$$

$$\epsilon'_{\text{vib}} = h_P\ \nu \left(n + \frac{1}{2} \right)$$

For electronic energy, no simple expression can be written, and hence, it will continue to be expressed simply as ϵ'_{el}.

$$\boxed{e_{\text{trans}} = \frac{3}{2}\ RT}$$

$$\boxed{e_{\text{rot}} = RT}$$

$$\boxed{e_{\text{vib}} = \frac{h_P \nu / kT}{e^{h_P \nu / kT} - 1}\ RT}$$

The *theorem of equipartition of energy* of kinetic theory states that

"*each thermal degree of freedom of the molecule contributes* $\frac{1}{2}\ kT$ *to the energy of each molecule, or* $\frac{1}{2}\ RT$ *to the energy per unit mass of gas*."

Hence, because of the equipartition of energy, the translational energy per unit mass should be

$$e_{\text{trans}} = 3 \left(\frac{1}{2}\ RT \right) = \frac{3}{2}\ RT$$

This is same as Equation (4.57) obtained from the modern principles of statistical thermodynamics.

Similarly, for a diatomic molecule, the rotational motion contributes two thermal degrees of freedom. Therefore,

$$e_{\text{rot}} = 2 \left(\frac{1}{2}\ RT \right) = RT$$

which is same as Equation (4.59).

For vibrational freedom, two degrees of freedom should result in

$$e_{\text{vib}} = 2\left(\frac{1}{2}\,RT\right) = RT$$

But this is not confirmed by Equation (4.61). Indeed, the factor

$$\frac{h_P\nu/kT}{(e^{-h_P\nu/kT}-1)}$$

is less than unity, except when $T \to \infty$, it approaches unity; thus, in general, $e_{\text{vib}} < RT$, in conflict with classical theory. This implies the following.

- The classical results based on macroscopic observations do not necessarily describe phenomena in the microscopic world of molecules.
- As a result, the equipartition of energy principle is misleading.

Equation (4.61), obtained from quantum mechanics considerations, is the proper expression for vibrational energy.

Thus, we have for atoms

$$e = \frac{3}{2}\,RT + e_{\text{el}}$$

This implies that for atoms,

Specific internal energy measured above zero-point energy (sensible energy)
= Translational energy + Electronic energy obtained directly from spectroscopic measurement

For molecules, we have the internal energy as

$$e = \frac{3}{2}\,RT + RT + \frac{h_P\nu/kT}{e^{h_P\nu/kT}-1}\,RT + e_{\text{el}}$$

The specific heat at constant volume is

$$c_v \equiv \left(\frac{\partial e}{\partial T}\right)_v$$

Thus, from Equation (4.62), we have the c_v for atoms as

$$\boxed{c_v = \frac{3}{2} + \frac{\partial e_{\text{el}}}{\partial T}}$$

For molecules, from Equation (4.63), we have the c_v as

$$\boxed{c_v = \frac{3}{2}\,R + R + \frac{(h_P\nu/kT)^2\; e^{h_P\nu/kT}}{(e^{h_P\nu/kT}-1)^2}\,R + \frac{\partial e_{\text{el}}}{\partial T}}$$

For a gas with only translational and rotational energy, we have the following.

For atoms,

$$c_v = \frac{3}{2} R$$

and for diatomic molecules,

$$c_v = \frac{5}{2} R$$

That is, c_v is a constant and independent of temperature. This is the case of a *calorically perfect gas*. For air around room temperature, being a perfect gas, we have

$$c_p - c_v = R$$

Therefore,

$$c_p = c_v + R$$

Substituting $c_v = \frac{5}{2} R$, we have

$$c_p = \frac{7}{2} R$$

Hence, the specific heats ratio γ becomes

$$\gamma = \frac{c_p}{c_v} = \frac{7}{5}$$
$$= 1.4$$

The *kinetic theory equivalent* of the perfect gas state equation is

$$\boxed{p\mathbb{V} = \frac{2}{3} E'_{\text{trans}}}$$

Another form of the kinetic theory equivalent of the perfect gas state equation is

$$\boxed{\frac{p}{\rho} = \frac{1}{3} \overline{C^2}}$$

The root-mean-square (RMS) velocity is given by

$$\sqrt{\overline{C^2}} = \sqrt{3RT}$$

The *single particle collision frequency*, Z', is

$$\boxed{Z' = n \pi d^2 \overline{C}}$$

The *mean free path*, λ, is defined as *the mean distance traveled by a molecule between two successive collisions*.

$$\boxed{\lambda = \frac{\overline{C}}{Z'} = \frac{1}{n\pi d^2}}$$

$$\boxed{\lambda \propto \frac{T}{p}}$$

Note that the collision frequency is *directly proportional* to the pressure, and the mean free path is *inversely proportional* to the pressure.

Most probable speed is

$$\boxed{C_{\text{mp}} = \sqrt{2RT}}$$

where R is the specific gas constant.

Average speed is

$$\boxed{\overline{C} = \sqrt{\frac{8RT}{\pi}}}$$

The root-mean-square (RMS) speed can be expressed as

$$\boxed{\sqrt{\overline{C}^2} = \sqrt{\frac{3R_u T}{M_m}}}$$

A flow is said to be in *local thermodynamic equilibrium* if a local Boltzmann distribution, given by

$$N_j^* = N \frac{e^{-\epsilon_j/kT}}{Q}$$

exists at each point in the flow at the local temperature T.

A flow is said to be in *local chemical equilibrium* if the local chemical composition at each point in the flow is the same as that determined by the chemical equilibrium calculations.

The equations of continuity, momentum, and energy for an inviscid compressible flow are the following.

Continuity equation:

$$\frac{\partial \rho}{\partial t} + \frac{\partial(\rho u)}{\partial x} + \frac{\partial(\rho v)}{\partial y} + \frac{\partial(\rho w)}{\partial z} = 0$$

Momentum equation (x-, y-, and z-components, respectively):

$$\rho\frac{\partial u}{\partial t} + \rho u\,\frac{\partial u}{\partial x} + \rho v\,\frac{\partial u}{\partial y} + \rho w\frac{\partial u}{\partial z} = -\frac{\partial p}{\partial x}$$

$$\rho\frac{\partial v}{\partial t} + \rho u\,\frac{\partial v}{\partial x} + \rho v\,\frac{\partial v}{\partial y} + \rho w\frac{\partial v}{\partial z} = -\frac{\partial p}{\partial y}$$

$$\rho\frac{\partial w}{\partial t} + \rho u\,\frac{\partial w}{\partial x} + \rho v\,\frac{\partial w}{\partial y} + \rho w\frac{\partial w}{\partial z} = -\frac{\partial p}{\partial z}$$

Energy equation:

$$\frac{\partial s}{\partial t} + u\,\frac{\partial s}{\partial x} + v\,\frac{\partial s}{\partial y} + w\,\frac{\partial s}{\partial z} = 0$$

This is a *specialized energy equation* for an adiabatic, inviscid flow.

- Continuity equation is a statement that the mass flow rate is conserved.
- Momentum equations are statements of Newton's second law, $F = ma$.
- Energy equation is a statement that entropy is constant along a streamline for an inviscid, adiabatic flow.

If entropy is constant along a streamline, then for an isentropic process of a calorically perfect gas, the quantity p/ρ^{γ} is also constant along a streamline, and we can write the above specialized energy equation in terms of the entropy in the following form.

$$\frac{\partial}{\partial t}\left(\frac{p}{\rho^{\gamma}}\right) + u\,\frac{\partial}{\partial x}\left(\frac{p}{\rho^{\gamma}}\right) + v\,\frac{\partial}{\partial y}\left(\frac{p}{\rho^{\gamma}}\right) + w\,\frac{\partial}{\partial z}\left(\frac{p}{\rho^{\gamma}}\right) = 0$$

Thus, the continuity, momentum, and energy equations in terms of entropy s are valid for a high-temperature, chemically reacting, inviscid, equilibrium flow.

The energy equation for an adiabatic inviscid flow, in terms of h_0, is

$$\boxed{\rho\,\frac{Dh_0}{Dt} = \rho\,\frac{\partial h_0}{\partial t} + \rho u\,\frac{\partial h_0}{\partial x} + \rho v\,\frac{\partial h_0}{\partial y} + \rho w\,\frac{\partial h_0}{\partial z} = \frac{\partial p}{\partial t}}$$

This equation is valid for *both equilibrium* and *nonequilibrium flows*.

Therefore, the governing equations for an inviscid, high-temperature, equilibrium flows are the following.

Continuity equation:

$$\frac{\partial \rho}{\partial t} + \nabla \cdot (\rho V) = 0$$

Momentum equation:

$$\rho \frac{DV}{Dt} = -\nabla p$$

Energy equation:

$$\rho\,\frac{Dh_0}{Dt} = \frac{\partial p}{\partial t}$$

The governing equations for the flow across a normal shock (one-dimensional flow) are

Continuity equation:

$$\rho_1 V_1 = \rho_2 V_2$$

Momentum equation:

$$p_1 + \rho_1 V_1^2 = p_2 + \rho_2 V_2^2$$

Energy equation:

$$h_1 + \frac{V_1^2}{2} = h_2 + \frac{V_2^2}{2}$$

These equations are general and *valid* for both reacting and nonreacting gases. For perfect gases, a series of closed-form algebraic relations for p_2/p_1, T_2/T_1, M_2, etc. as functions of M_1 can be obtained. But no such simple formulae can be obtained when the gas is vibrationally excited and/or chemically reacting.

To set up such a numerical scheme to solve for flow properties behind the normal shock, let us first rearrange Equations (4.101)–(4.103).

The enthalpy h_2 behind the shock is

$$\boxed{h_2 = h_1 + \frac{V_1^2}{2}\left[1 - \left(\frac{\rho_1}{\rho_2}\right)^2\right]}$$

As the flow properties ρ_1, V_1, p_1, h_1, etc. ahead of the shock are known, Equations (4.108) and (4.110) express p_2 and h_2, respectively, in terms of only one unknown, namely, the density ratio ρ_1/ρ_2.

There is a basic practical difference between the shock results for a calorically perfect gas and those for a chemically reacting gas.

For a calorically perfect gas, only the Mach number upstream of the shock, M_1, is required to obtain the ratio of flow properties across a normal shock wave.

But, for an equilibrium chemically reacting gas, we have seen that

$$\frac{p_2}{p_1} = g_1\,(V_1, p_1, T_1)$$
$$\frac{\rho_2}{\rho_1} = g_2\,(V_1, p_1, T_1)$$
$$\frac{h_2}{h_1} = g_3\,(V_1, p_1, T_1)$$

Note that, in this case, three freestream properties, namely, the velocity, pressure, and temperature are necessary to obtain the properties downstream of a normal shock wave.

The chemical reactions have the strongest effect on the temperature T. This is generally true for all types of chemically reacting flows – the temperature T is the most sensitive variable. In contrast, the pressure ratio is affected only by a small amount. Pressure is a "mechanically" oriented variable and governed mainly by the fluid mechanics of the flow, and not so much by the thermodynamic.

For high-speed flows,

$$\boxed{p_2 \approx \rho_1 V_1^2}$$

This is a common hypersonic approximation; note that p_2 is mainly governed by the freestream velocity and the thermodynamic effects are secondary.

An approximate expression for the shock detachment distance, δ, ahead of the nose of a blunt-nosed body, with spherical nose of radius R, in terms of the density ratio across the detached shock is

$$\boxed{\frac{\delta}{R} = \frac{\rho_1/\rho_2}{1 + \sqrt{2\,(\rho_1/\rho_2)}}}$$

$$\boxed{\tan(\beta - \theta) = \frac{V_{n_2}}{V_{n_1}}\,\tan\beta}$$

This relation in terms of θ, β, V_{n_2}, and V_{n_1} for the equilibrium high-temperature gases is the analog of the $\theta-\beta-M$ relation for calorically perfect gases.

- The $\theta-\beta-M$ behavior for equilibrium chemically reacting air is qualitatively similar to calorically perfect air.
- For the equilibrium chemically reacting results, the flow Mach number, M_1, upstream of the shock is not an important parameter. The results of an oblique shock wave in a chemically reacting flow depend on the upstream velocity, V_1, as well as on the pressure, p_1, and temperature, T_1, ahead of the shock.

The equilibrium chemically reacting flow through a nozzle is *isentropic*. It is a general result implying that the equilibrium chemical reactions do not introduce irreversibilities into the system. Thus, any shock-free, inviscid, adiabatic, equilibrium chemically reacting flow is isentropic.

One-dimensional flow is that in which the radius of curvature of the streamlines are very large and the cross-sectional area of the passage (streamtube) does not change abruptly.

The area–velocity relation can be expressed as

$$\boxed{\frac{dA}{du} = -\frac{A}{u}(1 - M^2)}$$

This is called the *area–velocity relation*. This is valid for any gas irrespective of whether it is perfect or chemically reacting.

For a calorically perfect gas, the nozzle flow characteristics are given by the local flow Mach number, M, only. In contrast, for an equilibrium chemically reacting gas, the area, temperature, and pressure ratios are given by

$$\frac{A}{A^*} = g_1\,(p_0, T_0, u)$$

$$\frac{T}{T_0} = g_2\ (p_0, T_0, u)$$

$$\frac{p}{p_0} = g_3\ (p_0, T_0, u)$$

Note that, as in the case of normal shock, the nozzle flow properties also depend on three parameters.

For nozzle flow, the equilibrium temperature is always higher than that for a calorically perfect gas. But for flow behind a shock wave, the equilibrium temperature is always lower than that for a calorically perfect gas. In the nozzle flow case, the reactions are *exothermic*, and energy is dumped into the translational molecular motion, but in the case of normal shock flow, the reactions are *endothermic* and energy is taken from the translational mode.

In the case of local equilibrium flow, the equilibrium properties of a moving fluid element demand instantaneous adjustment of local temperature, T, and pressure, p, as the element moves through the flow field. For this, the *reaction rates* have to be infinitely large. Therefore, equilibrium flow implies *infinite chemical* and *vibrational rates*. The opposite to this flow is that where the reaction rates are practically zero. Such a flow with no reaction is termed *frozen flow*. As a result, the chemical composition of frozen flow remains constant throughout the space and time.

For vibrationally frozen flow, vibrational energy remains constant throughout the flow. Because the temperature T is proportional to the translational energy, the frozen flow temperature distribution is less than that for equilibrium flow. In turn, the distribution of translational energy, e_{trans}, and rotational energy, e_{rot}, will be lower for vibrationally frozen flow.

A flow that is both chemically and vibrationally frozen has *constant specific heats*. This situation is the same as the calorically perfect gas. But no flow in reality is precisely an equilibrium flow or a frozen flow. However, there are a large number of flow applications that come very close to such a limiting situation of equilibrium frozen flow and thus can be analyzed using these assumptions.

$$c_p = \sum_i c_i\, c_{p_i} + \sum_i h_i \left(\frac{\partial c_i}{\partial T}\right)_p$$

This gives c_p for a *chemically reacting mixture*.

The c_p can be written as

$$\underset{\substack{\text{(Specific heat at}\\ \text{constant } p \text{ for}\\ \text{reacting mixture)}}}{c_p} = \underset{\substack{\text{(Frozen}\\ \text{specific heat)}}}{c_{p_f}} + \underbrace{\sum_i h_i \left(\frac{\partial c_i}{\partial T}\right)_p}_{\substack{\text{(Contribution because of}\\ \text{chemical reaction)}}}$$

$$c_v = \sum_i c_i \, c_{v_i} + \sum_i e_i \left(\frac{\partial c_i}{\partial T} \right)_v$$

This gives c_v for a *chemically reacting mixture*.

The c_v can be expressed as

$$\underset{\substack{\text{(Specific heat at constant } v \text{ for} \\ \text{reacting mixture)}}}{c_v} = \underset{\substack{\text{(Frozen} \\ \text{specific heat)}}}{c_{v_f}} + \underset{\substack{\text{(Contribution because of} \\ \text{chemical reaction)}}}{\sum_i e_i \left(\frac{\partial c_i}{\partial T} \right)_v}$$

The general expression for the speed of sound is

$$a = \sqrt{\left(\frac{\partial p}{\partial \rho} \right)_s}$$

This is a physical fact and is not changed by the presence of chemical reactions; hence, this relation for the speed of sound, a, is valid for both perfect gas flow and reacting gas flow.

The speed of sound in a perfect gas is given by

$$a = \sqrt{\gamma RT}$$

But this expression for the speed of sound is so restrictive and valid only for calorically perfect gases.

If the gas remains in local chemical equilibrium through the internal structure of the sound wave, the gas composition is changed locally within the wave according to the local variations of pressure and temperature. For this situation, the speed of sound wave is called *equilibrium speed of sound*, denoted by a_e. In turn, if the gas is in motion at the velocity V, then V/a_e is termed the *equilibrium Mach number*, M_e.

$$a_e^2 = \gamma RT \, \frac{[1 + (1/p)(\partial e/\partial v)_T]}{[1 - \rho \, (\partial h/\partial p)_T]}$$

This is the expression for *equilibrium speed of sound* in a chemically reacting mixture.

The governing equation for inviscid, nonequilibrium flows are the following.

Continuity equation:

$$\frac{\partial \rho}{\partial t} + \nabla \cdot (\rho V) = 0$$

Momentum equation:

$$\rho \frac{DV}{Dt} = -\nabla p$$

Energy equation:

$$\rho \frac{Dh_0}{Dt} = \frac{\partial p}{\partial t}$$

where

$$h_0 = h + \frac{V^2}{2}$$

These equations are valid for both equilibrium and nonequilibrium flows.

In addition to the continuity equation above, which is referred to as the *global continuity equation*, we must consider the species continuity equation for each individual chemical species in the mixture.

$$\boxed{\int\int\int_{\mathbb{V}} \rho_i \, d\,\mathbb{V} = -\int\int_s \rho_i \, V \cdot dS + \int\int\int_{\mathbb{V}} \dot{w}_i \, d\,\mathbb{V}}$$

This is the *integral form* of species continuity equation.

Using the divergence theorem, the *differential form* of the species continuity equation can be expressed as

$$\boxed{\frac{\partial \rho_i}{\partial t} + \nabla \cdot (\rho_i \, V) = \dot{w}_i}$$

The vibrational rate equation for a moving fluid element is

$$\boxed{\frac{De_{\text{vib}}}{Dt} = \frac{1}{\tau}(e_{\text{vib}}^{\text{eq}} - e_{\text{vib}})}$$

where e_{vib} is the local nonequilibrium value of vibrational energy per unit mass of gas.

The thin region where large gradients in temperature, pressure, and velocity occur and the transport phenomena of momentum (μ) and energy (K) are important is called the *shock*. Essentially, a shock is a compression front across which the flow properties *jump*.

For shocks in a calorically perfect gas flow or a chemically reacting equilibrium flow, the flow properties ahead of and behind the shock are uniform, and the gradients (that is, the jump) in flow properties take place almost discontinuously (that is, abruptly) within a thin region of not more than a few mean free path thickness ($\lambda \approx 6.6317 \times 10^{-8}$ m, for air at sea level).

However, in nonequilibrium flows, all chemical reactions and/or vibrational excitations take place at a finite rate. As the thickness of a shock wave is of the order of only a few mean free path, the molecules in a fluid element can experience only a few collisions, as the fluid element traverses the shock front. Consequently, the flow through the shock front is essentially *frozen*.

As the reaction is endothermic, the temperature, T, behind the shock decreases, whereas the density, ρ, increases.

For a given flow turning angle θ, the equilibrium shock angle β_e is always less than the frozen wave angle β_f (for $\gamma = 1.4$).

Nonequilibrium quasi-one-dimensional nozzle flows find application in high-temperature flows through rocket nozzle, high-enthalpy aerodynamic testing facilities, etc.

- In a rocket nozzle, nonequilibrium effects decrease the thrust and specific impulse.
- In a high-enthalpy (high temperature) wind tunnel, the nonequilibrium effects make the flow conditions in the test section somewhat uncertain. Both of these are adverse effects.
- In contrast, a gas dynamic laser creates a laser medium by intentionally fostering vibrational nonequilibrium in a supersonic expansion. Therefore, this application aims at obtaining the highest degree of nonequilibrium possible.

Widely accepted technique for solving nonequilibrium nozzle flows is the time-marching technique.

The governing equations for unsteady quasi-one-dimensional flow are the following.

Continuity equation:

$$\frac{\partial p}{\partial t} = -\frac{1}{A}\,\frac{\partial(\rho u A)}{\partial x}$$

Momentum equation:

$$\frac{\partial u}{\partial t} = -\frac{1}{\rho}\,\left(\frac{\partial p}{\partial x} + \rho u\,\frac{\partial u}{\partial x}\right)$$

Energy equation:

$$\frac{\partial e}{\partial t} = -\frac{1}{\rho}\,\left(p\,\frac{\partial u}{\partial x} + \rho u\,\frac{\partial e}{\partial x} + p u\,\frac{\partial \ln A}{\partial x}\right)$$

where A is the local cross-sectional area of the nozzle, p is the local pressure, and u is the local velocity.

In addition to these equations, for a nonequilibrium flow, the appropriate vibrational rate equation and species continuity equation are

$$\frac{\partial e_{\text{vib}}}{\partial t} = \frac{1}{\tau}(e_{\text{vib}}^{\text{eq}} - e_{\text{vib}}) - u\,\frac{\partial e_{\text{vib}}}{\partial x}$$

and

$$\frac{\partial C_i}{\partial t} = -u\,\frac{\partial C_i}{\partial x} + \frac{\dot{w}_i}{\rho}$$

The above equations are solved step by step in time, using the finite-difference predictor–corrector approach.

The nonequilibrium phenomena introduce an important new stability criterion for the time step Δt, in addition to the CFL criterion.

Nonequilibrium flow over a blunt nose not only resembles some of the characteristics of the equilibrium flow and perfect gas flow but also takes on some of the aspects of nonequilibrium flow behind shock waves. In the nose region, the chemical composition resembles that in a nonequilibrium region behind a normal shock wave. But for the streamline that goes through the stagnation point (abc), between a and b, the flow is compressed and decelerated; it reaches zero velocity at the stagnation point b. In doing so, it can be shown that a fluid element takes an infinite time to traverse the distance ab. This means that local equilibrium conditions must exist at the stagnation point b with its attendant highly *dissociated* and *ionized state*.

The random motion of atoms and molecules is the essence of molecular transport phenomena. The motion of molecules cause the transport of mass, momentum, and energy, popularly termed *transport phenomena*. The properties characterizing these transports are *diffusion coefficient*, D; *viscosity coefficient*, μ; and the *thermal conduction coefficient*, K, referring to the transport of mass, momentum, and energy, respectively.

The general transport equation is

$$\boxed{\Lambda = -2\, a\, n\, \overline{C}\, \lambda\, \frac{d\phi}{dy}}$$

The dynamic viscosity coefficient, μ, is given by

$$\boxed{\mu = 2\, a\, m\, n\, \overline{C}\, \lambda}$$

The thermal conductivity can be expressed as

$$\boxed{K = k\, n\, \overline{C}\lambda}$$

The binary diffusion coefficient for species A into B can be expressed as

$$\boxed{D_{AB} = 2\, a\, \overline{C}\lambda}$$

Exercise Problems

4.1 Determine $(\partial S/\partial E)$ and the Lagrange multiplier β for a gaseous system at 400°C.

[Answer: 1.486×10^{-3} 1/K, 1.08×10^{20} $s^2/(m^2\ kg)$]

4.2 A vacuum chamber has to be designed for fabricating reflective coatings. Inside this chamber, a small sample of metal will be vaporized so that its atoms travel in straight lines (the effects of gravity are negligible during the brief time of

flight of the atoms) to a surface where they land to form a very thin film. The sample of metal is at a distance of 30 cm from the surface to which the metal atoms will adhere. How low must the pressure in the chamber be so that the metal atoms only rarely collide with air molecules before they land on the surface, if the temperature is 300 K?

[Answer: 19.41×10^{-3} Pa]

4.3 A room is 6.0 m × 5.0 m × 3.0 m. (a) If the air pressure in the room is 1.0 atm and the temperature is 300 K, find the number of moles of air in the room. (b) If the temperature increases by 5.0 K and the pressure remains constant, how many moles of air leave the room?

[Answer: (a) 3.66×10^3 mol, (b) 60 mol]

4.4 Calculate the density and the RMS velocity for hydrogen at 101 kPa and 300 K.

[Answer: 0.081 kg/m^3, 1934.24 m/s]

4.5 Determine the mean free path and collision frequency for air at sea level. Take the radius of air molecule as 2×10^{-10} m.

[Answer: 2.095×10^{-7} m, 2.19×10^9 1/s]

4.6 Find the molar volume (in liters) of an ideal gas at temperature 0°C and pressure 101,325 Pa.

[Answer: 22.41 L]

4.7 Calculate the number of air molecules in a room of volume 30 m^3 at 300 K and 1 atm pressure.

[Answer: 7.342×10^{26}]

4.8 Calculate the molecular mass of air, made up of nitrogen (N_2) (78.084%), oxygen (O_2) (20.946%), argon (Ar) (0.9340%), carbon dioxide (CO_2) (0.0387%), neon (Ne) (0.001818%), helium (He) (0.000524%), methane (CH_4) (0.000179%), and krypton (Kr) (0.000114%).

[Answer: 28.967 g/mol]

4.9 If the density ratio across the shock at the nose of a blunt-nosed body of nose radius 1 m is 12, determine the shock detachment distance.

[Answer: 59.17 mm]

4.10 Express the most probable macrostate for fermions as

$$N_j^* = \frac{g_j}{e^{\alpha} e^{\beta \epsilon_j'} + 1}$$

4.11 Find the temperature at which the RMS speed of a molecule is 350 m/s if (a) the gas is air and (b) the gas is hydrogen.

[Answer: (a) 142.3 K, (b) 9.9 K]

4.12 Consider a system with energy levels $\epsilon_0 = 0\ \text{cm}^{-1}$, $\epsilon_1 = 12\ \text{cm}^{-1}$ and $\epsilon_2 = 23\ \text{cm}^{-1}$. Determine numerical values of the partition function at the temperature corresponding to $kT = 10\ \text{cm}^{-1}$, when the system consists a double degenerate ground state, and four exited states, as shown in Figure 4.40.

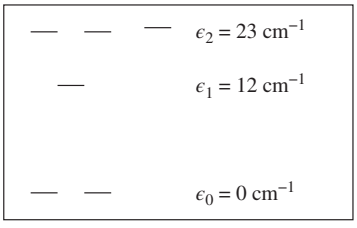

Figure 4.40 A system with three exited states.

[Answer: 2.602 units]

4.13 Calculate the number of microstates possible in the macrostate shown in Figure 4.2, using Fermi–Dirac statistics.
[Answer: 1800]

4.14 If the rotational energy content of 1 kg of nitrogen gas is 148.5 kJ, determine the temperature of the gas.
[Answer: 500.12 K]

4.15 Determine the translational energy content of a system containing 3 kg of oxygen gas at 35°C.
[Answer: 360.27 kJ]

4.16 If the root-mean-square velocity of air molecules in a system at 1.3 atm is 600 m/s, determine the specific volume of the gas.
[Answer: 0.911 m^3/kg]

4.17 If the number density of oxygen molecules in a system at 1.8 atm is $0.3185 \times 10^{20}\ 1/\text{m}^3$, find the temperature of the system.
[Answer: 414.95 K]

4.18 If the total kinetic energy of a system at 2.2 atm is $7.7 \times 10^6\ \text{m}^2/(\text{s}^2\ \text{mol})$, determine the temperature and the molar volume of the system.
[Answer: 617.43 K, 23.03 $\text{m}^3/(\text{kg mol})$]

4.19 A 5 L vessel contains 0.125 mol of an ideal gas at a pressure of 1.5 atm. What is the average translational kinetic energy of a single molecule?
[Answer: 1.51×10^{-20} J]

4.20 One mole of an ideal gas does 3000 J of work on its surroundings as it expands isothermally to a final pressure of 1 atm and volume of 25 L. Determine (a) the initial volume and (b) the temperature of the gas.
[Answer: (a) 7.652 L, (b) 304.68 K]

4.21 Find the limiting minimum value of shock detachment distance for perfect air stream past a blunt-nosed body of nose radius 56 mm.
[Answer: 5.92 mm]

4.22 Determine the specific heats ratio of nitrogen gas at 500 K.
[Answer: 1.4]

4.23 A blunt-nosed model is placed in a Mach 3 supersonic tunnel test section. If the settling chamber pressure and temperature of the tunnel are 10 atm and 315 K, respectively, calculate the pressure, temperature, and density at the nose of the model. Assume the flow to be one dimensional.
[Answer: 332.65 kPa, 315 K, 3.68 kg/m^3]

4.24 Air stream with a speed of 200 m/s and temperature 280 K is accelerated. If the temperature of the accelerated flow is 200 K, determine the speed.
[Answer: 448 m/s]

4.25 Determine the specific heat at constant volume, for sea level air, assuming it as a mixture of 78% of nitrogen, 21% of oxygen, and 0.3% of carbon dioxide, neglecting the contribution to the remaining species.
[Answer: 717.3 J/(kg K)]

References

[1] Rathakrishnan E., *Fundamentals of Engineering Thermodynamics*, 2nd ed. PHI Learning, New Delhi, India, 2005.
[2] Herzberg G., *Atomic Spectra and Atomic Structure*, Dover, New York, 1944.
[3] Herzberg G., *Molecular Spectra and Molecular Structure*, D. Van Nostrand, New York, 1963.
[4] Kennard E. H., *Kinetic Theory of Gases*, McGraw-Hill, New York, 1938.
[5] Hilsenrath J., and Klein M., "Tables of Thermodynamic Properties of Air in Chemical Equilibrium Including Second Virial Corrections from 1500 to 15000 K", Arnold Engineering Development Center Report No. AEDC-TR-65-68, 1965.
[6] Vincenti W. G., and Kruger C. H., *Introduction to Physical Gas Dynamics*, Krieger Publishing Company, 1975.
[7] Rathakrishnan E., *Applied Gas Dynamics*, John Wiley & Sons, Inc., 2010.
[8] Rathakrishnan E., *Gas Tables*, 3rd ed. Universities Press, Hyderabad, India, 2012.
[9] Hayes W. D., and Probstein R. F., *Hypersonic Flow Theory*, Academic Press, 1959.
[10] Anderson J. D., *Hypersonic and High Temperature Gas Dynamics*, McGraw-Hill, Inc., 1989.
[11] Bose T. K., *High Temperature Gas Dynamics*, Springer, 2004.
[12] Millikan R. C., and White D. R., "Systematics of vibrational relaxation", *J. Chem. Phys.*, Vol. 39, 1963, p. 3209.

5

Hypersonic Flows

5.1 Introduction

In the perfect gas dynamic theory, hypersonic flow is defined as the flow with Mach number greater than 5, where the change in flow Mach number is dictated by the change in the speed of sound. That is, in the hypersonic flow regime, the speed of sound is more dominant than the flow speed itself. But in problems such as the flow fields around blunt bodies begin to exhibit many of the characteristics of hypersonic flow when the Mach number is 4, or greater. By definition,

$$\boxed{M_\infty \equiv \frac{V_\infty}{a_\infty} \gg 1} \tag{5.1}$$

where M_∞ is the freestream Mach number, V_∞ is the flow speed, and a_∞ is the speed of sound. That is, the Mach number is greatly larger than unity ($M_\infty \gg 1$) is the basic assumption for all hypersonic flow theories. Thus, the internal thermodynamic energy of the freestream fluid particles is small compared to the kinetic energy of the freestream for hypersonic flows. In flight applications, this results because the volume of the fluid particles is relatively large. The limiting case, where M_∞ approaches infinity because the freestream velocity approaches infinity while the freestream thermodynamic state remains fixed, produces extremely high temperatures in the shock layer.

The high temperatures associated with hypersonic flight are difficult to match in ground-test facilities, such as hypersonic wind tunnel and shock tunnel. Therefore, in wind tunnel applications, hypersonic Mach numbers are achieved through relatively low speeds of sound. Thus, in the wind tunnel, the test-section Mach number, M_∞, approaches infinity because the speed of sound goes to *zero* while the freestream velocity is held fixed. As a result, the fluid temperatures in such wind tunnels remains below the levels that would damage the wind tunnel model.

High Enthalpy Gas Dynamics, First Edition. Ethirajan Rathakrishnan.

www.wiley.com/go/rathakrishnan

Another assumption common to hypersonic flow is that the ratio of the freestream density to the density just behind a shock is extremely small, that is,

$$\boxed{\epsilon \equiv \frac{\rho_\infty}{\rho_2} \ll 1} \tag{5.2}$$

where ρ_∞ is the freestream density and ρ_2 is the density behind the shock. Equation (5.2) is known as the *small-density-ratio* assumption. Thus, this assumption relates primarily to the properties of the gas downstream of the shock wave. Recall that for a perfect gas [1],

$$\epsilon \equiv \frac{\rho_1}{\rho_2} = \frac{\gamma - 1}{\gamma + 1} \tag{5.3}$$

for a normal shock wave as $M_\infty \to \infty$. Thus, ϵ is 1/6 for perfect gases with specific heats ratio $\gamma = 1.4$. It is important to note that a typical hypersonic wind tunnel operates at conditions where the test gas can be treated as perfect gas. However, during the reentry flights, the density ratio, ρ_∞/ρ_2, can approach as low as 1/20. Thus, the density ratio simulation in those wind tunnels where the airflow behaves as a perfect gas does not match the flight values. This will have a significant effect on the shock stand-off distance, as well as other flow parameters. To generate low-density ratios for wind tunnel simulations, gases other than air, such as hexafluoroethane (C_2F_6) for which $\gamma = 1.1$ or tetrafluoromethane (CF_4), also known as *carbon tetrafluoride*, for which $\gamma = 1.2$, may be used as the test gas.

5.2 Newtonian Flow Model

When the density ratio across the shock wave, illustrated in Figure 5.1, becomes small, the shock layer becomes very thin. For this kind of flow situation, we can assume that the speed and direction of the gas particles in the freestream remain unchanged until they strike the solid surface exposed to the flow. This flow model is termed *Newtonian flow model* because it is similar in character to that described by Newton in the seventeenth century. For Newtonian flow model, the normal component of momentum of the impinging fluid particle is wiped out, whereas the tangential component of momentum is conserved.

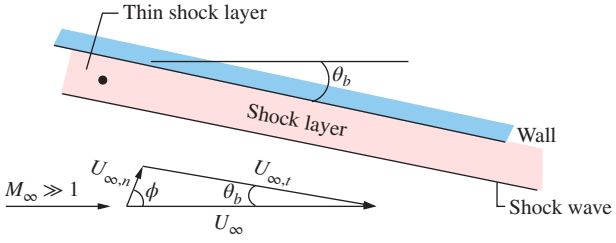

Figure 5.1 Illustration of Newtonian flow model.

The integral form of the momentum equation for a constant-area streamtube normal to the surface is

$$p_\infty + \rho_\infty V_{\infty,n}^2 = p_\infty + \rho_\infty [V_\infty \sin\ \theta_b]^2 = p_w \tag{5.4}$$

where p_∞, ρ_∞, and V_∞, respectively, are the pressure, density, and velocity of the freestream flow and p_w is the pressure at the wall surface, shown in Figure 5.1.

The pressure coefficient at the wall surface is given by

$$C_p = \frac{p_w - p_\infty}{\frac{1}{2}\rho_\infty V_\infty^2}$$

From Equation (5.4), we have the pressure coefficient as

$$C_p = 2 \sin^2\theta_b = 2 \cos^2\phi \tag{5.5}$$

This equation for the pressure coefficient is based on the Newtonian flow model, where 2 represents the pressure coefficient at the stagnation point, because $\theta_b = 90°$ at the stagnation point.

The pressure coefficient as a function of freestream Mach number, M_∞, for deflection angle, θ_b, of 10° and 30° for wedge and cone are compared with C_p of the Newtonian model (Equation (5.5)) in Figure 5.2.

As seen from Equation (5.5), the pressure coefficient for the Newtonian model is independent of Mach number and depends only on the angle between the freestream flow direction and the surface inclination. It is seen in Figure 5.2 that for flow past

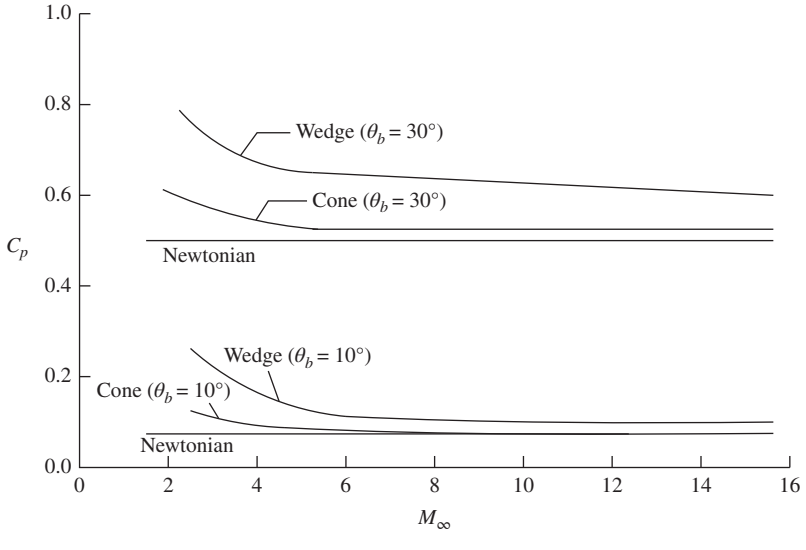

Figure 5.2 Pressure coefficient for air flow with $\gamma = 1.4$, past a wedge, a cone, and for the Newtonian flow model.

cone, the pressure coefficients for both 10° and 30° cone angles achieve Mach number independence once the freestream Mach number, M_∞, exceeds 5. But for the wedge, slightly higher freestream Mach numbers are required before the pressure coefficient exhibits Mach number independence.

It is seen in Figure 5.2 that for both deflection angles, there is relatively close correlation between the pressure coefficients for sharp cone and Newtonian model. For a sharp cone of vertex angle 20° in a Mach 10 stream of perfect air, the shock wave angle is 12.5°. If the cone angle is 60°, the shock wave angle is 34° [2]. Thus, the inviscid shock layer is relatively thin for a sharp cone in a hypersonic stream. As the Newtonian flow model assumes that the shock layer is very thin, the agreement between the pressure coefficient for these two flow models is expected. However, for a wedge placed in a Mach 10 stream of perfect air, the shock wave angle is 14.43° for wedge angle 20° and 38.52° for wedge angle 30°. Because the shock wave angle is higher at a higher angle of inclination, the pressure on the wedge surface is considerably higher than the pressure given by the Newtonian flow model, with the difference being greater for the larger deflection angle.

The Newtonian flow model and other theories for the shock layers related to the Newtonian approximation are based on the small-density-ratio approximation.

5.3 Mach Number Independence Principle

For slender configurations, such as sharp cones and wedges, the strong shock assumption is

$$\boxed{M_\infty \sin\ \theta_b \gg 1} \tag{5.6}$$

where M_∞ is the freestream Mach number and θ_b is the semi-angle of the nose. The concept termed the *Mach number independence principle* depends on this assumption.

The Mach number independence principle was derived for inviscid flow by Oswatitsh. The pressure forces are much larger than the viscous forces for blunt bodies or slender bodies at large angles of incidence when the Reynolds number exceeds 10^5; therefore, one would expect the Mach number independence principle to hold at these conditions.

Koppenwallner [3] demonstrates that there is a significant increase in the total drag coefficient for right circular cylinder because of the friction drag when the Knudsen number, defined as the ratio of mean-free path length to a characteristic dimension in the flow field, is greater than 0.01. Using the Reynolds number based on the flow conditions behind a normal shock wave as the characteristic parameter,

$$\boxed{Re_2 = \frac{\rho_2 V_2 d}{\mu_2}} \tag{5.7}$$

the friction drag for Re_2 is given by

$$\boxed{C_{D,f} = \frac{5.3}{(Re)^{1.18}}} \tag{5.8}$$

where subscript 2 refers to the condition behind the shock.

5.4 Hypersonic Flow Characteristics

The characteristics of hypersonic flow can be computed using the fluid-dynamic phenomena when the configuration geometry, the attitude, or orientation of the geometry to the freestream flow and the altitude at which the vehicle flies or the test conditions of a wind tunnel simulation are known. When computer-generated flow field solutions are used to define the aerothermodynamic environment, matching the fluid-dynamic similarity parameters becomes a secondary issue. However, it is essential to incorporate *critical* fluid-dynamic phenomena into the computational flow model. Now it is essential to note that what is a typically important fluid-dynamic phenomenon for one application may be irrelevant to another. For example, the drag coefficient for a cylinder whose axis is perpendicular to a hypersonic freestream will be essentially constant, independent of Mach number and Reynolds number, provided that the Mach number is sufficiently large so that the flow is hypersonic and the Reynolds number is sufficiently large so that the boundary layer is thin. For blunt bodies, where skin friction is a small fraction of the total drag, reasonable estimates of the force coefficient could be obtained from flow fields computed using flow models based on the Euler equation, that is, neglecting viscous terms in the equations of motion. However, in the rarefied (low-density) flows encountered at higher altitudes, viscous/inviscid interactions become important and the effects of viscosity can no longer be neglected.

5.4.1 Noncontinuum Considerations

At very high altitudes, the air becomes highly rarefied that the motion of the individual particles becomes important. Rarefied gas dynamics concerned with those phenomena related to the molecular description of a gas flow that occurs at sufficiently low density should be used to solve the flow field. The dimensionless parameter used to describe the regimes of rarefied gas dynamics is the Knudsen number, Kn, defined as the ratio of the mean-free path length, Λ, to some characteristic length, L, in the flow field. The criterion for free molecular flow is that the mean-free path becomes so large leading to the Knudsen number to become 10 or more. On the basis of Kn, the flow field is classified as follows.

- Continuum flow: $Kn < 0.01$.
- Slip flow: $0.01 < Kn < 0.1$.

- Transition flow: $0.1 < Kn < 1.0$.
- Free molecule flow: $Kn > 10$.

The continuum flow regime is termed the *vorticity interaction regime*. For a blunt-nosed body in a hypersonic (or supersonic) flow, there is a bow shock wave ahead of the nose. The bow shock generates vorticity in the inviscid flow outside of the boundary layer. The vorticity interaction regime identifies a condition when conventional boundary layer theory can no longer be used, because the vorticity in the shock layer external to the viscous region becomes comparable to that within the boundary layer.

The limits of applicability for the continuum flow theory and a discrete particle model are illustrated in Figure 5.3.

Thus, there is a portion of the flight environment when the flow can no longer be regarded as continuum and should be treated as free molecular flow for altitudes above about 145–160 km for a 300 mm radius sphere whose wall temperature is equal to the freestream temperature.

Flow field solutions for the nose region of the space shuttle Orbiter by Moss and Bird [4] indicate that both the direct simulation Monte Carlo (DSMC) and the viscous shock-layer (VSL) methods provide results that agree closely with the flight measurements at 92.35 km altitude.

From the above discussions, it is evident that there is no single, definite criterion for an upper-limit altitude above which the continuum model for the flow is no longer valid. Furthermore, because *Kn* is a characteristic dimensionless parameter for rarefied flows, these limits depends on vehicle size. That is, if the nose radius of the vehicle were increased by a factor of, say, 10 the corresponding density would be decreased by a factor of 10.

5.4.2 Stagnation Region

The air particles in the shock layer of a hypersonic reentry vehicle undergo vibrational excitation, dissociation, and even ionization. These chemical phenomena absorb energy, limiting the temperature increase as the kinetic energy of the hypervelocity

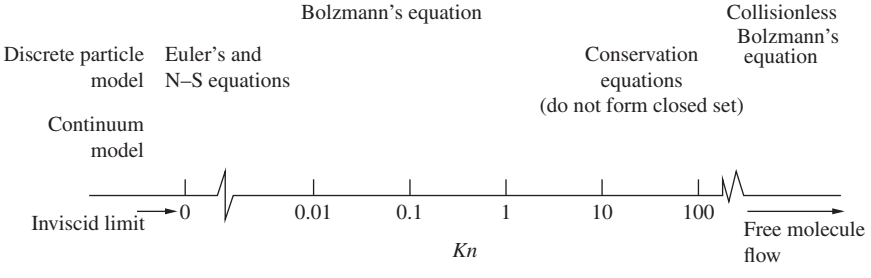

Figure 5.3 Classification of flow regimes.

particles, crossing the bow shock wave, is converted to thermal energy. At low altitudes, where the freestream density is sufficiently high, these chemical phenomenon tend to reach equilibrium. At higher altitudes, where the freestream density is relatively low, there are not sufficient collisions for the gas molecules to reach an equilibrium state. Therefore, the concentration of individual species and the energy contained in the different internal modes must be calculated by integrating the equations governing the phenomena.

Examine the flow near the stagnation point of a blunt-nosed body in a hypersonic stream illustrated in Figure 5.4. The flow passes through a normal shock portion of the detached shock and reaches state 2 and then decelerates isentropically to the stagnation state 02, which constitutes the outer-edge condition for the thermal boundary layer at the stagnation point. The streamline from the shock wave to the stagnation point may be curved for nonaxisymmetric flow fields.

The governing equations for steady, one-dimensional, inviscid, adiabatic flow in a constant-area streamtube are used to compute the conditions across a normal shock wave. The equations are the following.

Mass conservation or continuity equation:

$$\rho_1 V_1 = \rho_2 V_2 \tag{5.9}$$

Momentum equation:

$$p_1 + \rho_1 V_1^2 = p_2 + \rho_2 V_2^2 \tag{5.10}$$

Energy equation:

$$h_1 + \frac{V_1^2}{2} = h_2 + \frac{V_2^2}{2} = h_0 \tag{5.11}$$

where h_0 is the total or stagnation enthalpy of the flow.

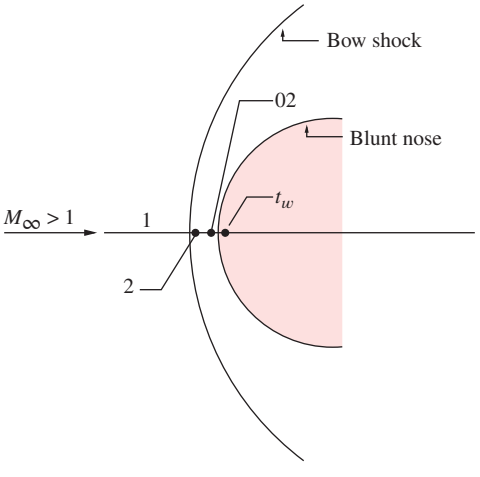

Figure 5.4 Flow past a blunt-nosed body.

Assuming the gas as thermally perfect, we have

$$p = \rho RT = \rho \frac{R_u}{M_o} T \tag{5.12}$$

where R_u is the universal gas constant and M_o is the molecular weight of the gas in the perfect (or reference) state. Introducing the assumption that the gas is calorically perfect, we have that the specific heat c_p is constant and

$$h = c_p T \tag{5.13}$$

If the gas is both thermally and calorically perfect, the ratio of values of the flow properties across the shock wave can be written as a unique function of the freestream Mach number M_1 (the Mach number ahead of the shock) and the specific heats ratio γ. These relations (the detailed theory and derivation of these are presented in Reference 1) are

$$\frac{p_2}{p_1} = 1 + \frac{2\gamma}{\gamma + 1}(M_1^2 - 1) \tag{5.14}$$

$$\frac{\rho_2}{\rho_1} = \frac{(\gamma + 1)M_1^2}{2 + (\gamma - 1)M_1^2} \tag{5.15}$$

$$\frac{T_2}{T_1} = \frac{h_2}{h_1} = \frac{a_2^2}{a_1^2} = 1 + \frac{2(\gamma - 1)}{(\gamma + 1)^2} \frac{(\gamma M_1^2 + 1)}{M_1^2}(M_1^2 - 1) \tag{5.16}$$

$$\frac{p_{02}}{p_{01}} = \left(1 + \frac{2\gamma}{\gamma + 1}(M_1^2 - 1)\right)^{-1/(\gamma-1)} \left\{ \frac{(\gamma + 1)M_1^2}{(\gamma - 1)M_1^2 + 2} \right\}^{\gamma/(\gamma-1)} \tag{5.17}$$

If we assume that the flow decelerates isentropically from the state 2 (just behind the normal shock portion of the detached shock) to the stagnation point 02 outside of the thermal boundary layer, combining Equations (5.14) and (5.17), we can express

$$\frac{p_1}{p_{02}} = \frac{\left(\frac{2\gamma}{\gamma + 1} M_1^2 - \frac{\gamma - 1}{\gamma + 1}\right)^{1/(\gamma-1)}}{\left(\frac{\gamma + 1}{2} M_1^2\right)^{\gamma/(\gamma-1)}} \tag{5.18}$$

This is known as the *Rayleigh supersonic pitot formula*.

For adiabatic flow across the shock, $T_{01} = T_{02}$, where T_{01} and T_{02} are the stagnation temperatures. Thus from isentropic relation,

$$\frac{T_{02}}{T_1} = \frac{T_{01}}{T_1} = \left(1 + \frac{\gamma - 1}{2} M_1^2\right) \tag{5.19}$$

It is essential to note that it is generally true that the stagnation enthalpy is constant across a normal shock wave in an adiabatic flow, but the stagnation temperature is

constant across a normal shock wave only for an adiabatic flow of a perfect gas. One more aspect to be noted is that Equations (5.14)–(5.19) relate the flow properties ahead of and behind (that is, the flow properties across) the normal shock wave.

It is seen that the properties ratios in Equations (5.14)–(5.19) depends only on the specific heats ratio, γ, and freestream Mach number, M_1 (that is, M_∞), and do not depend on the altitude.

In reality, for hypersonic flight, the temperature of the gas molecules that pass through the detached shock wave increases to very high levels, leading to the excitation of vibrational and chemical energy modes. This excitation lowers the specific heats ratio of the gas below the freestream value, if it is assumed that equilibrium exits and that dissociation is not driven to completion. A large amount of energy that would have gone into increasing the static temperature behind the bow shock wave for a perfect gas is used instead to excite the vibrational energy levels or dissociate the gas molecules. At sea level, at about 900 m/s, the vibrational energy of the air molecules begin to become important. Oxygen dissociation begins when the freestream velocity is in the range from 1800 to 2400 m/s. Nitrogen dissociation occurs when the freestream velocity exceeds 4500 m/s. When the freestream speed exceeds 9000 m/s, atoms get ionized. Note that the dissociation and ionization reactions are pressure dependent because each molecule yields two product particles, and such reactions are inhibited by high pressure. Therefore, high temperature and, consequently, higher velocity are required to produce the reaction at sea level than at high altitude where the pressure is much lower than the sea level pressure.

To account for the departure from the thermally perfect equation of state, $p = \rho RT$, because of the chemical reaction in air, the compressibility factor z is introduced. The compressibility factor is the ratio of the molecular weight of the undissociated air to the mean molecular weight at the conditions of interest. Thus

$$z = \frac{M_o}{\overline{M}} \tag{5.20}$$

where $\overline{M}$ is the mean molecular weight of the gas mixture at the conditions of interest. Accounting for the change in the gas composition, the equation of state becomes

$$p = \rho \frac{R_u}{\overline{M}} T = \rho \frac{M_o}{\overline{M}} \frac{R_u}{M_o} T = \rho z RT \tag{5.21}$$

Hansen and Heims [5] reported that the ionization reactions occur at very nearly the same energy changes so that they may be grouped together as a single reaction, for the purpose of approximation.

At this stage, it is essential to note that the compressibility factor z is not influenced by the vibrational excitation and, therefore, $z = 1$ until the dissociation of oxygen begins. As air contains about 20% of oxygen, $z \to 1.2$ as the oxygen dissociation approaches completion. Similarly, $z \to 2.0$ as the nitrogen dissociation approaches completion and all the molecules have dissociated into atoms. The ionization process produces further increase in z.

As energy is absorbed by the gas molecules entering the shock layer, the conservation laws and their thermophysics induce certain changes in the forebody flow (that is, the flow just ahead of the nose). The static temperature, the speed of sound, and the velocity in the shock layer are less for the equilibrium, real gas flow than for a perfect gas flow. The static pressure for air in thermodynamic equilibrium is slightly larger than the perfect gas value. The density is increased considerably, and as a result, the shock layer thickness is reduced significantly.

Computation of properties changes across a normal shock wave, using thermochemical equilibrium air properties [6] shows that for temperatures of 1600 K and below the air composition does not change in the shock-compression process. Therefore, for temperatures below 1600 K, the gas can be treated as thermally perfect. Furthermore, for temperatures below 800 K, it can be seen that the air can be treated as perfect with constant specific heats ratio of 1.4.

The governing Equations (5.9)–(5.11) are general and not just restricted to perfect gases alone and can be applied to high-temperature hypersonic flows. There are four unknowns, namely, p_2, ρ_2, h_2, and u_2 involved in the three Equations (5.9)–(5.11), therefore, to solve for these four variables, at least one more equation is necessary.

5.4.3 Stagnation Pressure behind a Normal Shock Wave

Variation of stagnation pressure downstream of a normal shock in reacting air in thermodynamic equilibrium and perfect air (with $\gamma = 1.4$) in the Mach number, M_∞, range from 4 to 24 at an altitude of 45,000 m, is presented in terms of dimensionless ratio p_{02}/p_∞ and the pressure coefficient at the stagnation point, C_{p02}, in Figures 5.5 and 5.6, respectively.

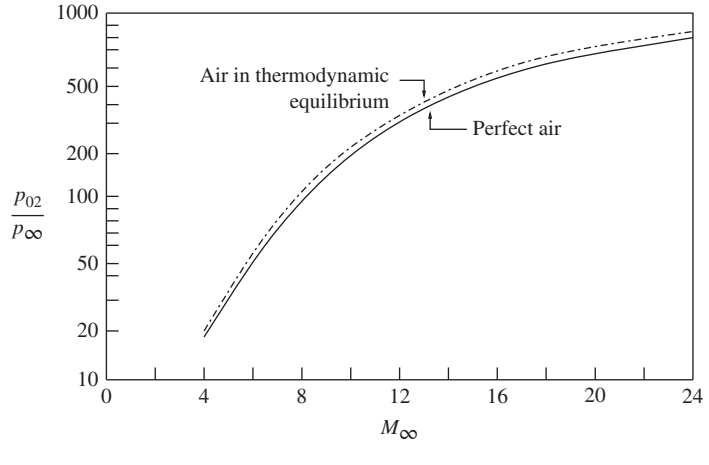

Figure 5.5 Variation of stagnation pressure downstream of a normal shock with freestream Mach number.

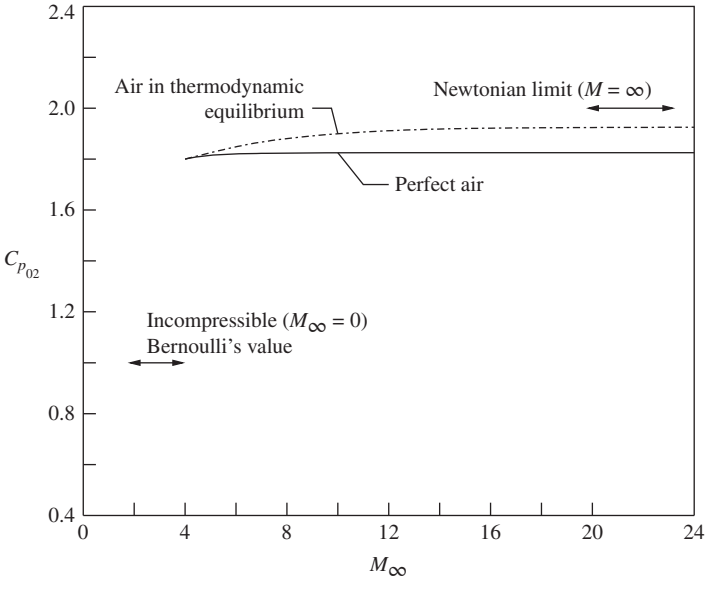

Figure 5.6 Stagnation pressure coefficient (behind a normal shock) with freestream Mach number.

From Figures 5.5, it is evident that the stagnation pressure computed for air in thermodynamic equilibrium is slightly larger than the perfect gas value. The stagnation pressure coefficient at Mach 4 is about 1.8 for both perfect air and air in thermodynamic equilibrium as seen from Figure 5.6. There is appreciable difference between the $C_{p_{02}}$ for perfect air and air in thermodynamic equilibrium, for Mach number greater than 4.

A two-dimensional hypersonic flow field that is ionized and in thermochemical nonequilibrium was solved numerically by Candler and MacCormack [7]. Comparing the surface pressures for a seven-species reacting gas flow model with those for a perfect gas flow model for $M_\infty = 25.9$ at 71 km altitude, they found that the surface is almost identical for each case. But the stagnation point pressure computed using the reacting gas flow model was slightly higher than the perfect gas value.

Note that for hypersonic flow across the normal shock wave portion of a bow shock,

$$p_1 \ll \rho_1 V_1^2 \quad \text{and} \quad p_2 \ll \rho_2 V_2^2$$

where subscripts 1 and 2, respectively, refer to the states ahead of and behind the shock wave. As a result, we have

$$p_2 \approx p_{02} \approx \rho_1 V_1^2$$

This can be expressed, by multiplying and dividing the terms by 2, as

$$p_2 \approx p_{02} \approx 2 \times \frac{1}{2} \rho_1 V_1^2$$

or

$$p_2 \approx p_{02} \approx 2q_1$$

Thus, the stagnation point pressure for hypersonic flow is independent of the flow chemistry and approximately twice the dynamic pressure, q_1, ahead of the shock.

At this stage, it is essential to note that this relative insensitivity of the pressure applies only to pressure downstream of the normal portion of the bow shock wave near the stagnation point. For locations away from the stagnation point, significant difference may exist. Although relatively simple techniques can provide first-order estimates of the pressures away from the stagnation point, there are phenomena that introduce large uncertainties in the pressure. The pressure distributions for flows involving shock/shock interactions, shock/boundary layer interactions, and flow separation, such as base flow, are very sensitive to a number of parameters.

The variation of the stagnation temperature behind a shock as a function of freestream Mach number, M_∞, at an altitude of 45 km, for perfect air and air at thermodynamic equilibrium are shown in Figure 5.7. It is seen that the energy absorbed by the dissociation process causes the reacting gas equilibrium temperature to lie significantly lower than the perfect gas temperature. This difference increases with increase in freestream Mach number, M_∞.

The specific heat correlation as a function of pressure and temperature presented by Hansen [8] may be used to identify the condition at which the dissociation of oxygen and nitrogen affects the properties. It is found that at all pressures, the dissociation of oxygen is essentially complete before the dissociation of nitrogen begins.

For a perfect gas, as we know, the changes in flow properties across a normal shock wave are functions of Mach number, M_1, ahead of the shock and the ratio of specific

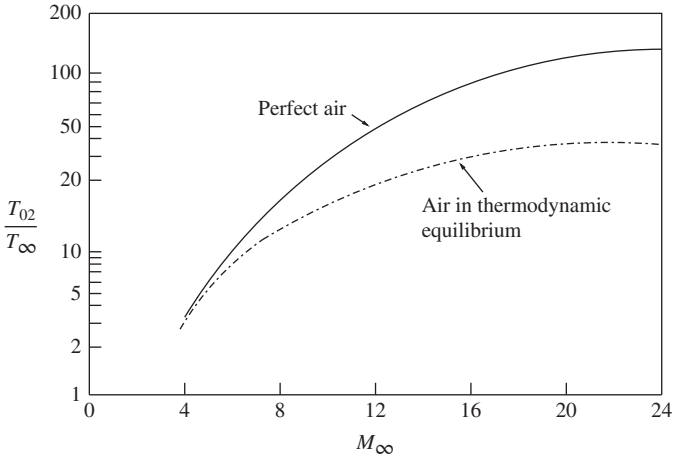

Figure 5.7 Variation of stagnation temperature (T_{02}/T_∞) downstream of a normal shock wave.

heats. That is,

$$\frac{p_2}{p_1} = f(M_1, \gamma)$$

But for a reacting gas in chemical equilibrium, three parameters are necessary to obtain the ratio of the properties across a normal shock, that is,

$$\frac{p_2}{p_1} = f(V_1, p_1, T_1)$$

The real gas effects have a significant effect on the temperature downstream of the shock wave, which will in turn have a significant impact on the density downstream of the shock wave.

5.5 Governing Equations

To solve the flow field between the bow shock wave and the surface of a vehicle flying at hypersonic speed, it is necessary to develop the governing equations of motion and the appropriate flow models. Here, the flow is assumed to be continuum. Let us consider the flow past a blunt-nosed body moving at a hypersonic speed, shown in Figure 5.8. Note that the entropy change across a shock wave depends on the freestream Mach number and the shock inclination angle. Thus, the entropy change across the bow shock wave depends on where the flow crosses the shock wave. The flow in the inviscid portion of the shock layer, that is, the flow between the shock wave and the boundary layer, is rotational. The inviscid flow in region 2 is subsonic. The flow downstream of that portion of the shock wave where the shock angle is relatively low, rendering the shock as weak as in region 3, is supersonic, in accordance with shock theory that the flow past a weak shock will be supersonic, with Mach number less than the upstream value.

Examine the flow field over the body. The flow process could be a chemical reaction or the exchange of energy among the various modes, for example, translational, rotational, vibrational, and electronic energies, of the atom and molecule. The transfer of energy between the various energy modes is accomplished through the collisions between the molecules and atoms. At high altitudes, where the air density is low,

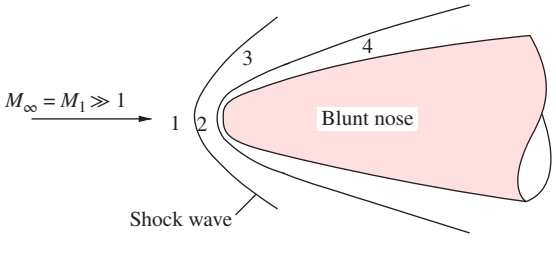

Figure 5.8 Hypersonic flow past a blunt-nosed body. (1) Free stream, (2) Subsonic, (3) Supersonic, (4) Boundary layer.

chemical states need not necessarily reach equilibrium. Nonequilibrium processes occur in a flow when the time required for a process to accommodate itself to the local conditions within a particular region is of the same order as the time it takes for the air particles to cross that region. If the time required for accommodation is longer than the transit time, the chemical composition remains "frozen" as the flow moves around the vehicle.

The shape and the stand-off distance of the bow shock wave are sensitive functions of the chemical state. The shape of the shock wave is affected by the chemical reaction, because the chemical reaction affects the temperature and, therefore, the density. Furthermore, the isentropic exponent of the gas process changes with reaction. This change in the isentropic exponent affects the pressure distribution over the vehicle. The magnitude of the pressure difference at a specific location, caused by this change in isentropic exponent, may be small, but the integrated effect on the pitching moment and on the stability of the vehicle may be significant.

5.5.1 Equilibrium Flows

At sufficiently high density, there are significant number of collisions between particles to allow the equilibrium of energy transfer between the various modes, the flow is in thermal equilibrium. For an equilibrium flow, any two thermodynamic properties, for example, p and T, can be used to uniquely define the state. As a result, the remaining thermodynamic properties and the composition of the gas can be determined.

5.5.2 Nonequilibrium Flows

Nonequilibrium state such as dissociation and recombination may result when the fluid particles pass through a strong shock wave and, when undergo a rapid expansion. In both these cases, the nonequilibrium occurs due to the lack of sufficient collisions to achieve equilibrium during the characteristic time of the fluid motion. If the rate at which fluid particles move through the flow field is greater than the chemical and thermodynamic reaction rates, the energy in the internal degrees of freedom, that is, the energy that would be released if the gas were chemically reacting, is *frozen* within the gas. Rakich *et al.* [9] reported that nonequilibrium effects can occur above an altitude of 40 km and at velocity greater than 4 km/s.

A dynamic behavior of the flow is significantly affected by the chemical reactions. Classical translational temperature is defined in terms of the average translational kinetic energy per particle. This temperature is classically associated with the *system temperature* in the one-temperature model. Park [10] found that the use of the one-temperature model in the computation of a nonequilibrium reacting flow leads to a substantial overestimation of the rate of equilibration.

Because of the slow equilibration rate of vibrational energy, multiple-temperature models are used to describe a flow that is out of equilibrium.

As per the three-temperature model recommended by Lee [11], "rotational temperature tends to equilibrate very fast with translational temperature and, hence, can be considered to be equal to heavy-particle translational temperature T. Electron temperature T_e deviates from heavy-particle translational temperature T because of the slow rate of energy transfer between electrons and heavy particles caused by the large mass disparity between them. Vibrational temperature T_v departs from both electron temperature T_e and heavy-particle translational temperature T because of the slow equilibrium of vibrational energy with electron and translational energies."

But Park [10] notes that the three-temperature chemical-kinetic model is complex and requires many chemical rate parameters. As a compromise between the three-temperature model and the conventional one-temperature model, Park proposed a two-temperature chemical-kinetic model. One temperature, T, is used to characterize the translational energy of both atoms and molecules and the rotational energy of the molecules. A second temperature, T_v, is used to characterize the vibrational energy of the molecules, the translational energy of the electrons, and the electronic excitation energy of the atoms and molecules. As per Park model [12] "without accounting for the nonequilibrium vibrational temperature, there is little chance that a computational fluid dynamics (CFD) calculation can reproduce the experimentally observed phenomena. In a one-temperature model, the temperature at the first node point behind a shock wave is very high, and so the chemical reaction rates becomes very large. In a two-temperature model, the vibrational temperature is very low behind the shock."

When a multi-temperature model is used, an independent conservation equation must be written for each part of energy characterized by that temperature.

5.5.3 Thermal, Chemical, and Global Equilibrium Conditions

A mixture of gases at a point is in local thermal equilibrium when the internal energies of each species form the Boltzmann distribution for the heavy-particle translational temperature T across each of their energy spectra. However, when the distribution of vibrational energies does not fit the Boltzmann distribution for temperature T, thermal nonequilibrium effects are present at that point. For the two-temperature model, the distribution of vibrational energies still forms the Boltzmann distribution but at a different temperature T_v. Thermal equilibrium exits when $T = T_v$.

A mixture of gases at a point is in local chemical equilibrium when the concentration of chemical species at that point are a function of the local pressure and the local temperature alone. Chemical equilibrium occurs when the chemical reaction rates are significantly faster than the time scales of the local fluid motion, so that the species conservation equations reduce to a balance between the production and destruction of the species because of the chemical reactions. If the effects of conservation and diffusion affect local species concentrations, the flow is in chemical nonequilibrium.

If the characteristic time scales for the fluid motion, the vibration relaxation process, and the chemical reactions are denoted by t_f, t_v, and t_c, respectively, then the

thermal equilibrium would prevail if $t_v \ll t_f$, everywhere in the mixture. For chemical equilibrium, $t_c \ll t_f$, everywhere in the mixture.

5.6 Dependent Variables

For a chemically reacting flow, the solution aims at determining the composition of the gas. For equilibrium process, once any two thermodynamic properties that are used as dependent variables have been determined, the equilibrium composition can be determined. But that is not the case for nonequilibrium process. For nonequilibrium flows, the mass density or number density for each of the species must be determined.

In the formulations of nonequilibrium hypersonic flows, the number of chemical species varies from four, that is, N_2, O_2, N, and O, which allows air to be approximately modeled by two species: molecules and atoms, to electrons, that is, N_2, O_2, N, O, N^+, O^+, N_2^+, O_2^+, NO^+, and e^-, which is used to approximate high-temperature air (for temperatures greater than 9000 K).

For mass fraction, C_i of species i is defined as

$$C_i = \frac{\rho_i}{\rho} = \frac{\rho_i}{\sum \rho_i} \tag{5.22}$$

where ρ is the overall mass density given by

$$\rho = \sum_{i=1}^{N} \rho_i \tag{5.23}$$

The expression for the density of the mixture can be expressed as

$$\rho_N = \rho - \sum_{i=1}^{N} \rho_i$$

or

$$C_N = 1 - \sum_{i=1}^{N} C_i$$

This approach allows a strong coupling, because ρ is directly a dependent variable evaluated from the governing conservation equations.

Summing the mass-production rates (per unit volume) over all of the N species, we obtain

$$\sum_{i=1}^{N} \dot{w} = 0 \tag{5.24}$$

The chemical source terms are determined from reactions that occur between components of the gas.

5.7 Transport Properties

For applying the equations of motion for a given application, it is essential to develop appropriate expressions for the transport coefficients that appear in the mass, momentum, and energy flux terms in these equations. Gradients of physical properties in the flow field cause a molecular transport that is directly proportional to the gradient but in the opposite direction. The momentum transport in the flow is proportional to the temperature gradient. In self-diffusion, the transport of molecules is proportional to the concentration gradient and presented by the mass diffusion coefficient. Thus the diffusion coefficient, viscosity coefficient, and thermal conductivity are known as *transport properties*.

The transport of mass, momentum, and energy are due to the collision of fluid particles in the flow field. Therefore, the theoretical prediction of the transport properties requires a knowledge of the energy potential that describes the interaction between the various colliding particles. Thus, in order to calculate the transport coefficients, once the relative populations of the constituents have been described, one must develop models that describe the collision cross section and the dynamics of the collisions between the particles that make up the flow field.

5.7.1 Viscosity Coefficient

Using the model describing the molecules physically as a rigid, impenetrable sphere surrounded by an inverse-power attractive force, Sutherland developed the following empirical relation to calculate the coefficient of viscosity:

$$\boxed{\mu = 1.46 \times 10^{-6} \left(\frac{T^{3/2}}{T + 111} \right)} \tag{5.25}$$

where T is the temperature in kelvin and the units of μ are in kg/(m s). This model is qualitatively correct for fluids in which the molecules attract one another when they are far apart and exert strong repulsive forces upon one another when they are close to each other.

It is found that Equation (5.25) closely represent the variation of μ with temperature for air over a fairly wide range of temperature [13]. However, the success of Sutherland's equation representing the variation of μ with T for several gases does not establish the validity of Sutherland's molecular model for those gases. In other words, in general, it is not adequate to represent the core of a molecule as a rigid sphere or to take molecular attraction into account to a first order only. The great rapidity of the exponential increase of μ with T, as compared to that of nonattractive rigid spheres, has to be explained as due partly to the "softness" of the repulsive field at small distances and partly to attractive forces that have more than a first-order

effect. Therefore, the Sutherland relation can be taken only as a simple interpolation formula over restricted range of temperature.

The Lennard–Jones model for the potential energy of an interaction, which takes into account both the softness of the molecules and their mutual attraction at large distances, has been used by Svehla [14] to calculate the viscosity and thermal conductivity of gases at high temperatures. It is found that there are significant differences between the values of viscosity based on these two models.

For temperatures below 3000 K, the viscosity of air is independent of pressure. The transport properties of air at high temperatures should take into account the collision cross section for atom/atom and atom/molecule collisions.

5.7.2 *Thermal Conduction*

The heat flux vector appearing in the energy equation includes contribution resulting from transport of energy because of heat conduction, the direct transport of enthalpy (sensible and formation) by species whose velocity V_i differs from the bulk (mass-averaged) velocity, the energy transferred by gas radiation, and higher-order effects.

The thermal conduction in terms of temperature can be expressed as [8]

$$\boxed{k = 1.993 \times 10^{-5} \frac{T^{3/2}}{T + 112}} \tag{5.26}$$

where T is the temperature in kelvin and the thermal conductivity k is in W/(cm K).

5.7.3 *Diffusion Coefficient*

In a multicomponent flow in which there are concentration gradients, the net mass flux of species i is the sum of the fraction of the mass transported by the overall fluid motion and that transported by diffusion. The diffusional velocity of a particular species is due to molecular diffusion, pressure gradients, and thermal diffusion. The effect because of thermal diffusion is a second-order collisional transport effect that moves lighter molecules to hotter regions of the gas.

The principal contributor to the diffusional transport is modeled in terms of the concentration gradients for most applications. According to Fick's law of diffusion,

$$C_i V_i = -D_i \nabla C_i \tag{5.27}$$

where C_i and V_i, respectively, are the mass fraction and velocity of the ith species. By Equation (5.22),

$$C_i = \frac{\rho_i}{\rho} = \frac{\rho_i}{\sum \rho_i}$$

Equation (5.27) can be expressed as

$$\rho_i V_i = -\rho D_i \nabla C_i \tag{5.28}$$

For mass conservation,

$$\sum_{i=1}^{N} C_i V_i = 0$$

At this stage, it should be noted that the Fick law violates the following realistic physical aspects:

- Chemical potential gradients, not concentration gradients, drive diffusion.
- When C_i goes to zero, diffusional velocities tend to infinity, according to Equation (5.27).

However, a diffusion coefficient can be a useful approximation in modeling the flow.

In practical applications, a multicomponent diffusion coefficient D_{ij} is calculated where collisions occur simultaneously among all species. Values for D_{ij} are usually found from binary collision theory, that is, considering as many binary mixtures as there are gas pairs in the mixture. The use of D_{ij} is an approximation, which is cost justifiable because of its convenience. Bartlett *et al.* [15] suggest an approximation of the form

$$D_{ij} = \frac{\overline{D}}{F_i F_j} \tag{5.29a}$$

where

$$F_i = \left(\frac{m_i}{26}\right)^{0.461} \tag{5.29b}$$

$$F_j = \left(\frac{m_j}{26}\right)^{0.461} \tag{5.29c}$$

$$\overline{D} = \frac{cT^{3/2}}{p} \tag{5.29d}$$

where m_i and m_j are the molecular weights of the ith and jth species, respectively, and c is a constant.

It is found that over a range of temperature, the thermal conductivity ratio, $k/k_{\text{Equation (5.26)}}$, is nearly proportional to the specific heat. Thus, until ionization occurs, the Prandtl number is 1 for air over a wide range of temperature. For this kind of flow, pressure plays a dominant role in the computation. For a Prandtl number of 1, Reynolds analogy indicates that the heat transfer coefficient is directly proportional to the skin friction coefficient for an incompressible flow [16]. The correlation between the skin friction and the heat transfer holds approximately for computing attached boundary layers.

5.8 Continuity Equation

The continuity equation is essentially a mass balance relation. It represents that the mass within a control volume plus the net outflow of the mass through the surface surrounding the control volume is equal to the rate at which mass is produced in the control volume. The general form of continuity equation is

$$\frac{\partial \rho_i}{\partial t} + \nabla \cdot (\rho(V + V_i)) = \dot{\omega}_i \tag{5.30}$$

where V is the mass-averaged velocity, V_i is the diffusion velocity of component (species) i of the gas mixture, ρ is the overall mass density, ρ_i is the density of species i, and $\dot{\omega}_i$ is the mass-production rate of the ith species. Thus, the net mass flux of species i is the sum of the fraction of the mass transported by the overall fluid motion and that transported by diffusion. On the basis of Fick's law of diffusion, the transport of species i by diffusion is proportional to the negative of the species concentration. Thus

$$\frac{\partial \rho_i}{\partial t} + \nabla \cdot (C_i \rho V) - \nabla \cdot (\rho D_i \nabla C_i) = \dot{\omega} \tag{5.31}$$

where $\partial \rho_i / \partial t$ is the rate of change of mass of species i per unit volume in the cell, $\nabla \cdot (C_i \rho V)$ is the flux of mass of species i convected across the cell walls with the mixture velocity, $\nabla \cdot (\rho D_i \nabla C_i)$ is the diffusion of species i across the cell walls, and $\dot{\omega}$ is the mass of species i produced because of chemical reactions.

Usually, instead of solving for the density, ρ_i, of every one of the individual species i, the overall (mixture) mass conservation equation is solved to obtain the overall density, ρ, of the mixture. This density, ρ, is used in the Navier–Stokes equation. The overall mass conservation equation is obtained by summing Equation (5.31) over all the species as

$$\boxed{\frac{\partial \rho}{\partial t} + \nabla \cdot (\rho V) = 0} \tag{5.32}$$

The differential form of the overall continuity equation in Cartesian coordinates is

$$\frac{\partial \rho}{\partial t} + \frac{\partial}{\partial x}(\rho u) + \frac{\partial}{\partial y}(\rho v) + \frac{\partial}{\partial z}(\rho w) = 0 \tag{5.33}$$

5.9 Momentum Equation

The momentum equation is the representation of Newton's law that the "sum of the forces acting on a system of fluid particles is equal to the time rate of change of linear momentum." The formulation of momentum equation includes both pressure forces and viscous forces acting on a surface in space but neglects the weight of the particles within the control volume. To relate the stresses to the fluid motion, it is assumed that the stress components may be expressed as a linear function of the components of the rate of strain. When all the velocity gradients are zero, that is, when

the shear stress vanishes, the stress components must reduce to the hydrostatic pressure, p. Using index notation, the component momentum equations may be written in Cartesian coordinates as

$$\frac{\partial}{\partial t}(\rho u_i) + \frac{\partial}{\partial x_j}(\rho u_i u_j) = -\frac{\partial p}{\partial x_j} + \frac{\partial}{\partial x_j}\left[\mu\left(\frac{\partial u_i}{\partial x_j} + \frac{\partial u_J}{\partial x_i}\right) - \frac{2}{3}\mu\frac{\partial u_k}{\partial x_k}\,\delta_{ij}\right] \tag{5.34}$$

The first term on the left-hand side (LHS) is the time rate of change of the ith component of momentum per unit volume in a cell, the second term on the left-hand side represents the ith component of momentum convected across the cell walls with mixture velocity u_i, the first term on the right-hand side is the pressure forces acting on the cell walls in the i-direction, and the second term on the right-hand side represents the viscous forces acting on the cell walls in the i-direction.

Taking $i = 1$ and summing over j in Equation (5.34), the x-component of the momentum equation is obtained as

$$\frac{\partial}{\partial t}(\rho u) + \frac{\partial}{\partial x}(\rho u^2) + \frac{\partial}{\partial y}(\rho uv) + \frac{\partial}{\partial z}(\rho uw) = -\frac{\partial p}{\partial x} + \frac{\partial}{\partial x}\left[2\mu\frac{\partial u}{\partial z} - \frac{2}{3}\mu\nabla\cdot V\right]$$
$$+ \frac{\partial}{\partial y}\left[\mu\left(\frac{\partial u}{\partial y} + \frac{\partial v}{\partial x}\right)\right] + \frac{\partial}{\partial z}\left[\mu\left(\frac{\partial u}{\partial z} + \frac{\partial w}{\partial x}\right)\right] \tag{5.34a}$$

Taking $i = 2$ and summing over j in Equation (5.34), the y-component of the momentum equation is obtained as

$$\frac{\partial}{\partial t}(\rho v) + \frac{\partial}{\partial x}(\rho uv) + \frac{\partial}{\partial y}(\rho v^2) + \frac{\partial}{\partial z}(\rho vw) = -\frac{\partial p}{\partial y} + \frac{\partial}{\partial x}\left[\mu\left(\frac{\partial v}{\partial x} + \frac{\partial u}{\partial y}\right)\right]$$
$$+ \frac{\partial}{\partial y}\left[2\mu\frac{\partial v}{\partial z} - \frac{2}{3}\mu\nabla\cdot V\right] + \frac{\partial}{\partial z}\left[\mu\left(\frac{\partial v}{\partial z} + \frac{\partial w}{\partial y}\right)\right] \tag{5.34b}$$

Taking $i = 3$ and summing over j in Equation (5.34), the z-component of the momentum equation is obtained as

$$\frac{\partial}{\partial t}(\rho w) + \frac{\partial}{\partial x}(\rho wu) + \frac{\partial}{\partial y}(\rho wv)\frac{\partial}{\partial z}(\rho w^2) = -\frac{\partial p}{\partial z} + \frac{\partial}{\partial x}\left[\mu\left(\frac{\partial w}{\partial x} + \frac{\partial u}{\partial z}\right)\right]$$
$$+ \frac{\partial}{\partial y}\left[\mu\left(\frac{\partial w}{\partial y} + \frac{\partial v}{\partial z}\right)\right] + \frac{\partial}{\partial z}\left[2\mu\frac{\partial w}{\partial z} - \frac{2}{3}\mu\nabla\cdot V\right] \tag{5.34c}$$

Momentum conservation is unaffected by chemical reaction or ionization. Even with ionization, there is no electrostatic force on the flow for approximate charge neutrality. However, multicomponent nature of the reacting flow affects the value of the viscosity, as well as the other transport coefficients (that is, the diffusion coefficient and the thermal conductivity coefficient). It is essential to note that the viscosity μ is affected by the multicomponent nature of the reacting flow but is not affected by the existence of multi-temperatures.

For many applications, the terms involving the product of the coefficient of viscosity times a viscosity gradient are negligible over extensive regions of the flow field. Let us use the term *inviscid flow* to describe the flow with viscous stress negligibly small. The term *inviscid flow* implies that the combined product of viscosity and the relevant viscosity gradient (or both normal and shear stresses) has a small effect on the flow field and not that the fluid viscosity is zero.

For inviscid flows, the momentum Equation (5.34) reduces to

$$\frac{\partial}{\partial t}(\rho u) + \frac{\partial}{\partial x}(\rho u^2) + \frac{\partial}{\partial y}(\rho uv) + \frac{\partial}{\partial z}(\rho uw) = -\frac{\partial p}{\partial x} \tag{5.35a}$$

$$\frac{\partial}{\partial t}(\rho v) + \frac{\partial}{\partial x}(\rho uv) + \frac{\partial}{\partial y}(\rho v^2) + \frac{\partial}{\partial z}(\rho vw) = -\frac{\partial p}{\partial y} \tag{5.35b}$$

$$\frac{\partial}{\partial t}(\rho w) + \frac{\partial}{\partial x}(\rho wu) + \frac{\partial}{\partial y}(\rho wv)\frac{\partial}{\partial z}(\rho w^2) = -\frac{\partial p}{\partial z} \tag{5.35c}$$

Equations (5.35a)–(5.35c) are called the *Euler equations*.

In reality, most continuum flows will contain regions where the viscous force can be ignored and the flow can be assumed to be inviscid and regions where the viscous forces cannot be neglected. For solving such flows, the flow may be divided into the following two layers.

- The viscous boundary layer adjacent to the wall.
- The inviscid flow outside the boundary layer.

5.10 Energy Equation

For developing the total energy equation, let us assume that the temperature of air is less than 9000 K, in order to neglect the ionization of atomic species. Also, let us assume that the transfer of energy by radiation is negligible. The overall thermodynamic energy per unit mass, that is, the specific internal energy, is defined as

$$e = \sum C_i e_i \tag{5.36}$$

The specific internal energy is the sum of the energy in heavy-particle translation, the energy in rotation, the energy in vibration, and the latent chemical energy of the species. The total energy, e_t, per unit mass is the sum of the specific internal energy and the kinetic energy of the molecules per unit mass

$$e_t = e + \frac{1}{2}(V \cdot V) = e + \frac{1}{2}V^2 \tag{5.37}$$

The overall specific enthalpy is defined as

$$h = \sum C_i h_i = \sum C_i e_i + \frac{p}{\rho} \tag{5.38}$$

This equation can be expressed as [17, 18]

$$\sum \rho_i \frac{\partial h_i}{\partial t} + \sum [\rho_i (V + V_i) \cdot \nabla] h_i + \sum \dot{w}_i h_i = \frac{dp}{dt} + \nabla \cdot (q) + \tau : (\nabla V) \tag{5.39}$$

where q is the heat flux vector and τ is the viscous shear stress tensor. Multiplying Equation (5.31) by h_i and summing over i, we get

$$\sum \dot{w}_i h_i = \sum h_i \frac{\partial \rho_i}{\partial t} + \sum h_i \nabla \cdot (\rho_i V) - \sum h_i \nabla \cdot (\rho D_i \nabla C_i) \tag{5.40}$$

Substituting this into Equation (5.39), we get

$$\frac{\partial}{\partial t}(\rho h) + \nabla \cdot \left(\sum \rho_i h_i V \right) - \nabla \cdot \left(\sum \rho h_i D_i \nabla C_i \right) = \frac{dp}{dt} - \nabla \cdot (q) + \tau : (\nabla V) \tag{5.41}$$

But

$$\sum \rho_i h_i = \rho \sum C_i h_i = \rho h$$

Therefore, Equation (5.41) becomes

$$h \frac{\partial \rho}{\partial t} + \rho \frac{\partial h}{\partial t} + h[\nabla \cdot (\rho V)] + \rho (V \cdot \nabla) h - \nabla \cdot \left[\sum h_i \rho D_i \nabla C_i \right] = \frac{\partial p}{\partial t} + (V \cdot \nabla) p - \nabla \cdot q + \tau : (\nabla V) \tag{5.42}$$

Multiplying the continuity equation by h, we get

$$h \left[\frac{\partial \rho}{\partial t} + \nabla \cdot (\rho V) \right] = h[0] = 0 \tag{5.43a}$$

Let us focus on the terms $\rho \frac{\partial h}{\partial t}$ and $\rho (V \cdot \nabla) h$ on the left-hand side and $\frac{\partial p}{\partial t}$ and $(V \cdot \nabla) p$ on the right-hand side of Equation (5.42) and analyze them as follows.

$$\rho \frac{\partial h}{\partial t} + \rho (V \cdot \nabla) h - \frac{\partial p}{\partial t} - (V \cdot \nabla) p = \rho \frac{\partial}{\partial t} \left(e + \frac{p}{\rho} \right) + \rho (V \cdot \nabla) \left(e + \frac{p}{\rho} \right) - \frac{\partial p}{\partial t} - (V \cdot \nabla) p$$

because $h = e + \frac{p}{\rho}$.

By expanding, we get

$$\text{LHS} = \rho \frac{\partial e}{\partial t} - \frac{p}{\rho} \frac{\partial \rho}{\partial t} + \frac{\partial p}{\partial t} + \rho (V \cdot \nabla) e - \frac{p}{\rho} [(V \cdot \nabla) \rho] + (V \cdot \nabla) p - \frac{\partial p}{\partial t} - (V \cdot \nabla) p$$

that is,

$$\text{LHS} = \rho \frac{\partial e}{\partial t} + \rho (V \cdot \nabla) e - \frac{p}{\rho} \left[\frac{\partial \rho}{\partial t} + (V \cdot \nabla) \rho \right] \tag{5.43b}$$

Multiplying the continuity Equation (5.32) by e, we get

$$e\frac{\partial \rho}{\partial t} + e\nabla \cdot (\rho V) = 0 \tag{5.43c}$$

By multiplying the following momentum equation

$$\rho\frac{dV}{dt} = -\nabla p + \nabla \cdot \tau$$

by the dot product of V, we get

$$V\rho \cdot \frac{dV}{dt} = -V \cdot \nabla p + V \cdot (\nabla \cdot \tau)$$

In terms of the tensor identity presented by Bird *et al.* [18],

$$\tau : \nabla V \equiv \nabla \cdot (\tau \cdot V) - V \cdot (\nabla \cdot \tau)$$

From the above two equations, we get

$$\tau : \nabla V \equiv V \cdot (\tau \cdot V) - V \cdot \nabla p - V\rho \cdot \frac{dV}{dt} \tag{5.43d}$$

and

$$\rho V \cdot \frac{dV}{dt} = \rho\frac{d}{dt}\left(\frac{V^2}{2}\right) \tag{5.43e}$$

Substituting Equations (5.43a)–(5.43e) into Equation (5.42), we get

$$\frac{\partial(\rho e)}{\partial t} + \nabla \cdot (\rho V e) + \rho\frac{\partial}{\partial t}\left(\frac{V^2}{2}\right) + \rho(V \cdot \nabla)\left(\frac{V^2}{2}\right) + V \cdot \nabla p - \frac{p}{\rho}\left[\frac{\partial \rho}{\partial t} + (V \cdot \nabla)\,\rho\right]$$
$$- V \cdot (\tau \cdot V) - \nabla \cdot q + \nabla \cdot \left[\sum h_i\, \rho D_i \nabla C_i\right] = 0 \tag{5.44}$$

The term $(V \cdot \nabla p)$ can be expanded as

$$V \cdot \nabla p \equiv \nabla \cdot (pV) - \frac{p}{\rho}(\rho \nabla \cdot V) \tag{5.45a}$$

Multiplying Equation (5.22) by $\frac{V^2}{2}$, we get

$$\frac{V^2}{2}\left[\frac{\partial \rho}{\partial t} + \nabla \cdot (\rho V)\right] = 0 \tag{5.45b}$$

Substituting Equations (5.45a) and (5.45b) into Equation (5.44), we get

$$\frac{\partial(\rho\ e)}{\partial t} + \nabla \cdot (\rho V e) + \rho\frac{\partial}{\partial t}\left(\frac{V^2}{2}\right) + \frac{V^2}{2}\left(\frac{\partial \rho}{\partial t}\right) + \rho V \cdot \nabla\left(\frac{V^2}{2}\right)$$
$$+ \frac{V^2}{2}\nabla \cdot (\rho V) + \nabla \cdot (pV) - \frac{p}{\rho}\left[\frac{\partial \rho}{\partial t} + (V \cdot \nabla)\,\rho + \rho \nabla \cdot V\right]$$
$$- V \cdot (\tau \cdot V) + \nabla \cdot q - \nabla \cdot \left[\sum h_i \rho D_i\ \nabla C_i\right] = 0 \tag{5.46}$$

Using Equations (5.32) and (5.37), this can be simplified to

$$\frac{\partial}{\partial t}(\rho e_t) + \nabla \cdot (\rho V e_t) + \nabla \cdot (pV) - \nabla \cdot (\tau \cdot V) + \nabla \cdot q - \nabla \cdot \left[\sum h_i \rho D_i \nabla C_i\right] = 0 \tag{5.47}$$

In Equation (5.47),

- the first term represents the rate of change of total energy per unit volume in a cell;
- the second term represents the flux of total energy through the cell walls;
- the third term gives the work done by the pressure forces;
- the fourth term gives the work done by the viscous forces;
- the fifth term represents the conduction of energy through the cell walls because of the temperature gradients;
- the sixth term represents the diffusion of enthalpy through the cell walls because of the concentration gradients.

For a two-dimensional flow, the total energy in Cartesian coordinates is expressed as

$$e_t = e + \frac{1}{2}(u^2 + v^2) = \sum C_i e_i + (u^2 + v^2)$$

Equation (5.47) simplifies to

$$\frac{\partial}{\partial t}(\rho e_t) + \frac{\partial}{\partial x}[u(\rho e_t + p)] - \frac{\partial}{\partial x}[u\tau_{xx} + v\tau_{xy} - q_x] - \frac{\partial}{\partial x}\left[\sum h_i \rho D_i \frac{\partial C_i}{\partial x}\right]$$
$$+ \frac{\partial}{\partial y}[v(\rho e_t + p)] - \frac{\partial}{\partial y}[u\tau_{yx} + v\tau_{yy} - q_y] - \frac{\partial}{\partial y}\left[\sum h_i \rho D_i \frac{\partial C_i}{\partial y}\right] = 0 \tag{5.48}$$

where

$$q_x = -k\frac{\partial T}{\partial x} - k_v \frac{\partial T_y}{\partial x} \tag{5.49a}$$

$$q_x = -k\frac{\partial T}{\partial y} - k_v \frac{\partial T_y}{\partial y} \tag{5.49b}$$

For a two-temperature model, there are two temperature gradients: one is because of the translational/rotational temperature T and the second is because of the vibrational temperature T_v, k represents the thermal conductivity relating to T and k_v designates the thermal conductivity relating to T_v.

5.11 General Form of the Equations of Motion

The general form of the equations of motion in conservation form may be expressed as

$$\frac{\partial U}{\partial t} + \frac{\partial (E_i - E_v)}{\partial x} + \frac{\partial (F_i - F_v)}{\partial y} + \frac{\partial (G_i - G_v)}{\partial z} = S \tag{5.50}$$

where subscript i denotes inviscid flow and subscript v denotes viscous flow, the vector of the chemical source terms in represented by S.

5.11.1 Overall Continuity Equation

Substituting $U = \rho,\ E_i = \rho u,\ F_i = \rho v,\ G_i = \rho w,$ and $E_v = F_v = G_v = S = 0$ in Equation (5.50), we obtain the overall continuity equation given by Equation (5.33) as

$$\frac{\partial \rho}{\partial t} + \frac{\partial}{\partial x}(\rho u) + \frac{\partial}{\partial y}(\rho v) + \frac{\partial}{\partial z}(\rho w) = 0$$

It is essential to note that even though the overall continuity equation applies to both inviscid and viscous regions, there are no terms relating uniquely to the viscous flow.

5.11.2 Momentum Equation

We know that neglecting the body forces, the x-momentum equation can be written as

$$\rho\frac{\partial u}{\partial t} + \rho u\frac{\partial u}{\partial x} + \rho v\frac{\partial u}{\partial y} + \rho w\frac{\partial u}{\partial z} = -\frac{\partial p}{\partial x} + \frac{\partial}{\partial x}\left[2\mu\frac{\partial u}{\partial x} - \frac{2}{3}\mu\ \nabla \cdot V\right] + \frac{\partial}{\partial y}\left[\mu\left(\frac{\partial u}{\partial y} + \frac{\partial v}{\partial x}\right)\right] + \frac{\partial}{\partial z}\left[\mu\left(\frac{\partial w}{\partial x} + \frac{\partial u}{\partial z}\right)\right] \tag{5.51}$$

or

$$\rho\frac{\partial u}{\partial t} + \rho u\frac{\partial u}{\partial x} + \rho v\frac{\partial u}{\partial y} + \rho w\frac{\partial u}{\partial z} = -\frac{\partial p}{\partial x} + \frac{\partial(\tau_{xx})}{\partial x} + \frac{\partial(\tau_{yx})}{\partial y} + \frac{\partial(\tau_{zx})}{\partial z} \tag{5.52}$$

where

$$\tau_{xx} = 2\mu\frac{\partial u}{\partial x} - \frac{2}{3}\mu\ \nabla \cdot V$$

$$\tau_{yx} = \mu\left(\frac{\partial u}{\partial y} + \frac{\partial v}{\partial x}\right)$$

$$\tau_{zx} = \mu\left(\frac{\partial u}{\partial z} + \frac{\partial w}{\partial x}\right)$$

Equations (5.51) and (5.52) are forms of the x-momentum equation that are commonly used in the study of boundary layers. But Equations (5.51) and (5.52) are not in conservation form. Multiplying the overall continuity Equation (5.32) by u and adding to Equation (5.52), we obtain the conservation-law form of the x-momentum equation as

$$\frac{\partial(\rho u)}{\partial t} + \frac{\partial}{\partial x}[(p + \rho u^2) - \tau_{xx}] + \frac{\partial}{\partial y}[(\rho uv) - \tau_{yx}] + \frac{\partial}{\partial z}[(\rho uw) - \tau_{zx}] = 0 \tag{5.53}$$

Comparing Equations (5.53) and (5.50), it is seen that

$$U = \rho u; \quad E_i = p + \rho u^2; \quad F_i = \rho uv; \quad G_i = \rho uw$$
$$E_v = \tau_{xx}; \quad F_v = \tau_{yx}; \quad G_v = \tau_{zx}; \quad S = 0$$

5.11.3 Energy Equation

The energy equation for two-dimensional flow, given by Equation (5.48), was obtained by expanding the vector expressions in Equation (5.47) for a two-dimensional flow. Following the same procedure for a three-dimensional flow, the energy equation for a three-dimensional flow can be obtained by substituting the following in Equation (5.50).

$$U = \rho e_t$$
$$E_i = u(\rho e_t + p)$$
$$E_v = u\tau_{xx} + v\tau_{xy} + w\tau_{xz} + q_x + \sum h_i \rho D_i \frac{\partial C_i}{\partial x}$$
$$F_i = v(\rho e_t + p)$$
$$F_v = u\tau_{yx} + v\tau_{yy} + w\tau_{yz} + q_y + \sum h_i \rho D_i \frac{\partial C_i}{\partial y}$$
$$G_i = w(\rho e_t + p)$$
$$G_v = u\tau_{zx} + v\tau_{zy} + w\tau_{zz} + q_z + \sum h_i \rho D_i \frac{\partial C_i}{\partial z}$$
$$S = 0$$

5.12 Experimental Measurements of Hypersonic Flows

In the design of a vehicle to fly at hypersonic Mach number, it is essential to integrate the experimental data obtained from tests in ground-based facilities with computational flow field solutions and data obtained from flight tests to define the aerothermodynamic environments that prevails during the flight of the vehicle. Only flight tests of the full-scale vehicle can provide the correct representation of the vehicle's environment. But the flight tests are very expensive and can be done only after an extensive design, development, and fabrication program has been completed. However, numerous researches employing elementary shapes, for example, blunt-nosed shapes, were conducted to understand the fundamentals of flow process.

As complete simulation of the flow field cannot be obtained in a ground-based facility, the first and most important step in planning a ground-based test program is establishing the test objectives. The following are the main objectives of the ground-based test.

- To obtain data defining the aerodynamic forces and moments and heat transfer distributions for complete configurations whose complex flow field resist computational modeling.
- To obtain data defining local flow phenomena, such as the inlet flow field, for a hypersonic air-breathing engine or the shock/boundary layer interaction using a fin or a wing mounted on a plane surface.
- To acquire detailed flow field data to be used in developing flow models for use in a computational algorithm.
- To measure the heat transfer and the drag, to be used in comparison with computed flow field solutions over a range of configuration geometries and flow conditions.
- To document aerodynamic effects of aerosurface settings, failures, etc.
- To certify air-breathing engines.

Experimental programs are needed to validate the numerical models used to represent physical process and flow chemistry and to calibrate the code to determine the range of conditions for which the values of the computed parameters are of acceptable accuracy.

5.13 Measurements of Hypersonic Flows

The parameters that can be measured using hypersonic experimental facilities are the following.

- The freestream Mach number.
- The freestream unit Reynolds number.
- The freestream velocity,
- The pressure altitude.
- The total enthalpy of the flow.
- The density ratio across the shock wave.
- The wall-to-total temperature ratio.
- The thermochemistry of the flow field.

Among these, some of the parameters are interrelated, for example, the freestream velocity and the total enthalpy of the flow, and the density ratio across the shock wave. Furthermore, in many instances where two parameters are related, for example, the freestream Mach number and the freestream velocity, one may simulate one parameter (say the Mach number) but not the other (the velocity, because neither the total enthalpy nor the speed of sound is matched).

Complete simulations of the flow field cannot be obtained in any one ground-based facility. Therefore, we must decide which parameters are critical to accomplishing the objectives of the test program. In fact, during the development of a particular vehicle, the designer will most unlikely utilize many different facilities with a run schedule, the model, the instrumentation, and the test conditions for each program tailors to answer specific questions.

For vehicles, such as the space shuttle, that operate at high angles of attack dominated by a blunt-nosed entropy layer, Mach number is not a significant parameter. However, for vehicles such as shuttle orbiter, designed to operate at lower angle of attack, Mach number and viscous effects become significant. Test facilities and development procedure, appropriate for one class of configurations, must be rethought when a different design is analyzed.

In addition to the nine parameters listed earlier, additional factors include the following.

- Model scale.
- Test time.
- Types of data available.
- Flow quality, such as uniformity, noise, cleanliness, and steadiness.

Let us consider a program that aims at acquiring experimental data to verify a code's ability to accurately model the physics and/or the chemistry of the flow, that is, code validation data. Measurements at the model surface, for example, heat transfer data and surface pressure, are not sufficient for validating a code. Code validation data must include information about the flow field away from the surface, for example, flow visualization data defining shock waves and density contours, velocity measurements, and gas-density measurements. In any test program, we must be able to define the freestream flow, because it is the upstream boundary condition for the flow around the model. Defining the freestream flow is critical for code validation test programs. Flow nonuniformity, unsteadiness, or noise may affect the validity of the data and make them unusable for code validation applications.

The test time is also an important parameter. As shown in Figure 5.9, the test time may vary from fraction of a millisecond for shock tube flows to hours for "conventional" wind tunnels.

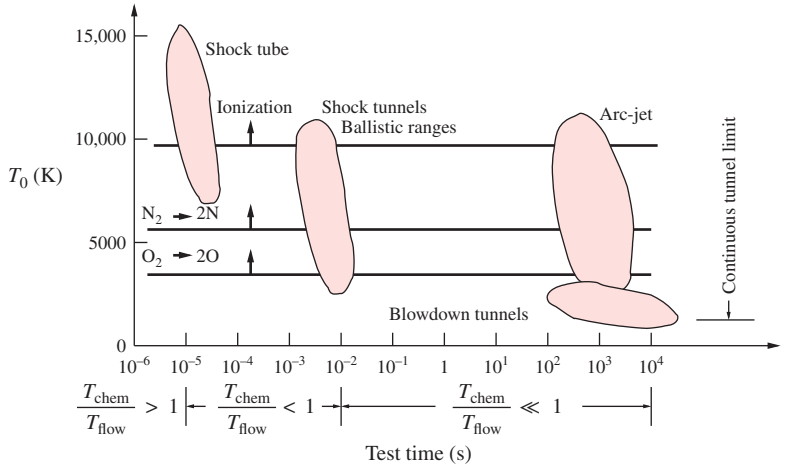

Figure 5.9 Stagnation temperature as a function of test time for some hypersonic facilities.

Continuous-flow wind tunnels using air as the test gas have maximum temperatures around 1000 K. If the flow involves nonequilibrium chemistry, the model scale affects the relation between the characteristic flow time and the characteristic reaction time. Furthermore, the specification of the instrumentation must reflect the test time and the model size. Thus, these many varied factors provide considerable challenge to the pretest planning effort.

For many applications, experimental data provide the information required for developing a realistic computational flow models and design data for flow fields whose complexity resists computer flow models. Thus, the ground-based testing and CFD play complimentary roles in the design of a hypersonic vehicle.

5.13.1 Hypersonic Experimental Facilities

It is essential to note that there is no single facility capable for simulating hypersonic flight environment; therefore, different facilities are used to address various aspects of the design problems associated with hypersonic flight. In this discussion, we will focus our attention on the types of facilities that are used to simulate the aerothermodynamic environment, that is, the aerodynamic forces and momentum, the heat transfer distribution, and the surface pressure distribution. Some of the primary experimental facilities meant for this are

- shock tubes;
- arc-tunnels;
- hypersonic wind tunnels;
- ballistic free-flight ranges.

5.14 Summary

Usually, hypersonic flow is defined as the flow with Mach number greater than 5, where the change in flow Mach number is dictated by the change in the speed of sound, except in problems such as the flow fields around blunt bodies begin to exhibit many of the characteristics of hypersonic flow when the Mach number is 4, or greater. By definition,

$$\boxed{M_\infty \equiv \frac{V_\infty}{a_\infty} \gg 1}$$

The Mach number is greatly larger than unity ($M_\infty \gg 1$) is the basic assumption for all hypersonic flow theories.

The high temperatures associated with hypersonic flight are difficult to match in ground-test facilities, such as hypersonic wind tunnel and shock tunnel. Therefore, in wind tunnel applications, hypersonic Mach numbers are achieved through relatively low speeds of sound.

Another assumption common to hypersonic flow is that the ratio of the freestream density to the density just behind a shock is extremely small, that is,

$$\boxed{\epsilon \equiv \frac{\rho_\infty}{\rho_2} \ll 1}$$

This is known as the *small-density-ratio* assumption.

When the density ratio across the shock wave becomes small, the shock layer becomes very thin. For this kind of flow situation, we can assume that the speed and direction of the gas particles in the freestream remain unchanged until they strike the solid surface exposed to the flow. This flow model is termed *Newtonian flow model* because it is similar in character to that described by Newton in the seventeenth century.

The pressure coefficient is given by

$$C_p = 2 \sin^2\theta_b = 2 \cos^2\phi$$

This equation for the pressure coefficient is based on the Newtonian flow model, where the 2 represents the pressure coefficient at the stagnation point, because $\theta_b = 90°$ at the stagnation point.

The pressure coefficient for the Newtonian model is independent of Mach number and depends only on the angle between the freestream flow direction and the surface inclination.

For slender configurations, such as sharp cones and wedges, the strong shock assumption is

$$\boxed{M_\infty \sin\ \theta_b \gg 1}$$

The concept termed the *Mach number independence principle* depends on this assumption.

Using the Reynolds number based on the flow conditions behind a normal shock wave as the characteristic parameter,

$$Re_2 = \frac{\rho_2 V_2 d}{\mu_2}$$

the friction drag for Re_2 is given by

$$\boxed{C_{D,f} = \frac{5.3}{(Re)^{1.18}}}$$

where subscript 2 refers to condition behind the shock.

A cylinder whose axis is perpendicular to a hypersonic freestream will be essentially constant.

In the rarefied flows, viscous/inviscid interactions become important and the effects of viscosity can no longer be neglected.

At very high altitudes, the air becomes highly rarefied so that the motion of the individual particles becomes significant. The dimensionless parameter used to describe the regimes of rarefied gas dynamics is the Knudsen number, Kn.

On the basis of Kn, the flow field is classified as follows.

- Continuum flow: $Kn < 0.01$.
- Slip flow: $0.01 < Kn < 0.1$.
- Transition flow: $0.1 < Kn < 1.0$.
- Free molecule flow: $Kn > 10$.

The continuum flow regime is termed the *vorticity interaction regime*.

The air particles in the shock layer of a hypersonic reentry vehicle undergo vibrational excitation, dissociation, and even ionization.

For adiabatic flow across the shock, $T_{01} = T_{02}$, where T_{01} and T_{02} are the stagnation temperatures. Thus from isentropic relation,

$$\frac{T_{02}}{T_1} = \frac{T_{01}}{T_1} = \left(1 + \frac{\gamma - 1}{2} M_1^2\right)$$

In reality, for hypersonic flight, the temperature of the gas molecules that pass through the detached shock wave increases to very high levels, leading to the excitation of vibrational and chemical energy modes.

The compressibility factor is the ratio of the molecular weight of the undissociated air to the mean molecular weight at the conditions of interest. Thus

$$z = \frac{M_o}{\overline{M}}$$

Accounting for the change in the gas composition, the equation of state becomes

$$p = \rho \frac{R_u}{\overline{M}} T = \rho \frac{M_o}{\overline{M}} \frac{R_u}{M_o} T = \rho z RT$$

For temperatures of 1600 K and below, the air composition does not change in the shock-compression process. Therefore, for temperatures below 1600 K, the gas can be treated as thermally perfect. Furthermore, for temperatures below 800 K, it can be seen that the air can be treated as perfect with constant specific heats ratio of 1.4.

The stagnation pressure computed for air in thermodynamic equilibrium is slightly larger than the perfect gas value.

For hypersonic flow across the normal shock wave portion of a bow shock,

$$p_1 \ll \rho_1 V_1^2 \quad \text{and} \quad p_2 \ll \rho_2 V_2^2$$

The stagnation point pressure for hypersonic flow is independent of the flow chemistry and approximately twice the dynamic pressure, q_1, ahead of the shock.

Nonequilibrium state such as dissociation and recombination may result when the fluid particles pass through a strong shock wave and undergo a rapid expansion.

A dynamic behavior of the flow is significantly affected by the chemical reactions. The use of a one-temperature model in the computation of a nonequilibrium reacting flow leads to a substantial overestimation of the rate of equilibration.

Because of the slow equilibration rate of vibrational energy, multiple-temperature models are used to describe a flow that is out of equilibrium.

A mixture of gases at a point is in local chemical equilibrium when the concentrations of chemical species at that point are a function of the local pressure and the local temperature alone.

For chemical equilibrium, $t_c \ll t_f$, everywhere in the mixture.

The transport of mass, momentum, and energy are due to the collision of fluid particles in the flow field.

The empirical relation to calculate the coefficient of viscosity is

$$\boxed{\mu = 1.46 \times 10^{-6} \left(\frac{T^{3/2}}{T + 111} \right)}$$

The thermal conduction in terms of temperature can be expressed as

$$\boxed{k = 1.993 \times 10^{-5} \frac{T^{3/2}}{T + 112}}$$

The general form of continuity equation is

$$\frac{\partial \rho_i}{\partial t} + \nabla \cdot (\rho(V + V_i)) = \dot{w}_i$$

The x-component of the momentum equation is

$$\frac{\partial}{\partial t}(\rho u) + \frac{\partial}{\partial x}(\rho u^2) + \frac{\partial}{\partial y}(\rho u v) + \frac{\partial}{\partial z}(\rho u w) = -\frac{\partial p}{\partial x} + \frac{\partial}{\partial x}\left[2\mu \frac{\partial u}{\partial z} - \frac{2}{3}\mu \nabla \cdot V\right] + \frac{\partial}{\partial y}\left[\mu\left(\frac{\partial u}{\partial y} + \frac{\partial v}{\partial x}\right)\right] + \frac{\partial}{\partial z}\left[\mu\left(\frac{\partial u}{\partial z} + \frac{\partial w}{\partial x}\right)\right]$$

The y-component of the momentum equation is

$$\frac{\partial}{\partial t}(\rho v) + \frac{\partial}{\partial x}(\rho u v) + \frac{\partial}{\partial y}(\rho v^2) + \frac{\partial}{\partial z}(\rho v w) = -\frac{\partial p}{\partial y} + \frac{\partial}{\partial x}\left[\mu\left(\frac{\partial v}{\partial x} + \frac{\partial u}{\partial y}\right)\right] + \frac{\partial}{\partial y}\left[2\mu \frac{\partial v}{\partial z} - \frac{2}{3}\mu \nabla \cdot V\right] + \frac{\partial}{\partial z}\left[\mu\left(\frac{\partial v}{\partial z} + \frac{\partial w}{\partial y}\right)\right]$$

The z-component of the momentum equation is

$$\frac{\partial}{\partial t}(\rho w) + \frac{\partial}{\partial x}(\rho w u) + \frac{\partial}{\partial y}(\rho w v)\frac{\partial}{\partial z}(\rho w^2) = -\frac{\partial p}{\partial z} + \frac{\partial}{\partial x}\left[\mu\left(\frac{\partial w}{\partial x} + \frac{\partial u}{\partial z}\right)\right] + \frac{\partial}{\partial y}\left[\mu\left(\frac{\partial w}{\partial y} + \frac{\partial v}{\partial z}\right)\right] + \frac{\partial}{\partial z}\left[2\mu\frac{\partial w}{\partial z} - \frac{2}{3}\mu\nabla\cdot V\right]$$

Momentum conservation is unaffected by chemical reaction or ionization.

For inviscid flows, the momentum equations reduce to

$$\frac{\partial}{\partial t}(\rho u) + \frac{\partial}{\partial x}(\rho u^2) + \frac{\partial}{\partial y}(\rho u v) + \frac{\partial}{\partial z}(\rho u w) = -\frac{\partial p}{\partial x}$$

$$\frac{\partial}{\partial t}(\rho v) + \frac{\partial}{\partial x}(\rho u v) + \frac{\partial}{\partial y}(\rho v^2) + \frac{\partial}{\partial z}(\rho v w) = -\frac{\partial p}{\partial y}$$

$$\frac{\partial}{\partial t}(\rho w) + \frac{\partial}{\partial x}(\rho w u) + \frac{\partial}{\partial y}(\rho w v)\frac{\partial}{\partial z}(\rho w^2) = -\frac{\partial p}{\partial z}$$

These are called the *Euler equations*.

The overall specific enthalpy is defined as

$$h = \sum C_i h_i = \sum C_i e_i + \frac{p}{\rho}$$

For a two-dimensional flow, the total energy in Cartesian coordinates is expressed as

$$e_t = e + \frac{1}{2}(u^2 + v^2) = \sum C_i e_i + (u^2 + v^2)$$

For a two-temperature model, there are two temperature gradients: one is because of the translational/rotational temperature T and the second is because of the vibrational temperature T_v, k represents the thermal conductivity relating to T and k_v designates the thermal conductivity relating to T_v.

The general form of the equations of motion in conservation form may be expressed as

$$\frac{\partial U}{\partial t} + \frac{\partial(E_i - E_v)}{\partial x} + \frac{\partial(F_i - F_v)}{\partial y} + \frac{\partial(G_i - G_v)}{\partial z} = S$$

The overall continuity equation is

$$\frac{\partial \rho}{\partial t} + \frac{\partial}{\partial x}(\rho u) + \frac{\partial}{\partial y}(\rho v) + \frac{\partial}{\partial z}(\rho w) = 0$$

It is essential to note that even though the overall continuity equation applies to both inviscid and viscous regions.

Neglecting the body forces, the x-momentum equation can be written as

$$\rho\frac{\partial u}{\partial t}+\rho u\frac{\partial u}{\partial x}+\rho v\frac{\partial u}{\partial y}+\rho w\frac{\partial u}{\partial z}=-\frac{\partial p}{\partial x}+\frac{\partial}{\partial x}\left[2\mu\frac{\partial u}{\partial x}-\frac{2}{3}\mu\ \nabla\cdot V\right]$$
$$+\frac{\partial}{\partial y}\left[\mu\left(\frac{\partial u}{\partial y}+\frac{\partial v}{\partial x}\right)\right]+\frac{\partial}{\partial z}\left[\mu\left(\frac{\partial w}{\partial x}+\frac{\partial u}{\partial z}\right)\right]$$

The conservation-law form of the x-momentum equation is

$$\frac{\partial(\rho u)}{\partial t}+\frac{\partial}{\partial x}[(p+\rho u^2)-\tau_{xx}]+\frac{\partial}{\partial y}[(\rho uv)-\tau_{yx}]+\frac{\partial}{\partial z}[(\rho uw)-\tau_{zx}]=0$$

In the design of a vehicle to fly at hypersonic Mach number, it is essential to integrate the experimental data obtained from tests in ground-based facilities with computational flow field solutions and data obtained from flight tests to define the aerothermodynamic environments that prevails during the flight of the vehicle.

The parameters that can be measured using hypersonic experimental facilities are the following.

- The freestream Mach number;
- The freestream unit Reynolds number;
- The freestream velocity;
- The pressure altitude;
- The total enthalpy of the flow;
- The density ratio across the shock wave;
- The wall-to-total temperature ratio;
- The thermochemistry of the flow field.

Complete simulations of the flow field cannot be obtained in any one ground-based facility. Therefore, we must decide which parameters are critical to accomplishing the objectives of the test program.

For many applications, experimental data provide the information required for developing a realistic computational flow models and design data for flow fields whose complexity resists computer flow models. Thus, the ground-based testing and CFD play complimentary roles in the design of a hypersonic vehicle.

There is no single facility capable for simulating hypersonic flight environment; therefore, different facilities are used to address various aspects of the design problems associated with hypersonic flight. Some of the primary experimental facilities meant for this are

- shock tubes;
- arc-tunnels;
- hypersonic wind tunnels;
- ballistic free-flight ranges.

Exercise Problems

5.1 Air at 82 atm and 740 K in a settling chamber runs a Mach 8 tunnel. Treating the expansion as isentropic, determine (a) the test-section static temperature, (b) static pressure, (c) velocity, (d) unit Reynolds number of the flow, and (e) dynamic pressure.

[Answer: (a) −219.53°C, (b) 851.13 Pa, (c) 1174.24 m/s, (d) 18.652×10^6 per unit length, (e) 38,130.36 Pa]

5.2 Find the (a) viscosity coefficient and (b) conduction coefficient of air at 620 K.
[Answer: (a) 3.083×10^{-5} kg/(m s), (b) 42.03×10^{-5} W/(m K)]

5.3 Show that for a compressible flow,

$$\ln\left(\frac{\rho_2}{\rho_1}\right)_{\text{isentropic}} \geq \ln\left(\frac{\rho_2}{\rho_1}\right)_{\text{shock}}$$

where subscript "shock" indicates the density ratio of a shock wave for which the pressure ratio is p_2/p_1 and the subscript "isentropic" denotes the density ratio for an isentropic process that spans the same pressure ratio p_2/p_1.

References

[1] Rathakrishnan E., *Applied Gas Dynamics*, John Wiley & Sons, Inc., Hoboken, NJ, 2010.
[2] Rathakrishnan E., *Gas Tables*, 3rd ed. Universities Press, Hyderabad, India, 2012.
[3] Koppenwallner G., "Experimentalelle Untersuchung der Druckverteilung und des Widerstands von querangestroemten Kreiszylindern bei hypersonischen Machzahlen in Bereich von Kontinuums – bis freier Molekularstromung", *Zeitshrift für Flugwissenchaften*, Vol. 17, No. 10, 1969, pp. 321–332.
[4] Moss J. N., and Bird G. A., "Direct Simulation of Transition Flow for Hypersonic Re-Entry Conditions", in H. F. Nelson (ed.), *Thermal Design of Aeroassisted Orbital Transfer Vehicles, Vol. 96 of Progress in Aeronautics and Astronautics*, AIAA, New York, 1985, pp. 338–360.
[5] Hansen C. F., and Heims S. P., "A review of thermodynamics, transport, and chemical reaction rate properties of high-temperature air", NACA TR R-4359, July 1958.
[6] Huber P. W., "Hypersonic Shock-Heated Flow Parameters for Velocities to 46,000 Feet Per Second and Altitudes to 323,000 Feet", NASA TR R-163, 1963.
[7] Candler G., and MacCormack R., "The Computation of Hypersonic Ionized Flows in Chemical and Thermal Nonequilibrium", AIAA Paper 88-0511, Reno, NV, Jan. 1988.
[8] Hansen C. F., "Approximations for the Thermodynamic and Transport Properties of High-Temperature Air", NACA TR R-50, Nov. 1957.
[9] Rakich J. V., Stewart D. A., and Lanfranco M. J., "Results of a Flight Experiment on the Catalytic Efficiency of the Space Shuttle Heat Shield", AIAA Paper 82-0944, St. Louis, MO, June 1982.
[10] Park C., "Assessment of Two-Temperature Kinetic Model for Ionizing Air", AIAA Paper 87-1574, Honolulu, HI, June 1987.
[11] Lee J. H., "Basic Governing Equations for the Flight Regimes of Aeroassisted Orbit Transfer Vehicles", H. F. Nelson (ed.), *Thermal Design of Aeroassisted Orbit Transfer Vehicles*, Vol. 96 of Progress in Astronautics and Aeronautics, AIAA, New York, 1985, pp. 353.

[12] Park C., *Nonequilibrium Hypersonic Aerothermodynamics*, John Wiley & Sons, Inc., New York, 1990.
[13] Chapman S., and Cowling T. G., *The Mathematical Theory of Non-Uniform Gases*, Cambridge University Press, Cambridge, 1960.
[14] Svehla R. A., "Estimated Viscosities and Thermal Conductivities of Gases at High Temperatures", NASA TR R-132, 1962.
[15] Bartlett E. P., Kendall R. M., and Rindal R. A., "An Analysis of the Coupled Chemically Reacting Boundary Layer and Charing Ablator, Part IV – A Unified Approximation for Mixture Transport Properties for Multicomponent Boundary-Layer Applications", NASA CR-1063, June 1968.
[16] Rathakrishnan E., *Elements of Heat Transfer*, CRC Press, Boca Raton, FL, 2012.
[17] Back L. H., "Conservation Equations of a Viscous Heat Conducting Fluid in Curvilinear Orthogonal Coordinates", Jet Propulsion Lab, TR-32-1332, Sep. 1968.
[18] Bird R. B., Stewart W. E., and Lightfoot E. N., *Transport Phenomena*, John Wiley & Sons, Inc., New York, 1960.

6

Aerothermodynamics

6.1 Introduction

Aerothermodynamics deals with the aerodynamic forces and moments and the heating distribution of a vehicle that flies at hypersonic speeds. Aerothermodynamics of a vehicle at hypersonic speeds may include boundary layer transition and turbulence, viscous/inviscid interactions, separated flows, nonequilibrium chemistry and the effects of catalycity, ablation, and noncontinuum effects. Most of the vehicles experiencing aerothermodynamic environment contain an air-breathing, scramjet propulsion system. A typical equipment with this kind of propulsion system is shown in Figure 6.1. The forebody of the vehicle serves as a compression surface for the inlet flow, and the afterbody serves as a nozzle. Therefore, we must deal with the transition process and subsequent three-dimensional turbulent boundary layer with reasonable accuracy to describe the flow past the forebody and the complex, three-dimensional flow field at the afterbody where chemistry and viscous/inviscid interactions are important.

The complex flow field associated with the vehicle shown in Figure 6.1 is usually studied by testing a scale model of the vehicle in a hypersonic wind tunnel or some other type of ground-based test facility. For a simple shape, properly nondimensionalized wind tunnel data can be comfortably applied to the flight environment. All ground-based tests are only partial simulations of the hypersonic flight environment. The extrapolation process becomes complicated for complex shapes.

Development of computer hardware and software led to the prediction of the data associated with the aerothermodynamics of a flying vehicle. Indeed, because of the continued improvements in computer hardware and software, computational fluid dynamics (CFD) plays an important role in the design process. The term *computational fluid dynamics* implies the integration of two disciplines, namely, the fluid dynamics and computation. Thus, in a CFD code developed for solving flow fields, approximations are made both in modeling fluid dynamic phenomena, for example, turbulence, and in the numerical formulation, for example, developing

High Enthalpy Gas Dynamics, First Edition. Ethirajan Rathakrishnan.

www.wiley.com/go/rathakrishnan

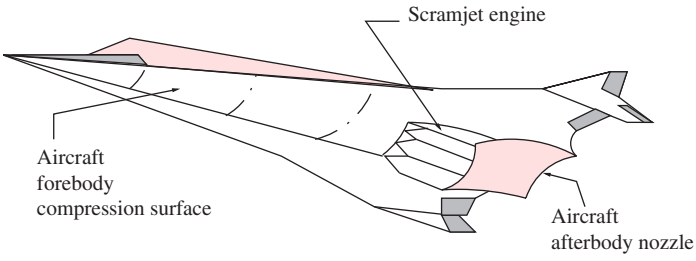

Figure 6.1 A hypersonic vehicle with air-breathing propulsion system.

grids to define the configurations and the flow field points where dependent variables are to be computed.

A CFD code development and application may follow the steps listed as follows.

- Select the physical process to be considered.
- Decide on mathematical and topographical models.
- Build body geometry and space grid.
- Develop a numerical solution method.
- Incorporate the above into a computer code.
- Calibrate and validate the code against benchmark data.
- Predict aerodynamic coefficients, flow parameters, and aerodynamic heatings.

At this stage, it is essential to note that the hypersonic design process must employ the synergistic integration of ground-based testing, basic analytic technologies, computational fluid dynamics, and flight testing. In some instances, data from ground-based tests are used to develop correlations for use at the design flight conditions. In other situations, the primary objective of a ground-test program is to generate high-quality data that can be used to develop, validate, and calibrate numerical codes. In all the cases, it is necessary to compare experimental measurements to the corresponding computed values.

6.2 Empirical Correlations

The wind tunnel data were usually used in dimensionless form to define the pressure distribution, the convective heat transfer distribution, and the aerodynamic forces and moments. For example, the convective heat transfer coefficient, h, measured at a specified location can be divided by a reference, stagnation-point heat transfer coefficient, $h_{t,\text{ref}}$, measured at the same flow conditions in a wind tunnel, resulting in a dimensionless ratio $h/h_{t,\text{ref}}$. Using this dimensionless rate, the local convective heat transfer rate at flight can be expressed as

$$\dot{q}_{\text{flt}} = \left(\frac{h}{h_{t,\text{ref}}}\right)\left(\dot{q}_{t,\text{ref}}\right)_{\text{flt}} \tag{6.1}$$

where subscripts ‘flt’ refers to flight condition.

Wind-tunnel-based empirical correlations complimented by analytical solutions provide reasonable estimates of the actual flight environment.

6.3 Viscous Interaction with External Flow

The effect of the boundary layer on the inviscid flow field may be represented by displacing the actual surface by boundary layer displacement thickness. As the boundary layer displaces the external stream, this stream deflection will change the shape of the shock wave and, therefore, the flow field. The growth of the boundary layer is determined by the pressure distribution, the flow properties at the edge of the boundary layer, while the values of these parameters, themselves, depend on the magnitude of the displacement effect. For instant, the lower the Reynolds number, the thicker the boundary layer and greater the viscous-interaction-induced effect on the flow field. Thus, this viscous/inviscid interactions is a complex phenomenon in which the boundary layer "history" plays a dominant role. Note that this phenomenon is more significant for slender bodies, such as slender cones, because the changes in the effective geometry due to boundary layer growth will be proportionally larger. Furthermore, the higher the Mach number, the shock wave will lie closer to the body.

To correlate the viscous/inviscid-interaction-induced flow field perturbations, Koppenwallner [1] identified two different parameters: one for the pressure and the other for the skin friction and the heat transfer. To correlate the pressure changes, the hypersonic viscous interaction parameter is

$$\chi = \frac{M_\infty^3 \sqrt{C_\infty}}{\sqrt{Re_{\infty,x}}} \tag{6.2}$$

where

$$C_\infty = \left(\frac{\mu_w}{\mu_\infty}\right)\left(\frac{T_\infty}{T_w}\right)$$

To correlate the viscous/inviscid-induced perturbations in the skin friction or the heat transfer, Koppenwallner recommends

$$V = \frac{M_\infty \sqrt{C_\infty}}{\sqrt{Re_{\infty,x}}} \tag{6.3}$$

as the viscous interaction parameter.

The induced pressure increase divided by the pressure for inviscid flow past a sharp cone is correlated in terms of the viscous interaction parameter [2]

$$\chi_c = \frac{M_c^3 \sqrt{C_c}}{\sqrt{Re_{c,x}}} \tag{6.4}$$

where subscript c refers to the inviscid flow properties at the surface of a sharp cone. Note that use of unperturbed, sharp-cone values of the edge properties in the correlation for the induced pressure, for example, Equation (6.4), rather than the use of

the freestream values, for example, Equation (6.2), is consistent with the analysis of Hayes and Probstein [3].

6.4 CFD for Hypersonic Flows

Computational fluid dynamics serves as a useful tool for solving the problems of hypersonic flow past flying machines. It is important to understand the grid scheme used to represent the body and the flow field, the numerical algorithms used to obtain the solution for the flow field, and the models used to represent fluid mechanic phenomena, thermodynamic phenomena, and flow properties for developing a computational code. The following are some of the books on CFD presenting the fundamental of this subject in detail.

1. Hirsh C, *Numerical Computation of Internal and External Flows, Volume 2: Computational Methods for Inviscid and Viscous Flows*, John Wiley & Sons, Chichester, England, 1990.
2. Hoffmann K. A, *Computational Fluid Dynamics for Engineers*, Engineering Education System, Austin, TX, 1989.

Computational fluid dynamics is essentially the numerical solutions of the equations of motion that describe the main governing equations, namely, the continuity, momentum, and energy equations. The most general form of these equations are the compressible Navier–Stokes equations for continuum flow regimes and the Boltzmann equation for rarefied or low-density flow regimes. Continuum flow fields have been well simulated for a variety of flow conditions involving viscous/inviscid interactions and/or flow separation by advancing these equations in time until a steady state is achieved. When there is no flow reversal and the flow in the stream-side direction is supersonic, these equations can be simplified by neglecting the streamwise viscous terms. These simplified equations are termed the *parabolized Navier–Stokes equations*. The solution to these equations can be obtained by streamwise marching techniques. When the viscous/inviscid interactions are weak, the equations can be further simplified by decoupling the viscous and inviscid regions from one another and simulating the regions separately in an interactive manner. Here the inviscid Navier–Stokes equations, termed the *Euler equations*, are solved in the inviscid region away from body surfaces. Near the body surface, the viscous-dominated boundary layer equations are solved. A fourth simplification that can be used for strong viscous/inviscid interactions is the viscous shock layer approximation. This method is used for the stagnation region of hypersonic blunt-nosed bodies between the bow shock and the body surface.

To account for the real-gas effects involving thermochemical nonequilibrium, leading to the finite rate process for chemical and energy exchange, and radiative transport, the concentration equations for each chemical species must be added to the governing

equations of the flow field. For dissociating and ionizing air, there are typically 11 species, namely, N_2, O_2, N, O, NO, O^+, N^+, NO^+, N_2^+, O_2^+, and e^-. Addition of concentration equations for each of these species nearly triples the number of equations to be solved. When there are combustion or gas/surface interactions or ablative products, the number of species increases further. To account for thermal nonequilibrium and radiative transport, there are additional energy equations to describe the energy exchange between the viscous energy modes, such as the translational, rotational, vibrational, and electronic energies. The range of time scales involved in thermochemical process is many orders of magnitude wider than the mean flow time scale. This is the single most *complicating factor* in the computation of aerothermodynamics.

Development of Navier–Stokes codes to generate flow field solutions for complex three-dimensional reacting gas flows is expensive and time consuming. Monnoyer *et al.* [4] show that the coupled solution of the second-order boundary layer and the Euler equations provides an efficient tool for the calculation of hypersonic viscous flows. But it is limited to flows with weak interaction only, and no shock/boundary layer or streamwise separation can be considered.

The zonal method is an approach to reduce computational efforts. In this method, the flow field is divided into zones according to the local flow characteristics. For example, the flow over the nose of a blunt-nosed vehicle may be divided into zones 1, 2, and 3 as shown in Figure 6.2.

Zones 1 and 2, being away from the surface, may be treated as inviscid. Also, flow in zone 1 is subsonic and thus elliptic type. Therefore, a time-iterative Euler code may be used to solve the elliptic equations characteristics of the subsonic inviscid flow in the nose region.

Flow in zone 2 is supersonic and thus hyperbolic in nature. This inviscid supersonic flow outside the boundary layer can be solved using a space-stepping Euler code meant for the hyperbolic equation.

Flow in zone 3 is adjacent to the surface is boundary layer flow and, hence, of parabolic type. We know that in the boundary layer, the diffusion in the direction

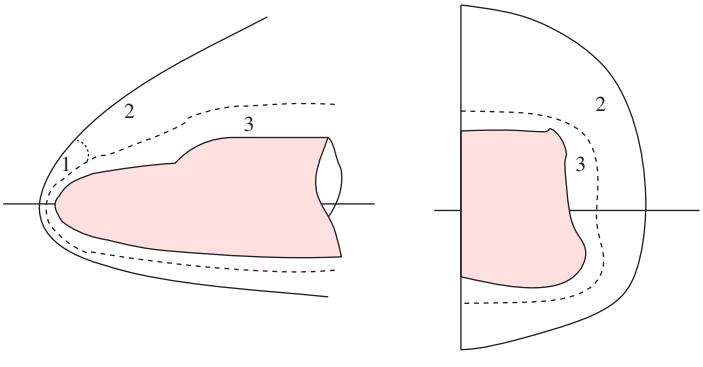

Figure 6.2 Flows zones for hypersonic flow past a blunt-nosed vehicle.

parallel to the surface can be assumed to be negligible and convection in the direction perpendicular to the wall is very small. The boundary layer equations being parabolic type, space-marching technique can be used for solving them.

At this stage, it is essential to note that this approach is reliable only if the boundary layer has little interaction with the inviscid flow. The level of simplifications that may be introduced into the method in order to obtain numerical solutions for the design process depends on the complexity of the application, time available, computer available, and accuracy desired.

6.4.1 Grid Generation

A code used for computing the aerothermodynamic environment requires a subprogram to define the geometric characteristics of the vehicle and a grid scheme to identify points or volumes within the flow field.

Large number of techniques have been developed for generating the computational grids that are required in the finite-difference, finite-volume, and finite-element solution of partial differential equations for arbitrary regions. Choosing the appropriate grid suitable for the numerical method used is the key for the successful calculation of results with acceptable accuracy.

Grids may be structured or unstructured. There are no a priori requirements on how grids are to be oriented. However, in some cases, the manner in which the flow modeling information is formulated may influence the grid structure. For instance, because the turbulence models are often formulated in terms of distance normal to the surface, the grid scheme utilized for these turbulent boundary layers employs surface-oriented coordinates where one of the coordinate axes is locally perpendicular to the body surface.

The computation of the heat transfer or the skin friction requires resolution of the flow very near the surface. The effect of grid density on the computed heat transfer rates for Mach 20 flow past a 5° semi-vertex angle cone was demonstrated by Neumann [5]. He found that there comes a time in the solution when adding additional grid points has no effect on the solution quality.

Siddiqui *et al.* [6] studied the grid-dependency effects on Navier–Stokes solvers for varying amounts of damping (that is, artificial viscosity) and different differentiating schemes. They found that the various algorithms investigated herein are found to be grip dependent, that is, the resolution of the grid affects the quality of the solution. Improper mesh sizes can result in underprediction of the heating rates by orders of magnitude. The degree of accuracy depends on the dissipative nature of the algorithm. The more dissipative a scheme, the finer the grid resolution that will be required for an accurate estimation of the heating loads.

At this stage, it is essential to note that it is not always wise to demand large computing capacity merely to push ahead a few more steps before exponentially growing instabilities caused by numerical truncations swamp the first few significant figures

in the calculations. A more sensible approach is to face the problem with analysis and attempt to suppress nonessential instabilities by appropriate numerical methods. The complexity of the problems makes complete mathematical region in these studies practically impossible; therefore, we are forced to rely on experience with linearized equations and familiarity with the physical problem for help in judging the accuracy of the solution obtained.

6.5 Computation Based on a Two-layer Flow Model

Many of the computer codes that are used to define the aerothermodynamic environment divide the shock-layer flow field (that is, the flow zone between the bow shock wave and the surface of the vehicle) into the following two regimes.

- A rotational, inviscid flow in which the viscous effects are negligible.
- The thin, viscous boundary layer adjacent to the surface.

These two flow zones are illustrated in Figure 6.2. The pressure distribution and the properties at the edge of the boundary layer are determined from the solution of the inviscid flow. Assuming the boundary layer is thin, the pressure is constant across the boundary layer. As a result, the pressure at the surface is equal to the pressure from the inviscid solution at the edge of the boundary layer. The skin friction and the convective heat transfer are determined from the boundary layer solution.

The codes offering a menu of pressure option with relatively simple methods for the boundary layer parameters is referred to as *conceptual design codes*, and the codes in which simplifications to the governing equations are introduced so that the Euler equations are solved to define the inviscid flow and the boundary layer equations are used to describe the inner region.

The term *two-layer* CFD code refers to the second category. Within each category, all individual code will include a number of approximations, representing a wide range of rigor in flow modeling.

6.5.1 Conceptual Design Codes

During the initial phases of a development program, the designer is faced with evaluating the performance of various configurations that might satisfy the mission requirements. Thus, the designer has need for computational tools that are capable of predicting the aerodynamic characteristics, that is, the aerothermodynamic environment, for a wide variety of configurations. The desired code should be economical and easy to use, employing engineering methods that represent realistic modeling of the actual flow about the required configurations over an entire trajectory. As the configurations may contain wings, fins, flaps, etc., the code should be able to model strong shock waves associated with viscous/inviscid interactions.

For computing the inviscid pressure acting on a panel, one of the simple impact or expansion methods can be used. These methods require the angle and, in some cases, the freestream Mach number.

Another approach for determining the local pressure includes the calculation of the interference effects of one component on another. This capability employs some of the simple impact methods but using the change in angle of an element from a previous point and the local flow conditions for that point determined from the flow field subroutine.

The challenging aspect of analyzing the flow over a complex shape is the calculation of the viscous flow due to difficulties in developing simple yet realistic models for turbulence, viscous/inviscid interactions, etc. A thorough knowledge of the local flow properties along surface streamlines is required for a realistic boundary layer solution. The code developed for supersonic/hypersonic arbitrary body program (S/HABP) [7] is an engineering approach for calculating the viscous force in a simple manner, retaining the essential characteristics of the boundary layer. The skin friction is calculated either using the relations for incompressible flow over a flat plate with correlation factors to account for compressibility and the heating (cooling) to the wall or using an integral boundary method.

The detailed distribution for the pressure and the skin friction that are computed using the approximate methods of a conceptual code may differ from the actual distributions.

6.5.2 Characteristics of Two-Layer CFD Models

Vehicle designed for hypersonic flight in the earth's atmosphere are with blunt nose. Owing to this, a detached shock is positioned at the nose of the vehicle, as illustrated in Figure 6.3. The entropy increase across the shock wave depends on the shock inclination angle; thus the entropy downstream of the shock wave is greatest for streamline 1 and least for streamline 3.

Because all the fluid particles originate in the freestream where the total enthalpy is uniform, the flow remains isentropic outside the boundary layer. The assumption that the flow outside the boundary layer is isentropic, that is, the total enthalpy is a constant, is reasonable, unless the temperatures in the inviscid shock-layer flow are sufficiently high so that gas radiate out through the shock layer, a phenomenon that occurs only at very high velocities, that is, in excess of 12 km/s. As the entropy is constant along a streamline for a steady inviscid adiabatic flow, the entropy will vary continuously through the shock layer.

A fluid particle crossing the shock wave at a particular location will retain the entropy and the stagnation pressure associated with the shock inclination at that point where it crossed the shock layer. The entropy and the stagnation pressure will be constant along a streamline until it enters the boundary layer. As the gas flows over the body, all of the high-entropy gas initially processed by the bow shock wave, which

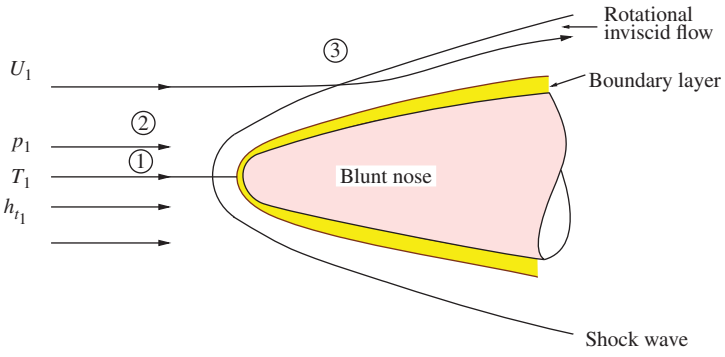

Figure 6.3 Flow past a blunt-nosed vehicle.

is termed the *entropy layer*, is entrained, or swallowed, by the boundary layer (for example, streamlines 1 and 2 in Figure 6.3). Additional gas subsequently entrained by the boundary layer is a cooler lower-entropy gas that has been traversed only the weaker portions of the shock wave (for example, streamline 3). Therefore, it is essential to include entropy-layer analysis to have accurate predictions of quantities such as the edge Mach number and the skin friction.

At low Reynolds number/high Mach number conditions, the interaction between the rotational external flow and the boundary layer would invalidate the two-layer approach. However, at moderate-to-high Reynolds numbers, a coupled Euler/boundary layer approach with features specific to hypersonic flows, for example, gas chemistry, surface catalycity, and entropy swallowing, provides an efficient tool for the calculation of hypersonic viscous flows over a wide range of conditions. The two-layer CFD models are restricted to flows with weak viscous/inviscid interactions. Thus, unless special compensation is introduced to the flow model, flows with streamwise boundary layer or shock/boundary layer interactions should not be considered.

The basic principle of a coupled inviscid region/boundary layer for the flow field is that the flows are matched at their interface. Although there are varieties of ways to compute the two-layer flow field, the classic approach is to solve the inviscid flow field just for the actual configuration. The inviscid flow field solution at the boundary surface provides conditions at the edge of the boundary layer, for example, the pressure, the entropy, and the velocity at the edge of the boundary layer. Subject to the boundary layer conditions at the edge and at the wall, the boundary layer solutions can be obtained. The spreading of adjacent streamlines can be used to define a scale factor or "equivalent cross-section radius," which is analogous to the cross-section radius for an axisymmetric flow. The equivalent cross-section radius determined from the divergence of the streamlines allows a three-dimensional flow to be modeled by the axisymmetric analogue, or small cross-section assumption [8]. As the boundary layer grows, more and more inviscid flow is entrained into the boundary layer. This has two

effects on the flow modeling. The effect of the boundary layer on the inviscid flow is represented by displacing the wall by the displacement thickness, that is, the distance the external streamlines are shifted to account for the mass-flow deficit due to the presence of the boundary layer. Boundary layer growth also changes the conditions at the edge of the boundary layer. The inviscid field might then be computed for the equivalent configuration, that is, the actual configuration plus the displacement thickness.

In a close-coupling strategy, an interactive procedure would be set up, containing until successive computations yielded a flow that is unchanged within some tolerance.

6.5.2.1 Two-Layer Flow Fields

Many codes have been developed to solve steady-state flow fields over complex three-dimensional bodies. In the treatment of Marconi *et al.* [9], all shock waves within the flow field are followed and the Rankine–Hugoniot relations are satisfied across them. Weilmuenster [10] scheme, referred to as *high alpha inviscid solution* (HALIS), using the conservation form of the Euler equations, can capture the shock that lie within the computational domain. To simplify the geometry, the upper surface of the Shuttle wing was filled with an elliptic-curve segment, which eliminated the need to deal with complex viscous-dominated flow field on the lee-side of the wing. With this approximation, the pressure field in the vicinity of the interaction between the fuselage-generated shock wave and the wing-generated shock wave can be computed. It is essential to note that a computer code developed for inviscid flows cannot provide information about the heat transfer to the surface. However, the flow phenomena identified in the computed pressure fields provide insights into the heating environment, including streaks of locally high heating. Weilmuenster found that the streaks originate at a point near the wing/body shock interaction and the severity of the heating decreases with increasing angle of attack that corresponds to a decreased strength of the interior wing shock as determined by the HALIS code.

At relatively high Reynolds numbers, the presence of the boundary layer has a second-order effect on the static pressure acting on the windward surface. At angles of attack where the flow on the lee-side of a slender body separates and forms a vortex pattern, the Euler-based flow models usually fail to represent the attached flow. When such a configuration is treated with an inviscid code, a cross-flow shock develops and the surface pressure ahead of the shock wave becomes unrealistically low. A more realistic lee-side flow pattern can be achieved with an Euler code by employing a semiempirical model in the inviscid flow properties at separation. This technique effectively changes the body surface to simulate flow separation.

6.5.3 Evaluating Properties at the Boundary Layer Edge

Vehicles designed for hypersonic flight through earth's atmosphere usually have blunt nose to reduce the convective heat transfer and alleviate asymmetric vortex effects

associated with subsonic portion of the flight. As a result, the bow shock wave is curved. The entropy increase caused by the shock is proportional to the local inclination of the shock wave and the freestream Mach number. For perfect gas flow, the entropy increase across the shock wave, with local inclination θ_{sw}, is given by [11]

$$s_2 - s_1 = R \ln \left(\frac{p_{01}}{p_{02}} \right) \tag{6.5}$$

where the pitot pressure ratio in terms of Mach number is

$$\frac{p_{02}}{p_{01}} = \left[1 + \frac{2\gamma}{\gamma + 1} \left(M_1^2 \sin^2 \theta_{sw} - 1 \right) \right]^{-1/(\gamma - 1)} \left[\frac{(\gamma + 1) M_1^2 \sin^2 \theta_{sw}}{(\gamma - 1) M_1^2 \sin^2 \theta_{sw} + 2} \right]^{\gamma/(\gamma - 1)}$$

Thus, as we saw (Figure 6.3), the streamline passing through the nearly normal portion of the bow shock wave (for example, streamline 1) experiences a larger entropy increase when crossing the shock than does the streamline passing through the more oblique portion of the shock wave (for example, streamline 3). As the entropy is constant along a streamline for an inviscid, adiabatic and steady flow, the entropy will vary continuously through the shock layer, depending on where the streamline crossed the shock wave. Fluid particles, having crossed the curved shock wave at a particular inclination, retain the entropy and the stagnation pressure associated with the shock inclination as they move through the inviscid shock layer. While moving downstream from the stagnation point, the boundary layer grows into the rotational inviscid flow. The flow entering the boundary layer is initially the hot high-enthalpy gas that has been stagnated, after passing through nearly normal portion of the bow shock wave. As the gas flows over the body, all of the high-entropy gas is eventually entrained, or swallowed, by the boundary layer. Additional gas subsequently entrained by the boundary layer is a cooler low-density gas that has passed through the weaker portion of the shock wave.

The entropy is constant between the streamline crossing the bow shock wave at the tangency point and the shock wave. However, the entropy gradients in the inviscid shock-layer flow that are produced when the flow passes through the curved bow shock wave persist for a considerable length.

The static pressure acting across the boundary layer is relatively insensitive to the flow field. However, significant entropy gradients can persist for considerable distances. Thus, when entropy layer swallowing is being considered, the location of the outer edge of the boundary layer must be defined. Because of rotational nature of the inviscid flow, the velocity and the temperature gradients are not zero at the outer edge of the boundary layer but have values associated with the rotational inviscid flow. The boundary layer edge is often defined as the location where the total enthalpy gradient goes to zero because the inviscid part of the shock layer is usually assumed to be adiabatic. However, the total enthalpy within the boundary layer can exceed the inviscid value of the total enthalpy in certain cases. In these cases, there will be at least two locations where the total enthalpy gradient goes to zero.

Example 6.1 Determine the entropy increase caused by a bow shock in a Mach 7 air stream along the stagnation streamline, treating air as a perfect gas.

Solution

Given $M_1 = 7$ and $\gamma = 1.4$. Along the stagnation streamline, the shock is almost normal with $\theta_w = 0°$.

$$s_2 - s_1 = R \ln \left(\frac{p_{01}}{p_{02}} \right)$$

The pitot pressure ratio in terms of Mach number is

$$\frac{p_{02}}{p_{01}} = \left[1 + \frac{2\gamma}{\gamma + 1} \left(M_1^2 \sin^2 \theta_{sw} - 1 \right) \right]^{-1/(\gamma - 1)} \left[\frac{(\gamma + 1) M_1^2 \sin^2 \theta_{sw}}{(\gamma - 1) M_1^2 \sin^2 \theta_{sw} + 2} \right]^{\gamma/(\gamma - 1)}$$

Therefore,

$$\begin{aligned} \frac{p_{02}}{p_{01}} &= \left[1 + \frac{2.8}{2.4} (7^2 - 1) \right]^{-1/0.4} \left[\frac{2.4 \times 7^2}{0.4 \times 7^2 + 2} \right]^{3.5} \\ &= (57)^{-2.5} (5.44)^{3.5} \\ &= \frac{375.49}{24{,}529.412} \\ &= 0.0153077 \\ \frac{p_{01}}{p_{02}} &= \frac{1}{0.0153077} \\ &= 65.3264 \end{aligned}$$

The increase of entropy caused by the shock is

$$\begin{aligned} \Delta s &= R \ln \left(\frac{p_{01}}{p_{02}} \right) \\ &= 287 \times \ln (65.3264) \\ &= 1199.47 \ \mathrm{m^2/(s^2\ K)} \end{aligned}$$

■

6.6 Calibration and Validation of the CFD Codes

Comparison of the flow properties over the surface and flow field, computed with a CFD code, with experimental data to verify the code's ability to accurately model the physics of the flow, is referred to as *calibration*. In other words, CFD code calibration implies comparison of computed results with experimental data for realistic geometries that are similar to the ones of design interest, made in order to provide a measure

of the code's ability to predict parameters that are required for the design without necessarily verifying that all the features of the flow are correctly modeled.

Some code developers prefer to compare the results computed using the code under development with the results computed using an established CFD code. When comparing absolute values, such as drag coefficient, all sources of experimental, as well as computational, errors must be evaluated. For example, because drag is sensitive to Reynolds number, the measurement accuracy of Reynolds number as well as the other parameters should be evaluated. As all initial and boundary conditions used in a computation cannot or have not been measured, code sensitivity to those conditions should be analyzed. All sources of error in the experimental data should be documented. The sensitivity of the computer code to grid size and shape, and the initial and boundary conditions, should be documented. This is essential when the code is run by users who did not develop the code.

Thus, the designer of a hypersonic vehicle must make use of both experimental and analytical tools available. Although neither ground-test facilities nor CFD provides the complete answer to a designer's needs, each offers certain advantages. CFD can give greater detail of a flow field than is possible in any wind tunnel, as all aerodynamic parameters are computed at each grid point. CFD provides a capability for configuration optimization for determining the effect of configuration changes before commitment to model construction is made. Thus, CFD helps in making more effective use of ground-test facilities. On the other hand, when integrated forces and moments are desired, CFD is subject to the inherent mathematical inaccuracies associated with small differences of large numbers.

6.7 Basic CFD – Intuitive Understanding

The purpose of this section is to provide plain explanation for CFD for beginners and undergraduate students.[1] Only essential key points of CFD are explained in an easy-to-understand way by omitting strictly organized theories. At the end of this section, a CFD technique is presented to solve a supersonic-flow problem based on the two-dimensional Euler equations in even-spacing orthogonal grid. For readers who already know CFD techniques and are looking for further and detailed knowledge of CFD, it is strongly recommended to see other textbooks specialized in CFD.

6.7.1 Governing Equations Based on Conservation Law

When we try to solve flow fields with CFD, the governing equations are usually written based on *conservation law*, that is, the equations describe the variation of *conserved*

[1] This section was developed by Dr. Yasumasa Watanabe, following some portion of the lectures of Professor Kojiro Suzuki in his course "Aerodynamics Lecture II-B, Department of Aeronautics and Astronautics, The University of Tokyo" for third year undergraduate students. Dr. Watanabe added a lot of material to help students, who are beginners to CFD, to understand the CFD basics.

quantity, for example, mass, momentum, and energy, at a certain *control volume*. Let q denote any conserved quantity per unit volume. Then, gross amount in a certain control volume V is $\iiint_V q dV$. Any change in conserved quantity in V can only take place via *flux* $\vec{\mathcal{F}}$ of q that goes through its boundary Ω, $\vec{\mathcal{F}} = q\vec{u}$. Net increase in the property q through the boundary Ω is written as $-\iint_\Omega \vec{\mathcal{F}} \cdot d\vec{S}$, where S denotes surface area. The reason for the minus sign in the above term is that the positive direction of $\vec{\mathcal{F}}$ is always in the direction going outside through the boundary. We can also think of extra change in q at volume V invoked by external factors such as gravity force. If we write such change by external factors per unit volume per unit time as $\dot{\varphi}$, we obtain general form of any conservation equations as

$$\frac{\partial}{\partial t}\iiint_V q dV = -\iint_\Omega \vec{\mathcal{F}} \cdot d\vec{S} + \iiint_V \dot{\varphi} dV \tag{6.6}$$

Substituting well-known Gauss's law $\iint_\Omega \vec{\mathcal{F}} \cdot d\vec{S} = \iiint_V \nabla \cdot \vec{\mathcal{F}} dV$, we get

$$\frac{\partial}{\partial t}\iiint_V q dV = -\iiint_V \nabla \cdot \vec{\mathcal{F}} dV + \iiint_V \dot{\varphi} dV \tag{6.7}$$

Therefore,

$$\frac{\partial q}{\partial t} + \nabla \cdot \vec{\mathcal{F}} = \dot{\varphi} \tag{6.8}$$

Expanding second term in the above equation, we finally get

$$\frac{\partial q}{\partial t} + \frac{\partial (qu)}{\partial x} + \frac{\partial (qv)}{\partial y} + \frac{\partial (qw)}{\partial z} = \dot{\varphi} \tag{6.9}$$

The control volume for this problem is as shown in Figure 6.4.

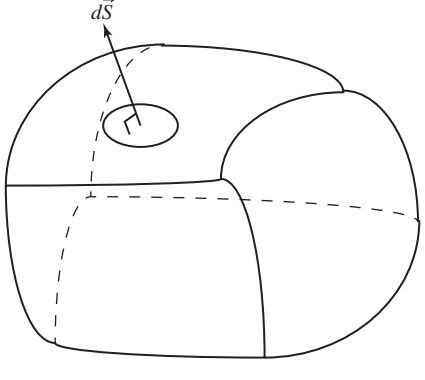

Figure 6.4 Control volume.

6.7.2 Euler Equations in Conservation Form

The Euler equations are composed of mass, momentum, and energy conservation equations. Substituting $q = \rho$, Equation (6.9) yields mass conservation equation.

$$q = \rho, \quad \dot{\varphi} = 0 \tag{6.10}$$

$$\frac{\partial \rho}{\partial t} + \frac{\partial(\rho u)}{\partial x} + \frac{\partial(\rho v)}{\partial y} + \frac{\partial(\rho w)}{\partial z} = 0 \tag{6.11}$$

Substituting $q = (\rho u, \rho v, \rho w)^T$, Equation (6.9) yields momentum equations.

$$q = \begin{pmatrix} \rho u \\ \rho v \\ \rho w \end{pmatrix}, \quad \dot{\varphi} = \begin{pmatrix} -\frac{\partial p}{\partial x} \\ -\frac{\partial p}{\partial y} \\ -\frac{\partial p}{\partial z} \end{pmatrix} \tag{6.12}$$

$$\frac{\partial}{\partial t}\begin{pmatrix} \rho u \\ \rho v \\ \rho w \end{pmatrix} + \frac{\partial}{\partial x}\begin{pmatrix} \rho u^2 \\ \rho uv \\ \rho uw \end{pmatrix} + \frac{\partial}{\partial y}\begin{pmatrix} \rho vu \\ \rho v^2 \\ \rho vw \end{pmatrix} + \frac{\partial}{\partial z}\begin{pmatrix} \rho wu \\ \rho wv \\ \rho w^2 \end{pmatrix} = \begin{pmatrix} -\frac{\partial p}{\partial x} \\ -\frac{\partial p}{\partial y} \\ -\frac{\partial p}{\partial z} \end{pmatrix} \tag{6.13}$$

In order to obtain the energy conservation equation, q is set to be $q =$(total energy per unit volume)$= E_t = \rho e + \frac{1}{2}(u^2 + v^2 + w^2)$, where $e = c_v T$ is the internal energy per unit mass. Ignoring works done by external body force and heat transfer and considering only the work done by the pressure, $\dot{\varphi}$ can be written as $\dot{\varphi} = \nabla \cdot (-p\vec{u})$. Finally, we obtain the energy equation as

$$q = E_t = \rho e + \frac{1}{2}(u^2 + v^2 + w^2), \quad \dot{\varphi} = \frac{\partial}{\partial x}(-pu) + \frac{\partial}{\partial y}(-pv) + \frac{\partial}{\partial z}(-pw) \tag{6.14}$$

$$\frac{\partial E_t}{\partial t} + \frac{\partial(uE_t)}{\partial x} + \frac{\partial(vE_t)}{\partial y} + \frac{\partial(wE_t)}{\partial z} = \frac{\partial}{\partial x}(-pu) + \frac{\partial}{\partial y}(-pv) + \frac{\partial}{\partial z}(-pw)$$

Therefore,

$$\frac{\partial E_t}{\partial t} + \frac{\partial[u(E_t + p)]}{\partial x} + \frac{\partial[v(E_t + p)]}{\partial y} + \frac{\partial[w(E_t + p)]}{\partial z} = 0 \tag{6.15}$$

There are, of course, the Euler equations in nonconservation form such as

$$\left(\frac{\partial}{\partial t} + u\frac{\partial}{\partial x} + v\frac{\partial}{\partial y}\right)\begin{pmatrix} u \\ v \\ \rho \\ T \end{pmatrix} = \begin{pmatrix} -\frac{1}{\rho}\frac{\partial p}{\partial x} \\ -\frac{1}{\rho}\frac{\partial p}{\partial y} \\ -\rho\nabla \cdot \vec{u} \\ -p\nabla \cdot \vec{u}/(\rho c_v) \end{pmatrix} \tag{6.16}$$

(an example of the 2D Euler equations)

However, in most cases, when we work on CFD for compressible gas dynamic problems, conservation form equations are numerically solved but nonconservation form equations are only occasionally employed as governing equations. This is because conservation laws and corresponding equations in conservation form equations are valid even if there are shock waves where discrete changes in properties would take place. By contraries, differential terms in nonconservation form, such as differentials of u, v, ρ, and T in Equation (6.16), cannot be defined at shock wave positions and they even diverges at shock waves.

6.7.3 Characteristics of Fluid Dynamic Equations

Before solving the practical gas dynamic problems, we will first check the characteristics of the one-dimensional Euler equations in order to guess what kind of numerical techniques are required in solving high-speed fluid dynamic problems.

The 1D Euler equations are given as

$$\frac{\partial Q}{\partial t} + \frac{\partial E}{\partial x} = 0 \tag{6.17}$$

where

$$Q = \begin{pmatrix} \rho \\ \rho u \\ E_t \end{pmatrix}, \quad E = \begin{pmatrix} \rho u \\ \rho u^2 + p \\ u(E_t + p) \end{pmatrix} \tag{6.18}$$

Equation (6.17) can be transformed into the following form with simple calculation.

$$\frac{\partial Q}{\partial t} + A \frac{\partial Q}{\partial x} = 0 \tag{6.19}$$

where

$$A = \frac{\partial E}{\partial Q} = \begin{pmatrix} 0 & 1 & 0 \\ \frac{\gamma-3}{2}u^2 & (3-\gamma)u & \gamma - 1 \\ \frac{\gamma-2}{2}u^3 - \frac{\gamma}{\gamma-1}\frac{p}{\rho}u & \frac{3-2\gamma}{2}u^2 + \frac{\gamma}{\gamma-1}\frac{p}{\rho} & \gamma u \end{pmatrix} \tag{6.20}$$

As the above Euler equations are a set of coupled equations, it would be a good idea to decouple the equations to see the essence of the same.

In order to decouple these equations, we can first find the eigenvalues of a matrix A by solving an equality

$$|\lambda I - A| = 0 \tag{6.21}$$

and three eigenvalues λ_1, λ_2, and λ_3 are obtained as

$$\begin{Bmatrix} \lambda_1 = u - c \\ \lambda_2 = u \\ \lambda_3 = u + c \end{Bmatrix} \tag{6.22}$$

where $c = \sqrt{\gamma \frac{p}{\rho}}$ is the local speed of sound.

Corresponding eigenvectors $\vec{q}_1$, $\vec{q}_2$, and $\vec{q}_3$ can also be obtained, and the matrix A can be diagonalized to be

$$A = R\Lambda R^{-1} \tag{6.23}$$

where

$$\Lambda = \begin{pmatrix} \lambda_1 & 0 & 0 \\ 0 & \lambda_2 & 0 \\ 0 & 0 & \lambda_3 \end{pmatrix} \tag{6.24}$$

$$R = (\vec{q}_1,\ \vec{q}_2,\ \vec{q}_3) = \begin{pmatrix} 1 & 1 & 1 \\ u-c & u & u+c \\ H-uc & \frac{1}{2}u^2 & H+uc \end{pmatrix} \tag{6.25}$$

$$R^{-1} = \begin{pmatrix} \frac{1}{2}\left(a+\frac{u}{c}\right) & -\frac{1}{2}\left(bu+\frac{1}{c}\right) & \frac{1}{2}b \\ 1-a & bu & -b \\ \frac{1}{2}\left(a-\frac{u}{c}\right) & -\frac{1}{2}\left(bu-\frac{1}{c}\right) & \frac{1}{2}b \end{pmatrix} \tag{6.26}$$

$$a = b\frac{u^2}{2}, \quad b = \frac{\gamma-1}{c^2} \tag{6.27}$$

and H is the total enthalpy.

$$H = \frac{c^2}{\gamma-1} + \frac{u^2}{2} = c_p T + \frac{u^2}{2} = h + \frac{u^2}{2} \tag{6.28}$$

Substituting Equation (6.23) into Equation (6.19) and multiplying R^{-1} from the left side, the one-dimensional Euler equations can be finally decoupled to be separate advection equations as

$$\frac{\partial}{\partial t}(R^{-1}Q) + \Lambda\frac{\partial}{\partial x}(R^{-1}Q) = 0 \tag{6.29}$$

The simplest form of the well-known advection equation is written as

$$\frac{\partial u}{\partial t} + a\frac{\partial u}{\partial x} = 0 \tag{6.30}$$

Here, a is the wave propagation speed because it is well known that the analytical solution can be written as $u = U_{\text{initial}}(x - at)$ (wave propagation). Therefore, the decoupled one-dimensional Euler equations given in Equation (6.29) reveals that in a flow field, any perturbation or waves will propagate with the speed of $\lambda_1 = u - c$, $\lambda_2 = u$, and $\lambda_3 = u + c$. It should be noted that eigenvalues $\lambda_1 = u - c$ and $\lambda_3 = u + c$ is the speed of acoustic wave in a flow field and the eigenvalue $\lambda_2 = u$ is the particle speed, suggesting that any information in fluid flow is conveyed by the acoustic wave or the particle's movement.

From the above discussions, we can see that numerical techniques to solve the one-dimensional advection equation can be a basis as well as a key point of solving the Euler equations.

6.7.4 *Advection Equation and Solving Techniques*

Let us consider the simplest form of the one-dimensional advection problem.

Governing Equation

$$\frac{\partial u(x,t)}{\partial t} + a\frac{\partial u(x,t)}{\partial x} = 0 \quad (a > 0) \tag{6.31}$$

Initial Condition

$$u(x,t) = u_0(x,t) \tag{6.32}$$

Boundary Condition

$$u(0,t) = u_1(t), \quad u(L,t) = u_2(t) \tag{6.33}$$

The computational domain is as shown in Figure 6.5.

In this problem, a numerical solution can be discretized in *t*-*x* plane (in Figure 6.5) as follows.

$$u_i^n = u(x_i, t_n) = u(i\Delta x, n\Delta t) \tag{6.34}$$

In case of a linear initial value problem such as the one in this section, the *Lax Evidence theorem* tells us what kind of numerical schemes should be employed to obtain accurate solution of the partial differential equation. According to the Lax Evidence

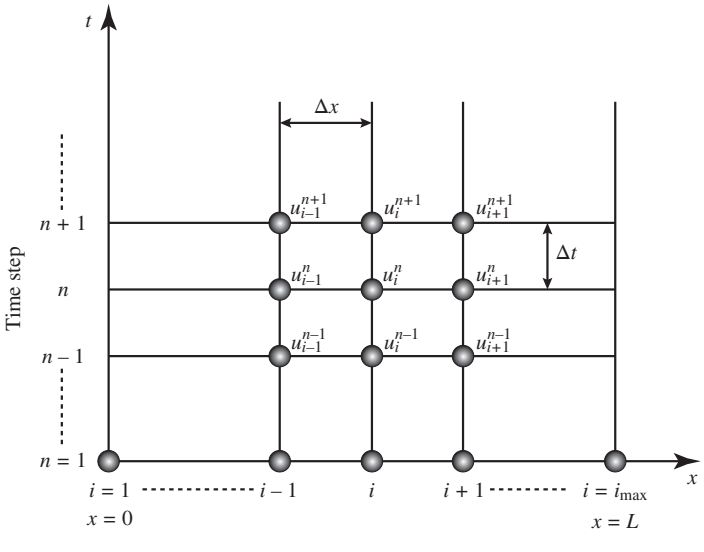

Figure 6.5 Computational domain.

theorem, if a *consistent finite difference scheme* is used and if the scheme is *stable*, obtained numerical solution converges to the exact solution of the partial differential equation.

Roughly speaking, the requirement for "consistent finite difference scheme" in the above theorem restricts the time step Δt in the computation.

If we discretize the advection equation with famous FTCS (forward-time central-space) scheme as

$$\frac{\partial u}{\partial t} = \frac{u_i^{n+1} - u_i^n}{\Delta t} \tag{6.35}$$

$$\frac{\partial u}{\partial x} = \frac{{u_{i+1}}^n - {u_{i-1}}^n}{2\Delta x} \tag{6.36}$$

The advection equation can be written in a discretized form as

$$u_i^{n+1} = u_i^n - \frac{1}{2}\frac{a\Delta t}{\Delta x}\left({u_{i+1}}^n - {u_{i-1}}^n\right) \tag{6.37}$$

Here, the term

$$\nu = \frac{a\Delta t}{\Delta x} \tag{6.38}$$

is called *Courant–Friedrichs–Lewy number* or just simply *Courant number*. The Courant number is interpreted as a ratio of "analytical (physical) wave propagation distance in time period Δt" ($= a \times \Delta t$) to "numerical domain of dependence" ($= \Delta x$). As the quantity u_i^{n+1} in the next time step is obtained by adding information from $(i-1)$th to $(i+1)$th grid point, this numerical information source region or the *numerical domain of dependence* Δx must contain *physical domain of dependence* $a\ \Delta t$ in which any perturbation only in this region affects the quantity in the next time step. The above statement can be expressed with an inequality

$$a\ \Delta t < \Delta x \tag{6.39}$$

Therefore,

$$\nu = \frac{a\ \Delta t}{\Delta x} < 1 \tag{6.40}$$

Hence, *Courant–Friedrichs–Lewy condition* provides confinement to the time step value Δt as

$$\Delta t < \nu\frac{\Delta x}{a} \tag{6.41}$$

The Courant condition is illustrated in Figure 6.6.

As to the other requirement for *stability*, we can roughly understand it as *to use numerical scheme that is appropriate for the phenomenon under consideration*, that is, we need to calculate properties in the next time step paying attention to the wave propagation direction, the accuracy of the scheme, and the monotonicity required to solve shock waves.

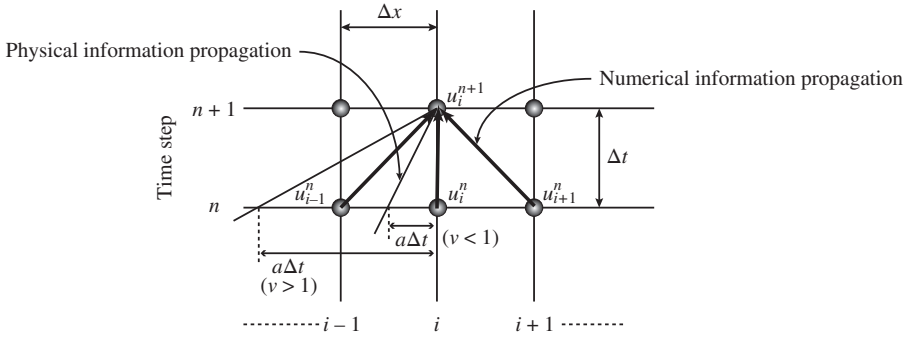

Figure 6.6 Courant condition.

6.7.4.1 Concept of Numerical Flux

In CFD, we usually describe numerical schemes using a concept of *numerical flux*. If we set $f = au$, then the linear advection equation can also be written as

$$\frac{\partial u}{\partial t} + \frac{\partial f}{\partial x} = 0, \quad (a > 0) \tag{6.42}$$

This equation can be discretized using numerical flux $\tilde{f}^n_{i+1/2}$ as

$$u_i{}^{n+1} = u_i{}^n - \frac{\Delta t}{\Delta x}\left(\tilde{f}^n_{i+1/2} - \tilde{f}^n_{i-1/2}\right) \tag{6.43}$$

Schematic concept of *numerical flux* $\tilde{f}^n_{i+1/2}$ is illustrated in Figure 6.7.

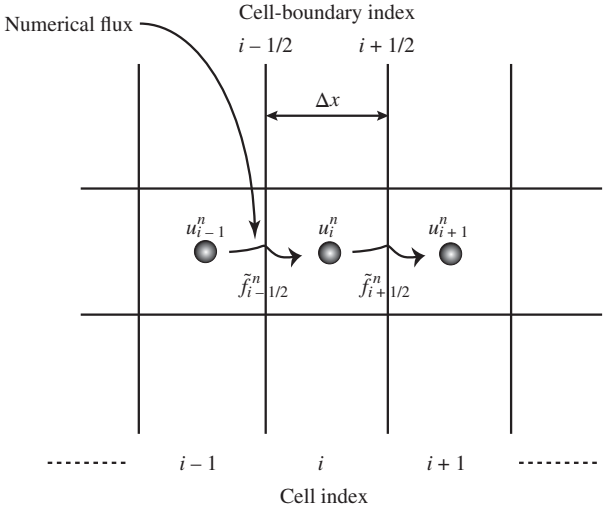

Figure 6.7 Numerical flux.

The numerical flux $\tilde{f}^n_{i+1/2}$ can be interpreted as a flux of a quantity, the quantity u in this case, going out from ith cell to $(i+1)$th cell. Here, we think of u^n_i as an averaged value in ith cell. By using the concept of numerical flux, the quantity u increases by $\frac{\Delta t}{\Delta x}\tilde{f}^n_{i-1/2}$ due to the flux coming into the ith cell through $(i-1/2)$th cell boundary. It also decreases by $\frac{\Delta t}{\Delta x}\tilde{f}^n_{i+1/2}$ due to the flux going out from the ith cell through $(i+1/2)$th cell boundary. Therefore, the net amount of change in an averaged property u in ith cell is evaluated to be $-\frac{\Delta t}{\Delta x}\left(\tilde{f}^n_{i+1/2}-\tilde{f}^n_{i-1/2}\right)$.

The difference of numerical schemes can also be stated as a difference between expressions of numerical flux term $\tilde{f}^n_{i+1/2}$.

Examples of flux expression for several conventional schemes are written as follows.

FTCS (Forward-Time Central-Space) Scheme

$$\tilde{f}^n_{i+1/2} = \frac{1}{2}(f^n_{i+1} + f^n_i) \tag{6.44}$$

First-Order Upwind Scheme

$$\tilde{f}^n_{i+1/2} = f^n_i \tag{6.45}$$

Lax–Wendroff Scheme

$$\tilde{f}^n_{i+1/2} = \frac{1}{2}(1-\nu)f^n_{i+1} + \frac{1}{2}(1+\nu)f^n_i \tag{6.46}$$

where $f^n_i = au^n_i$.

If we evaluate and expand ${u_{i+1}}^n$ or ${u_i}^{n+1}$ with Taylor expansion

$$u^n_{i+1} = u^n_i + \Delta t \cdot \frac{\partial u}{\partial t} + \frac{1}{2}\Delta t^2 \frac{\partial^2 u}{\partial t^2} + \frac{1}{6}\Delta t^3 \frac{\partial^3 u}{\partial t^3} + \cdots \tag{6.47}$$

$$u^{n+1}_i = u^n_i + \Delta x \cdot \frac{\partial u}{\partial x} + \frac{1}{2}\Delta x^2 \frac{\partial^2 u}{\partial x^2} + \frac{1}{6}\Delta x^3 \frac{\partial^3 u}{\partial x^3} + \cdots \tag{6.48}$$

we can easily see that the FTCS scheme is a second-order scheme, first-order upwind scheme is a first-order scheme, and Lax–Wendroff scheme is a second-order scheme. As numerical flux is a imaginary flux that goes through the cell boundary, its expressions can be defined arbitrarily. However, the accuracy must be evaluated by expanding the terms. It should be noted that FTCS scheme evaluates the flux $\tilde{f}^n_{i+1/2}$ as an average of neighboring cells, that is, it takes information evenly from both upstream $(-i)$ direction and downstream $(+i)$ direction. The first-order Upwind scheme evaluates the flux $\tilde{f}^n_{i+1/2}$ only taking the information from upstream cell in the $-i$ direction; therefore, it is called *upstream* scheme. The Lax–Wendroff scheme evaluates the flux $\tilde{f}^n_{i+1/2}$ as a weighted average of neighboring cells.

TVD Scheme

Let us solve the linear advection equation with the above three conventional schemes and see the advantages and characteristics of each schemes.

A sample code *wave.f* to solve 1D linear advection equation is given as follows:

```
      program ex6x1
c
c *** Sample code for 1d linear advection problem ***
c
      parameter (ndim=101)
      dimension x(ndim),uini(ndim),uan(ndim),u(ndim),flux(ndim)
c     <1> parameters
      mx    = 11
      nlast = 4
      cfl   =.5
      a     = 1.
      dx    = 1.
      dt    = cfl/(a/dx)
c     <2> grid
      do 100 i=1,mx
         x(i)=dx*float(i-1)
 100  continue
c     <3> initial condition
      do 200 i=1,mx
         if (x(i).lt.5.) then
            uini(i)=1.
         else
            uini(i)=0.
         end if
 200  continue
c     <4> analytical solution
      prop=float(nlast)*dt
      do 300 i=1,mx
         if (x(i).lt.5.+prop) then
            uan(i)=1.
         else
            uan(i)=0.
         end if
```

```
 300  continue
c     <5> numerical solution
      do 400 i=1,mx
         u(i)=uini(i)
 400  continue
      do 500 n=1,nlast
         do 510 i=1,mx-1
c     <5-1> FTCS
            flux(i)=.5*(a*u(i+1)+a*u(i))
c     <5-2> 1st-order Upwind
c            flux(i)=a*u(i)
c     <5-3> Lax-Wendroff
c            flux(i)=.5*(1-cfl)*a*u(i+1)+.5*(1+cfl)*a*u(i)
 510     continue
         do 520 i=2,mx-1
            u(i)=u(i)-dt/dx*(flux(i)-flux(i-1))
 520     continue
 500  continue
c     *** result file ***
      open(unit=50,file='wave.txt',form='formatted')
      write(50,*) ' x u(initial) u(analytical) u(numerical)'
      do 600 i=1,mx
         write(50,700) x(i),uini(i),uan(i),u(i)
 600  continue
 700  format(4E16.8)
      close(unit=50)
      stop
      end
```

Numerical solutions obtained by using FTCS, first-order upwind, and Lax–Wendroff schemes are shown in Figures 6.8–6.10.

It can be easily understood that in case of FTCS in Figure 6.8, the wave form is broken and the scheme failed to compute the solution. This is because FTCS takes wave propagation information evenly from both upstream (that is, u_{i-1}^n in $-i$ direction) and downstream sides. In case of first-order Upwind scheme, the wave form propagation was successfully captured by the computation but its discrete change in the initial wave form was smoothed by the scheme's dissipation effect because its accuracy is only up to first order. By contraries, the Lax–Wendroff scheme could successfully transfer the wave form with a good accuracy because the scheme is constructed with

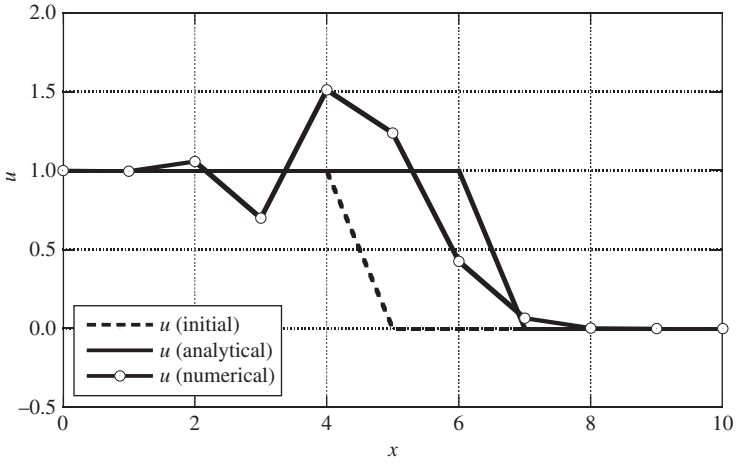

Figure 6.8 Numerical result with FTCS scheme after four steps with Courant number $\nu = 0.5$.

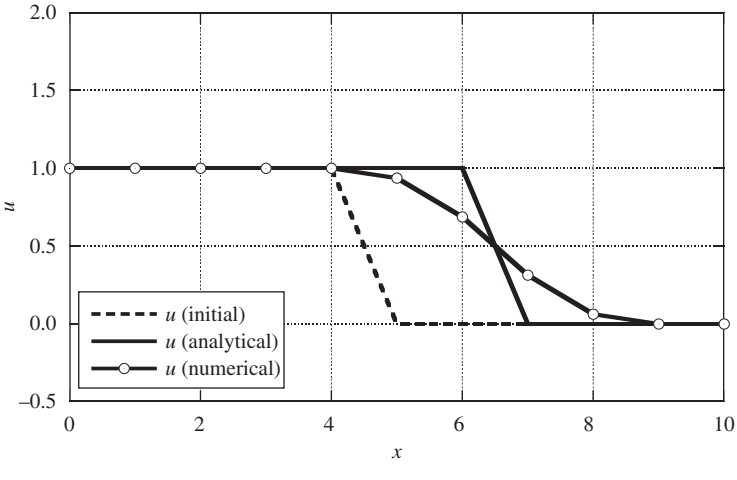

Figure 6.9 Numerical result with first-order Upwind scheme after four steps with Courant number $\nu = 0.5$.

an accuracy of second order. However, the wave form was slightly disturbed and we can see a spurious oscillation at $4 < x < 5$. This is a direct consequence of using high-order scheme because Lax–Wendroff scheme tries to capture the wave form using something like second-order polynomial. Therefore, it cannot allow the wave form to change suddenly as in a shock wave. Especially, the overshoot of properties in CFD becomes a serious problem when we deal with chemical reaction problems because any overshoot in temperature estimation lead to a huge misestimation of reaction rate and its result will suffer from the error caused by unreal overshoot. Therefore, we can combine and make use of both the advantage of the first-order Upwind

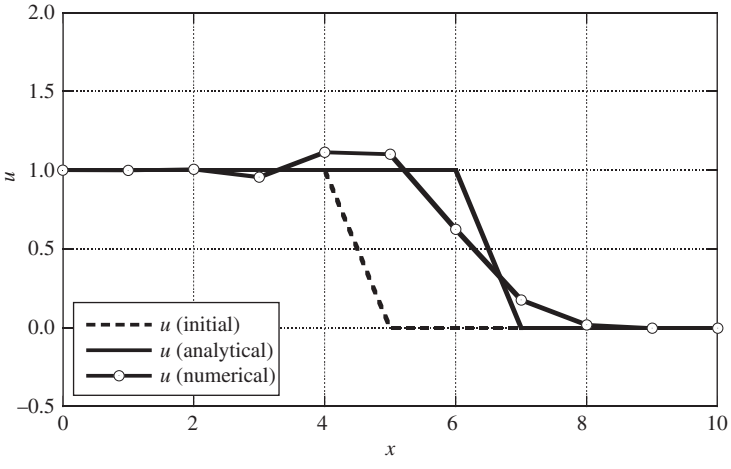

Figure 6.10 Numerical result with Lax–Wendroff scheme after four steps with Courant number $\nu = 0.5$.

scheme to capture the shock without any spurious oscillation and the advantage of the Lax–Wendroff scheme to accurately capture the waveform other than the shock.

Such kind of schemes to suppress spurious oscillations and realize high-order scheme other than shock waves are called total variation diminishing (TVD) scheme. As a hybrid scheme of first-order Upwind and Lax–Wendroff scheme, a general form of such flux can be written as

$$u_i^{n+1} = u_i^n - \frac{\Delta t}{\Delta x}\left(u_{i+1}{}^n - u_{i-1}{}^n\right) \tag{6.49}$$

$$\tilde{f}_{i+1/2}^n = a\left(u_i^n + \frac{1}{2}(1-\nu)B_{i+1/2}(u_{i+1}{}^n - u_i{}^n)\right) \tag{6.50}$$

When the term $B_{i+1/2} = 0$, Equation (6.50) yields first-order Upwind scheme, and when $B_{i+1/2} = 1$, Equation (6.50) gives Lax–Wendroff scheme. The idea is to control $B_{i+1/2}$ depending on the wave form so that we can make use of high-accuracy scheme, and therefore, the term $B_{i+1/2}$ is called *limiter function*. In case the wave form is smoothly changing, we can keep $B_{i+1/2}$ to be around 1.0 to realize high accuracy. On the other hand, when there is a discrete change in a wave form, $B_{i+1/2}$ should be set to 0.0. There are many well-known limiter functions such as

$$\begin{aligned} B_{i+1/2} &= \text{minmod}(1, r), \quad \text{minmod}(x_1, x_2) \\ &= \text{sign}(x_1) \cdot \max(0, \min(|x_1|, x_2 \cdot \text{sign}(x_1))) \end{aligned} \tag{6.51}$$

(Minmod function)

$$B_{i+1/2} = \max(0, \min(2r, 1), \min(2, r)) \tag{6.52}$$

(Superbee function)

Here, parameter r is an indicator of wave-form smoothness and defined as

$$r_i = \frac{u_i^n - u_{i-1}{}^n}{u_{i+1}{}^n - u_i^n} = \frac{\text{Increase of } u \text{ at upstream side}}{\text{Increase of } u \text{ at downstream side}} \tag{6.53}$$

When $r \sim 1$, then the wave form is almost straight and $B_{i+1/2}$ needs to be set to 1.0.

One of the conventional and famous TVD scheme was proposed by Yee [12] and is called *Yee's symmetric TVD scheme*. In this scheme, a numerical flux can be written as

$$\tilde{f}_{i+1/2}^n = a\left(u_i^n + \frac{1}{2}(1-\nu)B_{i+1/2}(u_{i+1}^n - u_i^n)\right) = \frac{1}{2}\left((f_{i+1}^n + f_i^n) + \phi_{i+1/2}\right) \tag{6.54}$$

where

$$\phi_{i+1/2} = -a(u_{i+1}^n - u_i^n) + a(1-\nu)B_{i+1/2}(u_{i+1}^n - u_i^n) \tag{6.55}$$

Let $B_{i+1/2}(u_{i+1}^n - u_i^n) = \widehat{Q}_{i+1/2}$, then

$$\phi_{i+1/2} = -(a\nu\widehat{Q}_{i+1/2} + a(u_{i+1}^n - u_i^n - \widehat{Q}_{i+1/2})) \tag{6.56}$$

The above equations are constructed assuming $a > 0$. If we generalize the equations and allow a to be $a < 0$, we can write

$$\phi_{i+1/2} = -\left(\frac{\Delta t}{\Delta x}a^2\widehat{Q}_{i+1/2} + |a|(u_{i+1}^n - u_i^n - \widehat{Q}_{i+1/2})\right) \tag{6.57}$$

Here, $\widehat{Q}_{i+1/2}$ is a limiter function and we can apply, for example,

$$\widehat{Q}_{i+1/2} = \text{minmod}(\Delta_{i-1/2}, \Delta_{i+1/2}, \Delta_{i+3/2}) \tag{6.58}$$

$$\widehat{Q}_{i+1/2} = \text{minmod}\left(2\Delta_{i-1/2}, 2\Delta_{i+1/2}, 2\Delta_{i+3/2}, \frac{1}{2}(\Delta_{i-1/2} + \Delta_{i+3/2})\right) \tag{6.59}$$

One thing that should be noted here is that when $|a| \ll 1$ and a is almost equal to zero,

$$\phi_{i+1/2} = -\left(\frac{\Delta t}{\Delta x}a^2\widehat{Q}_{i+1/2} + |a|(u_{i+1}^n - u_i^n - \widehat{Q}_{i+1/2})\right) \tag{6.60}$$

is also nearly zero and the numerical flux $\tilde{f}_{i+1/2}^n$ is evaluated as an FTCS scheme. In such a case, the wave form would be broken and the computation may fail to capture the wave propagation. In order to avoid such problems, $|a|$ in Equation (6.60) is replaced with

$$|a| \to \Psi(a) = \left\{ \begin{array}{ll} |a| & (\text{If} |a| > \delta) \\ \frac{a^2+\delta^2}{2\delta} & (\text{If} |a| < \delta) \end{array} \right\} \tag{6.61}$$

$$\phi_{i+1/2} = -\left(\frac{\Delta t}{\Delta x}a^2\widehat{Q}_{i+1/2} + \Psi_{i+1/2}(u_{i+1}^n - u_i^n - \widehat{Q}_{i+1/2})\right) \tag{6.62}$$

where $\delta \sim O(0.1)$. The above correction is called *entropy correction* because the manipulation of avoiding $\phi_{i+1/2}$ to be zero works as an increase in numerical

viscosity (nonphysical viscosity that accompanies numerical scheme) and thereby making entropy to increase to avoid the formation of nonphysical expansion shock in a computation. For more details, see an article by Yee [12].

There are many other TVD-type schemes. Readers are recommended to check other schemes because there is no all-purpose scheme applicable to all the problems.

Finally, the following sample code is a linear advection equation solver with Yee's symmetric TVD scheme.

```
      program ex6x2
c
c     FORTRAN sample code for 1d linear advection problem
c
      parameter (ndim=100)
      dimension x(ndim),uini(ndim),uan(ndim),u(ndim),flux(ndim)
c     <1> parameters
      mx    = 41
      nlast = 20
      cfl   =.5
      a     = 1.
      dx    = 0.25
      dt    = cfl/(a/dx)
      corr  = 0.1
c     <2> grid
      do 100 i=1,mx
         x(i)=dx*float(i-1)
 100  continue
c     <3> initial condition
      do 200 i=1,mx+1
         if (x(i).lt.5.) then
            uini(i)=1.
         else
            uini(i)=0.
         end if
 200  continue
c     <4> analytical solution
      prop=float(nlast)*dt
      do 300 i=1,mx
         if (x(i).lt.5.+prop) then
            uan(i)=1.
```

```
         else
            uan(i)=0.
         end if
 300  continue
c     <5> numerical solution
      do 400 i=1,mx+1
         u(i)=uini(i)
 400  continue
      do 500 n=1,nlast
        do 510 i=2,mx-1
         d1=u(i)-u(i-1)
         d2=u(i+1)-u(i)
         d3=u(i+2)-u(i+1)
         sg=sign(1.,d1)
         ql=sg*amax1(0.,amin1(2.*sg*d1,2.*sg*d2,2.*sg*d3,.5*sg*(d1+d3)))
         ph=abs(a)
         if(ph.lt.corr) then ph=(ph**2+corr**2)/(2.*corr)
         pha=-(dt/dx*a**2*ql+ph*(d2-ql))
         flux(i)=.5*(a*u(i+1)+a*u(i)+pha)
 510    continue
        do 520 i=3,mx-1
           u(i)=u(i)-dt/dx*(flux(i)-flux(i-1))
 520    continue
 500  continue
c     *** result file ***
      open(unit=50,file='wave.txt',form='formatted')
      write(50,*) ' x u(initial) u(analytical) u(numerical)'
      do 600 i=1,mx
         write(50,700) x(i),uini(i),uan(i),u(i)
 600  continue
 700  format(4E16.8)
      close(unit=50)
      stop
      end
```

The result is shown in Figure 6.11. The wave form propagation is successfully solved with high accuracy without any spurious oscillation.

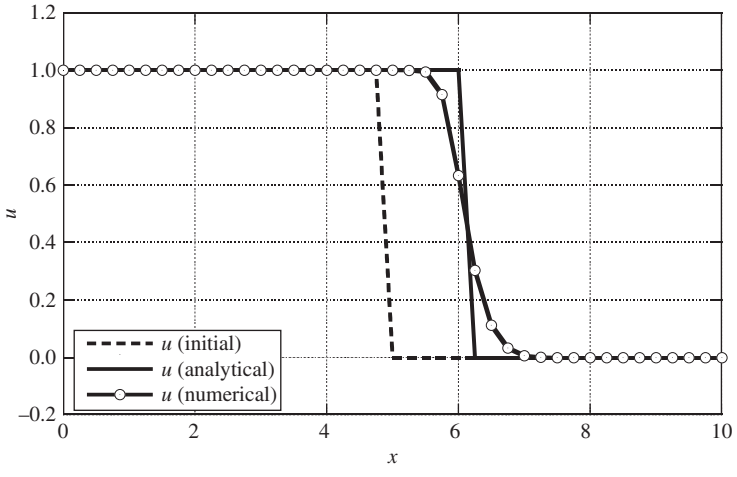

Figure 6.11 Numerical result with Yee's symmetric TVD scheme after 20 steps with Courant number $\nu = 0.5$.

6.7.5 Solving Euler Equations – Extension to System Equations

Yee's symmetric TVD scheme can be extended to system equations such as the 1D Euler equations as follows.

One-Dimensional Euler Equations

$$\frac{\partial Q}{\partial t} + \frac{\partial E}{\partial x} = 0 \tag{6.63}$$

where

$$Q = \begin{pmatrix} \rho \\ \rho u \\ E_t \end{pmatrix}, \quad E = \begin{pmatrix} \rho u \\ \rho u^2 + p \\ u(E_t + p) \end{pmatrix} \tag{6.64}$$

or

$$\frac{\partial Q}{\partial t} + A\frac{\partial Q}{\partial x} = 0 \tag{6.65}$$

where

$$A = \frac{\partial E}{\partial Q} = \begin{pmatrix} 0 & 1 & 0 \\ \frac{\gamma-3}{2}u^2 & (3-\gamma)u & \gamma - 1 \\ \frac{\gamma-2}{2}u^3 - \frac{\gamma}{\gamma-1}\frac{p}{\rho}u & \frac{3-2\gamma}{2}u^2 + \frac{\gamma}{\gamma-1}\frac{p}{\rho} & \gamma u \end{pmatrix} \tag{6.66}$$

As it is already stated earlier, the matrix A can be diagonalized to be

$$A = R\Lambda R^{-1} \tag{6.67}$$

where

$$\Lambda = \begin{pmatrix} \lambda_1 & 0 & 0 \\ 0 & \lambda_2 & 0 \\ 0 & 0 & \lambda_3 \end{pmatrix} \tag{6.68}$$

$$R = (\vec{q}_1,\ \vec{q}_2,\ \vec{q}_3) = \begin{pmatrix} 1 & 1 & 1 \\ u-c & u & u+c \\ H-uc & \frac{1}{2}u^2 & H+uc \end{pmatrix} \tag{6.69}$$

$$R^{-1} = \begin{pmatrix} \frac{1}{2}\left(a+\frac{u}{c}\right) & -\frac{1}{2}\left(bu+\frac{1}{c}\right) & \frac{1}{2}b \\ 1-a & bu & -b \\ \frac{1}{2}\left(a-\frac{u}{c}\right) & -\frac{1}{2}\left(bu-\frac{1}{c}\right) & \frac{1}{2}b \end{pmatrix} \tag{6.70}$$

$$a = b\frac{u^2}{2}, \quad b = \frac{\gamma-1}{c^2} \tag{6.71}$$

and H is the total enthalpy.

$$H = \frac{c^2}{\gamma-1} + \frac{u^2}{2} = c_p T + \frac{u^2}{2} = h + \frac{u^2}{2} \tag{6.72}$$

In a similar manner as in the solving procedure of the linear advection equation, the numerical flux can be written as

$$Q_i^{n+1} = Q_i^n - \frac{\Delta t}{\Delta x}\left(\tilde{E}_{i+1/2}^n - \tilde{E}_{i-1/2}^n\right) \tag{6.73}$$

Here, the numerical flux $\tilde{E}_{i+1/2}^n$ is given similarly as

$$\tilde{E}_{i+1/2}^n = \frac{1}{2}\left(E_{i+1}^n + E_i^n - |A_{i+1/2}^n|(Q_{i+1}^n - Q_i^n)\right) \tag{6.74}$$

where

$$|A_{i+1/2}^n| = R_{i+1/2}^n \Lambda_{i+1/2}^n {R_{i+1/2}^n}^{-1} \tag{6.75}$$

Roe Average

The problem at this step is how to evaluate properties such as $R_{i+1/2}^n$ or $\Lambda_{i+1/2}^n$ that are values on $(i+1/2)$th cell boundary. Let the subscript $_R$ denotes properties at right (that is, downstream) cell, which is the properties at $(i+1)$th cell in this case. Similarly, subscript $_L$ denotes properties at left (that is, upstream) cell, which is the properties at ith cell in this case. In the above numerical flux expression in system equations, we assumed that

$$\tilde{E}_R - \tilde{E}_L = A(Q_R, Q_L)\cdot(Q_R - Q_L) = A_{average}(Q_R - Q_L) \tag{6.76}$$

Therefore, the properties at $(i+1/2)$th cell boundary must satisfy

$$A(Q_R, Q_L) \cdot (Q_R - Q_L) = A(Q_{i+1/2}) \tag{6.77}$$

As such an averaged properties at $(i+1/2)$th cell boundary, Roe [13] introduced the *Roe average* as

$$\bar{u} = \frac{\sqrt{\rho_L}u_L + \sqrt{\rho_R}u_R}{\sqrt{\rho_L} + \sqrt{\rho_R}} \tag{6.78}$$

$$\overline{H} = \frac{\sqrt{\rho_L}H_L + \sqrt{\rho_R}H_R}{\sqrt{\rho_L} + \sqrt{\rho_R}} \tag{6.79}$$

$$\overline{c}^2 = (\gamma - 1)\left(\overline{H} - \frac{1}{2}\bar{u}^2\right) \tag{6.80}$$

Here, '$-$' stands for the Roe-averaged quantities where the properties and matrixes (at $(i+1/2)$th cell boundary) must be evaluated based on the above Roe average.

In light of the above discussions, we finally obtain Yee's symmetric TVD scheme for system equations as

$$\tilde{E}^n_{i+1/2} = \frac{1}{2}\left(E^n_{i+1} + E^n_i - \overline{R}^n_{i+1/2}\Phi^n_{i+1/2})\right) \tag{6.81}$$

$$\Phi^n_{i+1/2} = \begin{pmatrix}\phi^1\\ \phi^2\\ \phi^3\end{pmatrix} \tag{6.82}$$

$$\phi^\ell = -\left(\frac{\Delta t}{\Delta x}\overline{\lambda}_\ell{}^2\widehat{Q}^\ell_{i+1/2} + \Psi_{i+1/2}(\alpha^\ell_{i+1/2} - \widehat{Q}^\ell_{i+1/2})\right) \tag{6.83}$$

$$\alpha^\ell_{i+1/2} = (\overline{R}^{-1}(Q^n_{i+1} - Q^n_i))|_\ell \tag{6.84}$$

where $\widehat{Q}^\ell_{i+1/2}$ is the limiter function such as

$$\widehat{Q}^\ell_{i+1/2} = \text{minmod}\left(\alpha^\ell_{i-1/2}, \alpha^\ell_{i+1/2}, \alpha^\ell_{i+3/2}\right) \tag{6.85}$$

6.7.5.1 One-Dimensional Shock Tube Problem

Let us consider well-known shock tube problem. The problem settings are illustrated in Figure 6.12. The shock tube is filled with the air with the conditions in Figure 6.12.

In a shock tube, a high-pressure chamber at the left side and a low-pressure chamber at the right side are isolated at time $t = 0$ s. The computational techniques have already been explained in the previous sections. On the basis of Yee's symmetric TVD scheme, the shock tube problem was solved.

The sample code used in this shock tube problem is shown as follows.

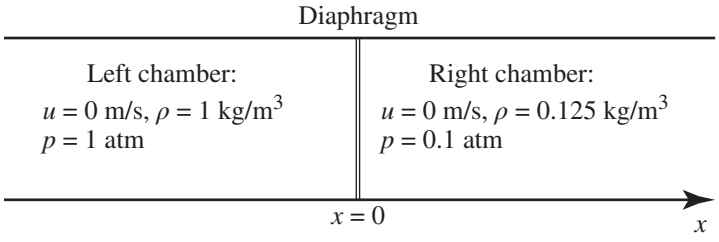

Figure 6.12 Shock tube problem.

```
      program shktub
c
c*******************************************************
c     Shock Tube Problem: 1D Euler eqs solver
c*******************************************************
      common/ grid1d/ mx,dx,x(-5:505)
      common/ cmpcnd/ cfl,dt,nlast,time,eps,g,rhol,ul,pl,rhor,ur,pr
     &              ,rags,cvgas,ecp
      common/ solute/ rho(-5:505),u(-5:505),p(-5:505),e(-5:505)
      common/ solver/ q(3,-5:505),qold(3,-5:505),flux(3,-5:505)
c
cc    (1)set grid
      mx   =  401
      xmin = -2.0
      xmax =  2.0
      dx   = (xmax-xmin)/float(mx-1)
      do 100 i=-2,mx+3
        x(i) = xmin+dx*float(i-1)
  100 continue
c     (2)set parameters
      atmpa= 1.013e05
      eps  = 1.0e-06
      g    = 1.4
      rgas =8.314e+03/28.96
      cvgas=rgas/(g-1.0)
c     (2-1) Left chamber
c     u(m/s),T(K),rho(kg/m3),P(atm)
      ul=0
      rhol=1.0
```

```
      platm=1.0
      pl=platm*atmpa
      tl=pl/(rgas*rhol)
c     (2-2) Right chamber
      ur=0
      rhor=0.125
      pratm=0.1
      pr=pratm*atmpa
      tr=pr/(rgas*rhor)
c     (2-3) Timestep settings
      tmsec=2.
      time= tmsec*1.0e-03
      cfl=0.1
c     (2-4) entropy
      ecp= 0.125
c
c     (3)numerical solutions
      uref=sqrt(g*rgas*amax1(tl,tr))
      dt   = cfl*dx/abs(uref)
      nlast= int(time/dt)
      time = dt*float(nlast)
c     (4) initialize properties
      do 300 i=1,mx
        if(x(i).lt.0.0) then
c     (4-1) Left chamber
          rho(i)= rhol
            u(i)=   ul
            p(i)=   pl
            e(i)= p(i)/((g-1.0)*rho(i))
        else
c     (4-2) Right chamber
          rho(i)= rhor
            u(i)=   ur
            p(i)=   pr
            e(i)= p(i)/((g-1.0)*rho(i))
        end if
c     (4-3) conserved quantitiy
        q(1,i)= rho(i)
```

```
        q(2,i)= rho(i)*u(i)
        q(3,i)= rho(i)*(e(i)+0.5*u(i)**2)
  300 continue
cc
      open(unit=60,file='sw.plt',form='formatted')
      write(60,*) 'VARIABLES="x, m","t, ms","rho, kg/m3","u, m/s",',
     &            '"p, Pa","t, K"'
      write(60,*) 'ZONE T="SW",I=',mx,',J=',nlast,
     &            ',F=POINT'
      do 410 i=1,mx
         write(60,9001) x(i),0.,rho(i),u(i),p(i),e(i)/cvgas
 410  continue
c     (5) Main loop: Time marching
      do 1000 n=1,nlast
c
        do 1010 i=1,mx
          qold(1,i)= q(1,i)
          qold(2,i)= q(2,i)
          qold(3,i)= q(3,i)
 1010   continue
c
        call calflx
        do 1100 i=4,mx-3
          q(1,i)= qold(1,i)-(dt/dx)*(flux(1,i)-flux(1,i-1))
          q(2,i)= qold(2,i)-(dt/dx)*(flux(2,i)-flux(2,i-1))
          q(3,i)= qold(3,i)-(dt/dx)*(flux(3,i)-flux(3,i-1))
          rho(i)= q(1,i)
            u(i)= q(2,i)/rho(i)
            p(i)= (g-1.0)*(q(3,i)-0.5*rho(i)*u(i)**2)
            e(i)= p(i)/((g-1.0)*rho(i))
 1100   continue
c
        if(mod(n,10).eq.0) write(6,*) ' .... step = ',n
        do 9010 i=1,mx
           write(60,9001) x(i),dt*n*1.e3,rho(i),u(i),p(i),e(i)/cvgas
 9010   continue
 9001   format(6f15.5)
 1000 continue
```

```
      close (unit=60)
c     waveform at t=2ms
      open(unit=70,file='waveform.txt',form='formatted')
      do 9200 i=1,mx
         write(70,9201) x(i),rho(i),u(i),p(i),e(i)/cvgas
 9200 continue
 9201 format(5e15.5)
      close (unit=70)
c
      write(6,*) 'DONE!'
c
      stop
      end
c
      subroutine calflx
c=======================================================================
c     Compute Flux with Yee's Symmetric TVD Scheme
c=======================================================================
      common/ grid1d/ mx,dx,x(-5:505)
      common/ cmpcnd/ cfl,dt,nlast,time,eps,g,rhol,ul,pl,rhor,ur,pr
     &              ,rags,cvgas,ecp
      common/ solute/ rho(-5:505),u(-5:505),p(-5:505),e(-5:505)
      common/ solver/ q(3,-5:505),qold(3,-5:505),flux(3,-5:505)
      dimension eigl(3,-5:505),rmat(3,3,-5:505),alpha(3,-5:505)
c
c     Find L/R values
      do 100 i=1,mx-1
        q1l= q(1,i  )
        q1r= q(1,i+1)
        q2l= q(2,i  )
        q2r= q(2,i+1)
        q3l= q(3,i  )
        q3r= q(3,i+1)
c
        dq1= q(1,i+1)-q(1,i  )
        dq2= q(2,i+1)-q(2,i  )
        dq3= q(3,i+1)-q(3,i  )
```

```
c
        rl= q1l
        ul= q2l/rl
        pl=(g-1.0)*(q3l-.5*rl*ul**2)
        hl=(q3l+pl)/rl
        rr= q1r
        ur= q2r/rr
        pr=(g-1.0)*(q3r-.5*rr*ur**2)
        hr=(q3r+pr)/rr
c     Roe Average at i+1/2
        ubar= (sqrt(rl)*ul+sqrt(rr)*ur)/(sqrt(rl)+sqrt(rr))
        hbar= (sqrt(rl)*hl+sqrt(rr)*hr)/(sqrt(rl)+sqrt(rr))
        abar= sqrt((g-1.0)*(hbar-0.5*ubar**2))
        abar= sqrt(amax1( abar, amin1(g*pl/rl, g*pr/rr) ) )
c     Eigen values and corresponding eigen vectors:
c          Matrix R&Lambda at i+1/2
          eigl(1,i)= ubar-abar
        rmat(1,1,i)= 1.0
        rmat(2,1,i)= ubar-abar
        rmat(3,1,i)= hbar-ubar*abar
          eigl(2,i)= ubar
        rmat(1,2,i)= 1.0
        rmat(2,2,i)= ubar
        rmat(3,2,i)= 0.5*ubar**2
          eigl(3,i)= ubar+abar
        rmat(1,3,i)= 1.0
        rmat(2,3,i)= ubar+abar
        rmat(3,3,i)= hbar+ubar*abar
c     alpha = R^(-1) . dQ_(j+1/2) = R^(-1) . (Q_(j+1)-Q_j)
        bb= (g-1.0)/abar**2
        aa= bb*ubar**2/2.0
        alpha(1,i)=
     1              .5*(aa+ubar/abar)    *dq1
     2             -.5*(bb*ubar+1./abar) *dq2
     3             +.5*bb                *dq3
        alpha(2,i)=
```

```
     1               (1.-aa)   *dq1
     2               +bb*ubar *dq2
     3               -bb       *dq3
        alpha(3,i)=
     1               .5*(aa-ubar/abar)     *dq1
     2              -.5*(bb*ubar-1./abar) *dq2
     3              +.5*bb                 *dq3
c
  100 continue
c     compute limiter func. and flux
      do 400 i=3,mx-3
        corr=ecp*amax1(abs(eigl(1,i)), abs(eigl(2,i)), abs(eigl(3,i)) )
c     : Lambda = u-c
        abc= abs(eigl(1,i))
        if(abc.lt.corr) abc= (abc**2+corr**2)*.5/corr
        sgn = sign(1., alpha(1,i))
        qlim= sgn*amax1(0.,amin1(sgn*2.*alpha(1,i-1),sgn*2.*alpha(1,i)
     &       ,sgn*2.*alpha(1,i+1),sgn*.5*(alpha(1,i-1)+alpha(1,i+1)) ))
        ph1= -(dt/dx)*eigl(1,i)**2*qlim-abc*(alpha(1,i)-qlim)
c     : Lambda = c
        abc= abs(eigl(2,i))
        if(abc.lt.corr) abc= (abc**2+corr**2)*.5/corr
        sgn = sign(1., alpha(2,i))
        qlim= sgn*amax1(0.,amin1(sgn*2.*alpha(2,i-1),sgn*2.*alpha(2,i)
     &       ,sgn*2.*alpha(2,i+1),sgn*.5*(alpha(2,i-1)+alpha(2,i+1)) ))
        ph2= -(dt/dx)*eigl(2,i)**2*qlim-abc*(alpha(2,i)-qlim)
c     : Lambda = u+c
        abc= abs(eigl(3,i))
        if(abc.lt.corr) abc= (abc**2+corr**2)*.5/corr
        sgn = sign(1., alpha(3,i))
        qlim= sgn*amax1(0.,amin1(sgn*2.*alpha(3,i-1),sgn*2.*alpha(3,i)
     &       ,sgn*2.*alpha(3,i+1),sgn*.5*(alpha(3,i-1)+alpha(3,i+1)) ))
        ph3= -(dt/dx)*eigl(3,i)**2*qlim-abc*(alpha(3,i)-qlim)
c     Phi_(i+1/2) = R . phi
        rphi1= rmat(1,1,i)*ph1+rmat(1,2,i)*ph2+rmat(1,3,i)*ph3
        rphi2= rmat(2,1,i)*ph1+rmat(2,2,i)*ph2+rmat(2,3,i)*ph3
```

```
        rphi3= rmat(3,1,i)*ph1+rmat(3,2,i)*ph2+rmat(3,3,i)*ph3
        q1l= q(1,i  )
        q1r= q(1,i+1)
        q2l= q(2,i  )
        q2r= q(2,i+1)
        q3l= q(3,i  )
        q3r= q(3,i+1)
         rl= q1l
         ul= q2l/rl
         pl= (g-1.0)*(q3l-.5*rl*ul**2)
         hl= (q3l+pl)/rl
         rr= q1r
         ur= q2r/rr
         pr= (g-1.0)*(q3r-.5*rr*ur**2)
         hr= (q3r+pr)/rr
        e1l= rl*ul
        e2l= rl*ul**2+pl
        e3l= ul*(q3l+pl)
        e1r= rr*ur
        e2r= rr*ur**2+pr
        e3r= ur*(q3r+pr)
        flux(1,i)= .5*(e1l+e1r+rphi1)
        flux(2,i)= .5*(e2l+e2r+rphi2)
        flux(3,i)= .5*(e3l+e3r+rphi3)
c
  400 continue
c
      return
      end
```

Results

The results of the shock tube problem are illustrated in Figures 6.13–6.15. As we can clearly see, the propagation of right running shock and the left running expansion fan are solved successfully. We can also see a contact surface in temperature result in Figure 6.15.

The variation of properties at time $t = 2$ ms after the removal of the diaphragm are shown in Figures 6.16–6.18.

For the analytical expressions governing the shock and expansion processes in the shock tube is given in Section 3.9 of Reference 11.

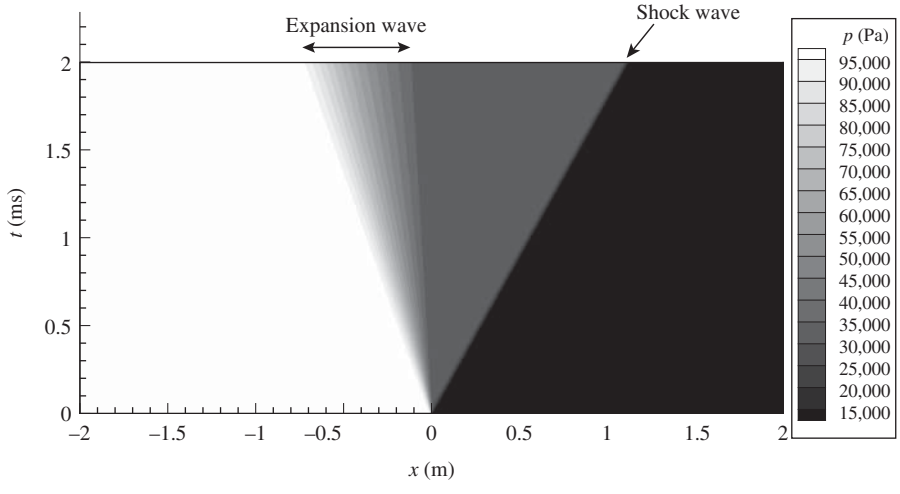

Figure 6.13 Result of shock tube problem – pressure.

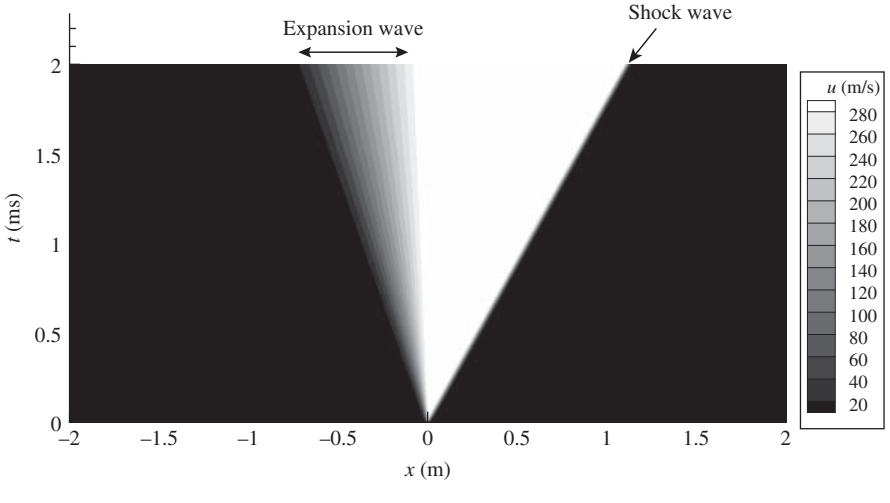

Figure 6.14 Result of shock tube problem – velocity.

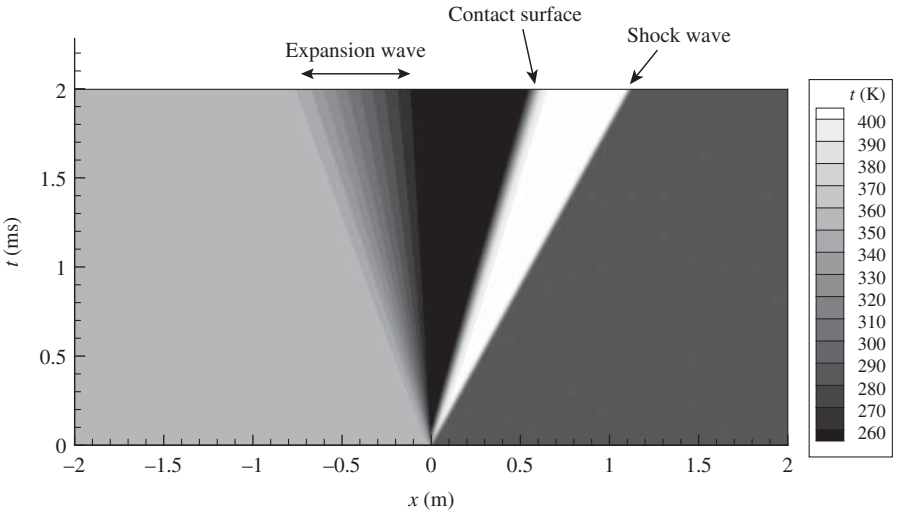

Figure 6.15 Result of shock tube problem – temperature.

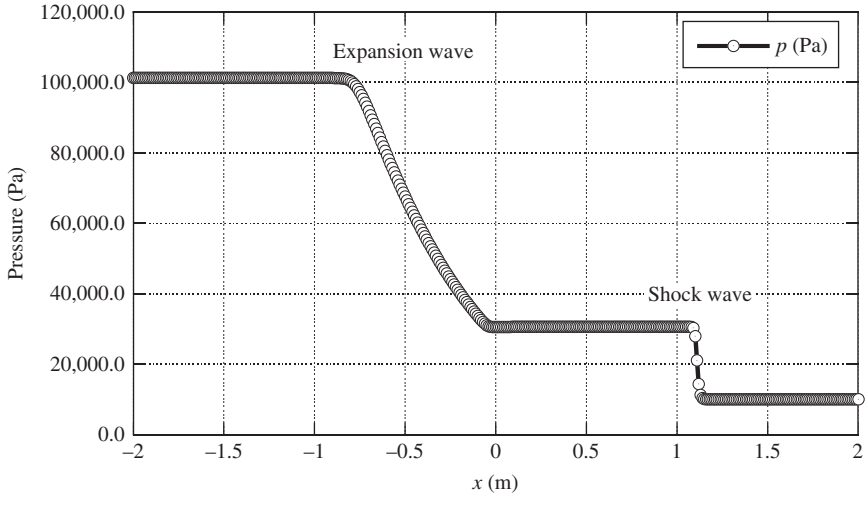

Figure 6.16 Result of shock tube problem - pressure at time $t = 2$ ms.

Note

The time integration was done with first-order accuracy in order to show the sample code as simple as possible. In the actual computations, it is strongly recommended to use much higher-order time integration schemes such as the Runge–Kutta method.

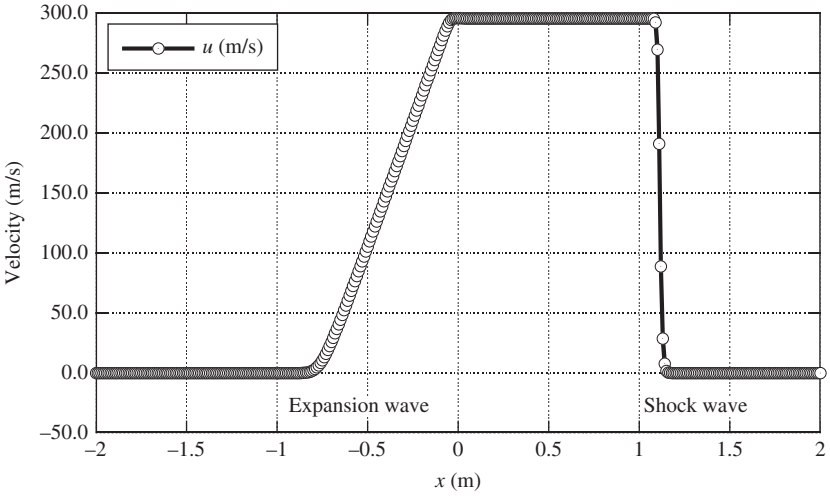

Figure 6.17 Result of shock tube problem – velocity at time $t = 2$ ms.

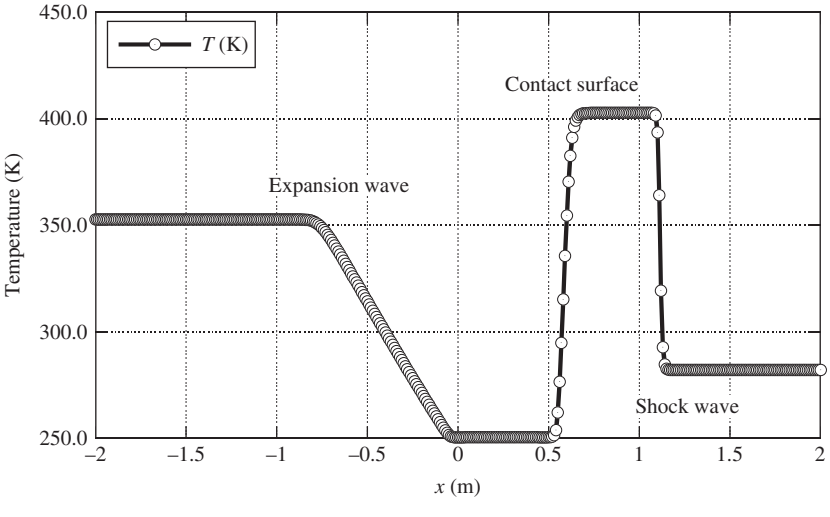

Figure 6.18 Result of shock tube problem – temperature at time $t = 2$ ms.

Example 6.2 For the pressure decrease of $p_3/p_4 = 0.3$, caused by the expansion (Figure 6.16), calculate the flow velocity V_3, caused by the expansion, with analytical expression, and compare this velocity with that in Figure 6.17.

Solution

Given $p_3/p_4 = 0.3$, $p_4 = 1$ atm, and $\rho_4 = 1\,\text{kg/m}^3$.

this gives the temperature T_4 as

$$\begin{aligned} T_4 &= \frac{p_4}{R\rho_4} \\ &= \frac{101325}{287 \times 1} \\ &= 353 \text{ K} \end{aligned}$$

The corresponding speed of sound is

$$\begin{aligned} a_4 &= \sqrt{\gamma R T_4} \\ &= \sqrt{1.4 \times 287 \times 353} \\ &= 376.6 \text{ m/s} \end{aligned}$$

The flow velocity V_3, caused by the expansion, by Equation (3.56) [11], is

$$\begin{aligned} V_3 &= \frac{2a_4}{\gamma_4 - 1}\left[1 - \left(\frac{p_3}{p_4}\right)^{(\gamma_4-1)/(2\gamma_4)}\right] \\ &= \frac{2 \times 376.6}{1.4 - 1}[1 - {}^{(1.4-1)/(2\times 1.4)}] \\ &= \frac{2 \times 376.6}{0.4} \times 0.158 \\ &= \boxed{298 \text{ m/s}} \end{aligned}$$

The value of V_3 in Figure 6.17 is 300 m/s. Thus the computed value of velocity agrees within $\pm 0.67\%$. ■

Multidimensional Problems

For CFD with the multidimensional Euler equations, such as the 2D Euler equations,

$$\frac{\partial Q}{\partial t} + \frac{\partial E}{\partial x} + \frac{\partial F}{\partial y} = 0 \tag{6.86}$$

This equation can be split into two parts:

$$\frac{\partial Q}{\partial t} + \frac{\partial E}{\partial x} = 0 \tag{6.87}$$

$$\frac{\partial Q}{\partial t} + \frac{\partial F}{\partial y} = 0 \tag{6.88}$$

We can first compute $\frac{\partial E}{\partial x}$ and then $\frac{\partial F}{\partial y}$. After that, time integration with the Runge–Kutta scheme or similar highly accurate method will be employed to obtain the result. For details and actual procedures, see Example 6.2.

Example 6.3 Solve an oblique shock problem with CFD computation under following conditions.

- Governing equations are the two-dimensional Euler equations.
- Half-angle of a wedge is 20°.
- Simulate flows with Mach numbers of 2, 3, and 5.
- Compare oblique shock angle with oblique shock equations.

Let us consider the oblique shock wave at the nose of the wedge of semi-vertex angle 20°, with the computional domain, as shown in Figure 6.19.

Solution

The computation code used in this exercise is given below.

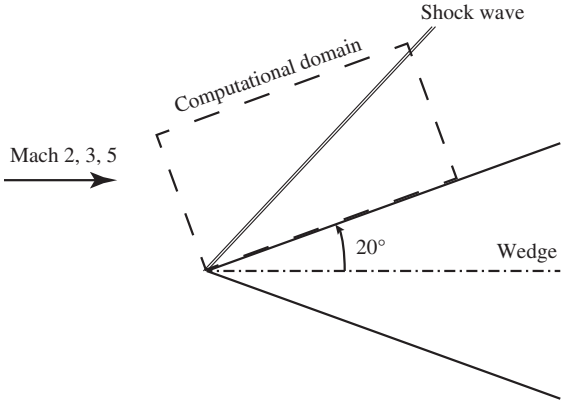

Figure 6.19 Oblique shock problem.

```
      program os2d
c**********************************************************************
c     2D Euler Eqs Solver for uniform spacing orthogonal grid
c     *** High Enthalpy Book Version ***
c**********************************************************************
c     flow conditions
      call setflw
c     solver
      call slvflw
      stop
      end
```

```
c
      subroutine setflw
c**********************************************************************
c     subroutine to set flow conditions
c**********************************************************************
      parameter( mdx = 202 , mdy = 102 )
      common /flwcnd/ g0,rgas,fm0,alpha,u0,v0,p0,rho0,t0
      common /cfdcnd/ cfl,dt,ecp,tol,nlast,nlp
      common /gridxy/ mx,my,grid,x(mdx,mdy),y(mdx,mdy),dx,dy
c
      write(6,*) ' *** 2-D inviscid flow ***'
      write(6,*) ' ** Schemes **'
      write(6,*) '    Time marching:  3-step TVD Runge Kutta method '
      write(6,*) '    Advection terms: 2nd order TVD scheme by Yee  '
c     (1) freestream conditions
      g0   =  1.4
      fm0  =  2.0
      alpha= 20.0
      rad  = 3.141592/180.
      u0   = 1.*cos(alpha*rad)
      v0   =-1.*sin(alpha*rad)
      p0   = 1./(g0*fm0**2)
      rho0 = 1.
      t0   = 1.
c     (2) gas constant
      rgas = 1./(g0*fm0**2)
c     (3) cfd conditions
      cfl  = .4
      ecp  = .15
      tol  = .01
      nlast=2000
      nlp  = 10
c     (4) grid settings
      xmin = 0.
      xmax = 1.
      mx   = 101
      dx   = (xmax-xmin)/float(mx-1)
      ymin = 0.
```

```
      ymax = 1.
      my   = 101
      dy   = (ymax-ymin)/float(my-1)
c
      do 100 i=1,mx
      do 100 j=1,my
         x(i,j) = xmin + dx*float(i-1)
         y(i,j) = ymin + dy*float(j-1)
 100  continue
      grid = float(mx*my)
      dsmin= amin1(dx,dy)
      dt   = cfl*dsmin
      write(6,*) ' +++ grid size +++'
      write(6,*) '  mx , my    = ', mx, my
      write(6,*) '  min grid spacing: ', dsmin
      write(6,*) ' +++ conditions +++'
      write(6,*) '  CFL number = ', cfl
      write(6,*) '  dt         = ', dt
      return
      end
c
      subroutine slvflw
c**********************************************************************
c     subroutine for flow solver: time marching
c**********************************************************************
      parameter( mdx = 202 , mdy = 102 )
      common /flwcnd/ g0,rgas,fm0,alpha,u0,v0,p0,rho0,t0
      common /cfdcnd/ cfl,dt,ecp,tol,nlast,nlp
      common /gridxy/ mx,my,grid,x(mdx,mdy),y(mdx,mdy),dx,dy
      common /flwprp/ u(mdx,mdy),v(mdx,mdy),p(mdx,mdy),t(mdx,mdy),
     &                rho(mdx,mdy)
      common /consvd/ q(4,mdx,mdy),qold(4,mdx,mdy)
      common /flwflx/ dq(4,mdx,mdy)
c     (1) set initial conditions
      call initfl
      call bndcnd
c     (2) time marching
      write(6,*) '3step TVD Runge Kutta time marching'
      do 1000 n=1,nlast
```

```
c     (2-1) copy previous variables
         do 100 l=1,4
         do 100 i=1,mx
         do 100 j=1,my
            qold(l,i,j) = q(l,i,j)
 100     continue
c     (2-2) step-1
         call calrhs
         do 200 l=1,4
         do 200 i=2,mx-1
         do 200 j=2,my-1
            q(l,i,j) = qold(l,i,j)+dq(l,i,j)
 200     continue
         call bndcnd
c     (2-3) step-2
         call calrhs
         do 300 l=1,4
         do 300 i=2,mx-1
         do 300 j=2,my-1
            q(l,i,j) = .75*qold(l,i,j)+.25*(q(l,i,j)+dq(l,i,j))
 300     continue
         call bndcnd
c     (2-4) step-3
         call calrhs
         do 400 l=1,4
         do 400 i=2,mx-1
         do 400 j=2,my-1
            q(l,i,j) = (qold(l,i,j)+2.*(q(l,i,j)+dq(l,i,j)))/3.
 400     continue
         call bndcnd
c     (2-5) residual
         res=0.
         do 500 l=1,4
         do 500 i=1,mx
         do 500 j=1,my
            res=res+(q(l,i,j)-qold(l,i,j))**2
 500     continue
         res=sqrt(res/grid)
```

```
c     (2-6) monitoring output for terminal
         if(mod(n,nlp).eq.0) write(6,*) 'step#',n,':      residual=',res
 1000 continue
c     (3) file output for Tecplot
      open(unit=50,file='plot2d.plt',form='formatted')
      write(50,*) 'VARIABLES="X","Y","U","V","P","T","RHO","MACH#"'
      write(50,*) 'ZONE T="EULER2D",I=',mx,',J=',my,',F=POINT'
      do 2000 j=1,my
      do 2000 i=1,mx
         write(50,2100) x(i,j),y(i,j),u(i,j),v(i,j),p(i,j),t(i,j),
     &        rho(i,j),(u(i,j)**2+v(i,j)**2)/sqrt(g0*rgas*t(i,j))
 2000 continue
 2100 format(8E16.8)
      close(unit=50)
      return
      end
c
      subroutine initfl
c**********************************************************************
c     subroutine for initial conditions
c**********************************************************************
      parameter( mdx = 202 , mdy = 102 )
      common /flwcnd/ g0,rgas,fm0,alpha,u0,v0,p0,rho0,t0
      common /cfdcnd/ cfl,dt,ecp,tol,nlast,nlp
      common /gridxy/ mx,my,grid,x(mdx,mdy),y(mdx,mdy),dx,dy
      common /flwprp/ u(mdx,mdy),v(mdx,mdy),p(mdx,mdy),t(mdx,mdy),
     &                rho(mdx,mdy)
      common /consvd/ q(4,mdx,mdy),qold(4,mdx,mdy)
      common /flwflx/ dq(4,mdx,mdy)
c     (1) initial condition
      do 1000 i=1,mx
      do 1000 j=1,my
         u(i,j) = u0
         v(i,j) = v0
         p(i,j) = p0
         t(i,j) = t0
         rho(i,j) = rho0
 1000 continue
```

```
c     (2) set conserved variables
      do 2000 i=1,mx
      do 2000 j=1,my
        q(1,i,j)=rho(i,j)
        q(2,i,j)=rho(i,j)*u(i,j)
        q(3,i,j)=rho(i,j)*v(i,j)
        q(4,i,j)=rho(i,j)*(rgas*t(i,j)/(g0-1.)+(u(i,j)**2+v(i,j)**2)/2.)
 2000 continue
      return
      end
c
      subroutine bndcnd
c**********************************************************************
c     subroutine for boundary conditions
c**********************************************************************
      parameter( mdx = 202 , mdy = 102 )
      common /flwcnd/ g0,rgas,fm0,alpha,u0,v0,p0,rho0,t0
      common /cfdcnd/ cfl,dt,ecp,tol,nlast,nlp
      common /gridxy/ mx,my,grid,x(mdx,mdy),y(mdx,mdy),dx,dy
      common /flwprp/ u(mdx,mdy),v(mdx,mdy),p(mdx,mdy),t(mdx,mdy),
     &                rho(mdx,mdy)
      common /consvd/ q(4,mdx,mdy),qold(4,mdx,mdy)
      common /flwflx/ dq(4,mdx,mdy)
c     (1) find flow properties
      do 100 i=2,mx-1
      do 100 j=2,my-1
         rho(i,j)=q(1,i,j)
         u(i,j)=q(2,i,j)/q(1,i,j)
         v(i,j)=q(3,i,j)/q(1,i,j)
         p(i,j)=(g0-1.)*(q(4,i,j)-.5*rho(i,j)*(u(i,j)**2+v(i,j)**2))
         t(i,j)=p(i,j)/(rgas*rho(i,j))
 100  continue
c     (2) i=1 freestream condition
      i=1
      do 200 j=1,my
         u(i,j) = u0
         v(i,j) = v0
         p(i,j) = p0
```

```
         t(i,j) = t0
         rho(i,j) = rho0
 200  continue
c     (3) j=my freestream condition
      j=my
      do 300 i=1,mx
         u(i,j) = u0
         v(i,j) = v0
         p(i,j) = p0
         t(i,j) = t0
         rho(i,j) = rho0
 300  continue
c     (4) j=my wall boundary
c      -- > normal velocity component = 0
c      -- > tangential velocity component ... extrapolation
c      -- > pressure ... normal gradient = 0
c      -- > temperature ... energy conservation condition
c      -- > density ... gas equation p=rho.R.t
      j=1
      cp = g0/(g0-1.) * rgas
      h0 = cp*t0 + (u0**2+v0**2)/2.
      do 400 i=1,mx
         u(i,1) = 2.*u(i,2)-u(i,3)
         v(i,1) = 0.
         p(i,1) = p(i,2)
         t(i,1) = (h0-.5*(u(i,1)**2-v(i,1)**2))/cp
         rho(i,1) = p(i,1)/(rgas*t(i,1))
 400  continue
c     (5) i=mx outflow condition
      i=mx
      do 500 j=1,my
         u(i,j) = 2.*u(i-1,j)-u(i-2,j)
         v(i,j) = 2.*v(i-1,j)-v(i-2,j)
         p(i,j) = 2.*p(i-1,j)-p(i-2,j)
         t(i,j) = (h0-.5*(u(i,j)**2-v(i,j)**2))/cp
         rho(i,j) = p(i,j)/(rgas*t(i,j))
 500  continue
```

```
c     (6) set conserved variables
      do 600 i=1,mx
      do 600 j=1,my
        q(1,i,j)=rho(i,j)
        q(2,i,j)=rho(i,j)*u(i,j)
        q(3,i,j)=rho(i,j)*v(i,j)
        q(4,i,j)=rho(i,j)*(rgas*t(i,j)/(g0-1.)+(u(i,j)**2+v(i,j)**2)/2.)
 600  continue
      return
      end
c
      subroutine calrhs
c**********************************************************************
c     subroutine for advection term evaluation
c       compute rhs term from q and store results in dq
c       discretization: 2nd order TVD scheme by Yee
c**********************************************************************
      parameter( mdx = 202 , mdy = 102 )
      common /flwcnd/ g0,rgas,fm0,alpha,u0,v0,p0,rho0,t0
      common /cfdcnd/ cfl,dt,ecp,tol,nlast,nlp
      common /gridxy/ mx,my,grid,x(mdx,mdy),y(mdx,mdy),dx,dy
      common /flwprp/ u(mdx,mdy),v(mdx,mdy),p(mdx,mdy),t(mdx,mdy),
     &                rho(mdx,mdy)
      common /consvd/ q(4,mdx,mdy),qold(4,mdx,mdy)
      common /flwflx/ dq(4,mdx,mdy)
      dimension um(mdx),vm(mdx),hm(mdx),cm(mdx)
      dimension uum(mdx),cmm(mdx),cpm(mdx)
      dimension a1(mdx),a2(mdx),a3(mdx),a4(mdx),dlt(mdx)
      dimension p1(mdx),p2(mdx),p3(mdx),p4(mdx)
      dimension flx1(mdx),flx2(mdx),flx3(mdx),flx4(mdx)
c     (1) inviscid flux: x
      do 1000 j=2,my-1
         do 1100 i=1,mx-1
c     (1-1) Roe's averaging at i+1/2
           dr   =sqrt(rho(i+1,j)/rho(i,j))
           um(i)=(dr*u(i+1,j)+u(i,j))/(dr+1.)
           vm(i)=(dr*v(i+1,j)+v(i,j))/(dr+1.)
           hm(i)=(dr*(q(4,i+1,j)+p(i+1,j))/rho(i+1,j)
```

```
     &              +(q(4,i  ,j)+p(i  ,j))/rho(i  ,j))/(dr+1.)
           cm2  =(g0-1.)*(hm(i)-.5*(um(i)**2+vm(i)**2))
           cm(i)=sqrt(amax1(cm2,amin1(g0*rgas*t(i,j),g0*rgas*t(i+1,j))))
           uum(i)=um(i)
           cmm(i)=uum(i)-cm(i)
           cpm(i)=uum(i)+cm(i)
           d1  =q(1,i+1,j)-q(1,i,j)
           d2  =q(2,i+1,j)-q(2,i,j)
           d3  =q(3,i+1,j)-q(3,i,j)
           d4  =q(4,i+1,j)-q(4,i,j)
           aa=(g0-1.)*(d1*(um(i)**2+vm(i)**2)/2.-d2*um(i)-d3*vm(i)+d4)
     &          /cm(i)**2
           bb=(-d1*um(i)+d2)/cm(i)
           a1(i)=(aa-bb)/2.
           a2(i)= d1-aa
           a3(i)=(aa+bb)/2.
           a4(i)=d1*vm(i)-d3
           dlt(i)=abs(uum(i))+abs(vm(i))+cm(i)*sqrt(2.)
1100       continue
           a1( 0)=a1(  1)
           a2( 0)=a2(  1)
           a3( 0)=a3(  1)
           a4( 0)=a4(  1)
           a1(mx)=a1(mx-1)
           a2(mx)=a2(mx-1)
           a3(mx)=a3(mx-1)
           a4(mx)=a4(mx-1)
           do 1200 i=1,mx-1
              ff1=(dt/dx)*cmm(i)**2
              ff2=abs(cmm(i))
              delta=dlt(i)*ecp
              if(ff2.lt.delta) ff2=0.5*(cmm(i)**2+delta**2)/delta
              s=sign(1. , a1(i-1))
              qq =s*amax1(0., amin1( s*a1(i-1), s*a1(i), s*a1(i+1) ))
              p1 (i)=-ff1*qq-ff2*(a1(i)-qq)
              ff1=(dt/dx)*cpm(i)**2
              ff2=abs(cpm(i))
              if(ff2.lt.delta) ff2=0.5*(cpm(i)**2+delta**2)/delta
```

```
            s=sign(1. , a3(i-1))
            qq =s*amax1(0., amin1( s*a3(i-1), s*a3(i), s*a3(i+1) ))
            p3 (i)=-ff1*qq-ff2*(a3(i)-qq)
            ff1=(dt/dx)*uum(i)**2
            ff2=abs(uum(i))
            if(ff2.lt.delta) ff2=0.5*(uum(i)**2+delta**2)/delta
            s=sign(1. , a2(i-1))
            qq =s*amax1(0.,amin1( s*2.*a2(i-1), s*2.*a2(i), s*2.*a2(i+1)
     &                          ,s*.5*(a2(i-1)+a2(i+1)) ))
            p2 (i)=-ff1*qq-ff2*(a2(i)-qq)
            s=sign(1. , a4(i-1))
            qq =s*amax1(0.,amin1( s*2.*a4(i-1), s*2.*a4(i), s*2.*a4(i+1)
     &                          ,s*.5*(a4(i-1)+a4(i+1)) ))
            p4 (i)=-ff1*qq-ff2*(a4(i)-qq)
 1200    continue
         do 1300 i=1,mx-1
            aa=p1(i)+p2(i)+p3(i)
            bb=-cm(i)*(p1(i)-p3(i))
            cc=-p4(i)
            flx1(i)= aa
            flx2(i)= um(i)*aa+bb
            flx3(i)= vm(i)*aa+cc
            flx4(i)= hm(i)*aa+um(i)*bb+vm(i)*cc-p2(i)*cm(i)**2/(g0-1.)
c     *
            e1  =q(2,i,j)+q(2,i+1,j)
            e2  =q(2,i,j)*u(i,j)+p(i,j)+q(2,i+1,j)*u(i+1,j)+p(i+1,j)
            e3  =q(2,i,j)*v(i,j)+q(2,i+1,j)*v(i+1,j)
            e4  =(q(4,i,j)+p(i,j))*u(i,j)+(q(4,i+1,j)+p(i+1,j))*u(i+1,j)
            flx1(i)=(e1+flx1(i))/2.
            flx2(i)=(e2+flx2(i))/2.
            flx3(i)=(e3+flx3(i))/2.
            flx4(i)=(e4+flx4(i))/2.
 1300    continue
         do 1400 i=2,mx-1
            dq(1,i,j)=-(flx1(i)-flx1(i-1))*dt/dx
            dq(2,i,j)=-(flx2(i)-flx2(i-1))*dt/dx
            dq(3,i,j)=-(flx3(i)-flx3(i-1))*dt/dx
            dq(4,i,j)=-(flx4(i)-flx4(i-1))*dt/dx
```

```
 1400    continue
 1000 continue
c     (2) inviscid flux: y
      do 2000 i=2,mx-1
         do 2100 j=1,my-1
c     (2-1) Roe's averaging at j+1/2
            dr   =sqrt(rho(i,j+1)/rho(i,j))
            um(j)=(dr*u(i,j+1)+u(i,j))/(dr+1.)
            vm(j)=(dr*v(i,j+1)+v(i,j))/(dr+1.)
            hm(j)=(dr*(q(4,i,j+1)+p(i,j+1))/rho(i,j+1)
     &              +(q(4,i  ,j)+p(i  ,j))/rho(i  ,j))/(dr+1.)
            cm2  =(g0-1.)*(hm(j)-.5*(um(j)**2+vm(j)**2))
            cm(j)=sqrt(amax1(cm2,amin1(g0*rgas*t(i,j),g0*rgas*t(i,j+1))))
            uum(j)=vm(j)
            cmm(j)=uum(j)-cm(j)
            cpm(j)=uum(j)+cm(j)
            d1  =q(1,i,j+1)-q(1,i,j)
            d2  =q(2,i,j+1)-q(2,i,j)
            d3  =q(3,i,j+1)-q(3,i,j)
            d4  =q(4,i,j+1)-q(4,i,j)
            aa=(g0-1.)*(d1*(um(j)**2+vm(j)**2)/2.-d2*um(j)-d3*vm(j)+d4)
     &           /cm(j)**2
            bb=(-d1*vm(j)+d3)/cm(j)
            a1(j)=(aa-bb)/2.
            a2(j)= d1-aa
            a3(j)=(aa+bb)/2.
            a4(j)=-d1*um(j)+d2
            dlt(j)=abs(uum(j))+abs(um(j))+cm(j)*sqrt(2.)
 2100    continue
         a1( 0)=a1(   1)
         a2( 0)=a2(   1)
         a3( 0)=a3(   1)
         a4( 0)=a4(   1)
         a1(my)=a1(my-1)
         a2(my)=a2(my-1)
         a3(my)=a3(my-1)
         a4(my)=a4(my-1)
```

```
      do 2200 j=1,my-1
         ff1=(dt/dy)*cmm(j)**2
         ff2=abs(cmm(j))
         delta=dlt(j)*ecp
         if(ff2.lt.delta) ff2=0.5*(cmm(j)**2+delta**2)/delta
         s=sign(1. , a1(j-1))
         qq =s*amax1(0., amin1( s*a1(j-1), s*a1(j), s*a1(j+1) ))
         p1 (j)=-ff1*qq-ff2*(a1(j)-qq)
         ff1=(dt/dy)*cpm(j)**2
         ff2=abs(cpm(j))
         if(ff2.lt.delta) ff2=0.5*(cpm(j)**2+delta**2)/delta
         s=sign(1. , a3(j-1))
         qq =s*amax1(0., amin1( s*a3(j-1), s*a3(j), s*a3(j+1) ))
         p3 (j)=-ff1*qq-ff2*(a3(j)-qq)
         ff1=(dt/dy)*uum(j)**2
         ff2=abs(uum(j))
         if(ff2.lt.delta) ff2=0.5*(uum(j)**2+delta**2)/delta
         s=sign(1. , a2(j-1))
         qq =s*amax1(0.,amin1( s*2.*a2(j-1), s*2.*a2(j), s*2.*a2(j+1)
     &                        ,s*.5*(a2(j-1)+a2(j+1)) ))
         p2 (j)=-ff1*qq-ff2*(a2(j)-qq)
         s=sign(1. , a4(j-1))
         qq =s*amax1(0.,amin1( s*2.*a4(j-1), s*2.*a4(j), s*2.*a4(j+1)
     &                        ,s*.5*(a4(j-1)+a4(j+1)) ))
         p4 (j)=-ff1*qq-ff2*(a4(j)-qq)
2200     continue
      do 2300 j=1,my-1
         aa=p1(j)+p2(j)+p3(j)
         bb=p4(j)
         cc=-cm(j)*(p1(j)-p3(j))
         flx1(j)= aa
         flx2(j)= um(j)*aa+bb
         flx3(j)= vm(j)*aa+cc
         flx4(j)= hm(j)*aa+um(j)*bb+vm(j)*cc-p2(j)*cm(j)**2/(g0-1.)
```

```
c     *
            f1  =q(3,i,j)+q(3,i,j+1)
            f2  =q(3,i,j)*u(i,j)+q(3,i,j+1)*u(i,j+1)
            f3  =q(3,i,j)*v(i,j)+p(i,j)+q(3,i,j+1)*v(i,j+1)+p(i,j+1)
            f4  =(q(4,i,j)+p(i,j))*v(i,j)+(q(4,i,j+1)+p(i,j+1))*v(i,j+1)
            flx1(j)=(f1+flx1(j))/2.
            flx2(j)=(f2+flx2(j))/2.
            flx3(j)=(f3+flx3(j))/2.
            flx4(j)=(f4+flx4(j))/2.
 2300     continue
          do 2400 j=2,my-1
             dq(1,i,j)=dq(1,i,j)-(flx1(j)-flx1(j-1))*dt/dy
             dq(2,i,j)=dq(2,i,j)-(flx2(j)-flx2(j-1))*dt/dy
             dq(3,i,j)=dq(3,i,j)-(flx3(j)-flx3(j-1))*dt/dy
             dq(4,i,j)=dq(4,i,j)-(flx4(j)-flx4(j-1))*dt/dy
 2400     continue
 2000 continue
      return
      end
```

The time integration was computed with the three-step TVD Runge–Kutta method. The discretization of advection terms was done using the second-order Yee's Symmetric TVD method.

The results of the flow field studied are shown in the following figures. The grids generated for solving the flow past the oblique shock in Mach 2, Mach 3, and Mach 5 freestream flows are shown in Figure 6.20(a)–(c), respectively.

The Mach number contour plots for the flow past the oblique shock in Mach 2, Mach 3, and Mach 5 freestream flows are shown in Figure 6.21(a)–(c), respectively.

The Pressure contour plot with streamlines, for the flow past the oblique shock in Mach 2, Mach 3, and Mach 5 freestream flows are shown in Figure 6.22(a)–(c), respectively.

As it can be clearly seen from Figure 6.21, the oblique shock formed over the 20° wedge can be successfully solved with numerical computation. As it can also be seen in Figure 6.22, streamlines suddenly change their direction at the shock. The shock angle was measured as in Figure 6.23. From this figure, the shock angle was measured to be about 52°–53°. This value of shock angle is identically the same as that given in the oblique shock table given in Reference 11.

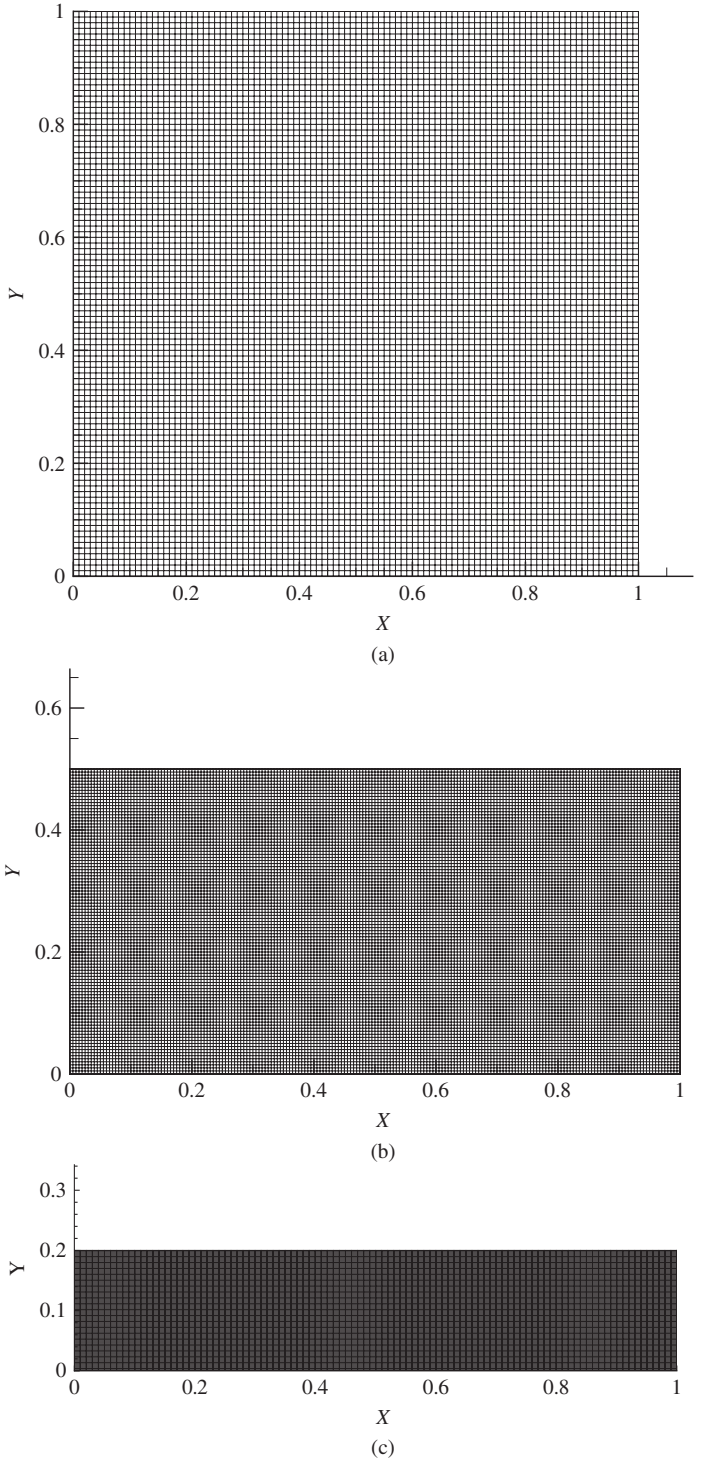

Figure 6.20 Computational grid for oblique shock problem. (a) Grid for Mach-2 flow, (b) grid for Mach-3 flow, and (c) grid for Mach-5 flow.

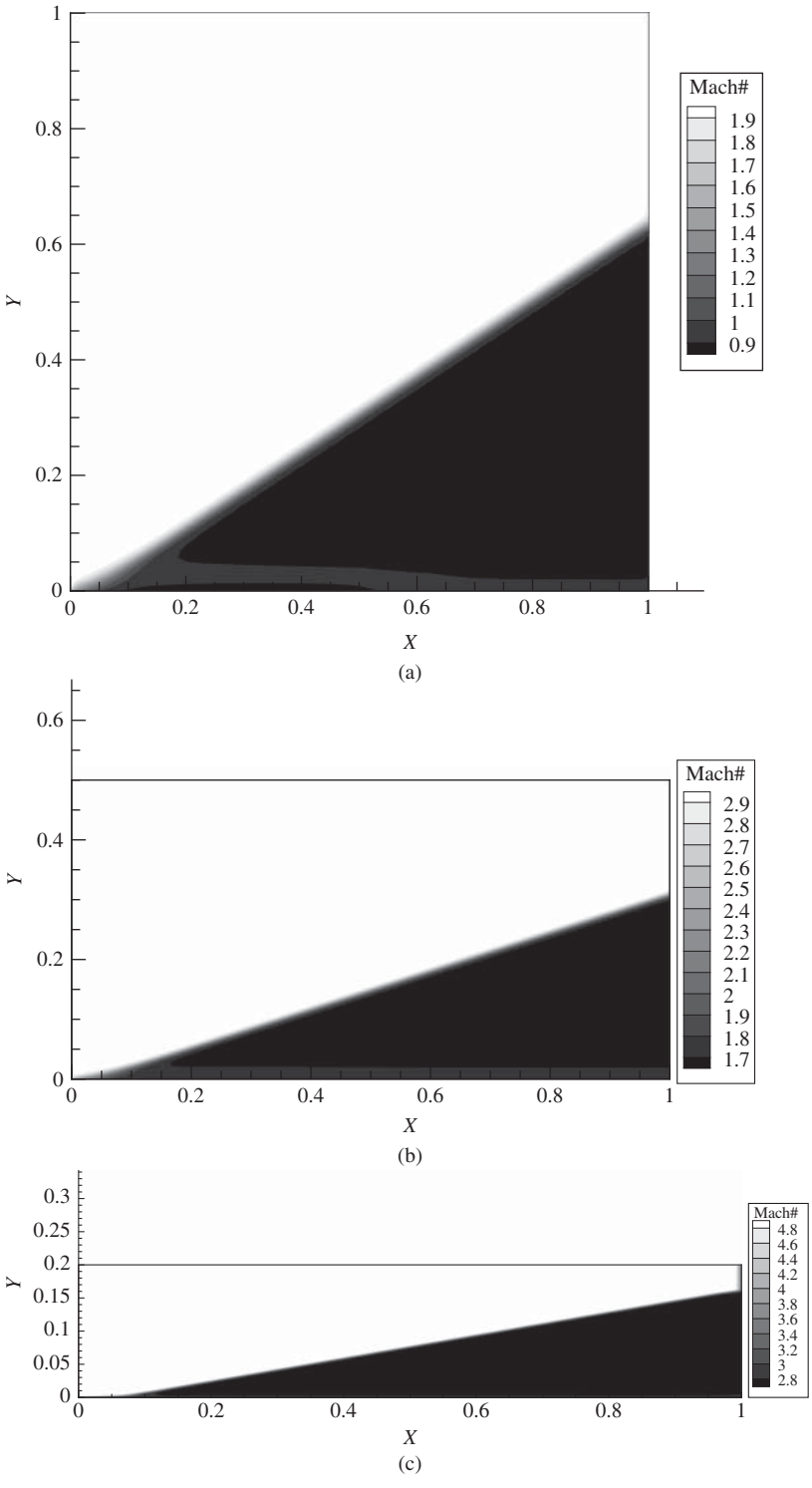

Figure 6.21 Mach number contour plot. (a) Mach 2 flow, (b) Mach 3 flow, and (c) Mach 5 flow.

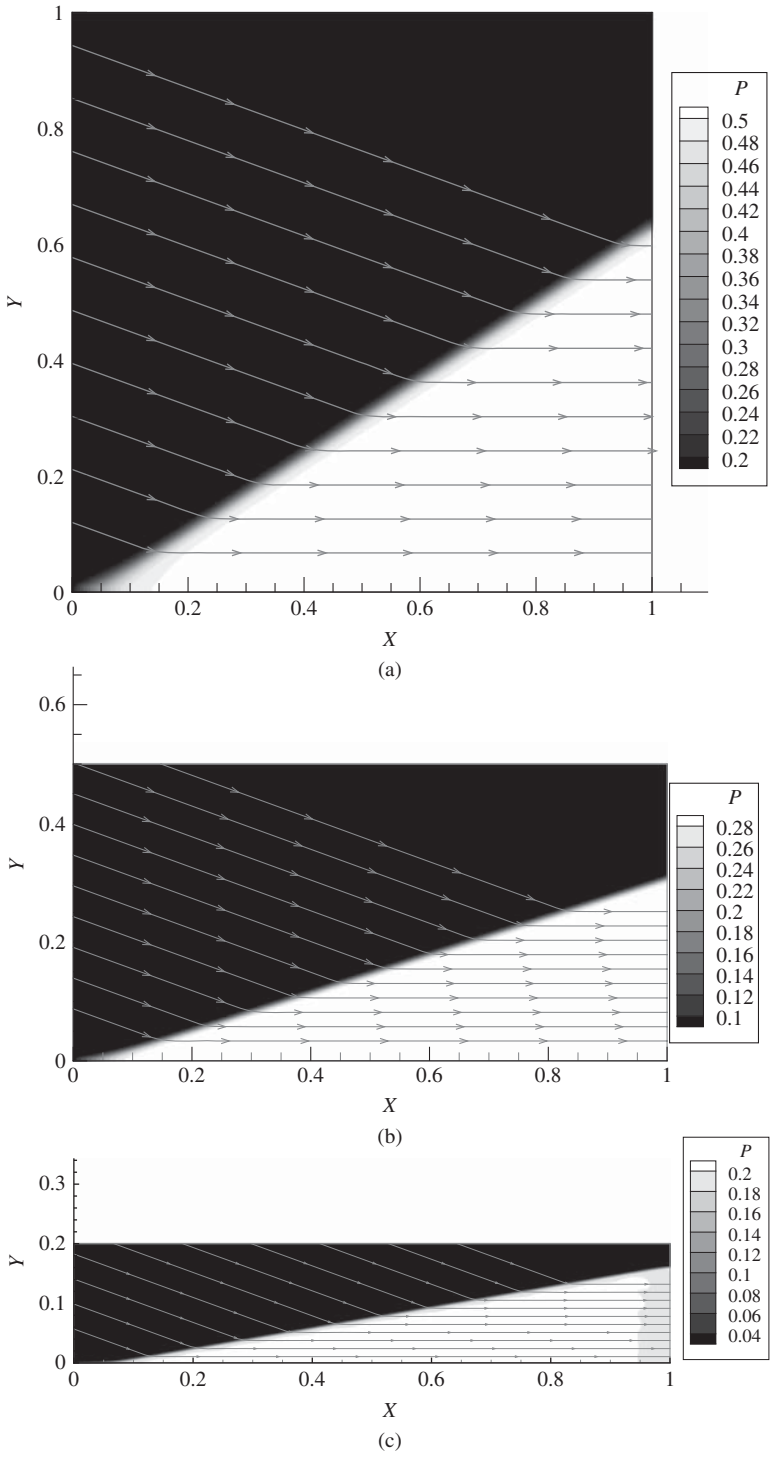

Figure 6.22 Pressure contour plot with streamlines (pressure is nondimensionalized with $\rho U_\infty{}^2$). (a) Mach 2 flow, (b) Mach 3 flow, and (c) Mach-5 flow.

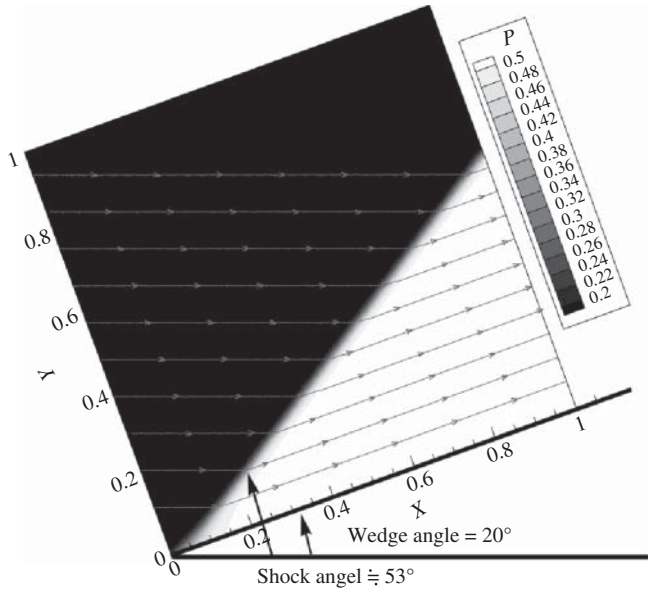

Figure 6.23 Oblique shock angle in Mach 2 flow.

■

6.8 Summary

Aerothermodynamics deals with the aerodynamic forces and moments and the heating distribution of a vehicle that flies at hypersonic speeds. Most of the vehicles experiencing aerothermodynamic environment contain an air-breathing, scramjet propulsion system.

The complex flow field associated with the vehicle is usually studied by testing a scale model of the vehicle in a hypersonic wind tunnel or some other type of ground-based test facility.

Computational fluid dynamics implies the integration of two disciplines, namely, the fluid dynamics and computation.

A CFD code development and application may follow the following steps.

- Select the physical process to be considered.
- Decide upon mathematical and topographical models.
- Build body geometry and space grid.
- Develop a numerical solution method.
- Incorporate the above into a computer code.
- Calibrate and validate the code against benchmark data.
- Predict aerodynamic coefficients, flow parameters, and aerodynamic heatings.

The wind tunnel data were usually used in dimensionless form to define the pressure distribution, the convective heat transfer distribution, and the aerodynamic forces

and moments. Wind-tunnel-based empirical correlations complimented by analytical solutions provide reasonable estimates of the actual flight environment.

The effect of the boundary layer on the inviscid flow field may be represented by displacing the actual surface by boundary layer displacement thickness.

The viscous/inviscid interactions is a complex phenomenon in which the boundary layer "history" plays a dominant role. This phenomenon is more significant for slender bodies.

To correlate the viscous/inviscid-interaction-induced flow field perturbations, Koppenwallner [1] identified two different parameters: one for the pressure and the other for the skin friction and the heat transfer. To correlate the pressure changes, the hypersonic viscous interaction parameter is

$$\chi = \frac{M_\infty^3 \sqrt{C_\infty}}{\sqrt{Re_{\infty,x}}}$$

To correlate the viscous/inviscid-induced perturbations in the skin friction or the heat transfer, Koppenwallner recommends

$$V = \frac{M_\infty \sqrt{C_\infty}}{\sqrt{Re_{\infty,x}}}$$

as the viscous interaction parameter.

Computational fluid dynamics serves as a useful tool for solving the problems of hypersonic flow past flying machines. Computational fluid dynamics is essentially the numerical solutions of the equations of motion that describe the main governing equations, namely, the continuity, momentum, and energy equations.

To account for the real-gas effects involving thermochemical nonequilibrium, leading to finite rate process for chemical and energy exchange, and radiative transport, the concentration equations for each chemical species must be added to the governing equations of the flow field.

Development of Navier–Stokes codes to generate flow field solutions for complex three-dimensional reacting gas flows is expensive and time consuming. The coupled solution of the second-order boundary layer and the Euler equations provides an efficient tool for the calculation of hypersonic viscous flows.

The zonal method is an approach to reduce computational efforts. In this method, the flow field is divided into zones according to the local flow characteristics.

Large number of techniques have been developed for generating the computational grids that are required in the finite-difference, finite-volume, and finite-element solutions of partial differential equations for arbitrary regions. Grids may be structured or unstructured.

The computation of the heat transfer or the skin friction requires resolution of the flow very near the surface. The effect of grid density on the computed heat transfer rates for Mach 20 flow past a 5° semivertex angle cone was demonstrated by Neumann [5].

Improper mesh sizes can result in underprediction of the heating rates by orders of magnitude. The degree of accuracy depends on the dissipative nature of the algorithm.

Many of the computer codes that are used to define the aerothermodynamic environment divide the shock-layer flow field (that is, the flow zone between the bow shock wave and the surface of the vehicle) into the following two regimes.

- A rotational inviscid flow where the viscous effects are negligible.
- The thin viscous boundary layer adjacent to the surface.

During the initial phases of a development program, the designer has need for computational tools that are capable of predicting the aerodynamic characteristics.

For computing the inviscid pressure acting on a panel, one of the simple impact or expansion methods can be used. These methods require the angle and, in some cases, the freestream Mach number.

Another approach for determining the local pressure includes the calculation of the interference effects of one component on another.

The challenging aspect of analyzing the flow over a complex shape is the calculation of the viscous flow due to difficulties in developing simple yet realistic models for turbulence, viscous/inviscid interactions, etc.

The detailed distribution for the pressure and the skin friction that are computed using the approximate methods of a conceptual code may differ from the actual distributions.

At low Reynolds number/high Mach number conditions, the interaction between the rotational external flow and the boundary layer would invalidate the two-layer approach. However, at moderate-to-high Reynolds numbers, a coupled Euler/boundary layer approach with features specific to hypersonic flows, for example, gas chemistry, surface catalycity, and entropy swallowing, provides an efficient tool for the calculation of hypersonic viscous flows over a wide range of conditions.

The basic principle of a coupled inviscid region/boundary layer for the flow field is that the flows are matched at their interface. The inviscid flow field solution at the boundary surface provides conditions at the edge of the boundary layer. Boundary layer growth changes the conditions at the edge of the boundary layer. The inviscid field might then be computed for the equivalent configuration, that is, the actual configuration plus the displacement thickness.

Many codes have been developed to solve steady state flow fields over complex three-dimensional bodies.

At relatively high Reynolds numbers, the presence of the boundary layer has a second-order effect on the static pressure acting on the windward surface. At angles of attack where the flow on the lee-side of a slender body separates and forms a vortex pattern, the Euler-based flow models usually fail to represent the attached flow.

Vehicles designed for hypersonic flight through earth's atmosphere usually have blunt nose to reduce the convective heat transfer and alleviate asymmetric vortex

effects associated with subsonic portion of the flight. As a result, the bow shock wave is curved. The entropy increase caused by the shock is proportional to the local inclination of the shock wave and the freestream Mach number.

The static pressure acting across the boundary layer is relatively insensitive to the flow field. However, significant entropy gradients can persist for considerable distances. Thus, when entropy layer swallowing is being considered, the location of the outer edge of the boundary layer must be defined.

CFD code calibration implies comparison of computed results with experimental data for realistic geometries that are similar to the ones of design interest, made in order to provide a measure of the code's ability to predict parameters that are required for the design without necessarily verifying that all the features of the flow are correctly modeled.

The designer of a hypersonic vehicle must make use of both experimental and analytical tools available. CFD can give greater detail of a flow field than that is possible in any wind tunnel, as all aerodynamic parameters are computed at each grid point. CFD provides a capability for configuration optimization for determining the effect of configuration changes before commitment to model construction is made. Thus, CFD helps in making more effective use of ground-test facilities.

Exercise Problem

6.1 If the entropy increase along the stagnation streamline of the blunt-nosed object, flying in air, is 0.8 kJ/(kg K), determine (a) the freestream Mach number and (b) the shock strength along the stagnation streamline.

[Answer: (a) 5, (b) 28]

References

[1] Koppenwallner G., *Hypersonic Aerothermodynamics*, Lecture Series 1984-01, von Karman Institute for Fluid Dynamics, 1984.

[2] Talbot L., Koga T., and Sherman P. M., "Hypersonic viscous flow over slender cones", *Journal of Aerospace Sciences*, Vol. 26, No. 11, 1959, pp. 723–730.

[3] Hayes W. D., and Probstein R. F., *Hypersonic Flow Theory*, Academic Press, New York, 1959.

[4] Monnoyer F., Mundt C., and Pfitzner M., "Calculation of the Hypersonic Viscous Flow Past Reentry Vehicles with an Euler-Boundary Layer Coupling Method", AIAA Paper 90-0417, Reno, NV, Jan. 1990.

[5] Neumann R. D,, "Defining the Aerothermodynamic Methodology", J. J. Bertin, R. Glowinski, and J. Periaux (eds.), *Hypersonics: Defining Hypersonic Environment*, Vol. I, Birkauser Boston, Boston, MA, 1989.

[6] Siddiqui M. S., Hoffmann K. A., Chiang S. T., and Rutledge W. H,, "A comparative Study of Navier-Stokes Solvers with Emphasis on the Heat Transfer Computations of High Speed Flows", AIAA Paper 92-0835, Reno, NV, Jan. 1992.

[7] Gentry A. E., Smyth D. N., and Oliver W. R., *The Mark IV Supersonic-Hypersonic Arbitrary-Body Program*, AFFDL-TR-73-159, Nov. 1973.

[8] Cooke J. C., *An Axially Symmetric Analogue for General Three-Dimensional Boundary Layers*, British Aeronautical Research Council, R&M No. 3200, 1961.

[9] Marconi F., Salas M., and Yeager L., "Development of a Computational Code for Calculating the Steady Super/Hypersonic Flow Around Real Configurations, Volume I - Computational Technique", NASA CR-2675, Apr, 1976.

[10] Weilmuenster K. J., "Comparison of inviscid computations with flight data for the shuttle orbiter", *Journal of Spacecraft and Rockets*, Vol. 22, No. 3, 1985, pp. 297–303.

[11] Rathakrishnan E., *Applied Gas Dynamics*, John Wiley & Sons, Inc., Hoboken, NJ, 2010.

[12] Yee H. C., "A Class of High-Resolution Explicit and Implicit Shock-Capturing Methods", NASA TM-101088, 1989.

[13] Roe P. L., "Approximate riemann solvers, parameter vectors, and difference schemes", *Journal of Computational Physics*, Vol. 43, 1981, pp. 357–372.

7

High-Enthalpy Facilities

7.1 Introduction

High-enthalpy facilities are devices to provide hypersonic air flows at high-enthalpy and high-pressure total conditions. In such a device, real-gas effects are large causing experimental difficulties to assess the test-section freestream characteristics. Also, flow contamination is a problem for total enthalpy determination. Some of the popular high-enthalpy facilities are free-piston tunnels, shock tubes, shock tunnels, hot shot tunnels, arc tunnels, and gun tunnels. The knowledge of the actual enthalpy is not an obvious task for high-enthalpy wind tunnels, as it could be for cold hypersonic wind tunnels. These are experimental aerodynamic facilities that allow testing and research at velocities considerably above those achieved in the wind tunnels meant for tests at subsonic and supersonic speeds. The high velocities in these facilities are achieved at the expense of other parameters, such as Mach number, pressure, and/or run time.

From the technical features of supersonic and hypersonic tunnels, it is obvious that the aerodynamic problems of high-speed flight are not completely answered by tests in these facilities, where the tunnel operating temperature is only high enough to avoid liquefaction. Also, we know that if the static temperatures and pressures in the test section of a wind tunnel have to be equal to those at some altitude in the atmosphere and at the same time that the velocity in the wind tunnel equals the flight velocity of a vehicle at that altitude, then the total temperatures and pressures in the wind tunnel must be quite high. It is important to keep the static temperature, static pressure, and velocity in the test section be the same as those in the actual flight condition, because only then the temperature and pressure in the vicinity of the model (behind shock waves and in boundary layers) would correspond to conditions for the vehicle in flight.

Having the proper temperature and pressure in the vicinity of the model is considered important because at high temperatures, the characteristics of air are completely different from those at low temperatures. Experimental facilities that have been

High Enthalpy Gas Dynamics, First Edition. Ethirajan Rathakrishnan.

www.wiley.com/go/rathakrishnan

developed to simulate realistic flow conditions at high speeds and are used extensively for high-speed testing are

- Hotshot tunnels.
- Plasma jets.
- Shock tubes.
- Shock tunnels.
- Light gas guns.

Although it is not our aim to discuss these facilities in this book, let us briefly see them to have an idea about the facilities that are expected to dominate the experimental study in the high-speed regime in the future.

7.2 Hotshot Tunnels

Hotshot tunnels are devices meant for the generation of high-speed flows with high temperatures and pressures for a short duration. The high temperatures and pressures required at the test section are obtained by rapidly discharging a large amount of electrical energy into an enclosed small volume of air, which then expands through the nozzle and the test section. The main parts of a typical hotshot tunnels are shown schematically in Figure 7.1.

The arc chamber is filled with air at pressures up to 270 MPa. The rest of the circuit is evacuated and kept at low pressures at the order of few micropascals. The high- and low-pressure portions are separated by a thin metallic or plastic diaphragm located slightly upstream of the nozzle throat. Electrical energy from a capacitance or inductance energy storage system is discharged into the arc chamber over a time interval of a few milliseconds. The energy added to the air causes an increase in its temperature and pressure, and this makes the diaphragm to get ruptured. When the diaphragm ruptures, the air at high temperature and pressure in the arc chamber expands through the nozzle and establishes a high-velocity flow. The high-velocity flow typically lasts for

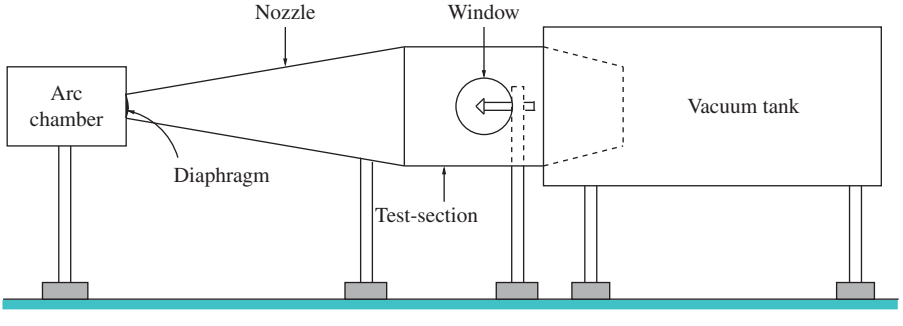

Figure 7.1 Main parts of hotshot tunnel.

10–100 ms periods but varies continuously during the period. The variation of flow velocity is due to the decay of the pressure and temperature in the arc chamber with time. The high-velocity flow is terminated when the shock that passed through the tunnel at the starting of the flow is reflected from a downstream end of the vacuum tank and arrives back upstream at the model.

Presently, the common operating pressure and temperature of hotshot tunnels are about 20 MPa and 4000°C, respectively. The flow Mach number is usually 20 and above, although there is much variation between facilities. Data collection in hotshot tunnels are much more difficult than the conventional tunnels because of the short run times.

7.3 Plasma Arc Tunnels

Plasma arc tunnels are devices capable of generating high-speed flows with very high temperature. It uses a high-current electric arc to heat the test gas. Unlike hotshot tunnels, plasma arc tunnels may be operated for periods of the order of many minutes, using direct or alternating current. Temperatures of the order of 13,000°C or more can be achieved in the test gas.

A typical plasma arc tunnel consists of an arc chamber, a nozzle usually for a Mach number less than 3, an evacuated test chamber into which the nozzle discharges, and a vacuum system for maintaining the test chamber at a low pressure, as shown in Figure 7.2.

In the plasma arc tunnel, a flow of cold test gas is established through the arc chamber and the nozzle. An electric arc is established through the test gas between an insulated electrode in the arc chamber and some surface of the arc chamber. The electric arc raises the temperature of the test gas to an ionization level, rendering the test gas as a mixture of free electrons, positively charged ions, and neutral atoms. This mixture is called *plasma*, and it is from this that the plasma arc tunnel gets its name.

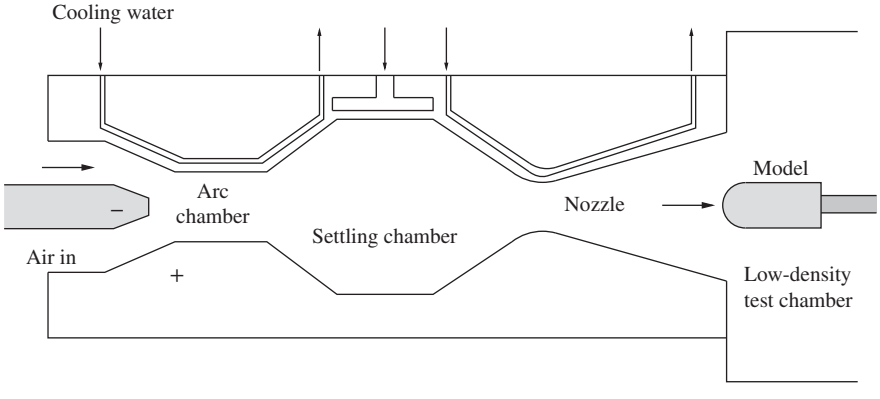

Figure 7.2 Schematic of plasma arc tunnel.

Plasma tunnels operate with low stagnation pressures of the order of 700 kPa or less, with gases other than air. The enthalpy level of the test gas and, consequently, the temperature and velocity in a given nozzle are higher for a given power input when the pressure is low. Argon is often used as the test gas because high temperature and high degree of ionization can be achieved with a given power input; also the electrode will not get oxidized in argon environment.

Mostly, plasma arc tunnels are used for studying materials for reentry vehicles. Surface material ablation tests, which are not possible in low-temperature tunnels or high-temperature short-duration tunnels, can be made. These tunnels can also be used for "magneto-aerodynamics" and plasma chemistry fields to study the electrical and chemical properties of the highly ionized gas in a flow field around a model.

Example 7.1 If the test-section temperature of a arc tunnel run by stagnation state at 700 kPa and 3200 K is 2000 K, determine the test-section Mach number, assuming the gas as perfect gas with specific heats ratio 1.5 and molecular weight 28.

Solution

Given $T_0 = 3200$ K, $T = 2000$ K, $M_m = 28$, and $\gamma = 1.5$.
For the test gas, the gas constant is

$$\begin{aligned} R &= \frac{R_u}{M_m} \\ &= \frac{8314}{28} \\ &= 296.93 \text{ J/(kg K)} \end{aligned}$$

The specific heat at constant pressure is

$$\begin{aligned} c_p &= \frac{\gamma}{\gamma - 1} R \\ &= \frac{1.5}{1.5 - 1} \times 296.93 \\ &= 890.79 \text{ J/(kg K)} \end{aligned}$$

By energy equation,

$$h + \frac{V^2}{2} = h_0$$

where $h = c_p T$ and $h_0 = c_p T_0$; therefore,

$$\begin{aligned} V^2 &= 2(h_0 - h) \\ V &= \sqrt{2c_p(T_0 - T)} \\ &= \sqrt{2 \times 890.79 \times (3200 - 2000)} \\ &= 1461.5 \text{ m/s} \end{aligned}$$

The speed of sound at the test section is

$$\begin{aligned} a &= \sqrt{\gamma RT} \\ &= \sqrt{1.5 \times 296.93 \times 2000} \\ &= 943.82 \text{ m/s} \end{aligned}$$

Thus the Mach number is

$$\begin{aligned} M &= \frac{V}{a} \\ &= \frac{1461.5}{943.82} \\ &= \boxed{1.55} \end{aligned}$$

■

7.4 Shock Tubes

The shock tube is a device that is used to produce high-speed flow with high temperatures by traversing normal shock waves that are generated by the rupture of a diaphragm that separates a high-pressure gas from a low-pressure gas. Shock tube is a very useful research tool for investigating not only the shock phenomena but also the behavior of the materials and objects when subjected to very high pressures and temperatures. A shock tube and its flow process are shown schematically in Figure 7.3.

The diaphragm between the high- and low-pressure sections is ruptured and the high-pressure driver gas rushes into the driven section, setting up a shock wave that compresses and heats the driven gas. The pressure variation through the shock tube at the instant of diaphragm rupture and two short intervals later are shown in Figure 7.3. The wave diagram simply shows the position of the important waves as a function of time.

When the shock wave reaches the end of the driven (low-pressure) tube, all of the driven gas will have been compressed and will have a velocity in the direction of shock wave travel. On striking the end of the tube, the shock gets reflected and starts traveling back upstream. As it passes through the driven gas and brings it to rest, additional compression and heating is accomplished. The heated and compressed gas sample at the end of the shock tube will retain its state except for heat losses until the shock wave reflected from the end of the tube passes through the driver-gas-driven interface and sends a reflected wave back through the stagnant gas sample, or the rarefaction wave reflected from the end of the driver (high-pressure) section reaches the gas sample. The high-temperature gas samples that are generated make the shock wave useful for studies of the chemical physics problems of high-speed flight, such as dissociation and ionization.

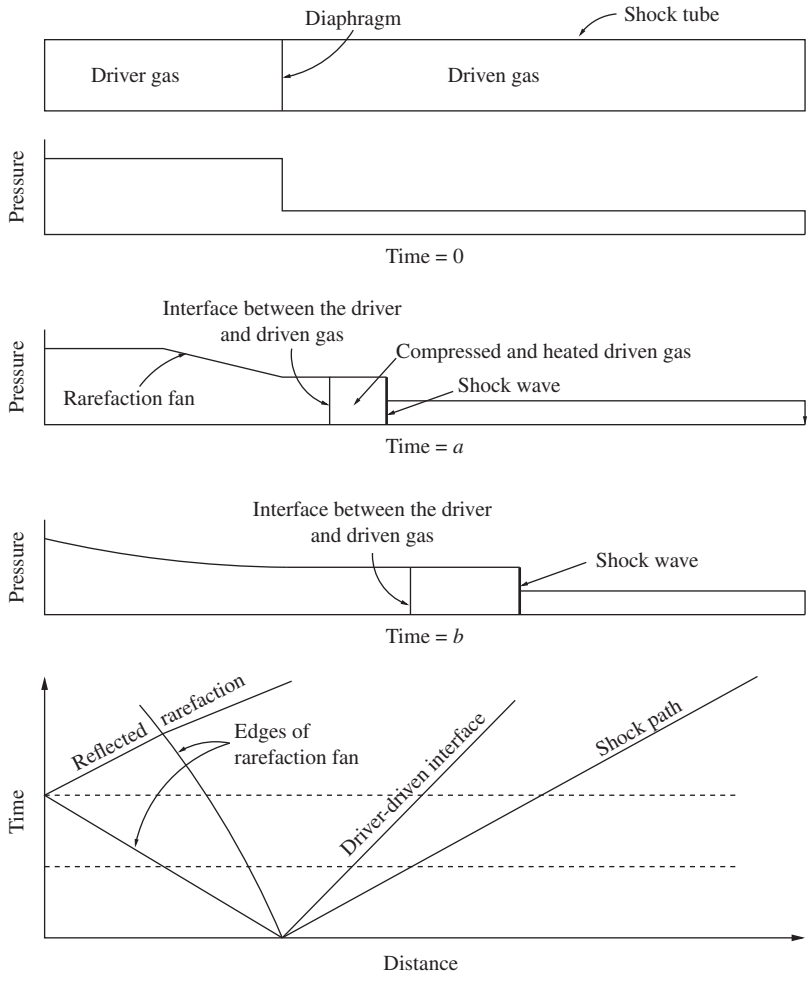

Figure 7.3 Pressure and wave diagram for a shock tube.

7.4.1 Shock Tube Applications

Shock tube being a device capable of producing established flow with uniform temperatures and pressure at high values, which cannot be achieved with conventional tunnels, finds application in numerous fields in science and engineering.

1. The uniform flow behind the shock wave may be used as a short-duration wind tunnel. In this role, the shock tube is similar to an intermittent or blowdown tunnel, but the duration of flow is much shorter, usually of the order of a millisecond. But the operating conditions (particularly the high stagnation enthalpies), which are possible, cannot be easily obtained with other types of facility.

2. The abrupt changes of flow condition at the shock front may be utilized for studying transient aerodynamic effects and for studies of dynamic and thermal response.
3. Shock tubes can also be used for studies on relaxation effects, reaction rates, dissociation, ionization, etc.

Finally, note that in the shock tube relations, we use different "γ" for every flow zone. This is because in most of the applications, the temperatures experienced by the gas at these zones are appreciably above the level to assume the gas as perfect gas, and hence, γ takes different values corresponding to the local temperature.

Example 7.2 A shock tube is filled with air. The temperature in the low-pressure chamber is atmospheric. (a) If the shock generated by rupturing the diaphragm moves at Mach number 10, treating the air traversed by the shock as perfect gas, determine the stagnation temperature of the air behind the shock. (b) What will be the test time available for testing a model located at 8 m from the diaphragm?

Solution

Let subscripts 1 and 2, respectively, refer to states ahead of and behind the shock.

(a) Given $M_s = 10$, $T_1 = 15°\text{C} = 288.15$ K, and $\gamma = 1.4$.
The speed of sound in the low-pressure chamber is

$$\begin{aligned} a_1 &= \sqrt{\gamma R T_1} \\ &= \sqrt{1.4 \times 287 \times 288.15} \\ &= 340.3 \text{ m/s} \end{aligned}$$

Thus the shock speed is

$$\begin{aligned} C_s &= M_s a_1 \\ &= 10 \times 340.3 \\ &= 3403 \text{ m/s} \end{aligned}$$

The pressure ratio across the shock is

$$\begin{aligned} \frac{p_2}{p_1} &= 1 + \frac{2\gamma}{\gamma + 1}(M_s^2 - 1) \\ &= 1 + \left(\frac{2 \times 1.4}{1.4 + 1}\right) \times (10^2 - 1) \\ &= 116.5 \end{aligned}$$

For $M_s = 10$, from normal shock table [1],

$$\frac{\rho_2}{\rho_1} = 5.71429, \qquad \frac{T_2}{T_1} = 20.387$$

The flow speed of the field traversed by the shock, by Equation (3.45) [2], is

$$\begin{aligned} V_2 &= C_s \left(1 - \frac{\rho_1}{\rho_2}\right) \\ &= 3403 \times \left(1 - \frac{1}{5.71429}\right) \\ &= 2807.48 \text{ m/s} \end{aligned}$$

The temperature of air stream traversed by the shock is

$$\begin{aligned} T_2 &= 20.387\ T_1 \\ &= 20.387 \times 288.15 \\ &= 5874.5 \text{ K} \end{aligned}$$

The Mach number of the air stream traversed by the shock is

$$\begin{aligned} M_2 &= \frac{V_2}{a_2} \\ &= \frac{V_2}{\sqrt{\gamma R T_2}} \\ &= \frac{2807.48}{\sqrt{1.4 \times 287 \times 5874.5}} \\ &= 1.83 \end{aligned}$$

From $M_2 = 1.83$, from isentropic table,

$$\frac{T_2}{T_{02}} = 0.599$$

The flow across the shock is adiabatic; hence, $T_{02} = T_{01}$. Thus, the stagnation temperature of air behind the shock is

$$\begin{aligned} T_{02} &= \frac{T_2}{0.599} \\ &= \frac{5874.5}{0.599} \\ &= \boxed{9807.2 \text{ K}} \end{aligned}$$

(b) Let l be the distance between the model and the diaphragm. The test time t is equal to $l/V_2 - l/C_s$. Thus

$$\begin{aligned} t &= \frac{l}{V_2} - \frac{l}{C_s} \\ &= \frac{8}{2807.48} - \frac{8}{3403} \\ &= \boxed{4.99 \times 10^{-4} \text{ s}} \end{aligned}$$

■

7.5 Shock Tunnels

Shock tunnels are wind tunnels that operate at Mach numbers of the order of 25 or higher for time intervals up to a few milliseconds by using air heated and compressed in a shock tube. Schematic diagram of a shock tunnel, together with wave diagram, is shown in Figure 7.4.

As shown in the figure, a shock tunnel includes a shock tube, a nozzle attached to the end of the driven section of the shock tube, and a diaphragm between the driven tube and the nozzle. When the shock tube is fired and the generated shock reaches the end of the driven tube, the diaphragm at the nozzle entrance is ruptured. The shock is reflected at the end of the driven tube, and the heated and compressed air behind the reflected shock is available for operation of the shock tunnel. As the reflected shock travels back through the driven section, it travels only a relatively short distance before striking the contact surface; it will be reflected back toward the end of the driven section. When the reflected shock reaches the end of the driven section, it will result in a change in pressure and temperature of the gas adjacent to the end of the driven section. If the change in the conditions of the driven gas is significant, the flow in the nozzle will be unsatisfactory and the useful time will be terminated. The stagnation pressure and temperature in shock tunnels are about 200 MPa and 8000 K, respectively, to provide test times of about 6.5 ms.

7.6 Gun Tunnels

The gun tunnel is quite similar to the shock tunnel in operation. It has a high-pressure-driver section and a low-pressure-driven section with a diaphragm separating the two, as shown in Figure 7.5.

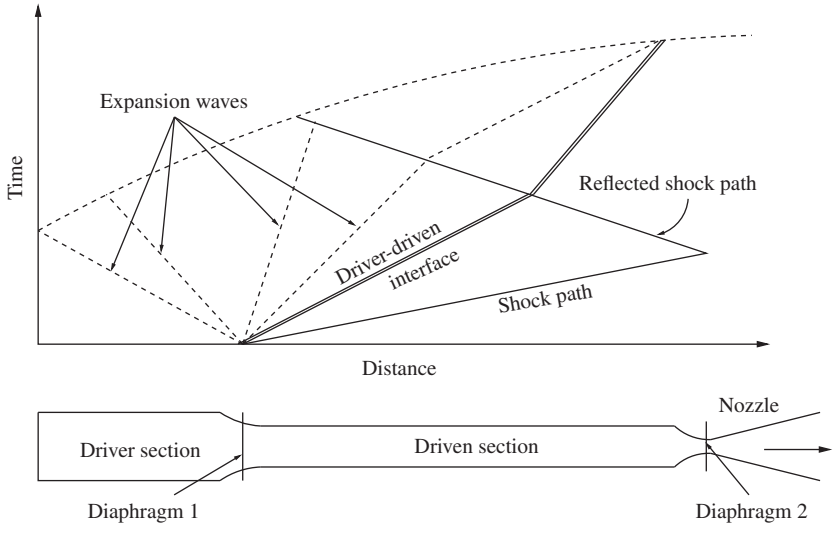

Figure 7.4 Schematic of shock tunnel and wave diagram.

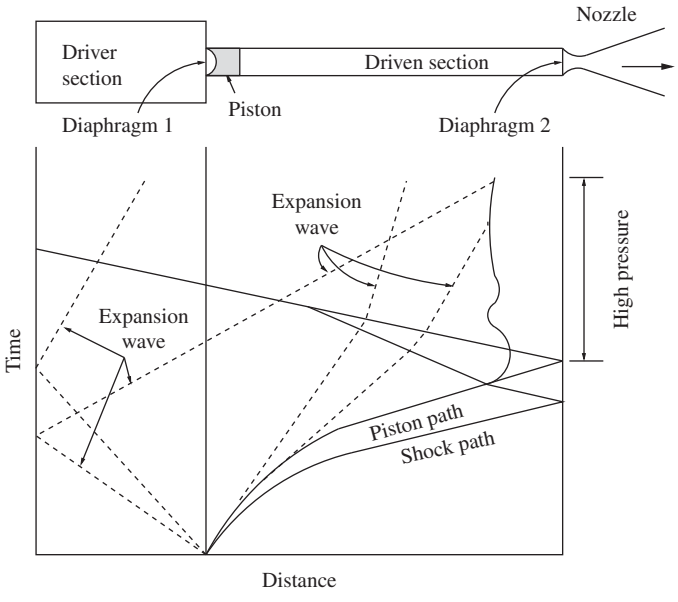

Figure 7.5 A gun tunnel and its wave diagram.

A piston is placed in the driven section, adjacent to the diaphragm, so that when the diaphragm ruptures, the piston is propelled through the driven tube, compressing the gas ahead of it. The piston used is so light that it can be accelerated to velocities significantly above the speed of sound in the driven gas. This causes a shock wave to precede the piston through the driven tube and heat the gas. The shock wave will be reflected from the end of the driven tube to the piston, causing further heating of the gas. The piston comes to rest with equal pressure on its two sides, and the heated and compressed driven gas ruptures a diaphragm and flows through the nozzle.

As can be inferred, gun tunnels are limited in the maximum temperature that can be achieved by the piston design. The maximum temperatures normally achieved are about 2000 K. Run times of an order of magnitude higher than the shock tunnels are possible in gun tunnels. In general, the types of tests that can be carried out in gun tunnels are the same as those in the hotshot tunnels and the shock tunnels.

7.7 Some of the Working Facilities

Some popular facilities meant for experiments at high-enthalpy and hypersonic environments are given in this section, to get an idea about the various parameters associated with such flows. The facilities listed here are meant for gaining a bird's eye view about the requirements of facilities meant for generating high-enthalpy environment.

In addition to what is listed here, there are large number of facilities in active use all over the world.

7.7.1 Hypersonic Wind Tunnel

The hypersonic wind tunnel Cologne (H2K) at Department Wind tunnels facilities is one of the busy facilities. The H2K is a "blowdown" wind tunnel with a free jet test section. It uses contoured, axially symmetrical and replaceable nozzles. For aerodynamic testing, nozzles for Mach numbers of 4.8, 5.3, 6.0, 7.0, 8.7, and 11.2 are available. For aerothermal tests on probes, smaller nozzles with Mach numbers of 3.0 and 5.0 are also in use.

In order to achieve the pressure ratio required for building up the nozzle flow for about 30 s, the pressure in the test chamber is reduced by a vacuum sphere. Owing to the large expansion of the air in the nozzle, its static temperature decreases significantly. To prevent condensation of air particles and for tests at high temperatures, the air is preheated. Eight electric heaters with a maximum electrical power of 5 MW heat the air for up to 1100 K. Depending on the test setup, between 8 and 10 tests per day can be carried out.

Application areas

The following are some of the specific applications for which the above H2K wind tunnel is used.

1. For simulation of the air flow around models of future spacecrafts at Mach numbers of between 4.8 and 11.2.
2. For the measurement of aerodynamic and aerothermodynamic loads on complete hypersonic flight configurations and their components.
3. For investigations on the interaction of hot plume nozzle flows with the external base flow.

7.7.2 High-Enthalpy Shock Tunnel (HIEST)

This facility is the largest high-enthalpy shock tunnel of free-piston-driven type (commonly called HIEST) in the world, constructed by Mitsubishi Heavy Industries limited, Japan. It simulates airflow of very high temperature and high pressure that returnable spacecrafts (that is, HOPE X and spaceplanes) encounter when they reenter the atmosphere. The purposes of this facility are to understand aerodynamic and aerothermodynamic characteristics of the real gas by simulations using scale models of spacecrafts and to clarify combustion process and characteristics of ram jet engines and scramjet engines.

The main specifications and performance parameters are given in the following text.

Specifications

Secondary reservoir	Wrap-around type
Type/capacity	7.7 m^3
Compression	
Tube length/diameter	42 m/600 mm
Shock tube	
Length/diameter	17 m/180 mm
Piston weight	300/440/580 kg
Nozzle exit diameter	500/1200 mm

Performance

Stagnation pressure	150 MPa
Maximum enthalpy	25 MJ/kg
Maximum stagnation temperature	10,500 K
Test duration	2.0 ms

- *Piston Blasting System*. The world's first system, developed in coordination with the National Aerospace Laboratory of Japan, is adopted.
- *Piston Shock Absorber*. The world's first long-life damper made from urethane is adopted.

Features

(i) The largest shock wind tunnel in the world.
(ii) It can simulate both very high temperature and very high pressure at the same time. The stagnation enthalpy established in this facility is suppose to be the largest stagnation enthalpy in the world.
(iii) It can perform tests of the longest duration in the world.
(iv) It can perform returnable spacecraft's aerodynamic and aerothermodynamic tests as well as scramjet engine's combustion tests.

Types of tests

(i) Aerodynamic and aerothermodynamic tests on scale models of returnable spacecrafts.
(ii) Combustion process tests on scramjet engines.

7.7.3 Hypersonic and High-Enthalpy Wind Tunnel

The hypersonic and high-enthalpy wind tunnel at Kashiwa Campus of the University of Tokyo has provision for two-mode operation. Using the high-pressure and high-temperature air generator, it can used either as a hypersonic wind tunnel (that is, very high-speed flow) or as a high-enthalpy wind tunnel (that is, very high temperature flow).

This facility is used for studying *planetary science*, *high-speed aerospace transport*, *spacecraft*, and *high-temperature material test*.

Heater

Pebble-bed air heater is used to produce the high-temperature gas with the heat exchange between the air and preheated pebbles. The height of the heater is about 3 m. The wall inside the heater is covered by heat-resistant bricks. Alumina pebbles are filled in the heater. The air from high-pressure tank is introduced to the heater from the bottom to the top, after the pebbles are preheated by the burner at the top of the heater, producing very high temperature air at more than 1200°C. Such high-temperature air is necessary not only for the experiments with hot air but also for energizing the air to accelerate to hypersonic speeds in the hypersonic wind tunnel.

Nozzle

Hypersonic nozzle of the tunnel converts the thermal energy obtained through the heater to the kinetic energy. The choked air flow through the very narrow throat is accelerated by expanding it in the divergent portion downstream of the throat. As the degree of acceleration depends on the area ratio between the throat and the outlet, the nozzle throat for the hypersonic wind tunnel is very narrow. The diameter of the nozzle exit is 200 mm. The curve of the bell-shaped nozzle is smooth and carefully designed to produce the uniform flow at the test section. Two nozzles for Mach numbers 7 and 8 are available.

Pressure system

Compressor and vacuum pump are used to charge the air in the high-pressure tank and reduce the pressure in the vacuum tank, respectively. Both are installed in the special compartment to avoid the spillage of the noise and vibration to the outside. Both tanks are installed outside. High-pressure vessel is a cylindrical tank of volume 4 m^3, which can store the high-pressure dry air produced by the compressor system to a maximum pressure level of 5 MPa. The stagnation pressure of the air flow is controlled by the regulator. The temperature of air is raised by pebble-bed heater.

The maximum flow duration is about 60 s for the hypersonic wind tunnel and 200 s for the high-enthalpy wind tunnel. The vacuum tank is a spherical tank of volume 180 m^3, and 7 m in diameter, and very low pressure level at less than 100 kPa can be kept for several days. The pressure in the vacuum tank is decreased using a vacuum pump before the experiment. The air of the hypersonic wind tunnel flow is exhausted to the tank.

Test section of high-enthalpy wind tunnel

High-temperature air from the heater is injected to the atmosphere as a free jet flow. The flows are exhausted to outside through the silencer tower. Users can set up the supersonic nozzle and test-section layout freely, depending on the objectives of each experiments.

Air cooler

Air cooler used in this facility is a water-cooled heat exchanger to cool the air of hypersonic wind tunnel before exhausted to the vacuum tank.

Test section of hypersonic wind tunnel

In the test section, the hypersonic flow around the test model can be observed and measured. This section is an airtight chamber because the pressure inside is much lower than the atmospheric pressure during the experiment. There are windows of 200 mm diameter, for the observation, for example, Schlieren images. The model injection system is installed in the test section. The model is injected to the hypersonic flow after the flow establishes stably. The angle of attack with respect to the uniform flow (that is pitch angle) can be controlled from $-10°$ to $+10°$ from control room remotely. Owing to the constraint of the blockage ratio, the model size is limited to about 4 cm in diameter.

7.7.4 Von Karman Institute Longshot Free-Piston Tunnel

The Von Karman Institute (VKI) Longshot free-piston tunnel is a short-duration facility that can be operated with either nitrogen or carbon dioxide, and it is designed to provide the attainment of very high Reynolds number hypersonic flows.

It has a Mach number of 14 contoured nozzle of 0.43 m exit diameter and a 6° conical nozzle of 0.60 m exit diameter that can be used throughout the Mach number ranging from 14 to 20. Typical Reynolds numbers at Mach number 14 range from 5×10^3 to 15×10^6 (that is these Reynolds numbers are per unit length). A high precision incidence mechanism for pitch, roll, and yaw is mounted in the open-jet 4 m^3 test section. Instrumentation includes a force/moment balance, accelerometers, thin-film

and coaxial thermocouples for heat flux measurements, piezoresistive pressure transducers, and a Schlieren system.

7.7.5 MHD Acceleration in High-Enthalpy Wind Tunnels

The interest in transporting goods, people, and military equipment around the world as fast as possible has lead to the development of hypersonic technologies. In order to utilize these technologies, they must be proven safe, economical, and efficient. High-enthalpy wind tunnels provide important data required to verify and optimize specific designs of hypersonic vehicles, such as reentry vehicles. However, hypersonic facilities that utilize classical adiabatic expansion for gas acceleration require an incredible amount of resources and have critical limitations. In the late 1950s, researchers began searching for an alternative method for accelerating flow in high-enthalpy wind tunnels. The use of magnetohydrodynamics (MHD) was implemented into the flow chain of a wind tunnel to accelerate the gas to higher speeds. MHD avoids the complications of ultra-high precombustion values by directly increasing the kinetic energy of the flow implementing Lorentz forces[1].

The MHD generator transforms thermal energy and kinetic energy directly into electricity. MHD generators are different from traditional electric generators in that they operate at high temperatures without moving parts. MHD was developed because the hot exhaust gas of an MHD generator can heat the boilers of a steam power plant, increasing overall efficiency. MHD was developed as a topping cycle to increase the efficiency of electric generation, especially when burning coal or natural gas. MHD dynamos are the complement of MHD propulsors, which have been applied to pump liquid metals and in several experimental ship engines.

An MHD generator, similar to a conventional generator, relies on moving a conductor through a magnetic field to generate electric current. The MHD generator uses hot conductive plasma as the moving conductor. The mechanical dynamo, in contrast, uses the motion of mechanical devices to accomplish this. MHD generators are technically practical for fossil fuels but have been overtaken by other, less expensive technologies, such as combined cycles in which a gas turbine's or molten carbonate fuel cell's exhaust heats steam to power a steam turbine.

Natural MHD dynamos are an active area of research in plasma physics and of great interest to the geophysics and astrophysics communities, because the magnetic fields of the earth and sun are produced by these natural dynamos.

7.7.6 Measurement Techniques

The measurement techniques are force/moment measurements with six-component dynamic monitoring service (DMS)- based balances; pressure distribution

[1] In physics, particularly electromagnetism, the Lorentz force is the combination of electric and magnetic forces on a point charge due to electromagnetic fields.

measurements; temperature and heat flux measurements with thermocouples and infrared cameras; flow visualization by means of Schlieren optics and oil flow method (up to 150 kHz); and determination of dynamic derivatives with the free and forced oscillation methods.

7.8 Just a Recollection

To aid in understanding the different topics discussed, in the previous chapters, and to provide background material for interested readers who may not have specialized training in this field, a brief summary of the fundamental attributes of hypersonic flows is given here. Many of the topics that are introduced in this section are elaborated further in contributions related to specific subjects related to sustained hypersonic flight, in the open literature. The differences between the thermal and chemical aspects of hypersonic flow and supersonic flow are therefore highlighted. The age of some of the literature in the open source reflects the fact that the problems of hypersonic flight are not newly discovered.

The hypersonic flight regime includes atmospheric entry and reentry, ground testing, and flight for both powered and unpowered vehicles. Even though it is not currently certified for flight, there is one operational hypersonic vehicle: the space shuttle of NASA. At least 20 years before the development of the shuttle, a significant activity in hypersonic flight research was conducted by the US Air Force in their X-15 program. This vehicle has reached a flight Mach number of 6.7 on its final flight, which is also used to test a hypersonic ramjet engine. Direct shock impingement on the pylon holding a dummy engine caused severe heating and structural damage, and this was one of many lessons learned from the program. Owing to the design of the X-15, it was not capable of long-duration powered flight, but it provided a great deal of information on technical problems that still remain a serious obstacle to the development of new hypersonic vehicles. It is still astonishing to look back on the rapid development of high-speed flight in the years after the World War II. The challenge is to build on this experience and to accomplish the development of a new generation of flight vehicles.

Although unpowered hypersonic vehicles are not the topic of this book, it is important to note that there have been many more successful developments of these types of vehicle, predominantly in the reentry of manned and unmanned spacecraft of Russian, American, and European origin into earth's atmosphere. For example, the Apollo reentry conditions were 53 km of altitude, 11 km/s of velocity, 270 K of temperature, and speed of sound of 338 m/s that gave a reentry Mach number of $M = 32.5$. There have also been a number of missions to other planets (more vehicles going to these planets than that have been developed for sustained hypersonic flight within the atmosphere) and the entry speeds into those atmospheres have been even greater. A recent noteworthy example of this was the Galileo probe to Jupiter that was designed to

enter the Jovian atmosphere at 60 km/s at an altitude of 1000 km. At this altitude, the temperature is approximately 800 K, and the atmosphere was assumed to consist of hydrogen and helium at a mixture of 89 : 11 by mass. Therefore, the entry Mach number was about 28 for this mission. Even though the entry speed was greater than that of the Apollo reentry, the Mach number is lower owing to the greater value of the speed of sound in the hydrogen–helium atmosphere.

Clearly, Mach number is not the only parameter that must be considered for hypersonic flight; in fact, it is often only of secondary importance. In earth's atmosphere, for example, the temperature of the outer atmosphere is quite low, so the speed of sound is lower than that at sea level and higher Mach numbers can be achieved there at lower speeds. A better measure is the speed itself, because it can also give an indication of the kinetic energy involved in the trajectory. For hypersonic craft, the flight enthalpy can usually be estimated very quickly from the speed as $h = u^2/2$. The amount of aerothermodynamic heating that the vehicle must deal with is linearly dependent on the kinetic energy of the vehicle. This is a very important aspect of hypersonic flight through planetary atmospheres. The vehicle encounters such severe heating that a significant part of the design and development effort is concerned with providing sufficient protection of the payload without using all payload capacity for doing this. Other general characteristics of hypersonic flows are that molecules behind a high-velocity shock wave become vibrationally excited, partially or completely dissociated depending on their bond energy, and, at very high speeds, partially ionized. These aspects of hypersonic flow are typically called *real-gas* effects. To clarify what is meant by "real-gas effects," it is useful to recall the definitions in the following subsections.

7.8.1 Thermally Perfect Gas

A thermally perfect gas is one that obeys the ideal gas equation of state,

$$p = \rho RT$$

From compressible flow theory, this relationship implies that internal energy and enthalpy depend only on temperature.

7.8.2 Calorically Perfect Gas

A calorically perfect gas has constant values of specific heats (that is, constant c_p and c_v) independent of temperature.

7.8.3 Perfect or Ideal Gas

This designation refers to a gas that is both thermally and calorically perfect.

7.8.4 Thermal Equilibrium

A single temperature can be used to describe the different molecular internal energy modes (which are described in detail in the following). This single temperature describes the energy modes of all molecules and it is the same as the temperature of the surroundings.

7.8.5 Chemical Equilibrium

All chemical reactions are in balance and the system does not spontaneously undergo any change in chemical composition, no matter how slow. For this situation, the distribution of species is uniquely described by two thermodynamic variables, such as density and temperature.

Note that a "real gas" is not defined, because it is used by fluid dynamicists to describe all of the situations that are not perfect. However, it will be shown later that the most important real or imperfect gas effects for hypersonic flight in earths atmosphere are caloric.

As in other flow regimes, non-dimensional parameters are used to describe hypersonic flow. Most of these parameters are encountered in other flow domains, including subsonic and supersonic flow, but they are summarized here for convenience.

1. *Reynolds number*, $Re = VL/\nu$. This can be taken as a measure of the viscous flow time over the mean flow time.
2. *Mach number*, $M = V/a$. This is a measure of the flow speed relative to the acoustic propagation speed.
3. *Knudsen number*, $Kn = \lambda/L$ $(= M = Re)$. This is an indication of the collision path length relative to the flow scale.
4. *Prandtl number*, $Pr = \nu/k$. A measure of the thermal diffusion time relative to the viscous diffusion time.
5. *Schmidt number*, $Sc = \nu/D$. This is an indication of the species diffusion time relative to the viscous diffusion time.
6. *Eckert number*, $E = u^2/h$. This indicates the relative magnitudes of kinetic and thermal energy for the flow.
7. *Damkohler number*, $Da = \tau_f/\tau_c$. This dimensionless parameter is the ratio of the characteristic flow time (such as a residence time) to the characteristic chemical reaction time. When it is very large, the chemical reactions can be complete, and the flow will likely be in chemical equilibrium. When it is very small, the chemical reactions will not be complete and the flow chemistry is considered to be frozen. For hypersonic flow, in contrast to other flow regimes, the Damkohler number plays an important role, determining whether or not the flow is in equilibrium.

To relate the discussion of thermodynamic and gas dynamic considerations to applications of interest, it is useful to consider first general high-temperature gas effects

that are encountered in the hypersonic flight of a typical vehicle (it should be noted that apart from compressibility, none of the attributes mentioned in the following are found in the supersonic flow regime).

7.8.6 Caloric and Chemical Effects

The atmospheric composition behind a normal shock ahead of a hypersonic vehicle will differ greatly from the atmosphere ahead of the shock. Diatomic molecules will be vibrationally excited and dissociated to some extent, and the resulting atoms and remaining molecules can be partially ionized. Thus, for the remaining post-shock molecules, the assumption that they behave as calorically perfect gases is no longer valid. Within a vehicle boundary layer, there is sufficient viscous dissipation to affect the stream chemistry and this can lead to chemically reacting boundary layers. As specific heats are no longer constant owing to vibrational excitation and chemical reaction, their ratio, $\gamma = c_p/c_v$, is also no longer constant and also depends on the temperature. For air, this begins at around 800 K.

7.8.7 Aerodynamic Forces

Another important aspect of hypersonic flight is that the variation in the ratio of specific heats, γ, can significantly influence the pressure distribution over a vehicle or its control surfaces. This is because γ, which is also the isentropic exponent, directly influences the rate of expansion or compression of the flow. This can manifest itself in the setting of control surface angles or even in the trim angle of attack for a vehicle, which can be larger than that predicted for the perfect gas value of γ by $2°-4°$. This was actually observed during the first Shuttle reentry. It was found that there is a small but consistent difference in pressure values that are slightly higher for the forward region and lower in the aft region for the reacting case. When integrated over the vehicle surface, this produces a net moment that provided additional pitch-up to the shuttle nose and required manual control to override. Note that other explanations have also been given for this, which illustrates how difficult it is to isolate interacting physical phenomena.

7.8.8 Plasma Effects

For air at 1 atm pressure, oxygen dissociation begins near 2000 K and is complete at about 4000 K. Nitrogen dissociation begins at about 4000 K and is complete near 9000 K. At higher post-shock temperatures, ionization becomes important. In a partially ionized flow, the free electrons absorb and reflect electromagnetic radiation, usually in the frequency band of communication systems. In addition, at some level of ionization, the flow will behave quite differently than a weakly ionized or neutral

flow, because the interatomic forces will have a strong electrical interaction component, which will lead to differences in transport properties.

7.8.9 Viscous and Rarefaction Effects

For flows at very high speeds and low density, which might correspond to a high atmospheric altitude, the mean free path, λ, which is the average distance that a molecule or atom travels between collisions with its neighbors, can be larger than a characteristic length, L, of the vehicle. This effect is represented by the Knudsen number λ/L, and it is known that when the mean free path is too large, and Kn approaches unity, then the familiar Navier–Stokes equations can no longer be closed. Another approach to modeling the flow must be used. The viscous interaction parameter,

$$\overline{V'_\infty} = M_\infty \frac{\sqrt{\overline{C'_\infty}}}{\sqrt{Re_{\infty L}}}$$

where

$$\overline{C'_\infty} = (\mu_\infty T')/(\mu' \, T_\infty)$$

is the Chapman–Rubesin viscosity coefficient based on the reference temperature conditions. In fact, inviscid analysis can only be used in the "hypersonic" regime, which is characterized by high Reynolds number and low Mach number conditions. At higher altitudes, the reverse situation of high Mach number and low Reynolds number requires careful handling of the viscous interactions that influences the inviscid flow.

7.8.10 Trajectory Dependence

As mentioned earlier, air chemistry is significantly different at the high temperatures encountered in hypersonic flight applications. Vibrational excitation of molecules, dissociation, and ionization will all occur as temperature is increased. However, with the exception of vibrational excitation, the onset and the range of these effects will also vary with density or pressure.

7.8.11 Nonequilibrium Effects

In addition to these effects, when the characteristic flow time is much shorter than the time to complete chemical reactions or energy exchange mechanisms, then the flow can be in a nonequilibrium state. It is in this aspect that the Damkohler number plays a determining role. Note that for a given situation, there can be thermal nonequilibrium, chemical nonequilibrium, or both. This is a subject of considerable importance, as the interpretation of physical and chemical phenomena in hypersonic flow applications

often depend on the assumption of thermal and chemical equilibriums, which allows for a simpler characterization of the thermal and chemical states of the flow. This assumption is often used without justification, and it is the objective of many present research activities to investigate the limits of this assumption.

7.8.12 Ground Test

It is apparent, even to the casual observer, that hypersonic vehicles are not yet readily available for human transportation. At present, there is only the Space Shuttle, and the lifetime of this vehicle has already been officially fixed (even though it is already operating *beyond* the design lifetime). Consequently, there is very little empirical data on vehicle design and performance and many design parameters have been barely explored. Part of the reason for this is the difficulty in simulating flight conditions on the ground. The relationship between actual flight data and the data from measurements in ground test facilities is not yet well understood. Unfortunately, flight experiments are expensive, and even ground tests in high-enthalpy facilities are not cheap, so there is relatively little data to guide the development of analytical and numerical tools for these applications.

7.8.13 Real-Gas Equation of State

Although most of the discussion concerns thermally perfect gases, it is instructive to look at other equations of state that can be used for nonperfect gas situations. The most well known of these equations is the Van der Waal's equation,

$$p = \frac{RT}{v - b} - \frac{a}{v^2}$$

This equation expresses the relationship between the thermodynamic variables in the same way as the perfect gas equation, but with an important modification to account for the attractive forces of real-gas behavior at high density in the second term. Recall that the long-range attractive potential scaling was $\approx -A/R^6$ [3], and note that the second term in the Van der Waal's equation of state above is $-a/v^2$. Clearly, the second term is intended to account for the attractive potential, which becomes important as density increases. This equation provides a useful qualitative picture of real-gas behavior, but it is not quantitative. For example, the onset of the real-gas behavior also depends on temperature, and this effect is not included in the above equation.

Fortunately, for most applications involving hypersonic flows of air, the departure from thermal perfection is minimal. For CO_2, this is not the case, and as some hypersonic ground test facilities, such as the VKI Longshot Facility use CO_2, it is important to take into account its thermal imperfection when considering the test conditions.

7.9 Summary

High-enthalpy facilities are devices to provide hypersonic air flows at high-enthalpy and high-pressure total conditions. Some of the popular high-enthalpy facilities are free-piston tunnels, shock tubes, shock tunnels, hot shot tunnels, arc tunnels, and gun tunnels. These are experimental aerodynamic facilities that allow testing and research at velocities considerably above those achieved in the wind tunnels meant for tests at subsonic and supersonic speeds.

Experimental facilities that have been developed to simulate realistic flow conditions at high speeds and are used extensively for high-speed testing are

- Hotshot tunnels.
- Plasma jets.
- Shock tubes.
- Shock tunnels.
- Light gas guns.

Hotshot tunnels are devices meant for the generation of high-speed flows with high temperatures and pressures for a short duration. The high-velocity flow typically lasts for 10–100 ms periods but varies continuously during the period. Presently, the common operating pressure and temperature of hotshot tunnels are about 20 MPa and 4000°C, respectively. The flow Mach number is usually 20 and above.

Plasma arc tunnels are devices capable of generating high-speed flows with very high temperature. It uses a high-current electric arc to heat the test gas. Unlike hotshot tunnels, plasma arc tunnels may be operated for periods of the order of many minutes, using direct or alternating current. Temperatures of the order of 13,000°C or more can be achieved in the test gas. Plasma tunnels operate with low stagnation pressures of the order of 700 kPa or less, with gases other than air. Mostly, plasma arc tunnels are used for studying materials for reentry vehicles. Surface material ablation tests, which are not possible in low-temperature tunnels or high-temperature short-duration tunnels, can be made.

Shock tube is a device that is used to produce high-speed flow with high temperatures by traversing normal shock waves that are generated by the rupture of a diaphragm that separates a high-pressure gas from a low-pressure gas. Shock tube is a very useful research tool for investigating not only the shock phenomena but also the behavior of the materials and objects when subjected to very high pressures and temperatures. Shock tube being a device capable of producing established flow with uniform temperatures and pressure at high values, which cannot be achieved with conventional tunnels, finds application in numerous fields in science and engineering.

Shock tunnels are wind tunnels that operate at Mach numbers of the order of 25 or higher for time intervals up to a few milliseconds by using air heated and compressed in a shock tube. A shock tunnel includes a shock tube, a nozzle attached to the end of the driven section of the shock tube, and a diaphragm between the driven tube and the

nozzle. The stagnation pressure and temperature in shock tunnels are about 200 MPa and 8000 K, respectively, to provide test times of about 6.5 ms.

The gun tunnel is quite similar to the shock tunnel in operation. It has a high-pressure-driven section and a low-pressure-driven section with a diaphragm separating the two. A piston is placed in the driven section, adjacent to the diaphragm, so that when the diaphragm ruptures, the piston is propelled through the driven tube, compressing the gas ahead of it. The piston used is so light that it can be accelerated to velocities significantly above the speed of sound in the driven gas. This causes a shock wave to precede the piston through the driven tube and heat the gas.

The hypersonic wind tunnel Cologne (H2K) at Department Wind tunnels facilities is one of the busy facilities. The H2K is a "blowdown" wind tunnel with a free jet test section. It uses contoured, axially symmetrical and replaceable nozzles. For aerodynamic testing, nozzles for Mach numbers of 4.8, 5.3, 6.0, 7.0, 8.7, and 11.2 are available. For aerothermal tests on probes, smaller nozzles with Mach numbers of 3.0 and 5.0 are also in use. The H2K wind tunnel above can be used for simulation of the air flow around models of future spacecrafts at Mach numbers of between 4.8 and 11.2. Measurement of aerodynamic and aerothermodynamic loads on complete hypersonic flight configurations and their components. Investigations on the interaction of hot plume nozzles flows with the external base flow.

HIEST is the largest high-enthalpy shock tunnel of free-piston-driven type in the world. It simulates airflow of very high temperature and high pressure that returnable spacecrafts encounter when they reenter the atmosphere.

The hypersonic and high-enthalpy wind tunnel at Kashiwa Campus of the University of Tokyo has facility for two-mode operation, using a high-pressure and high-temperature air generator, that is, hypersonic wind tunnel mode (very high-speed flow) and high-enthalpy wind tunnel mode (very high temperature flow).

The MHD generator transforms thermal energy and kinetic energy directly into electricity. MHD generators are different from traditional electric generators in that they operate at high temperatures without moving parts.

The hypersonic flight regime includes atmospheric entry and reentry, ground testing, and flight for both powered and unpowered vehicles.

Although unpowered hypersonic vehicles are not the topic of this book, it is important to note that there have been many more successful developments of unpowered hypersonic vehicle, predominantly in the reentry of manned and unmanned spacecraft of Russian, American, and European origin into earths atmosphere. There have also been a number of missions to other planets (more vehicles going to these planets than have been developed for sustained hypersonic flight within the atmosphere) and the entry speeds into those atmospheres have been even greater.

Mach number is not the only parameter that must be considered for hypersonic flight. A better measure is the speed itself, because it can also give an indication of the kinetic energy involved in the trajectory. For hypersonic craft, the flight enthalpy can usually be estimated very quickly from the speed as $h = u^2/2$. The amount of aerothermodynamic heating that the vehicle must deal with is linearly dependent on

the kinetic energy of the vehicle. This is a very important aspect of hypersonic flight through planetary atmospheres.

A thermally perfect gas is one that obeys the ideal gas equation of state,

$$p = \rho RT$$

A calorically perfect gas has constant values of specific heat independent of temperature. This designation refers to a gas that is both thermally and calorically perfect.

Reynolds number, $Re = VL/\nu$. This can be taken as a measure of the viscous flow time over the mean flow time.

Mach number, $M = V/a$. This is a measure of the flow speed relative to the acoustic propagation speed.

Knudsen number, $Kn = \lambda/L$ $(= M = Re)$. This is an indication of the collision path length relative to the flow scale

Prandtl number, $Pr = \nu/k$. A measure of the thermal diffusion time relative to the viscous diffusion time.

Schmidt number, $Sc = \nu/D$. This is an indication of the species diffusion time relative to the viscous diffusion time.

Eckert number, $E = u^2/h$. This indicates the relative magnitudes of kinetic and thermal energy for the flow.

Damkohler number, $Da = \tau_f/\tau_c$. This dimensionless parameter is the ratio of the characteristic flow time (such as a residence time) to a characteristic chemical reaction time.

The atmospheric composition behind a normal shock ahead of a hypersonic vehicle will differ greatly from the atmosphere ahead of the shock. Diatomic molecules will be vibrationally excited and dissociated to some extent, and the resulting atoms and remaining molecules can be partially ionized. Within a vehicle boundary layer, there is sufficient viscous dissipation to affect the stream chemistry and this can lead to chemically reacting boundary layers. As specific heats are no longer constant owing to vibrational excitation and chemical reaction, their ratio $\gamma = c_p/c_v$ is also no longer constant and also depends on the temperature. For air, this begins at around 800 K.

Another important aspect of hypersonic flight is that the variation in the ratio of specific heats, γ, can significantly influence the pressure distribution over a vehicle or its control surfaces.

For air at 1 atm pressure, oxygen dissociation begins near 2000 K and is complete at about 4000 K. Nitrogen dissociation begins at about 4000 K and is complete near 9000 K. At higher post-shock temperatures, ionization becomes important. In a partially ionized flow, the free electrons absorb and reflect electromagnetic radiation, usually in the frequency band of communication systems. In addition, at some level of ionization, the flow will behave quite differently than a weakly ionized or neutral flow, because the interatomic forces will have a strong electrical interaction component, which will lead to differences in transport properties.

For flow at very high speeds and low density, the mean free path can be larger than a characteristic length of the vehicle. This effect is represented by the Knudsen number λ/L.

Air chemistry is significantly different at the high temperatures encountered in hypersonic flight applications. Vibrational excitation of molecules, dissociation, and ionization will all occur as temperature is increased. However, with the exception of vibrational excitation, the onset and range of these effects will also vary with density or pressure.

When the characteristic flow time is much shorter than the time to complete chemical reactions or energy exchange mechanisms, then the flow can be in a nonequilibrium state.

Hypersonic vehicles are not yet readily available for human transportation. At present, there is only the Space Shuttle, and the lifetime of this vehicle has already been officially fixed (even though it is already operating *beyond* the design lifetime). Consequently, there is very little empirical data on vehicle design and performance and many design parameters have been barely explored. Part of the reason for this is the difficulty in simulating flight conditions on the ground. The relationship between actual flight data and the data from measurements in ground test facilities is not yet well understood.

Other equations of state that can be used for nonperfect gas situations. The most well-known equation of state used for nonperfect gas is the Van der Waal's equation,

$$p = \frac{RT}{v - b} - \frac{a}{v^2}$$

This equation expresses the relationship between the thermodynamic variables in the same way as the perfect gas equation but with an important modification to account for the attractive forces of real-gas behavior at high density in the second term.

Fortunately, for most applications involving hypersonic flows of air, the departure from thermal perfection is minimal.

Exercise Problems

7.1 A shock tube has still air at 0.1 atm and 270 K in its low-pressure chamber. A normal shock generated by rupturing the diaphragm separating the high-pressure chamber from the low-pressure chamber moves at 2100 m/s. Determine (a) the pressure in the high-pressure chamber at the time of diaphragm rupture and (b) the pressure, temperature, and Mach number of the air traversed by the shock. Treat air as a perfect gas.

[Answer: (a) 230.9 atm, (b) 4.75 atm, 2137 K, 1.89]

7.2 If a shock tube filled with air at 300 and 400 K at its low- and high-pressure chambers, respectively, has to generate a shock to traverse air to attain 600 K.

(a) What should be the shock strength? (b) Also, determine the velocity of the contact surface and the shock speed.

[Answer: (a) 5.32, (b) $V_2 = 559.60$ m/s, $C_s = 818.66$ m/s]

7.3 Mach number of 4.3 air stream flows over a blunt-nosed body. Determine the pressure coefficient at the stagnation point of the nose, with reference to the flow (a) ahead of and (b) behind the bow shock at the nose.

[Answer: (a) 1.82, (b) 1]

References

[1] Rathakrishnan E., *Gas Tables*, 3rd ed. Universities Press, Hyderabad, India, 2012.

[2] Rathakrishnan E., *Applied Gas Dynamics*, John Wiley & Sons, Inc., Hoboken, NJ, 2010.

[3] Sutton, A. P., and Chen, J., "Long-range finnis-sinclair potentials", *Philisophical Magazine Letters*, Vol. 61, 1990, pp. 139–146.

Index

High Enthalpy Gas Dynamics, First Edition. Ethirajan Rathakrishnan.

www.wiley.com/go/rathakrishnan

Index

High Enthalpy Gas Dynamics, First Edition. Ethirajan Rathakrishnan.

www.wiley.com/go/rathakrishnan